# OFFSHORE WIND TURBINES IN MARMARA REGION, TÜRKİYE: SITE SELECTION AND PRELIMINARY GEOTECHNICAL DESIGN OF MONOPILES

A THESIS SUBMITTED TO
THE GRADUATE SCHOOL OF NATURAL AND APPLIED SCIENCES
OF
MIDDLE EAST TECHNICAL UNIVERSITY

BY

ERAY CACEOĞLU

IN PARTIAL FULFILLMENT OF THE REQUIREMENTS
FOR
THE DEGREE OF MASTER OF SCIENCE
IN
CIVIL ENGINEERING

JUNE 2023

Approval of the thesis:

**OFFSHORE WIND TURBINES IN MARMARA REGION, TÜRKİYE: SITE SELECTION AND PRELIMINARY GEOTECHNICAL DESIGN OF MONOPILES**

submitted by **ERAY CACEOĞLU** in partial fulfillment of the requirements for the degree of **Master of Science in Civil Engineering, Middle East Technical University** by,

Prof. Dr. Halil Kalıpçılar
Dean, Graduate School of **Natural and Applied Sciences** _____

Prof. Dr. Erdem Canbay
Head of the Department, **Civil Engineering** _____

Assoc. Prof. Dr. Nejan Huvaj Sarıhan
Supervisor, **Civil Engineering, METU** _____

Assoc. Prof. Dr. Elif Oğuz
Co-Supervisor, **Civil Engineering, METU** _____

**Examining Committee Members:**

Assoc. Prof. Dr. Nabi Kartal Toker
Civil Engineering, METU _____

Assoc. Prof. Dr. Nejan Huvaj Sarıhan
Civil Engineering, METU _____

Prof. Dr. Sami Oğuzhan Akbaş
Civil Engineering, Gazi University _____

Assoc. Prof. Dr. Elif Oğuz
Civil Engineering, METU _____

Asst. Prof. Dr. Gülizar Özyurt Tarakcıoğlu
Civil Engineering, METU _____

Date: 22.06.2023

**I hereby declare that all information in this document has been obtained and presented in accordance with academic rules and ethical conduct. I also declare that, as required by these rules and conduct, I have fully cited and referenced all material and results that are not original to this work.**

Name Lastname: Eray Caceoğlu

Signature:

## ABSTRACT

### OFFSHORE WIND TURBINES IN MARMARA REGION, TÜRKİYE: SITE SELECTION AND PRELIMINARY GEOTECHNICAL DESIGN OF MONOPILES

Caceoğlu, Eray
Master of Science, Civil Engineering
Supervisor: Assoc. Prof. Dr. Nejan Huvaj Sarıhan
Co-Supervisor: Assoc. Prof. Dr. Elif Oğuz

June 2023, 177 pages

In this study, first, Analytical Hierarchy Process and Geographic Information Systems have been applied to detect suitable sites for future offshore wind power plants in Marmara Region, Türkiye. Site selection criteria have been determined based on literature review, then relative importances of these criteria have been computed based on a questionnaire answered by 11 international experts on offshore wind power plant site selection. In total, 5 regions are identified as suitable sites. In the second stage, three idealized seabed soil profiles have been identified which could represent Southern Marmara Sea and 12 preliminary monopile design cases have been studied considering different idealized soil profiles, pile diameters and p-y curve recommendations. Considered p-y curve recommendations include the current and the newly proposed recommendations of the American Petroleum Institute. It is found that newly proposed p-y curve recommendation could result in 20-30% reduced monopile penetration depth leading to a more economical foundation solution. Also, it is found that in certain soil/loading conditions, it

may provide a satisfactory design while the current p-y recommendation cannot.

Keywords: Offshore Wind Energy, Analytical Hierarchy Process, Geographic Information Systems, Monopile Design, p-y Curves

# ÖZ

## MARMARA BÖLGESİ, TÜRKİYE'DE DENİZ ÜSTÜ RÜZGAR TÜRBİNLERİ: SAHA SEÇİMİ VE TEKİL KAZIK GEOTEKNİK ÖN TASARIMI

Caceoğlu, Eray
Yüksek Lisans, İnşaat Mühendisliği
Tez Yöneticisi: Doç. Dr. Nejan Huvaj Sarıhan
Ortak Tez Yöneticisi: Doç. Dr. Elif Oğuz

Haziran 2023, 177 sayfa

Bu çalışmada, ilk olarak Marmara Bölgesi'nde kurulabilecek deniz üstü rüzgar enerji santrallerinin olası sahalarını tespit etmek için Analitik Hiyerarşi Prosesi ve Coğrafi Bilgi Sistemleri kullanılmıştır. Saha seçim kriterleri literatür taramasına dayalı olarak belirlenmiş, ardından bu kriterlerin göreceli önemleri, deniz üstü rüzgar enerji santrali saha seçimi konusunda 11 uluslararası uzmanın cevapladığı bir ankete dayalı olarak hesaplanmıştır. Toplamda 5 bölge uygun saha olarak belirlenmiştir. İkinci aşamada, farklı idealize zemin profilleri, kazık çapları ve p-y eğrisi tavsiyeleri dikkate alınarak tekil kazıklar için 12 farklı durumda ön tasarım çalışması yapılmıştır. Güney Marmara Denizi'ni temsil edebilecek idealize edilmiş üç zemin profili tanımlanmıştır. Analizlerde kullanılan p-y eğrisi tavsiyeleri, Amerikan Petrol Enstitüsü'nün mevcut ve gelecekteki tavsiyelerini içermektedir. Yeni önerilen p-y eğrilerinin, mevcut yöntemlerle karşılaştırıldığında tekil kazık penetrasyon derinliğini %20-30 oranında azaltabileceği ve mevcut önerilerin yapamadığı zemin/yükleme koşullarında, yeni önerilerin kabul edilebilir tasarımlar verebileceği görülmüştür.

Anahtar Kelimeler: Deniz Üstü Rüzgar Enerjisi, Analitik Hiyerarşi Prosesi, Coğrafi Bilgi Sistemleri, Tekil Kazık Tasarımı, p-y Eğrileri

To my beloved ones...

## ACKNOWLEDGMENTS

I am deeply grateful to my supervisor Assoc. Prof. Nejan Huvaj Sarıhan for her continuous guidance and valuable suggestions, which changed my perception of professional life and helped to shape my future plans, for the last 4 years including the last year of my undergraduate studies. Also, I really appreciate the support that my co-advisor Assoc. Prof. Elif Oğuz provided to me whenever I needed her. It has been a great pleasure for me to study with them.

I feel indescribably thankful to my family, Hasan, Aliye and Ceyda Caceoğlu. I know you always wanted me to be happy and achieve the best since my childhood. Without your nice parenting and sibship, I would not be at the point where I am. Other than my family, I feel the same way for my girlfriend, Esin Yandımata, although I knew her shorter than my family. I just want to say your endless love and support made my life much better.

Furthermore, my sincere good wishes go to all my friends from Geotechnics Division (Arda, Berkan, Elife, Hayri, Mehmet, Sefa and Tuğçe), who all tried their best to help me when I felt desperate about my study and future. We had many opportunities to discuss a lot of technical and daily life topics and we had lots of laughs together. I will not forget the good times we had.

Finally, I would like to mention the institutions who provided valuable financial support to me during my Master of Science studies. First, I thank to The Scientific and Technological Research Council of Türkiye (TÜBİTAK) for their continuous financial support for 2 years via 2210-A National MSc/MA Scholarship Program. Second, I thank to DANIDA Fellowship Centre for their support for 1 year during my project assistantship in WindFlag project.

## TABLE OF CONTENTS

ABSTRACT ..... v

ÖZ ..... vii

ACKNOWLEDGMENTS ..... ix

TABLE OF CONTENTS ..... x

LIST OF TABLES ..... xiv

LIST OF FIGURES ..... xvi

LIST OF ABBREVIATIONS ..... xx

LIST OF SYMBOLS ..... xxii

CHAPTERS

1 INTRODUCTION ..... 1

1.1 Offshore Wind Energy ..... 1

1.2 Problem Statement ..... 4

1.3 Research Objectives ..... 6

2 LITERATURE REVIEW ..... 7

2.1 Offshore Wind Power Plant Site Selection ..... 7

2.1.1 Site Selection Criteria ..... 8

2.1.2 Multi-Criteria Decision Making (MCDM) Methods & Analytical Hierarchy Process (AHP) ..... 11

2.1.3 Calculations in AHP ..... 13

2.1.3.1 Relative Weights of Decision Criteria ..... 14

2.1.3.2 Alternative Site Scores ..... 19

2.1.4 Existing Studies in Türkiye ..... 21

2.2 Monopile Design ..... 25
2.2.1 Monopiles ..... 25
2.2.2 Design Considerations ..... 27
2.2.2.1 Load Combinations ..... 27
2.2.2.2 Ultimate Limit State (ULS) ..... 29
2.2.2.2.1 Lateral Ultimate Capacity of a Monopile ..... 29
2.2.2.2.2 Partial Load and Resistance Factors ..... 31
2.2.2.3 Serviceability Limit State (SLS) ..... 32
2.2.2.4 Natural Frequency ..... 33
2.2.2.4.1 Method of Arany et al. (2016) ..... 35
2.2.2.5 Other Considerations ..... 38
2.2.3 Design Methodologies ..... 38
2.2.4 1D Finite Difference Method by p-y Curves ..... 39
2.2.5 American Petroleum Institute p-y Curves for Sands ..... 42
2.2.6 Matlock (1970) p-y Curves for Soft Clays ..... 44
2.2.7 p-y curves for Stiff Clays without Free Water ..... 46
2.2.8 Jeanjean et al. (2022) p-y Curves for Clays ..... 47
2.3 Offshore Soil Conditions in Marmara Sea ..... 52
3 OFFSHORE WIND POWER PLANT SITE SELECTION ..... 57
3.1 Workflow of Site Selection Study ..... 57
3.2 Study Area ..... 59
3.3 Site Selection Criteria in This Study ..... 61
3.3.1 Decision Criteria ..... 61
3.3.2 Exclusion Criteria ..... 70

3.4 Alternative Sites ..... 74
3.5 Results and Discussion of Site Selection ..... 77
3.5.1 Relative Weights of Decision Criteria ..... 77
3.5.2 Alternative Site Scores ..... 81
3.5.3 Final Alternative Site Scores and Discussion ..... 87
4 PRELIMINARY MONOPILE DESIGN ..... 89
4.1 Workflow of Monopile Design ..... 90
4.2 Idealized Soil Profiles ..... 93
4.2.1 Soil Profile 1 ..... 95
4.2.2 Soil Profile 2 ..... 96
4.2.3 Soil Profile 3 ..... 96
4.3 Selected Wind Turbine ..... 97
4.4 Load Calculations ..... 98
4.5 Creation and Validation of Jeanjean et al. (2022) p-y Curves ..... 103
4.5.1 Monotonic Curves ..... 103
4.5.2 Cyclic Curves ..... 105
4.5.3 Comparison of Monotonic and Cyclic Curves ..... 106
4.5.4 Check of p-y Curves in LPILE ..... 109
4.6 Design Criteria and Assumptions ..... 110
4.7 Results and Discussion of Monopile Design ..... 112
4.7.1 Example Design Problem (Soil Profile 1 – L=70 m & D=9.5 m Using Current Practice) ..... 112
4.7.1.1 Ultimate Limit State (ULS) Checks ..... 113
4.7.1.2 Serviceability Limit State (SLS) Checks ..... 117

4.7.2 Summary of Results ..... 120
4.7.2.1 Ultimate Limit State (ULS) ..... 121
4.7.2.2 Serviceability Limit State (SLS) ..... 125
4.7.2.3 Suggested Monopile Dimensions ..... 127
4.7.3 Comparison of Results ..... 128
5 CONCLUSION AND FUTURE WORK ..... 131
5.1 Conclusion ..... 131
5.2 Future Work ..... 133
REFERENCES ..... 135
APPENDICES
A. Site Selection AHP Questionnaire ..... 151
B. Wind Load Calculations ..... 154
C. Wave Load Calculations ..... 156
D. LPILE Ultimate Limit State Analysis Results ..... 160
E. LPILE Serviceability Limit State Analysis Results ..... 172

## LIST OF TABLES

TABLES

Table 2.1. Examples of Conflicts on OWPP Sites in Europe ..... 8
Table 2.2. Relative Importance Values in AHP (Saaty, 1987) ..... 15
Table 2.3. Recommended RI Values in AHP (Saaty, 1987) ..... 18
Table 2.4. Relative Desirability Values Used for Alternative Sites Comparison ..... 19
Table 2.5. Existing Studies on Turkish OWPP Site Selection ..... 21
Table 2.6. Site Selection Criteria Summary ..... 23
Table 2.7. Example relative weights from existing literature ..... 24
Table 2.8. Critical Load Combinations for Geotechnical Design of Monopiles (Arany et al., 2017) ..... 28
Table 2.9. Partial Load Factors (Det Norske Veritas, 2014) ..... 31
Table 2.10. Recommended Modulus of Subgrade Reaction Values (American Petroleum Institute, 2014) ..... 43
Table 2.11. Normalized p-y Relations Under Cyclic Loads (Matlock, 1970) 45
Table 2.12. Cyclic Loading Modification Factors (Jeanjean et al., 2022) ..... 51
Table 3.1. Summary of Decision Criteria ..... 62
Table 3.2. Summary of Exclusion Criteria ..... 71
Table 3.3. Main Properties of 5 Alternative Sites ..... 76
Table 3.4. First Candidate Group PCM ..... 77
Table 3.5. Final Group PCM ..... 78
Table 3.6. Summary of Consensus Iterations ..... 79
Table 3.7. Alternative Site Scores for WND ($CR = 0.040$) ..... 81
Table 3.8. Alternative Site Scores for FSH ($CR = 0.037$) ..... 82
Table 3.9. Alternative Site Scores for SHP ($CR = 0.031$) ..... 82
Table 3.10. Alternative Site Scores for PRT ($CR = 0.038$) ..... 83
Table 3.11. Alternative Site Scores for SOC ($CR = 0.035$) ..... 83
Table 3.12. Alternative Site Scores for WD ($CR = 0.038$) ..... 84

Table 3.13. Alternative Site Scores for EQH ($CR = 0.075$) ..... 84
Table 3.14. Alternative Site Scores for BRD ($CR = 0.009$) ..... 85
Table 3.15. Alternative Site Scores for DKBA ($CR = 0.054$) ..... 85
Table 3.16. Alternative Site Scores for OFC ($CR = 0.049$) ..... 86
Table 3.17. Alternative Site Scores for ONC ($CR = 0.057$) ..... 86
Table 3.18. Final Alternative Site Scores ..... 87
Table 4.1. Studied Design Cases ..... 92
Table 4.2. Considered Wind Turbines ..... 97
Table 4.3. Calculated Wind Loads ..... 99
Table 4.4. Calculated Non-Amplified Wave Loads ..... 99
Table 4.5. Pile Properties Used for Validation (Jeanjean et al., 2022) ..... 103
Table 4.6. Cyclic p-y Curve Model Parameters for North Sea (Jeanjean et al., 2022) ..... 105
Table 4.7. Ultimate Pile Capacity Values for the Example Monopile ..... 114
Table 4.8. Estimated ULS Natural Frequencies for the Example Monopile 115
Table 4.9. Amplified ULS Loads and Moments Acting on the Example Monopile ..... 116
Table 4.10. Safety Check for the Example Monopile ..... 117
Table 4.11. Estimated SLS Natural Frequencies for the Example Monopile 118
Table 4.12. Amplified SLS Loads and Moments Acting on the Example Monopile ..... 118
Table 4.13. Pile Head Deflection and Rotation of the Example Monopile .. 119
Table 4.14. Monopile Penetration Depths Satisfying ULS Requirements ... 125
Table 4.15. Concluded Preliminary Monopile Penetration Depths ..... 127

## LIST OF FIGURES

FIGURES

Figure 1.1. Hornsea 2 OWPP (Ørsted, 2019) ..... 2
Figure 1.2. Share of Foundation Cost in OWPPs (Oh et al., 2018) ..... 4
Figure 2.1. General Representation of an AHP Hierarchy (Zabel, 2012) ..... 14
Figure 2.2. Monopile Foundations (Bhattacharya, 2019) ..... 26
Figure 2.3. Estimation of Ultimate Lateral Capacity Using Numerical Analysis Results (Haiderali & Madabhushi, 2013) ..... 30
Figure 2.4. Dynamic Loads Affecting Monopiles (modified from Prendergast & Gavin, 2016) ..... 34
Figure 2.5. Calculation of Spring Coefficients (modified from Isenhower et al., 2019) ..... 37
Figure 2.6. Discretization of a Pile Using p-y Curves (Rocscience Inc., 2022) ..... 40
Figure 2.7. Recommended Values of $C1, C2$ and $C3$ (American Petroleum Institute, 2014) ..... 42
Figure 2.8. (a) Flow-around and (b) passive wedge mechanisms (Fleming et al., 1985) ..... 44
Figure 2.9. Normalized p-y Relations for Matlock (1970) (Isenhower et al., 2019) ..... 46
Figure 2.10. Normalized p-y Relations for Stiff Clays without Free Water (Isenhower et al., 2019) ..... 47
Figure 2.11. Normalized p-y Relations Under Monotonic Loads (Jeanjean et al., 2022) ..... 50
Figure 2.12. Seabed Soil Textures in Southern Marmara Sea (Vardar & Alpar, 2016) ..... 52
Figure 2.13. (a) Seabed sediments (upper 30 cm soil) in Marmara Sea according to Folk-7 sediment classification (EMODnet, 2021) (b) Folk-7 sediment classification (Guinan et al. 2021) ..... 53

Figure 2.14. Soil Profile Cross-Sections in Gemlik Bay (Yilmaz & Üstünkaya, 2004) ..... 54
Figure 2.15. Soil Profile Cross-Section in İzmit Bay (Oguz & Huvaj, 2020) 55
Figure 2.16. Undrained shear strength with depth for investigations in water depths greater than 10 m (values in parentheses are: rate of increase of undrained shear strength with depth (kPa/m); standard deviation in kPa) (Oğuz and Huvaj, 2020)..... 56
Figure 3.1. Workflow of Site Selection Study..... 58
Figure 3.2. Study Area of the Thesis ..... 60
Figure 3.3. Average Annual Offshore Wind Speed Map of Türkiye at 100 m Height (Modified from Global Wind Atlas (n.d.) by Caceoğlu et al., 2022).. 60
Figure 3.4. Average Annual Wind Speed at 100 m at the Study Area ..... 63
Figure 3.5. Hierarchy of Decision Criteria in This Study..... 64
Figure 3.6. Commercial Fishery at The Study Area ..... 65
Figure 3.7. Shipping Routes at The Study Area ..... 65
Figure 3.8. Existing Ports and Distance to Ports at the Study Area..... 66
Figure 3.9. (a) Water Depth (b) Bathymetry Contours (Shown with Red) with 100 m Intervals at the Study Area..... 67
Figure 3.10. Key Biodiversity Areas (KBAs) at the Study Area..... 68
Figure 3.11. Bird Migration Routes at the Study Area ..... 68
Figure 3.12. Earthquake Fault Lines at the Study Area ..... 69
Figure 3.13. High Voltage Electricity Cable Lines at the Study Area..... 70
Figure 3.14. Airports and Aviation Communication Devices at the Study Area ..... 71
Figure 3.15. Shipwrecks at the Study Area..... 72
Figure 3.16. Existing Subsea Communication Cables and Natural Gas Pipelines at the Study Area ..... 73
Figure 3.17. Alternative Sites (indicated with yellow) ..... 75
Figure 3.18. Relative Weights of Decision Criteria..... 80
Figure 4.1. Workflow of Monopile Design..... 90

Figure 4.2. Idealized Soil Profiles Used in This Study ..... 94
Figure 4.3. Representative Test Results in Very Soft Clay Layer..... 95
Figure 4.4. Calculated (a) Lateral Force and (b) Bending Moments at the Pile Head..... 101
Figure 4.5. Validation of Undrained Shear Strength Profiles ..... 104
Figure 4.6. Validation of Monotonic Lateral Bearing Capacity Factors..... 104
Figure 4.7. Example p-y Curves from Soil Profile 2, ULS, L=31 m, D=7.5 m (Depth of rotation under monotonic loading: 21 m) ..... 106
Figure 4.8. Example p-y Curves from Soil Profile 1, SLS, L=58 m, D=8.5 m (Depth of rotation under monotonic load: 47 m)..... 107
Figure 4.9. Example p-y Curves from Soil Profile 3, ULS, L=36 m, D=8.5 m (Depth of rotation under monotonic load: 25 m)..... 108
Figure 4.10. Comparison of Calculated and Extracted Cyclic p-y Curves at (a) 32 m, (b) 38 m, (c) 42 m and (d) 46 m depth (ULS, Soil Profile 1, D=9.5 m) ..... 109
Figure 4.11. ULS Analysis Plot for the Example Monopile ..... 114
Figure 4.12. (a) Pile Head Deflection and (b) Rotation Values for Increased Pile Lengths for the Example Monopile..... 120
Figure 4.13. Estimated Natural Frequencies of the Design Cases ..... 121
Figure 4.14. Ultimate Limit State Load Demands and Pile Capacities for Load Combination 1 ..... 122
Figure 4.15. Ultimate Limit State Load Demands and Pile Capacities for Load Combination 2 ..... 123
Figure 4.16. Ultimate Limit State Load Demands and Pile Capacities for Load Combination 3 ..... 123
Figure 4.17. Ultimate Limit State Load Demands and Pile Capacities for Load Combination 4 ..... 124
Figure 4.18. Summary of SLS Analysis Showing Lateral Deflection of Pile Head..... 125
Figure 4.19. Summary of SLS Analysis Showing Rotation of Pile Head..... 126

Figure 4.20. (a) Pile Head Deflection and (b) Rotation Values for Increased Pile Lengths (Jeanjean et al. (2022) Soil Profile 1 – D=9.5 m) ..... 127
Figure 4.21. Effect of Diameter in Pile Head Deflection and Rotation (Soil Profile 1 – Current Recommendation – SLS – Load Combination 3) ..... 128
Figure 4.22. (a) Lateral Deflection and (b) Mobilized Soil Reactions for Example Comparison (SLS, Soil Profile 1, D=9.5 m) ..... 129

## LIST OF ABBREVIATIONS

| | |
|---|---|
| 1P | Rotor passing frequency |
| 3P | Blade passing frequency |
| AHP | Analytical Hierarchy Process |
| ALS | Accidental Limit State |
| BRD | Distance to bird migration routes |
| CI | Consistency index |
| CPT | Cone Penetration Test |
| CR | Consistency ratio |
| DAF | Dynamic amplification factor |
| DKBA | Distance to Key Biodiversity Areas |
| EGC | Electricity grid connection |
| ENV | Environmental concerns |
| EQH | Earthquake hazard |
| Exp. | Expert |
| FEM | Finite Element Method |
| FLS | Fatigue Limit State |
| FSH | Commercial fishery |
| GCI | Group consensus index |
| GIS | Geographic Information Systems |
| GW | Gigawatts |
| HUM | Existing human activities |
| KBA | Key Biodiversity Areas |
| MCDM | Multi Criteria Decision Making |
| MN | Meganewtons |
| MN·m | Meganewton meters |
| MSP | Marine spatial planning |
| MW | Megawatt |

| | |
|---|---|
| MWh | Megawatt hours |
| NM | Nautical miles |
| OCR | Overconsolidation ratio |
| OFC | Required offshore cable length |
| ONC | Required onshore cable length |
| OWPP | Offshore wind power plant |
| OWT | Offshore wind turbine |
| PCM | Pairwise comparison matrix |
| PI | Plasticity index |
| PRT | Distance to ports |
| RI | Random index |
| rpm | Revolutions per minute |
| RW | Relative weight |
| SHP | Distance to shipping routes |
| SLS | Serviceability Limit State |
| SOC | Social acceptance |
| tan | Tangent |
| TEİAŞ | Turkish Electricty Transmission Cooperation |
| UK | United Kingdom |
| ULS | Ultimate Limit State |
| UU | Unconsolidated undrained |
| WD | Water depth |
| WND | Average annual wind speed at 100 m height |

## LIST OF SYMBOLS

| | |
|---|---|
| $a_{ij}$ | Element in i$^{th}$ row and j$^{th}$ column in individual pairwise comparison matrix |
| $\bar{a}_{ij}$ | Element in i$^{th}$ row and j$^{th}$ column in normalized pairwise comparison matrix |
| $a_{ij}^{*}$ | Element in i$^{th}$ row and j$^{th}$ column in modified pairwise comparison matrix |
| $a_{ij,r}$ | Element $a_{ij}$ in pairwise comparison matrix for r$^{th}$ expert |
| $f$ | Natural frequency of the regular wave under consideration |
| $f_{FB}$ | Fixed base natural frequency of the wind turbine |
| $f_{FB,T}$ | Fixed base natural frequency of tower |
| $f_n$ | Natural frequency of the OWT – foundation system |
| $g_{ij}$ | Element in i$^{th}$ row and j$^{th}$ column in group pairwise comparison matrix |
| $h$ | Length of discretized pile element (m) |
| $k$ | Modulus of subgrade reaction (MN/m$^3$) |
| $m$ | Number of alternative sites |
| $m_{RNA}$ | Mass of rotor-nacelle assembly (tons) |
| $m_t'$ | Euqivalent tower mass (tons) |
| $n$ | Number of decision criteria |
| $p$ | Mobilized soil reaction (MN/m) |
| $p_{cy}$ | Mobilized soil reaction under cyclic loads (MN/m) |
| $p_{mod}$ | Modification factor for mobilized soil reaction under cyclic loads |
| $p_{mo}$ | Mobilized soil reaction under monotonic loads (MN/m) |
| $p_u$ | Ultimate mobilized soil reaction (kN/m) |
| $s$ | Number of experts |
| $s_{m,final}$ | Final score of m$^{th}$ alternative |
| $s_u$ | Undrained shear strength (kPa) |

| | |
|---|---|
| $s_{u0}$ | Undrained shear strength at seabed (kPa) |
| $s_{u1}$ | Change rate of undrained shear strength with depth (kPa/m) |
| $t_{avg}$ | Average tower wall thickness (m) |
| $y_{cy}$ | Lateral deflection under cyclic loads (m) |
| $y_m$ | Lateral deflection of $m^{th}$ discretized pile element (m) |
| $y_{mod}$ | Modification factor for lateral deflection under cyclic loads |
| $y_{mo}$ | Lateral deflection under monotonic loads (m) |
| $z$ | Depth (m) |
| $z_{rot}$ | Depth of rotation or zero-deflection (m) |
| $D$ or $D_{pile}$ | Monopile diameter (m) |
| $D_{avg}$ | Average tower thickness (m) |
| $D_b$ | Diameter of tower at the bottom (m) |
| $D_t$ | Diameter of tower at the top (m) |
| $EI_{top}$ | Bending stiffness of tower at the top (MN·m$^2$) |
| $E_T I_T$ | Bending stiffness of tower (MN·m$^2$) |
| $E_P I_P$ | Bending stiffness of monopile (MN·m$^2$) |
| $GCI_r$ | Group Comparison Index for r$^{th}$ expert |
| $H_{ult}$ | Ultimate lateral pile capacity (MN) |
| $K_L$ | Lateral spring stiffness (MN/m) |
| $K_{LR}$ | Cross-coupling spring stiffness (MN) |
| $K_R$ | Rotational spring stiffness (MN·m/rad) |
| $L_S$ | Distance between mudline and top of transition piece (m) |
| $L_T$ | Tower height (m) |
| $M$ | Bending moment at seabed level (MN·m) |
| $N_{eq}$ | Equivalent number of cycles |
| $N_p$ | Lateral bearing capacity factor |
| $P_x$ | Axial load (MN) |
| $V$ | Lateral force at seabed level (MN) |
| $W_i$ | Relative weight of i$^{th}$ decision criteria |

| | |
|---|---|
| $\alpha_{ave}$ | Average adhesion factor through the monopile |
| $\delta$ | Lateral deflection at pile head (m) |
| $\theta$ | Rotation at pile head (rad) |
| $\varepsilon_c$ or $\varepsilon_{50}$ | Lateral strain at half of the shear strength |
| Φ’ | Angle of internal friction (°) |
| $\gamma'$ | Submerged unit weight (kN/m$^3$) |
| $\xi$ | Damping ratio |
| $\rho$ | Opinion weight of experts |

# CHAPTER 1

# INTRODUCTION

## 1.1 Offshore Wind Energy

Long before the invention of electricity, wind energy was utilized to perform many simple mechanical tasks such as water pumping and irrigation (Allamehzadeh, 2017). However, the first large wind turbine to produce electricity has been installed in Cleveland, Ohio in 1888, and small wind turbines were common in Denmark during World War I (Kaldellis & Zafirakis, 2011). Yet, the recent interest in wind energy started with the global oil crisis in 1970s, which paved the way for large scale onshore wind farms in California (Kaldellis & Zafirakis, 2011).

While Vindeby, Denmark (11 turbines with 450 kW power commissioned in 1991) is the first commercial offshore wind power plant (OWPP), the largest operational OWPP as of December 2022 is Hornsea 2 (illustrated in Figure 1.1) in the UK with an installed capacity of 1386 MW (165 turbines with 8.4 MW power) (Ørsted, 2019). Power capacities of Vindeby and Hornsea 2 shows the enormous development of offshore wind energy sector in just three decades.



Figure 1.1. Hornsea 2 OWPP (Ørsted, 2019)

Global Wind Energy Council (2021) provides the following statistics on the status of the market by the end of 2020.

- Global offshore wind market grew 22% per year in the last decade, and cumulative installed capacity reached to 35.3 GW.
- New installations reached to 6.1 GW in 2020 from 2.2 GW in 2016.
- Europe is the market leader with 70% of the installed capacity.
- The United Kingdom had the largest cumulative installed capacity (28.9% of the total global capacity), followed by China (28.3%) and Germany (21.9%). However, China overtook the United Kingdom in 2021.

This rapid development can be explained by the advantages of offshore wind energy. The advantages of offshore wind energy over onshore counterparts can be listed as follows (Bilgili et al., 2011; Esteban et al., 2011):

- Offshore environment typically provides faster winds than onshore. Therefore, energy potential is significantly higher.
- Offshore wind is not only faster but also more stable, i.e., less turbulent.
- Onshore wind turbines must be transported using roads, which sets a practical limit on the size of the turbines. However, there is no such limit for offshore wind turbines since logistics bases are usually large ports.
- Potential areas for onshore wind farms are usually restricted by human activities. However, there is much less restrictions on the sea. This enables to construct wind farms over larger areas.

On the other hand, the main disadvantage of the offshore wind energy is the considerably higher cost, which includes specialized installation, operation, and maintenance equipment (Irawan et al., 2017). However, as experience grows worldwide, the industry has started to be more economically competitive. Buljan (2021a) reported that levelized cost of energy for offshore wind has decreased by 28-49% between 2014-2019. The reason is attributed to "increased use of competitive procurement" and continuous technological advances. Also, Ørsted (2019) reported that in Northwest Europe, levelized cost of energy for newly built OWPPs was 61 €/MWh, which is lower than nuclear (169 €/MWh), natural gas (93 €/MWh) and coal (83 €/MWh) energy.

Apart from the reduction in costs, two more trends can be observed following WindEurope (2021). First, installed wind turbines are getting more powerful. Average turbine capacity was about 4 MW in 2014, but this number doubled in 2020. Second, wind energy is being extracted further from the coast with higher water depths. There are examples of OWPPs at permission stage which are located as far as 200 km from the coastline.

Today, offshore wind energy forms the backbone of renewable energy plans in many countries. For example, The United Kingdom Government (2020) ambitiously aims to reach 40 GW of installed offshore wind energy by 2030, which is "more than enough electricity to power every home in the country".

Republic of Türkiye has established the goal of 5 GW installed offshore wind energy until 2035 (Ministry of Energy and Natural Resources, 2022).

## 1.2 Problem Statement

Offshore wind turbine (OWT) foundations have the crucial task to transfer the loads to the undersea soils in a safe and serviceable manner. However, as Bhattacharya (2014) states, OWT foundations are critical not only in terms of safety of OWPP, but also in financial viability of the overall project because the foundations typically make up 25-34% of the overall cost. Oh et al. (2018) comes up with a similar interval (19-36%) as visualized in Figure 1.2.

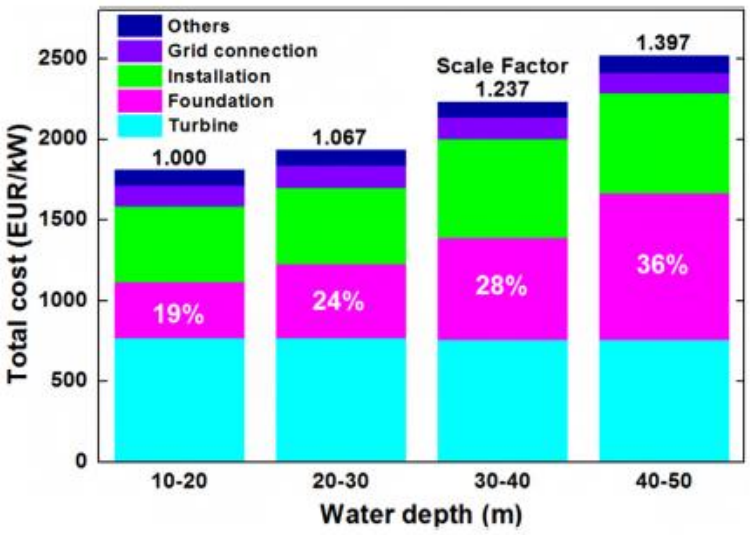



Figure 1.2. Share of Foundation Cost in OWPPs (Oh et al., 2018)

From Figure 1.2, it can be seen that the total cost per kW increases in deeper waters. More interestingly, costs other than the foundations do not change dramatically with water depth. This indicates the importance of reducing foundation costs to achieve a more economical OWPP.

Although being responsible for a considerable portion of the cost, current design methodologies, especially for monopiles (the most common foundation type as will be introduced in Section 2.2), are either underestimating the soil response (i.e. a conservative design approach) or time-consuming. Both issues increase the cost. As a result, recently, new design methodologies have been developed which aims to reach more economical design while spending less time. This includes American Petroleum Institute, whose recommendations are commonly followed in the industry. The institute will update its recommendation of design methodologies soon (Jeanjean et al., 2022). Mathematical expressions for the new recommendations have been published in the literature. Yet, to the best knowledge of the author, the effect of using the future and current recommendations of American Petroleum Institute on the pile dimensioning has not been studied.

On the other hand, the first step of OWPP implementation is the suitable site selection. Site selection is not a straightforward problem as there are many constraints and the suitable site needs to satisfy various criteria in addition to strong wind resource. So, in order to reach to an objective decision, Multi-Criteria Decision-Making (MCDM) method can be used. As will be shown in Section 2.1, in Türkiye, there are prior studies concerning site selection for future OWPPs using MCDM methods. However, none of the previous studies used Analytical Hierarchy Process (AHP) which gathers the opinions of multiple experts when deciding on the weights of each site selection criteria. Instead, decisions relied solely on the opinion of the researchers which may have caused biased results.

## 1.3 Research Objectives

In this thesis, two problems, mentioned in previous section, will be addressed.

First one is about site selection for an OWPP in Marmara Region. This part aims to identify suitable sites for OWPP implementation in Geographical Information Systems (GIS) environment. This will enable to analyze spatial data to be able to study multiple site selection simultaneously. Then, by considering international expert opinions from various backgrounds, which will be combined using consensus analysis through Anaytical Hierarchy Process, these suitable sites will be ranked to investigate their relative desirability among the others.

Second research objective is about preliminary monopile dimensioning in Marmara Sea. The current and newly developed/future recommendations of American Petroleum Institute will be applied on different idealized soil profiles in Marmara Sea. This part aims to provide an insight to possible challenges and reasonable dimensions for monopiles for possible future OWPP applications in Türkiye. On the other hand, comparisons of the methods will be a focus point which will attempt to estimate the reduction in monopile dimensions. This quantification is deemed as important since optimization of OWPP foundations would have a contribution for offshore wind energy to be more economically competitive.

# CHAPTER 2

# LITERATURE REVIEW

This chapter presents the conducted literature review on the subject organized as three main subjects: offshore wind power plant site selection (Section 2.1), monopile design (Section 2.2) and offshore soil conditions in Marmara Sea (Section 2.3).

## 2.1 Offshore Wind Power Plant Site Selection

Site selection is a crucial task since it is the first step in any OWPP project. Site selection should be done such that sufficient energy can be produced with no/minimal conflict with restrictions of local/environmental/social conditions.

As stated in Chapter 1, large areas are available for offshore wind turbines to be implemented, yet restrictions, some of which are unique to offshore projects, still exist that needs to be considered during OWPP site selection. Section 2.1.1 discusses these restrictions and parameters affecting the choice of the "best" site, collectively referred to as site selection criteria.

Section 2.1.2 introduces the Multi-Criteria Decision Making (MCDM) methods used in this study and their example applications. In the most basic sense, these methods aim to reach to a decision, in complex problems which depend on more than one criterion, using quantitative algorithms.

Finally, Section 2.1.4 discusses the previous studies on site selection for a potential future OWPP in Türkiye in detail.

### 2.1.1 Site Selection Criteria

OWPP site selection is an inter-disciplinary study during which concerns from different aspects should be considered. For example, the project developer/owner desire to produce the highest possible energy in a strongly windy area with the minimum cost, while electrical engineers may desire an OWPP where it is feasible to connect to the existing electric transmission system and will not cause problems in the operation of the national electrical grid. On the other hand, the concerns of different occupations (such as environmental engineers, civil engineers, marine biologists, regional planners, and social scientists) may conflict with each other. To illustrate, a site too far from a port would increase the cost, but a site too close may pose problems for shipping traffic. In the light of this discussion, it is seen that site selection is a complicated task. Despite being undesired, complications may require revisions in the selected site afterwards. In European practice, there exists some examples of this situation, as exemplified in Table 2.1.

Table 2.1. Examples of Conflicts on OWPP Sites in Europe

| **Country** | **Reference** | **Action/Revision** | **Reason** |
|---|---|---|---|
| The Netherlands | European MSP Platform (2018) | Site relocated to be farther from the coast | Concerns for possible effects on tourism |
| Germany | European MSP Platform (2018) | Size of the site reduced to one-third of the original plan | Visual impact and possible loss of revenue for local fisheries |
| Estonia | European MSP Platform (2018) | Cancellation of the project | Potential effects on the local nature and |

Table 2.1 (cont'd)

| Country | Reference | Action/Revision | Reason |
|---|---|---|---|
| Denmark | Buljan (2021b) | Tendering procedure paused to search for new sites | Unforeseen soil conditions with very soft deep clay |

These examples illustrate the importance of the preliminary site selection. Hence, the multi-disciplinary nature of OWPP site selection should be kept in mind, and as much data as possible should be obtained to assist in selecting a reasonable site.

The topic has been increasingly popular throughout the world in the last decade. There is an abundance of studies, some of which are even meta-analyzed by other researchers. Two examples of these meta-analyses are given here.

First, Spyridonidou & Vagiona (2020) analyzed 23 OWPP site selection studies. In their database, all studies have been published after 2010. According to this study, wind speed, water depth, distance to existing electricity grid system, distance to ports and verified shipping routes are the most considered "assessment criteria". On the other hand, military zones, bird migration routes and habitats, underwater cables and pipelines and civil/military aviation areas are among widely considered "exclusion criteria", on which OWPPs should not/cannot be installed.

Second, Peters et al. (2020) aimed to provide statistics and insight on the recent trends about GIS usage in offshore wind industry. Their database includes 49 studies, 14 of which are site selection studies. These 14 studies considered an average of 7 site selection criteria, but this number tends to increase in more recent ones. Interestingly, they noted that despite having the common aim, site

selection studies have considerable deviations. They believe that this might be due to site selection studies being more prone to bias of the researchers.

Despite being a comprehensive task, criteria selection is only a portion of OWPP site selection process. It is important to identify unsuitable areas for OWPPs. Literature review revealed that researchers came up with different limits for unsuitable areas supporting the ideas of Peters et al. (2020). Before summarizing the findings, some definitions are made:

- *Decision criteria:* Site selection criteria that has an effect on the preference of the "best" alternative site
- *Exclusion criteria:* Site selection criteria that directly results in elimination of some areas, commonly referred to as "no-go zones" in the practice
- *Buffer zone:* Zone, on which no turbine would be constructed, defined around potential source of conflict with OWPP
- *Suitable limit:* Minimum or maximum quantitative limit applied on a criterion to pre-eliminate potentially uneconomical sites

World Bank (2019) considers areas with annual average offshore wind speed at 100 m height smaller than 7 m/s as unsuitable for OWPPs. However, Cradden et al. (2016), Vasileiou et al. (2017) and Tercan et al. (2020) considers this limit as 6 m/s while Caceoğlu et al. (2022) as 6.5 m/s. Tricoli et al. (2006) puts the suitability limit as 6 m/s at 60 m height. Note that all studies consider wind speed as a decision criterion. However, Emeksiz & Demirci (2019) considered it as an exclusion criterion and eliminated sites with lower wind speed than 3 m/s at 50 m height.

Regarding the distance to shipping routes, Jay (2009) recommends a buffer zone of 3.6 km. Hong & Möller (2011) comes up with a more complex recommendation of 1, 3 and 3.6 km for low, medium and high intensity routes respectively. Isiacik Colak et al. (2021) excluded sites closer than 1 NM (1852 m) to the shipping routes. On the other hand, Díaz & Soares (2021) considers a

smaller buffer zone of 500 m. The UK Maritime and Coastguard Agency (2021) defines 0.5 NM (926 m) of buffer zone as unacceptable for OWPPs in the UK.

Maximum water depth is typically regarded as an important suitable limit. Vasileiou et al. (2017) and Tercan et al. (2020) stated 70 m, whereas Isiacik Colak et al. (2021) considered 60 m as a reasonable limit. On the other hand, 50 m is more commonly applied as the maximum water depth limit (Díaz & Soares, 2021; Kim et al., 2018; World Bank, 2019). It should be noted that those limits are given as boundary values below which fixed-bottom foundations and above which floating foundations are economically preferable. Emeksiz & Demirci (2019) also applied a lower limit of 3 m/s and studied sites with 25-50 m water depth.

Distance to shore is another concern. A site too close to the shore may drive social acceptance problems although a site too far may increase the costs too much. Tercan et al. (2020) considered sites 1.5-25 km distant from the shore as suitable sites.

Pipelines and undersea cables are potential source of conflicts for OWPPs. Therefore, buffer zones are suggested by different researchers as 0.1 NM (185 m) (Isiacik Colak et al., 2021), 250 m (Tercan et al., 2020) and 500 m (Emeksiz and Demirci, 2019).

### 2.1.2 Multi-Criteria Decision Making (MCDM) Methods & Analytical Hierarchy Process (AHP)

Langemeyer et al. (2016) defines MCDM methods as a "multi-step process consisting of a set of methods to structure and formalize decision-making processes in a transparent and consistent manner." Also, they state that MCDM allows the decision makers to compare some alternatives based on decision criteria, whose weights can be assigned quantitatively. When there are a high number of alternatives, finding the "best" alternative becomes important, which

can be achieved by MCDM methods (Zlaugotne et al., 2020). As a result, these methods help enormously on complicated tasks, which includes OWPP site selection.

In the literature, countless MCDM methods can be found. However, this study focuses on AHP because there is extensive knowledge/experience on AHP, which is a widely accepted and applied MCDM method.

Since its introduction to the literature by Saaty (1980) AHP has been a popular MCDM method. There are example applications in geotechnical engineering practice as well. To name a few, Saadatkhah et al. (2015) developed an index to assess shallow landslide susceptibility based on factors such as slope inclination and lithology. Providakis et al. (2021) investigated tunnel-induced settlement vulnerability considering six parameters: groundwater table, hydraulic conductivity, undrained shear strength, density, elastic modulus, and unit weight.

Some advantages of AHP method are given below (Karthikeyan et al., 2016; Oguztimur, 2011):

- The method is simple since it is not necessary to use sophisticated datasets.
- The method is based on expert opinions.
- The consistency of the decision maker can be measured easily.
- The method can be applied in a fast manner using computer software.
- It is possible to consider any level of details. In other words, sub-criteria are possible to be applied.

On the other hand, some disadvantages are noted as follows (Karthikeyan et al., 2016; Oguztimur, 2011).

- Number of calculations is high even if the problem is small, i.e., there is low number of decision criteria.
- Relying on expert opinions means that the obtained result is subjective.

AHP has been extensively used on OWPP site selection problems worldwide. For example, Díaz & Soares (2021) ranked 4 pre-selected alternative sites in Canary Islands, Spain using AHP. They considered a notably wide range of site selection criteria (6 main criteria and 23 sub-criteria) including meteorological oceanographic (met-ocean) conditions, viability, logistics, facilities, marine environment and techno-economic criteria. Their alternative sites are in very deep waters at which there is no commercial OWPP available today. Vagiona & Karanikolas (2012) applied AHP with 5 decision criteria (wind speed, distance to protection areas, distance from shipping routes, distance from shore and electricity connection) to rank 10 sites in Greece. They found that electricity connection and distance from the shore as the most important ones. In Nigeria, Mayaki et al. (2018) compared 3 alternative sites. They used only 4 decision criteria, but different from other studies, they included "power demand" and "distance from airports" in their decision along with wind speed and distance to shipping routes. Abdel-Basset et al. (2021) searched for suitable OWPP sites in Egyptian waters by studying 7 main and 22 subcriteria. They developed a hybrid MCDM method, in which AHP is combined with other methods. The role of AHP is limited to find the relative weights of decision criteria. Final example is the study of Fetanat & Khorasaninejad (2015), which studied OWPP site selection in Iran territorial waters.

### 2.1.3 Calculations in AHP

In this section, calculations of AHP are explained step by step as they are applied in this study. Calculations consist of two sub-steps: relative weights of decision criteria and alternative site scores.

#### 2.1.3.1 Relative Weights of Decision Criteria

**Step 1: Formation of the hierarchy**

This step includes defining the goal, selecting the criteria that affects the decision and setting up the relationships between the goal and decision criteria. The hierarchy consists of three or four levels, which is visualized in Figure 2.1.

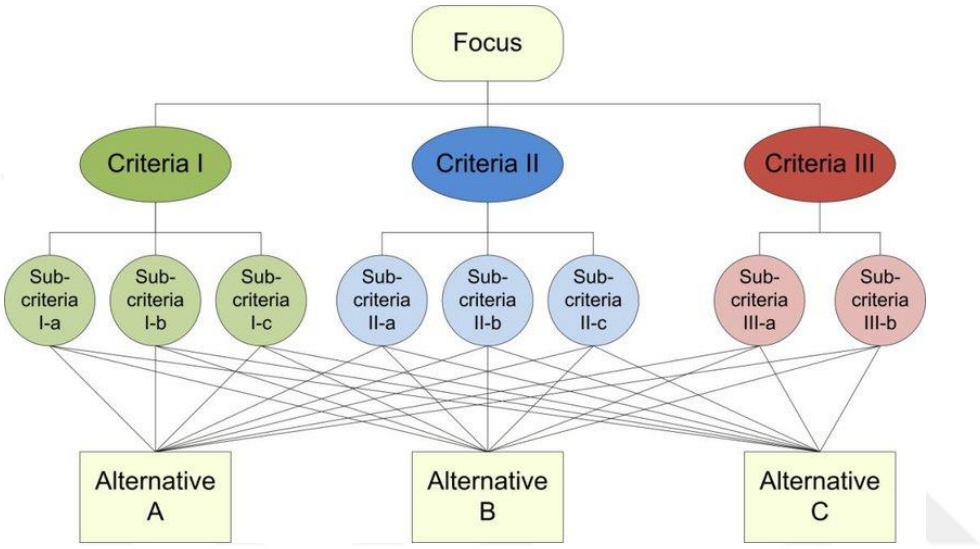



Figure 2.1. General Representation of an AHP Hierarchy (Zabel, 2012)

In Figure 2.1, "Focus" refers to the goal of the hierarchy and "Criteria" to decision criteria. It should be observed that the goal is affected by a series of decision criteria and all alternatives are evaluated for each decision criterion. It is possible to have some or all the criteria with no subcriteria.

**Step 2: Formation of the Pairwise Comparison Matrix (PCM)**

PCM has the dimensions of $n \times n$. In this matrix, any element $a_{ij}$ represents the relative importance of the $i^{th}$ decision criterion over the $j^{th}$ decision criterion. The relative importance is quantified as given in Table 2.2.

Table 2.2. Relative Importance Values in AHP (Saaty, 1987)

| **Importance value** | **Definition** | **Explanation** |
|---|---|---|
| 1 | Equal importance | Two criteria have an *equal* contribution to the decision. |
| 3 | Moderate importance | Experience and judgment *slightly* favor one criterion. |
| 5 | Strong importance | Experience and judgment *strongly* favor one criterion. |
| 7 | Very strong importance | *Evidence* favoring one criterion *exists* in the industry. |
| 9 | Extreme importance | *Evidence* favors one criterion *at the highest level* possible. |
| 2, 4, 6, 8 | Intermediate values in the case of compromise needed between two adjacent judgments | |
| Reciprocals of above values | Indicates $j^{th}$ decision criterion has more importance over $i^{th}$ decision criterion | |

There are three observations from Table 2.2. First, the explanations of the values are qualitative, which is the reason of the subjectivity of the method. However, it seems to be a reasonable way to quantify the opinion of the expert or the decision maker. Second, all diagonal elements are equal to 1 since any decision criterion has equal importance over itself. Third, last row implies that $a_{ij} = 1/a_{ji}$. As a result, for $n$ decision criteria, a decision maker has to perform $n(n-1)/2$ pairwise comparisons.

**Step 3: Consensus analysis**

In some cases, like this study, more than one expert may be consulted. This necessitates a consensus analysis as experts would naturally have different opinions on priority of decision criteria. At the end, for $p$ experts, there would be $p$ number of $n \times n$ pairwise comparison matrices. Consensus analysis combines these "individual" PCMs into a single "group PCM". Note that this step is not necessary for applications with a single expert.

In the literature, different algorithms of consensus analysis can be found like suggestions of Altuzarra et al., (2009), Wu & Xu (2012) and Dong & Saaty, (2014). This thesis utilizes Dong & Saaty (2014) as it is deemed as simpler to apply on a spreadsheet. The next paragraphs explain this iterative method.

Each iteration starts by forming a candidate group PCM. This $n \times n$ matrix is obtained by Eq. (2.1).

$$g_{ij} = \prod_{r=1}^{p} (a_{ij,r})^{\rho_r} \tag{2.1}$$

In Eq. (2.1), $\rho_r$ represents the opinion weight of $r^{th}$ expert. Different experts may be assigned different opinion weight. However, Eq. ((2.2) must always hold.

$$\sum_{r=1}^{p} \rho_r = 1 \tag{2.2}$$

In this thesis, all experts are assigned the same opinion weight, i.e., $\rho_r = 1/s = 0.125$ for all 8 experts.

Next, group consensus index $(GCI)$ is calculated for each expert. Eq. 3.3 shows the utilized equation to compute $GCI$ for $r^{th}$ expert.

$$GCI_r = \frac{1}{n^2} \sum_{i=1}^{n} \sum_{j=1}^{n} a_{ij,r}\, g_{ji} \tag{2.3}$$

Eq. (2.3) includes an elementwise multiplication of individual PCMs with transpose of candidate group comparison matrix. If an individual PCM is identical with candidate group PCM, then $GCI_r = 1$. As a result, expert with the highest $GCI$ has the largest deviation from the group. A stop condition should be set at this stage. In this thesis, it is considered that if standard deviation of $GCI_r$ for all experts is smaller than 0.01, then the consensus has been reached, and final group PCM is the one formed by Eq. (2.1). Once the consensus has been reached, Step 4 can start.

If consensus is not reached, the expert with the highest $GCI$ is invited to modify his/her individual PCM by applying Eq. (2.4).

$$a_{ij}^{*} = \left(a_{ij}\right)^{\alpha}\left(g_{ij}\right)^{1-\alpha} \tag{2.4}$$

Here, $\alpha \in [0, 1]$ and it indicates how dramatic the update of the individual PCM is going to be. For example, $\alpha = 0$ is the most dramatic update, which equates the updated individual PCM to the group PCM. On the other hand, $\alpha = 1$ does not result any change in individual PCM. In this thesis, it is assumed that $\alpha = 0.5$ for each iteration. This assumption is needed since a physical discussion environment could not be set.

After applying Eq. (2.4), the current iteration ends and the next one starts by Eq. (2.1).

**Step 4: Calculation of relative weights of the decision criteria**

There are two calculations in this step. First, the resultant group PCM is normalized column-wise as shown in Eq. (2.5). In the normalized pairwise matrix, elements in the same column add up to 1.

$$\bar{a}_{ij} = a_{ij} \Big/ \sum_{k=1}^{n} a_{ik} \tag{2.5}$$

Second, average of the elements at the same row is calculated, which gives the relative weight of decision criterion that is represented by the respective row. The calculation is given in Eq. (2.6).

$$W_i = \frac{1}{n}\sum_{k=1}^{n} \bar{a}_{ki} \tag{2.6}$$

**Step 5: Checking the consistency of PCM**

From Step 2, it can be observed that the method requires an extensive amount of pairwise comparison especially for large $n$, which may easily yield inconsistent comparisons. Thus, consistency check is a crucial step of the method.

The first calculation is to normalize PCM with relative weights calculated in Step 4. This is achieved by Eq. (2.7). Note that $b_i$ is a single number.

$$b_i = \frac{1}{W_i}\sum_{k=1}^{n} W_i a_{ik} \tag{2.7}$$

Second, the largest eigenvalue of the PCM can be found from Eq.(2.8).

$$\lambda_{max} = \frac{1}{n}\sum_{k=1}^{n} b_i \tag{2.8}$$

Third, consistency ratio, CR, can be calculated using Eq.(2.9).

$$CR = \frac{CI}{RI} = \frac{\lambda_{max} - n}{(n-1)RI} \tag{2.9}$$

Here, $RI$ is a function of $n$ with larger $RI$ for larger $n$. The suggested values are given in Table 2.3.

Table 2.3. Recommended RI Values in AHP (Saaty, 1987)

| $n$ | 3 | 4 | 5 | 6 | 7 | 8 | 9 | 10 |
|---|---|---|---|---|---|---|---|---|
| $RI$ | 0.58 | 0.90 | 1.12 | 1.24 | 1.32 | 1.41 | 1.45 | 1.49 |

No consistency check is required for $n = 2$ since there is only one pairwise comparison in this case. At the end, a PCM is said to be consistent if $CR \leq 0.1$. If not, the respective PCM should not be trusted in decision making.

#### 2.1.3.2 Alternative Site Scores

The calculations have the same logic with previous part, but slight modifications are needed as explained below.

**Step 1: Identification of alternative sites**

This is a crucial step in the process, yet more details are given in Section 3.5 on identified alternative sites.

**Step 2: Pairwise comparison of alternative sites in terms of each decision criterion**

Similar with pairwise comparison of decision criteria, the same grading scale is used for pairwise comparison of alternative sites. However, Table 2.2 is slightly modified as presented in Table 2.4.

Table 2.4. Relative Desirability Values Used for Alternative Sites Comparison

| **Desirability value** | **Definition** |
|---|---|
| 1 | Equal desirability |
| 3 | Moderate desirability |
| 5 | Strong desirability |
| 7 | Very strong desirability |
| 9 | Extreme desirability |
| 2, 4, 6, 8 | Intermediate values in the case of compromise needed between two adjacent values |

Values in Table 2.4 are used to compare alternative sites for each decision criterion. In other words, for $m$ alternative sites and $n$ decision criteria, $n$ number of $m \times m$ PCMs have been formed by judgement of the author.

Since there is only one set of PCMs for alternative sites by the author, there is no need for consensus analysis.

**Step 3: Calculation of alternative site scores in terms of each decision criterion**

The only difference with the previous section is the size of the PCM ($m \times m$). Eqs. (2.10) - (2.11) yield the alternative site scores of each alternative.

$$\bar{a}_{ij} = a_{ij} / \sum_{k=1}^{m} a_{ik} \tag{2.10}$$

$$s_{t,i} = \frac{1}{m} \sum_{k=1}^{m} \bar{a}_{ki} \tag{2.11}$$

**Step 4: Consistency checks**

Similarly, the only difference is the size of the matrix. However, as an important result, $RI$ value is different as can be seen in Table 2.3.

**Step 5: Calculation of final alternative site scores**

Section 2.1.3.1 already have provided the relative weights of decision criteria. Also, alternative site scores for each decision criterion have been obtained by previous steps in this section. The final alternative site score, given in Eq. (2.12), basically combines these two to obtain a single number for each alternative site.

$$s_{t,final} = \sum_{i=1}^{n} W_i s_{t,i} \tag{2.12}$$

It is to be noted that final alternative site scores must add up to 1. Alternatives with higher final scores obtain higher rankings.

### 2.1.4 Existing Studies in Türkiye

OWPP site selection has taken the attention of Turkish researchers in the last decade and the interest is ever increasing.

Table 2.5 summarizes some of the prior studies on the subject. In this table, 11 studies are given, oldest of which was published in 2012.

Table 2.5. Existing Studies on Turkish OWPP Site Selection

| **Study** | **Area of study** | **Suitable wind speed limit** | **Suitable water depth limit** | **Utilization of GIS** | **Utilization of MCDM methods** |
|---|---|---|---|---|---|
| Güzel (2012) | Bozcaada & Gökçeada | Not specified | ≤ 45 m | No | No |
| Özdilim (2017) | All Türkiye | ≥7 m/s | ~ 30 m | No | No |
| Akalın (2018) | Bozcaada & Gökçeada | ≥ 6.5 m/s | 15-50 m | Yes | Yes |
| Argin et al. (2019) | All Türkiye | ≥3 m/s (at 50m) | ≤ 45 m | No | No |
| Emeksiz & Demirci (2019) | All Türkiye | >3.5 m/s at 50 m | 25-50 m | Yes | Yes |
| Aydıner (2020) | Aegean Sea | ≥ 6.5 m/s | ≤ 50 m | Yes | Yes |
| Tercan et al. (2020) | Aegean Sea | ≥ 6 m/s | ≤ 70 m | Yes | Yes |

Table 2.5 (cont'd)

| **Study** | **Area of study** | **Suitable wind speed limit** | **Suitable water depth limit** | **Utilization of GIS** | **Utilization of MCDM methods** |
|---|---|---|---|---|---|
| Genç et al. (2021) | All Türkiye | ≥ 7 m/s | ≤ 50 m | Yes | Yes |
| Isiacik Colak et al. (2021) | Bozcaada | ≥ 4 m/s | ≤ 60 m | Yes | Yes |
| Yıldız (2021) | Aegean and Mediterranean Seas | ≥ 6.5 m/s | ≤150 m | Yes | No |
| Caceoğlu et al. (2022) | Northwest Türkiye | ≥ 6.5 m/s | ≤100 m | Yes | Yes |

From Table 2.5, it can be clearly seen that OWPP site selection has become a hot topic in the country in the last 5 years. Also, utilization of MCDM methods and GIS has clearly increased. The probable reason would be that the complex nature of OWPP site selection has been realized better over time. On the other hand, considered water depth limitations imply that fixed-bottom foundations were considered primarily, except for Yıldız (2021) and Caceoğlu et al. (2022). However, considered water depth values increased over time which indicates that recent developments have been considered in more recent studies. Finally, different researchers came up with different suitable limits for wind speed values. It is a good example of subjective nature of site selection process.

Like the case with wind speed and water depth, existing studies differ in terms of considered site selection criteria as well. Table 2.6 summarizes the counts of utilized site selection criteria in the above-mentioned 11 studies.

Table 2.6. Site Selection Criteria Summary

| **Site selection criterion** | **Number of studies** | **Site selection criterion** | **Number of studies** |
|---|---|---|---|
| Wind speed | 11 | Airports / civil aviation | 6 |
| Water depth | 10 | Electricity grid connection | 5 |
| Shipping routes | 10 | Ports | 5 |
| Military areas | 8 | Fishery areas | 4 |
| Environmental concerns | 8 | Earthquake fault lines | 4 |
| Existing subsea cables/pipelines | 8 | Tourism areas | 2 |
| Territorial water boundaries | 7 | Nuclear power plants | 1 |

From Table 2.6, it is clear that wind speed, water depth and shipping routes constitute mostly considered site selection criteria. They are followed by military areas, environmental concerns and existing subsea cables/pipelines, each of which was evaluated in 8 studies. On the other hand, tourism areas and nuclear power plants are the least considered ones. Earthquake fault lines seem to be overlooked by many studies with only 4 study considering earthquake fault lines. This may be an important site selection criterion considering the high seismic activity of Türkiye.

Existing studies differ not only in considered criteria but also in concluded relative weights. Three example studies are presented in Table 2.7.

Table 2.7. Example relative weights from existing literature

| **Criteria** | **Akalın (2018)** | **İsiacik Colak et al. (2020)** | **Tercan et al. (2020)** |
|---|---|---|---|
| Water depth | 0.11 | 0.25 | 0.20 |
| Wind speed | 0.27 | 0.40 | 0.25 |
| Distance to shipping routes | 0.06 | 0.13 | 0.09 |
| Distance to substations | 0.25 | 0.05 | - |
| Distance to earthquake fault lines | 0.31 | - | - |
| Distance to shore | - | 0.08 | 0.13 |
| Distance to ports | - | 0.03 | 0.18 |
| Distance to subsea cables | - | 0.02 | - |
| Distance to urban areas | - | 0.04 | - |
| Environmental & military concerns | - | - | 0.15 |

First of all, there are only three criteria that all studies considered: water depth, wind speed and distance to shipping routes. Wind speed turned to be one of the most two important criteria in all studies with a relative weight between 25-40%. In general, water depth tended to be assigned a lower relative weight, followed by distance to shipping routes. Regarding the remaining criteria, the

most interesting results are related with distance to substations. One study did not study substations at all whereas two remaining studies assigned significantly different relative weights. A similar observation can be made for distance to ports as well. These exemplify the subjective nature of site selection studies.

## 2.2 Monopile Design

This section is subdivided into eight subsections. First monopiles are briefly introduced (Section 2.2.1), followed by design considerations (Seciton 2.2.2) and design methodologies (Section 2.2.3). Then, Section 2.2.4 discusses 1D Finite Difference Method, which forms the basis of monopile design in this thesis. Finally, Sections 2.2.5 - 2.2.8 presents different p-y curve recommendations used in this thesis.

### 2.2.1 Monopiles

Monopiles are single tubular piles, which are usually made of steel and driven into the seabed. A monopile is connected to the turbine tower via transition piece (Figure 2.2).

Monopiles are the most common fixed-bottom foundation types for offshore wind turbines located in water depths typically less than 50 m (World Bank, 2018). In fact, 4.681 out of 5.764 (81%) OWTs in Europe have been supported by monopiles (WindEurope, 2021).The reason is attributed to their simplicity with only three major design parameters: embedded length, diameter and wall thickness (Lesny & Richwien, 2011).

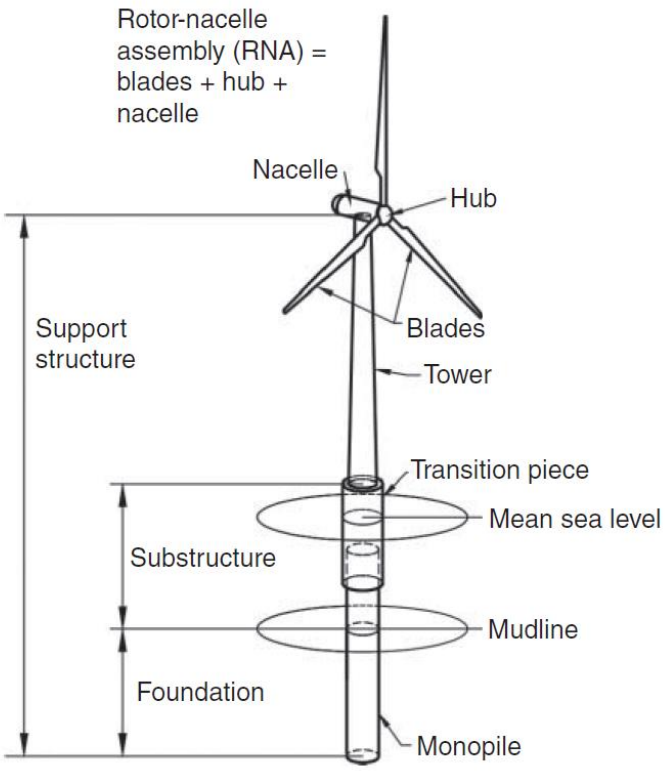



Figure 2.2. Monopile Foundations (Bhattacharya, 2019)

Monopiles are free-head piles with ability to rotate at the pile head. They transfer the wind and wave loads as lateral load into the soil. Therefore, it is crucial to have shallow soil with sufficient lateral capacity (Lesny & Richwien, 2011).

For a 5MW OWT (95 m hub height and 125 m rotor diameter) installed in the North Sea, Lesny & Wiemann (2005) estimates that at the mudline, the axial load would be 35 MN, extreme horizontal load would be 16 MN, creating a bending moment of 562 MN·m. Therefore, it can be understood that lateral loads constitute a major design concern for monopiles.

Arany et al. (2017) compiled some existing monopile dimensions. In their database, monopile diameters range between 3-7 m, and wall thickness between 35-126 mm. Also, they noted that monopiles in London Array OWPP have the

following properties: 4.7 – 5.7 m diameter (d), 40 m embedded length (L) and 44-87 mm wall thickness. It should be noted that $L/d \cong 7 - 8.5$. Similarly, Negro et al. (2017) presents a database of monopile dimensions as well. Their compilations included monopiles with diameters of 3-7 m, total lengths of 20-85 m and total weight of 200 – 800 tons. These piles were applied in water depths shallower than 30 m. However, these databases consist of 3.6 MW turbines at most, which are considered too small nowadays.

Hermans & Peeringa (2016) recommended a 9.6 m diameter monopile for a 10 MW OWT. As of February 2023, the largest manufactured monopile has a diameter of 9.6 m, which will be installed in the United States (Lewis, 2023). Also, monopiles with 9.5 m diameter and 110 m total length have been successfully installed in Arcadis Ost 1 OWPP in 2022 (DEME Group, 2022).

### 2.2.2 Design Considerations

Monopile design is a multi-disciplinary task incorporating hydrodynamic, structural and geotechnical aspects of civil engineering. In this section, design considerations of a monopile are discussed with a focus on geotechnical aspects.

#### 2.2.2.1 Load Combinations

In the most commonly used guidelines, critical load combinations assume a return period of 50 years or 2% probability of annual exceedance (Det Norske Veritas, 2014), although OWPPs are usually planned to operate about 20-25 years. Although numerous load combinations are given in Det Norske Veritas (2014), Arany et al. (2017) stated that 5 load combinations are critical for geotechnical concerns. These combinations are tabulated in Table 2.8.

Table 2.8. Critical Load Combinations for Geotechnical Design of Monopiles (Arany et al., 2017)

| Combination No | Wind load | Wave load | Direction of application |
|---|---|---|---|
| 1 | Normal turbulence at rated wind speed | 1-year extreme sea state | Collinear |
| 2 | Extreme turbulence at rated wind speed | 50-year extreme wave height | Collinear |
| 3 | Extreme operating gust at rated wind speed | 1-year extreme wave height | Collinear |
| 4 | Extreme operating gust at cut-out speed | 50-year extreme wave height | Collinear |
| 5 | Extreme turbulence at rated wind speed | 50-year extreme wave height | 90° misalignment |

Definitions of these load cases are summarized below from Arany et al. (2017).

**Normal turbulence at rated wind speed:** Rated wind speed is the wind speed at which the turbine produces the maximum electricity that it can. Wind force is maximum at rated wind speed. However, turbulence creates extra loads, which can be calculated from Det Norske Veritas (2014). Turbulence loads needs to be considered as well.

**Extreme turbulence at rated wind speed:** The only difference from the previous case is that turbulence loads are higher under extreme turbulence.

**Extreme Operating Gust at Rated Wind Speed:** This case corresponds to the maximum possible wind load. Therefore, it can be considered as an abnormal load case with low probability. Extreme gust speed can be calculated using

statistical distribution parameters, usually from Weibull distribution, of wind measurements.

**Extreme Operating Gust at Cut-out Speed:** At very high wind speeds, turbine stops generating electricity for safety reasons. This is referred as cut-out speed of the turbine. It may be comprehended as the most critical wind load case, however, after rated wind speed, drag coefficient starts to reduce thanks to pitch-control system of the turbine, therefore, wind force starts to decrease.

**1-year Extreme Sea State:** This represents the sea state during a storm with a return period of 1-year. The sea state is characterized by significant wave height, which corresponds to the wave height with 13.6% probability of exceedance during a storm.

**1-year Extreme Wave Height:** Different from Extreme Sea State, Extreme Wave height case considers the largest wave, which can be either directly measured or estimated using significant wave height.

**50-year Extreme Wave Height:** This load case corresponds to the most critical wave loads as it considers the largest wave during a large storm.

#### 2.2.2.2 Ultimate Limit State (ULS)

A monopile must provide sufficient capacity to avoid failure under extreme axial loads, lateral loads and moment. This condition is known as the Ultimate Limit State. Thus, in ULS calculations, lateral and axial pile capacity needs to be estimated. In the literature, it is noted that lateral loads usually govern ULS concerns (Arany et al., 2017; Bhattacharya, 2019).

##### 2.2.2.2.1 Lateral Ultimate Capacity of a Monopile

Long-lasting and well-known analytical methods proposed by Broms (1964a, 1964b) and Fleming et al. (1985) can be applied for preliminary assessment of

ultimate lateral load capacity of monopiles. However, Broms (1964a, 1964b) method may underestimate the ultimate capacity because no soil reaction is assumed at the top 1.5D length of the pile, which corresponds to a noteworthy portion of a monopile. Also, this is an overly simplified assumption.

Ultimate lateral capacity could be estimated using numerical analysis results as well. In the literature, one example is suggested by Haiderali & Madabhushi (2013), which is illustrated in Figure 2.3.

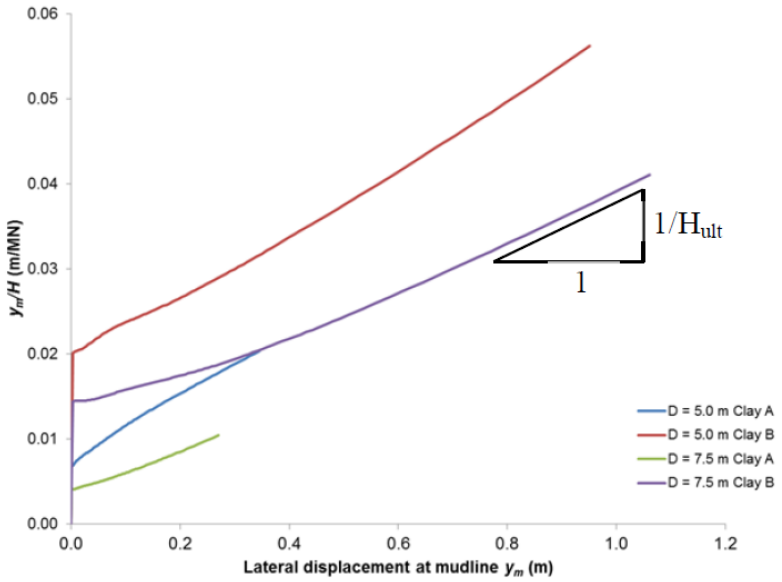



Figure 2.3. Estimation of Ultimate Lateral Capacity Using Numerical Analysis Results (Haiderali & Madabhushi, 2013)

In Figure 2.3, lateral deflection at pile head is plotted in horizontal axis whereas ratio of lateral displacement to applied lateral load is given in vertical axis. After a certain point, the relationship is linear whose slope is $1/H_{ult}$. The method may be expected to produce more reliable results for rigid piles since pile head deflections tend to increase quickly under increasing large loads in flexible piles.

Furthermore, LeBlanc et al. (2010) performed experiments to establish a failure criterion for rigid piles. A clear point could not be established, but they have suggested that the load that causes a rotation of 4° at the pile head could be taken as the ultimate capacity for a rigid pile.

#### 2.2.2.2.2 Partial Load and Resistance Factors

To ensure a certain safety level, partial load and resistance factors are applied in ULS analysis.

Table 2.9 summarizes the widely used partial load factors.

Table 2.9. Partial Load Factors (Det Norske Veritas, 2014)

| | **Dead load** | **Variable load** | **Environmental loads** | **Deformation loads** |
|---|---|---|---|---|
| Set 1 | 1.25 | 1.25 | 0.70 | 1.00 |
| Set 2 | 1.00 | 1.00 | 1.35 | 1.00 |
| Set 3 (for abnormal wind loads) | 1.00 | 1.00 | 1.10 | 1.00 |

As it is seen in Table 2.9, Set 1 gives more consideration to vertical dead loads whereas the other two increase the importance of lateral environmental loads. Set 3 applies to abnormal wind loads, which corresponds to the Load Combination 3 in Table 2.8.

As a result, it is reasonable to check vertical capacity using Set 1, and lateral capacity using Sets 2 and 3. In all cases, load factor of deformation loads, i.e., second order effects due to vertical dead load, is set to 1.

On the other hand, partial resistance factors are applied to the characteristic strength parameters of soil. These factors are recommended as 1.25 to undrained shear strength for clays (total stress analysis) and 1.15 (effective stress analysis) for sands (Det Norske Veritas, 2014). It is not specified whether this factor should be directly applied to angle of internal friction (Φ') or tangent of it, tan(Φ').

#### 2.2.2.3 Serviceability Limit State (SLS)

In this limit state, monopile is checked against excessive rotation and lateral deflection throughout the design life of the structure. This is a crucial design check as it may be the governing limit state (Senanayake, 2016).

Serviceability requirements include lateral deflection and rotation at the pile head. A literature review revealed two different acceptable lateral deflection limits: 12 cm at the pile head and 2 cm at the pile toe, which has been stated as the experience gained in TU Delft (Velarde, 2016), and 20 cm at the pile head (Arany et al., 2017; Nasab et al., 2022). The latter criterion is also mentioned in Krolis et al. (2007).

Regarding the pile head rotation, sometimes referred to as tilt, a maximum permanent tilt of 0.5° has been recommended (Det Norske Veritas, 2014) although this limit has been criticized as being too low by Arany et al., (2015).

It is important to note that these limitations apply to accumulated deflection and rotation due to cyclic loads as well. Therefore, as described by Cuéllar (2011), SLS can be subdivided into two categories: short-term and long-term.

Although long-term deformations are likely to be more critical, its estimation requires much detailed information of waves and soil behavior. Firstly, it is a difficult task to estimate the sequence of wave loads imposed by successive storms. In the literature, effect of successive storms has been studied. Anh Quang (2012) recommended that a comprehensive probabilistic model of

possible storm patterns should be examined in monopile design. Secondly, estimating plastic soil deformation is also challenging under millions of load cycles. Simple analytical methods have been proposed to estimate long term deflections (Cuéllar, 2011; LeBlanc et al., 2010; Page et al., 2021). However, these are mostly developed from experiments with low number of cycles compared to what a monopile experiences. In any case, cyclic laboratory tests are essential in estimation of long-term behavior of soil-monopile interaction.

Short-term serviceability is relatively easier to estimate where the monopile is exposed to a powerful storm for about 3 hours (Det Norske Veritas, 2014). In this case, the pile is subjected to extreme loads which are expected to occur only once throughout the service life. This case has been studied in preliminary design problems in the literature assuming the intact shear strength properties of soil. However, Cuéllar (2011) points out that it is not necessarily the case. He suggests classifying the behavior as undrained, partially drained or drained, which again requires a comprehensive laboratory testing program.

#### 2.2.2.4 Natural Frequency

It is important to ensure that natural frequency of OWT foundations do not result in significant dynamic amplification of forces, i.e., resonance. This is because OWT foundations are under dynamic loads from various sources. These sources include waves, rotor spinning frequency (1P) and blade passing frequency (3P for a typical three blade OWT). Furthermore, waves have a random nature, and rotor spinning and blade passing frequency changes with wind speed, which creates an interval of natural frequencies which OWT-foundation system should avoid. The concept is visualized in Figure 2.4.

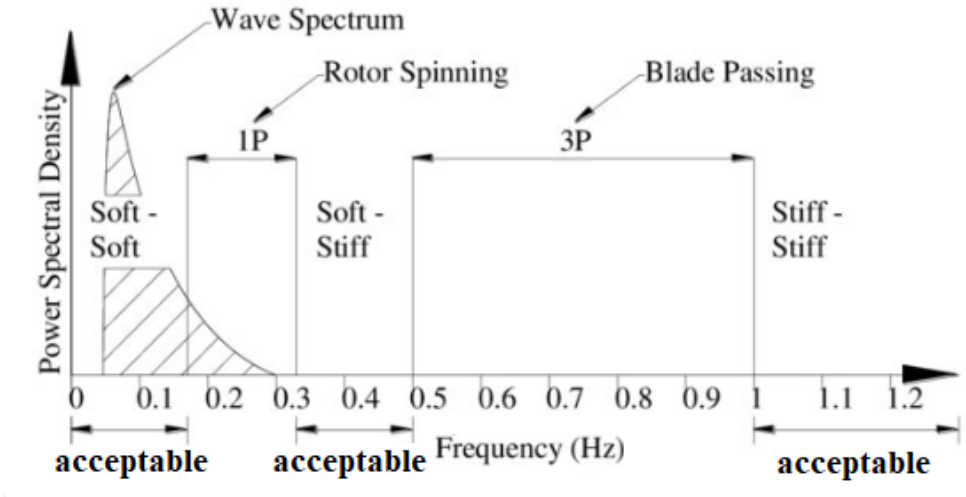



Figure 2.4. Dynamic Loads Affecting Monopiles (modified from Prendergast & Gavin, 2016)

From Figure 2.4, it is observed that natural frequency of an OWT-foundation system may fall into three acceptable regions referred as **soft-soft** (both the turbine tower and foundation deform considerably), **soft-stiff** and **stiff-stiff** (neither of the turbine tower and foundation deforms considerably). In the literature, it has been reported that monopiles typically fall into soft-stiff region (Andersen et al., 2012; Wan et al., 2023). This is why natural frequency of the system needs to be estimated accurately since both underestimation and overestimation may be unsafe.

Provided numbers in Figure 2.4 are stated as “typical values” for an application in North Sea as of 2016. However, 1P-3P ranges are different for each turbine, where 3P range boundaries are exactly as three times as 1P range boundaries. For example, turbine presented in Figure 2.4 has a 1P range of 0.17-0.33 Hz and 3P range of 0.5-1 Hz. On the other hand, LW 8MW turbine blades rotate with a frequency between 6.3-10.5 rpm (Desmond et al., 2016), which results in 1P range of 0.105-0.165 Hz and 3P range of 0.305-0.495 Hz.

In dealing with 1P-3P frequency ranges, the common practice is to avoid them with a 10% factor of safety (Det Norske Veritas, 2014).

On the other hand, wave spectrum, which can be developed by analyzing wave measurements, naturally differs for each sea environment. Random nature of waves makes it impractical to avoid concurrence with wave period. So, waves are usually dealt by applying a dynamic amplification factor (DAF) given in Eq. (2.13), also recommended by Det Norske Veritas (2014).

$$DAF = \frac{1}{\sqrt{\left(1 - \frac{f}{f_n}\right)^2 + \left(2\xi \frac{f}{f_n}\right)^2}} \tag{2.13}$$

The next section presents the method used in this study to calculate the natural frequency of OWT – monopile system.

#### 2.2.2.4.1 Method of Arany et al. (2016)

This is a semi-empirical method which consists of three steps, explained in detail below.

**Step 1: Fixed-base natural frequency**

In this step, the turbine is considered as an elastic cantilever beam fixed at the seabed. Then, fixed-base natural frequency of tower is given by Eq. (2.14).

$$f_{FB,T} = \frac{1}{2\pi} \sqrt{\frac{3E_T I_T}{L_T^3 \left(m_{RNA} + \frac{33}{140} m'_T\right)}} \tag{2.14}$$

Since tower diameter and wall thickness changes throughout the turbine tower, the tower is idealized as a perfect cylinder in this approximation. As a result, moment of inertia of the tower ($I_T$) is calculated using average diameter ($D_{avg}$) and average wall thickness ($t_{avg}$) from Eq. (2.15).

$$I_T = \frac{1}{8}\pi D_{avg} t_{avg} \tag{2.15}$$

Similarly, $m'_T$ in Eq. (2.14) refers to the mass of this idealized perfectly cylindrical tower.

So far, only the tower above transition piece is considered. The next calculations are done to evaluate the effect of the portion of the monopile between transition piece and seabed. This is dealt via of two ratios: bending stiffness ratio of the tower and monopile ($X$), and platform/tower length ratio ($\psi$). These parameters are calculated by Eqs. (2.16) and (2.17).

$$X = \frac{E_T I_T}{E_P I_P} \tag{2.16}$$

$$\psi = \frac{L_S}{L_T} \tag{2.17}$$

At the end, natural frequency of the fixed-end turbine can be calculated using Eq. (2.18).

$$f_{FB} = f_{FB,t}\sqrt{\frac{1}{1 + (1+\psi)^3 X - X}} \tag{2.18}$$

**Step 2: Non-dimensional foundation stiffness parameters**

At this step, foundation is represented by three springs: lateral ($K_L$), rotational ($K_R$) and cross-coupling springs ($K_{LR}$) (Figure 2.5). Estimated spring coefficients are utilized in three non-dimensionless foundation stiffness parameters. First, a parameter called $f(q)$ is calculated by Eq. (2.19)

$$f(q) = \frac{1}{3}\frac{2q^2(q-1)^3}{2q^2\ln(q) - 3q^2 + 4q - 1}, where\ q = \frac{D_b}{D_t} \tag{2.19}$$

Second, $f(q)$ parameter is used to normalize the bending stiffness of the tower with respect to the bending stiffness at the top as given in Eq. (2.20).

$$EI_\eta = EI_{top} \times f(q) \tag{2.20}$$

Then, the needed non-dimensionless parameters can be calculated by Eq. (2.21).

$$\eta_L = \frac{K_L L_T^3}{EI_\eta}, \eta_{LR} = \frac{K_{LR} L_T^2}{EI_\eta}, \eta_R = \frac{K_R L_T}{EI_\eta} \tag{2.21}$$

It should be kept in mind that foundation stiffness coefficients may be estimated either using closed-form analytical equations or using computer analysis. Although researchers provided analytical equations to estimate spring coefficients, they stated that computer analyses are more reliable.

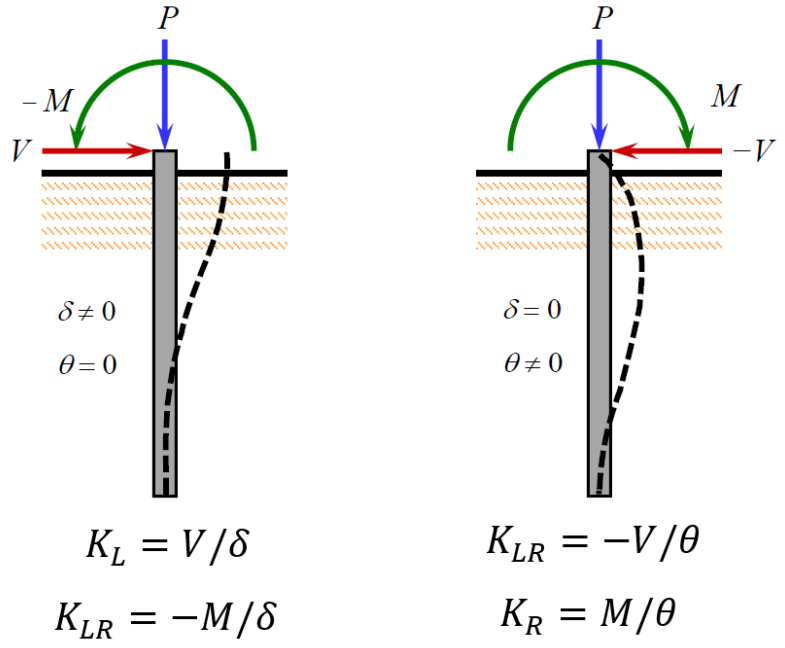



Figure 2.5. Calculation of Spring Coefficients (modified from Isenhower et al., 2019)

**Step 3: First natural frequency on a deformable foundation**

At this stage, two empirical parameters ($C_R$ *and* $C_L$) are calculated in Eqs. (2.22) and (2.23). In these equations, 0.6 and 0.5, respectively, are empirical constants.

$$C_R = 1 - \frac{1}{1 + 0.6\left(\eta_R - \frac{\eta_{LR}^2}{\eta_L}\right)} \tag{2.22}$$

$$C_L = 1 - \frac{1}{1 + 0.5\left(\eta_L - \frac{\eta_{LR}^2}{\eta_R}\right)} \tag{2.23}$$

Finally, first natural frequency of the tower – monopile system can be estimated using Eq. (2.24).

$$f_n = C_R C_L f_{FB} \tag{2.24}$$

Arany et al. (2016) noted that applicability conditions of Eq. (2.24) are as given in Eq. (2.25).

$$\eta_R > 1.2\frac{\eta_{LR}^2}{\eta_L} \;\; \& \;\; \eta_L > 1.2\frac{\eta_{LR}^2}{\eta_R} \tag{2.25}$$

#### 2.2.2.5 Other Considerations

There are more monopile design considerations that are not addressed in this thesis. These considerations include installation effects, Fatigue Limit State (FLS), Accidental Limit State (ALS), scour protection, marine growth, earthquake loading and corrosion.

### 2.2.3 Design Methodologies

Monopile design methodologies have a wide range from preliminary simple hand calculations to sophisticated 3D Finite Element Method (FEM) models.

Arany et al. (2017) proposed a simple iterative procedure for preliminary dimensioning, which can be performed by hand calculations. The required inputs are basic turbine properties, met-ocean data (wind and wave statistical parameters) and geotechnical data (soil stiffness variation with depth). On the

other hand, although using suitable constitutive models and soil parameters 3D FEM models can approximate the complex pile-soil interaction problems accurately, they are computationally more expensive to optimize the monopile design for the whole OWPP (Murphy et al., 2018). More importantly, a high number of soil parameters is needed for accurate modelling.

1D Finite Difference Method by p-y curves are commonly used in monopile design as a faster alternative to 3D FEM models. However, p-y curves currently recommended by American Petroleum Institute have been developed by field test on flexible piles, so their applicability for monopiles have been questioned (Wang et al., 2022). New methods have been proposed to deal with this problem.

Byrne et al. (2020) developed a new method called PISA (Pile Soil Analysis). This method is developed specifically for monopiles. In this method, soil parameters are calibrated by 3D Finite Element Method models, which are then fed as inputs to 1D Finite Difference Method. On the other hand, Jeanjean et al. (2022) chose adhering to the same logic of existing p-y curves but brought major updates to p-y curves. They compared their recommendations with PISA method and noted very good physical agreement although differences exist in mathematical expressions.

This thesis concentrates on 1D Finite Difference Method by p-y curves because the method is not as complicated as 3D FEM, also there are different p-y curves available in the literature which gives the chance to compare these methods.

### 2.2.4 1D Finite Difference Method by p-y Curves

1D Finite Difference Method is a simple and fast way of analyzing laterally loaded piles. In this method, the pile is discretized (Figure 2.6) and a lateral non-linear Winkler spring is attached to each pile element to model the soil.

Load-deformation relationship of these non-linear springs are referred to as p-y curves. The pile is considered as a deformable elastic beam.

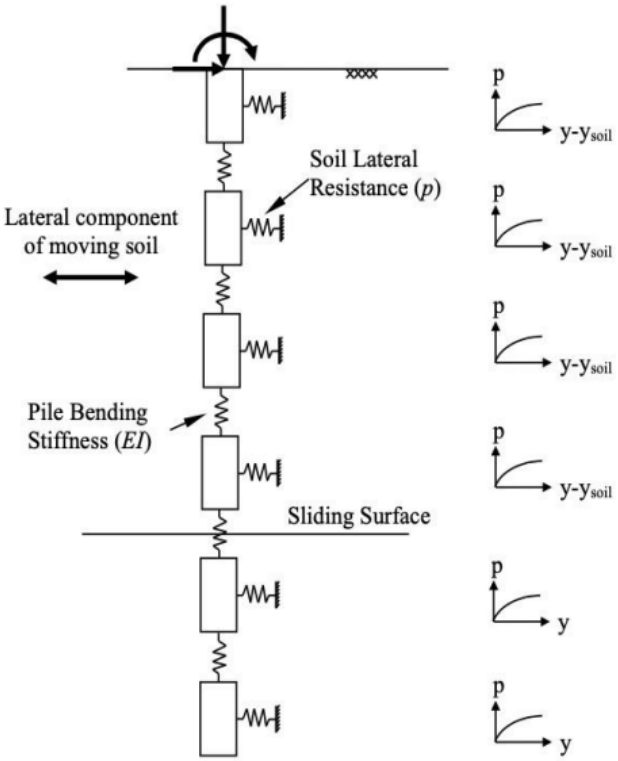



Figure 2.6. Discretization of a Pile Using p-y Curves (Rocscience Inc., 2022)

Commonly used software like LPile and RSPile implement this theory, which is summarized in the next paragraphs from Isenhower et al. (2019).

The governing equation is given in Eq. (2.26), which correlates the distributed load and deflection of an elastic beam. In the case of a laterally loaded pile, distributed load is mobilized soil reaction ($p$).

$$p = EI\frac{d^4y}{dx^4} + P_x\frac{d^2y}{dx^2} \tag{2.26}$$

Using central difference method, a numerical method to estimate derivative of a function, Eq. (2.26) can be rewritten as in Eq. (2.27).

$$p = EI\left(\frac{y_{m-2} - 4y_{m-1} + 6y_m - 4y_{m-1} + y_{m+2}}{h^4}\right) + P_x\left(\frac{y_{m-1} - y_m + y_{m+1}}{h^2}\right) \tag{2.27}$$

This equation needs to be solved at each pile element. Mobilized soil reaction is already quantified in terms of lateral displacement at each element thanks to p-y curves, i.e., $p = f(y_m)$.

It should be noted that two imaginary points need to be introduced at the head ($y_{-1}$ and $y_0$ when $m = 1$) and tip ($y_{(m_{max})+1}$ and $y_{(m_{max})+2}$ when $m = m_{max}$) of the pile. This results in introduction of 4 extra unknowns, which can be dealt by boundary conditions. For a free-headed monopile, 4 boundary conditions are as follows:

1. At the pile tip, moment is zero.
2. At the pile tip, shear is zero.
3. At the pile head, moment coming from the superstructure is known.
4. At the pile head, shear coming from the superstructure is known.

It should be noted that shear and moment along the pile are also derived from elastic beam deflection equations, and central difference method is applied to them as well (Eqs. (2.28) - (2.29)).

$$V = EI\frac{d^3y}{dx^3} + P_x\frac{dy}{dx}$$

$$V = EI\left(\frac{-y_{m-2} + 2y_{m-1} - 2y_{m+1} + y_{m+2}}{2h^3}\right) + P_x\left(\frac{y_{m-1} + y_{m+1}}{2h}\right) \tag{2.28}$$

$$M = EI\frac{d^2y}{dx^2} = EI\left(\frac{y_{m-1} - y_m + y_{m+1}}{h^2}\right) \tag{2.29}$$

Therefore, at the end, pile response problem reduces to a system of equations with $m_{max} + 4$ unknowns and $m_{max} + 4$ equations for a pile discretized in $m_{max}$ elements. Once lateral deflection of an element is known, shear (Eq.

(2.28)), moment (Eq. (2.29)) and rotation (Eq. (2.30)) at this element can be calculated using elastic beam deflection formulations.

$$S = \frac{dx}{dy} = \frac{y_{m-1} + y_{m+1}}{2h} \tag{2.30}$$

In Finite Difference Method, choice of p-y curves has a direct effect on pile response. Therefore, next sections introduce p-y curves used in this study.

### 2.2.5 American Petroleum Institute p-y Curves for Sands

These p-y curves are employed in commonly used recommended practices (American Petroleum Institute, 2014; Det Norske Veritas, 2014). In this method, the ultimate mobilized soil reaction is given by Eq. (2.31).

$$p_u = \min\big((C_1 z + C_2 D)\gamma' z,\ C_3 D \gamma' z\big) \tag{2.31}$$

In this equation, $C_1, C_2$ and $C_3$ constants depend on angle of internal friction, which are visualized in Figure 2.7.

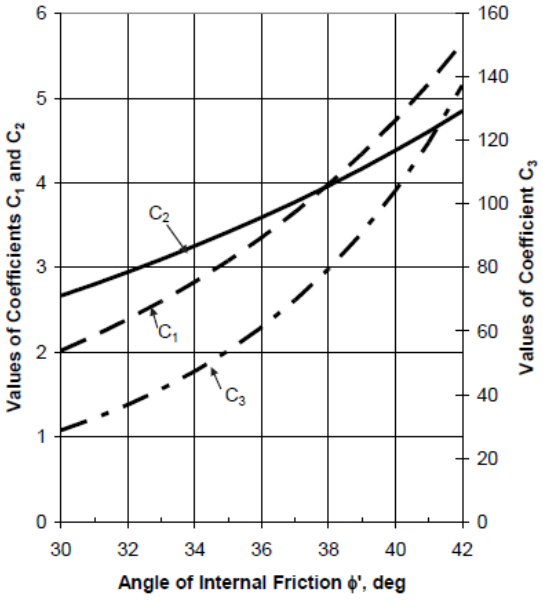



Figure 2.7. Recommended Values of $C_1, C_2$ and $C_3$ (American Petroleum Institute, 2014)

As expected, higher values for $C_1, C_2$ and $C_3$ are recommended with increasing angle of internal friction. On the other hand, since $C_3$ is larger than $C_1$ & $C_2$, the first term in Eq. (2.31) dominates the ultimate mobilized soil reaction at shallower depths whereas the second term is more pronounced at larger depths. Mobilized soil reaction ($p$) vs pile head lateral deflection ($y$) relationship is given by Eq. (2.32).

$$p = Ap_u \tanh\left(\frac{kz}{Ap_u} y\right) \tag{2.32}$$

In this equation, $A$ is an empirical constant whose value is 0.9 for cyclic loading and between 0.9 – 3 for monotonic loading. This implies that up to 70% reduction in mobilized soil reaction under cyclic loads is anticipated. Another note is related with modulus of subgrade reaction ($k$). Recommended values in American Petroleum Institute (2014) are given in Table 2.10.

Table 2.10. Recommended Modulus of Subgrade Reaction Values (American Petroleum Institute, 2014)

| **Angle of internal friction** | $\boldsymbol{k}$ $(\boldsymbol{MN/m^3})$ |
|---|---|
| 25° | 5.4 |
| 30° | 11 |
| 35° | 22 |
| 40° | 45 |

It is possible use linear interpolation for intermediate values. However, as noted by Orakcı (2022), angle of internal friction of sand should be between 30-40° to avoid any extrapolation of parameters presented in Figure 2.7 and Table 2.10. For friction angle values smaller than 25° and larger than 40°, American Petroleum Institute (2014) recommends carrying out pile tests, while some

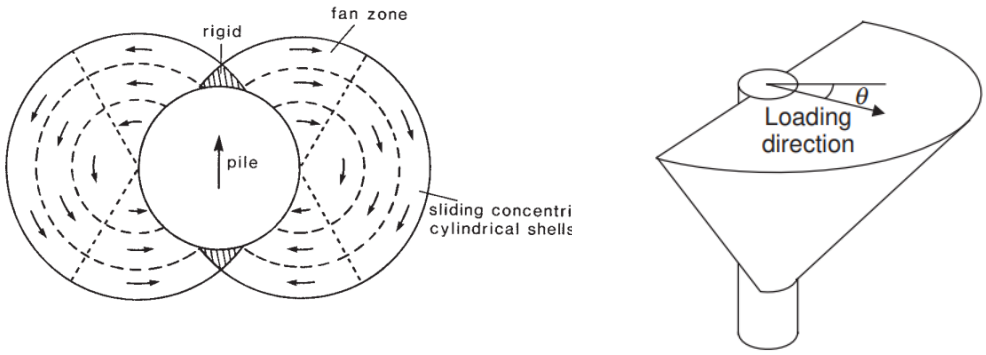
researchers such as Orakci et al. (2022) used capping at the maximum value of $k$. Orakci (2022) reminded that extrapolation may give unreasonable results.

### 2.2.6 Matlock (1970) p-y Curves for Soft Clays

Traditionally, the method proposed by Matlock (1970) has been implemented in American Petroleum Institute (2014) and Det Norske Veritas (2014) for clays.

$$p_u = \min\left(3s_u + \gamma' z + \frac{Js_u z}{D}, 9s_u D\right) \tag{2.33}$$

In this equation, two terms refer to two different failure mechanisms: passive wedge and flow-around failures (Figure 2.8) respectively. At shallower depths, passive wedge governs the ultimate mobilized soil reaction. At these depths, lateral bearing capacity factor is less than 9. After a certain point, which is denoted as $z_R$ and calculated by Eq. (2.34), flow-around mechanism is dominant. Lateral bearing capacity factor for flow-around mechanism is recommended as 9.




(a) (b)

Figure 2.8. (a) Flow-around and (b) passive wedge mechanisms (Fleming et al., 1985)

$$z_R = \frac{6D}{\frac{\gamma' D}{s_u} + J} \tag{2.34}$$

It should be noted that $J$ is an empirical factor between 0.25 – 0.5. American Petroleum Institute (2014) recommends $J = 0.5$ soft clays like these in Gulf of Mexico.

Normalized p-y curves for clays are presented in Table 2.11.

Table 2.11. Normalized p-y Relations Under Cyclic Loads (Matlock, 1970)

| $z > z_R$ | | $z < z_R$ | |
|---|---|---|---|
| $p/p_u$ | $y/y_c$ | $p/p_u$ | $y/y_c$ |
| 0 | 0 | 0 | 0 |
| 0.23 | 0.1 | 0.23 | 0.1 |
| 0.33 | 0.3 | 0.33 | 0.3 |
| 0.50 | 1.0 | 0.50 | 1.0 |
| 0.72 | 3.0 | 0.72 | 3.0 |
| 0.72 | ∞ | $0.72z/z_R$ | 15 |
| | | $0.72z/z_R$ | ∞ |

Values in Table 2.11 can be visualized as given in Figure 2.9, on which $z_R$ is referred to as $x_n$.

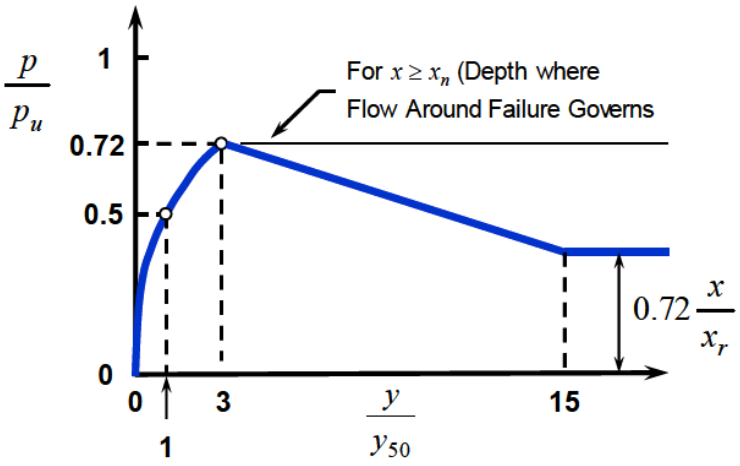



Figure 2.9. Normalized p-y Relations for Matlock (1970) (Isenhower et al., 2019)

$y_c$ (referred to as $y_{50}$ in Figure 2.9), calculated by Eq. (2.35), is referred to as the lateral deflection at which the mobilized soil reaction reaches to half of its maximum value. It should be noted that $y_c$ is a function of $\varepsilon_c$ which is defined as strain when stress is half of the maximum deviator stress in laboratory testing. Alternatively, it can be estimated by Eq. (2.36).

$$y_c = 2.5\varepsilon_c D \tag{2.35}$$

$$\varepsilon_c = \begin{cases} 0.02 & if\ s_u < 48\ kPa \\ 0.01 & if\ 48 \le s_u < 96\ kPa \\ 0.007 & if\ s_u \ge 96\ kPa \end{cases} \tag{2.36}$$

American Petroleum Institute (2014) states that this method is applicable for clays having undrained shear strength less than 100 kPa.

### 2.2.7 p-y curves for Stiff Clays without Free Water

Free water refers to water that may exist in pile-soil interface especially under submerged conditions like offshore. So, it is likely to be present in the case of pile-soil separation, also known as scour, under cyclic loads. However, as noted

in Parker et al. (2018), this situation is appropriate only for stiff clays at or near ground surface, i.e., seabed in offshore environment. Also, in a design problem, "without free water" conditions may be assumed as Gilbert et al. (2015) did, but this necessitates to ensure no significant pile-soil separation. It means scour protection would be needed.

In the case of no free water, ultimate mobilized soil reaction ($p_u$) of stiff clays ($s_u > 100\ kPa$) can be calculated as the same way as Matlock (1970). The suggested p-y curves are provided in Figure 2.10. In this method, it should be noted that $y_{50} = 2.5\varepsilon_{50}D$, also the method is applicable up to $s_u \approx 400\ kPa$ (Isenhower et al., 2019).

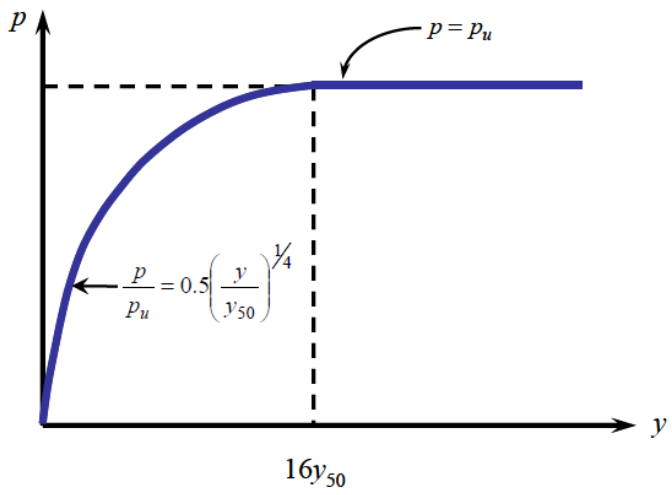



Figure 2.10. Normalized p-y Relations for Stiff Clays without Free Water (Isenhower et al., 2019)

### 2.2.8 Jeanjean et al. (2022) p-y Curves for Clays

This method is expected to be the official recommendation of American Petroleum Institute in the near future, as of February 7, 2022. In fact, Jeanjean et al. (2022) in their study entitled "The New ISO/API P-Y Curves in Clays and their Reconciliation with the PISA Framework" referred to this method as

"Draft International Standard ISO 19901-4". The proposed mathematical expressions are based on accumulated experience and observations gained from many field pile load tests performed for a long time as first mentioned in Jeanjean (2009).

This method is slightly more complicated compared to the previously presented ones and consists of two steps: p-y curves under monotonic action and under cyclic actions.

**Step 1: p-y curves under monotonic action**

In principle, ultimate soil reaction is calculated as the same way as the current methods as can be seen in Eq. (2.37).

$$p_u = N_p s_u D \tag{2.37}$$

Therefore, the difference lies in lateral bearing capacity factor ($N_p$). Also similar with the current methods, two failure mechanisms are considered: passive wedge and flow-around mechanisms. However, bearing capacity factor for flow around mechanism ($N_{pd}$) is a value between 9-12 depending on undrained shear strength of clay Eq. (2.38).

$$N_{pd} = 9 + 3\alpha_{ave} \tag{2.38}$$

In this equation, $\alpha_{ave}$ is the average adhesion factor along the monopile. On the other hand, lateral bearing capacity factor ($N_p$) is given by Eq. (2.39).

$$N_p = \begin{cases} N_{p0} + \dfrac{\gamma' z}{s_u} \leq N_{pd} \; if \; gapping \; is \; assumed \\ 2N_{p0} \leq N_{pd} \; if \; no \; gapping \; is \; assumed \end{cases} \tag{2.39}$$

Gapping conditions are quantitatively provided; however, it has been stated that gapping preference rests with the designer. If gapping is assumed, an anisotropy correction should be applied as well.

$N_{p0}$ is a model parameter given in Eq. (2.40).

$$N_{p0} = 12 - (1 - \alpha_{ave}) - 8.78\left[1 - \left(\frac{z}{dD}\right)^{0.6}\right]^{1.35} \leq N_{pd} \tag{2.40}$$

Finally, another model parameter "$d$", which is a function of pile diameter ($D$) and shear strength profile ($s_{u\,@depth\,z} = s_{u0} + s_{u1}z$), is given in Eq. (2.41).

$$d = 16.8 - 2.3\log_{10}\left(\frac{s_{u0}}{s_{u1}D}\right) \geq 14.5 \tag{2.41}$$

Please note that Eq. (2.41) enables to use the method in both constant and linearly increasing with depth shear strength profiles. For constant shear strength profiles, $s_{u1} \cong 0$ to prevent divergence of the parameter $d$.

A noteworthy difference is that Jeanjean et al. (2022) considers the effect of shear strength profile. Therefore, the ultimate mobilized soil reaction depends on undrained shear strength not only at considered depth, but also the variation within the profile. On the other hand, current recommendations focus only on the undrained shear strength at the depth under consideration.

Normalized p-y curves are provided for 6 different cases depending on plasticity index and overconsolidation ratio of the soil, therefore, normalized curves are presented as a plot for a better representation in Figure 2.11.

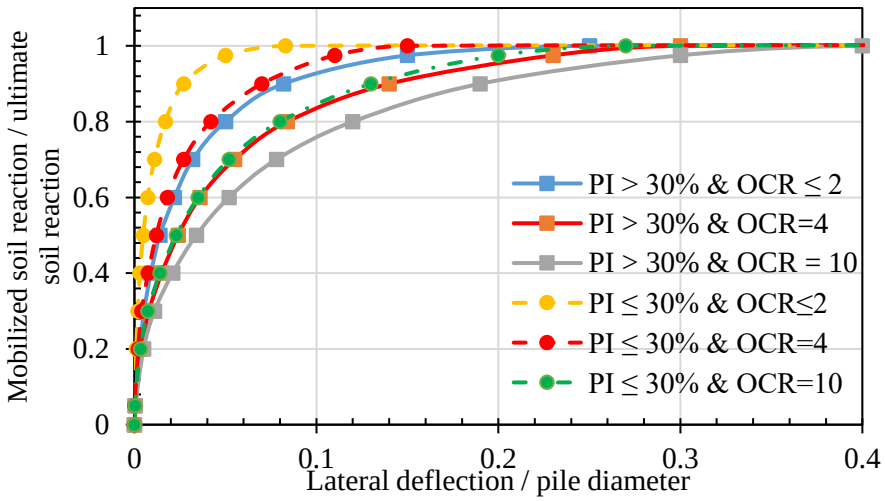



Figure 2.11. Normalized p-y Relations Under Monotonic Loads (Jeanjean et al., 2022)

**Step 2: p-y curves under cyclic actions**

In a nutshell, to obtain cyclic p-y curves under wave loads ($p_{cy}$ and $y_{cy}$) , monotonic p-y curves are modified by two modification factors ($p_{mod}$ and $y_{mod}$) for ultimate soil reaction and lateral deflection as in Eq. (2.42). These modifications apply to each point on monotonic p-y curves.

$$p_{cy} = p_{mod}\, p_{mo} \quad \& \quad y_{cy} = y_{mod}\, y_{mo} \tag{2.42}$$

Modification factors ($p_{mod}$ & $y_{mod}$) depend on the sea environment and soil behavior. So far, experiments have been conducted only on North Sea and Gulf of Mexico. The parameters are given in Table 2.12. The researchers noted that if sea conditions are dramatically different from North Sea and Gulf of Mexico, local field tests need to be performed for more accurate estimation of pile behavior.

Table 2.12. Cyclic Loading Modification Factors (Jeanjean et al., 2022)

| **Condition** | **Modification factor for mobilized soil resistance ($p_{mod}$)** | **Modification factor for lateral deflection ($y_{mod}$)** |
|---|---|---|
| Gulf of Mexico | $1.47 - 0.14\ln(N_{eq})$ | $1.2 - 0.14\ln(N_{eq})$ |
| Soft clay in North Sea | $1.63 - 0.15\ln(N_{eq})$ | $1.2 - 0.17\ln(N_{eq})$ |
| Stiff clay in North Sea | $1.45 - 0.17\ln(N_{eq})$ | $1.2 - 0.17\ln(N_{eq})$ |

The term $N_{eq}$ is referred as "equivalent number of cycles" and it could be a real number between 1 and 25. Calculation of $N_{eq}$ is given in Eq. (2.43).

$$N_{eq} = \left(\frac{2}{1 - h_f}\right)^g \tag{2.43}$$

In this equation, $g$ and $h_f$ are model parameters. Recommended $g$ values are

- $g = 1.0$ for Gulf of Mexico
- $g = 1.25$ for soft clay in North Sea
- $g = 2.5$ for stiff clay in North Sea

The other model parameter, $h_f$ is also known as hybrid factor and calculated by Eq. (2.44). Note that $-1 \leq h_f \leq 1$.

$$h_f = \begin{cases} \frac{p_{mo}}{p_u} - \left(\frac{z}{z_{rot}}\right)^2 & if\ z \leq z_{rot} \\ \frac{p_{mo}}{p_u} - 1 & if\ z > z_{rot} \end{cases} \tag{2.44}$$

The final parameter is the depth of center of rotation under monotonic actions ($z_{rot}$). Therefore, a prior analysis under monotonic loads is required to produce cyclic p-y curves.

## 2.3 Offshore Soil Conditions in Marmara Sea

In this section, a selection of existing studies in the literature regarding the soil types and properties of Marmara Sea are summarized. Detailed geotechnical site investigation studies are not available in the literature although there is an abundance of geophysical studies.

Among the geophysical studies, Ergin et al. (1999) reported ~10 m thick fine-grained deposit which is underlain by coarser-grained deposits in Bandırma Bay, Southern Marmara Sea. Vardar & Alpar (2016) also studied the same area, and presented the soil types at seabed level based on texture (Figure 2.12).

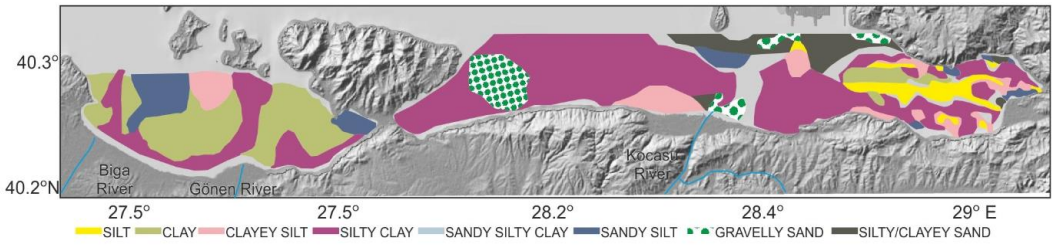
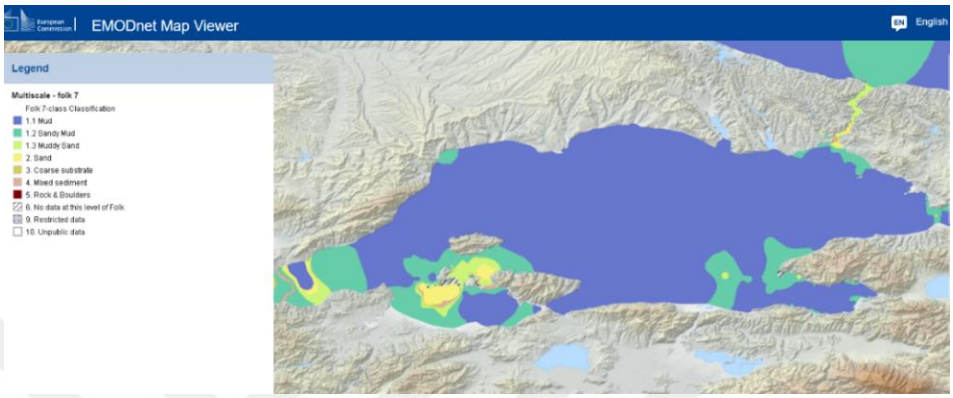



Figure 2.12. Seabed Soil Textures in Southern Marmara Sea (Vardar & Alpar, 2016)

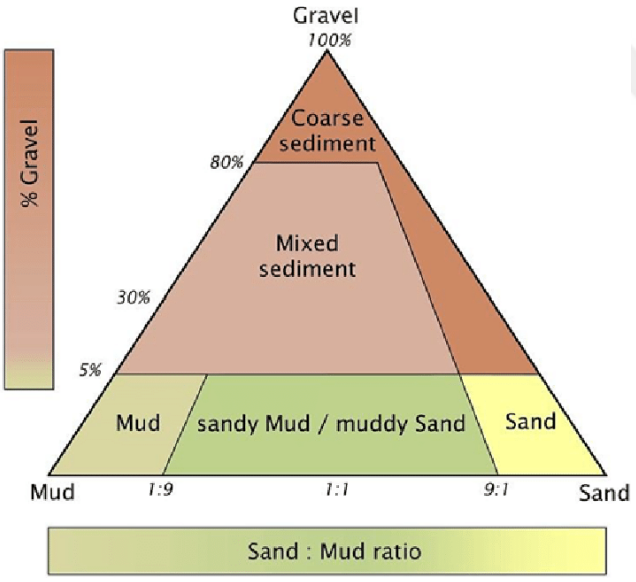
Figure 2.12 reveals that the dominant seabed soil type is silty clay in Bandırma Bay, which is in line with findings of Ergin et al. (1999). On the other hand, seabed soil at Gemlik Bay (eastern end at Figure 2.12) is more variable.

The EMODnet Geology (2021) presents marine geological data using Folk's sediment triangle with 16, 7 and 5 substrate classes. The data describes the seabed substrate from the uppermost 30 cm of the sediment column and the data has been generalized into a target scale of 1:1000000. The data therefore gives an overview of the marine regions, and it is not suitable for local/detail scale analysis

Figure 2.13 (a) demonstrates that the seabed sediments near the surface is dominantly "mud" according to Folk-7 classification (Figure 2.13 (b)) which indicates fine-grained soils, and in some areas, there are "sandy mud", "muddy sand" and "sand".




(a)




(b)

Figure 2.13. (a) Seabed sediments (upper 30 cm soil) in Marmara Sea according to Folk-7 sediment classification (EMODnet, 2021) (b) Folk-7 sediment classification (Guinan et al. 2021)

For geotechnical engineering purposes, Yilmaz & Üstünkaya (2004) studied Gemlik Bay at the eastern end of Marmara Sea. They performed 13 Standard Penetration Tests nearshore where water depth has a maximum value of ~20 m. They constructed three cross-sections, which are given in Figure 2.14.

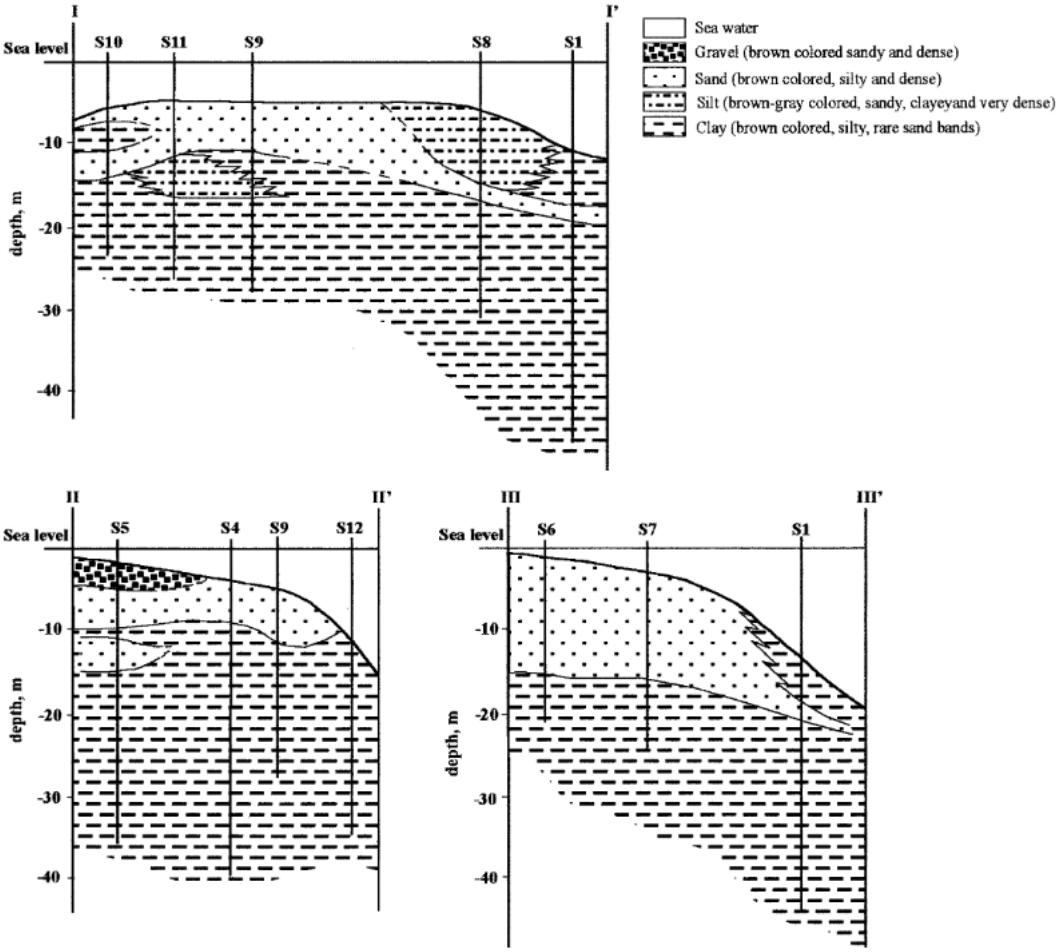



Figure 2.14. Soil Profile Cross-Sections in Gemlik Bay (Yilmaz & Üstünkaya, 2004)

From Figure 2.14, deep clay layers can be clearly observed. At shallow waters, these layers are overlain by sand layers along with occasional gravel layers. These coarse-grained layers tend to become thinner as water depth increases.

Researchers further studied the geotechnical properties of existing clay. They found that clay layers mostly have low plasticity with an average plasticity index of 19% and liquid limit of 38.7%. Yet, average water content was found as 40.1%, which is higher than liquid limit. Furthermore, average overconsolidation ratio and undrained shear strength values were reported as 0.53 ∓ 0.08 and 23.8 ∓ 3.7 kPa, respectively. As a result, deep clay layers in Gemlik Bay are found to be soft unconsolidated deposits. However, no experiments on remolded samples were conducted to study possible sensitivity of soft clay.

Another geotechnical study has been conducted by Oguz & Huvaj (2020) in İzmit Bay, at Northeastern Marmara Sea. Their database includes 65 Cone Penetration Tests with water depth ranging between 1.5 – 64.2 m (45 of the CPT's were in water depths greater than 10 m). The deepest test extends until 200 m below sea level. They detected multi-layer profiles as shown in Figure 2.15. In this figure, "Zones" refer to the classification system suggested by Robertson & Cabal (2012). Furthermore, they noted that the seabed soils in the study area are not uniform with depth, they are composed of interlayers of "clays" (silty clay, clayey silt, clay) and "sands" (clean sand, silty sand, sandy silt, gravelly sand) with varying thicknesses.

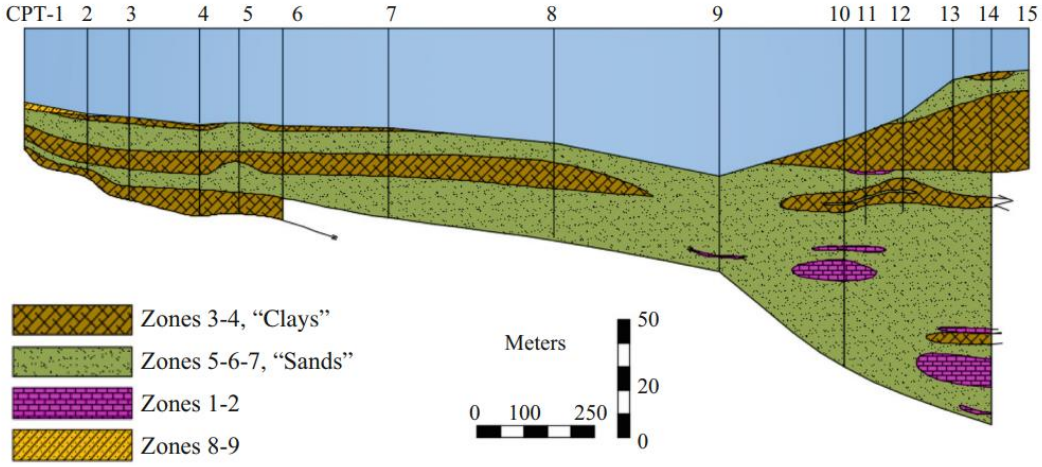



Figure 2.15. Soil Profile Cross-Section in İzmit Bay (Oguz & Huvaj, 2020)

As can be noticed from Figure 2.15, soil profile mostly consists of alternating clayey and sandy layers with only CPT-9 detecting mostly sand. Occasionally, sensitive clays are observed in the vicinity of CPT-10.

Regarding the geotechnical parameters of clay, most are classified as high-plasticity clay. Out of 174 Atterberg limit test samples, 166 samples were classified as clay (71% CH and 25% CL) according to the Unified Soil Classification System. Undrained shear strength at seabed is reported as 37 – 55 kPa. Increase of this value with depth is estimated as 0.73 – 2.46 kPa/m (based on laboratory test data such as in Figure 2.16, for water depths greater than 10 m). For "sands" at both nearshore (less than 10 m water depth) and offshore (greater than 10 m water depth) seem to have similar relative density, values that are generally less than 50% (i.e., sands are in loose to medium-dense state). Finally, they reported very low spatial correlation length values, which imply highly variable soil parameters within small distances.

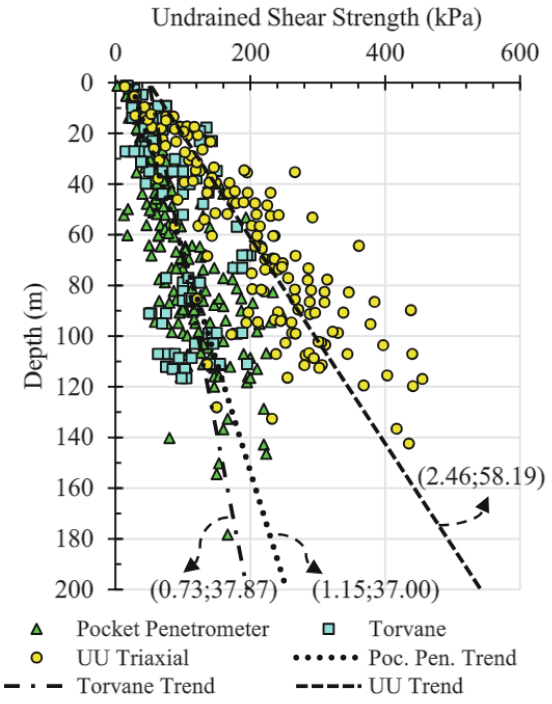



Figure 2.16. Undrained shear strength with depth for investigations in water depths greater than 10 m (values in parentheses are: rate of increase of undrained shear strength with depth (kPa/m); standard deviation in kPa) (Oğuz and Huvaj, 2020)

# CHAPTER 3

# OFFSHORE WIND POWER PLANT SITE SELECTION

This chapter presents offshore wind power plant site selection in detail. First, the workflow is presented in Section 3.1. Then, Section 3.2 explains why the study concentrates to Marmara Region. Section 3.3 summarizes the site selection criteria used in this thesis, which is followed by alternative sites (Section 3.4) satisfying the criteria set in Section 3.3. Finally, Section 3.5 includes the results and the discussion on site selection.

The reader should keep in mind that this chapter does not intend to investigate suitable sites for monopiles only.

## 3.1 Workflow of Site Selection Study

The general workflow is given in next page in Figure 3.1.

First, the study area has been determined based on three preliminary indicators, which are explained in Section 3.2.

Second, literature review, already presented in Section 2.2, has been done. As a result of this review, site selection criteria have been decided, and categorized as decision and exclusion criteria along with setting buffer zones and suitability limits. Then, open-source GIS data has been found for the decided site selection criteria. The selected criteria and data sources are given in Section 3.4.

The next step is to analyze the obtained data in accordance with set buffer zones and suitability limits to identify suitable areas, referred as “alternative sites”, introduced in Section 3.4. ArcGIS Pro software has been used in this step. Then, GIS data has been utilized for pairwise comparison of selected alternative sites.

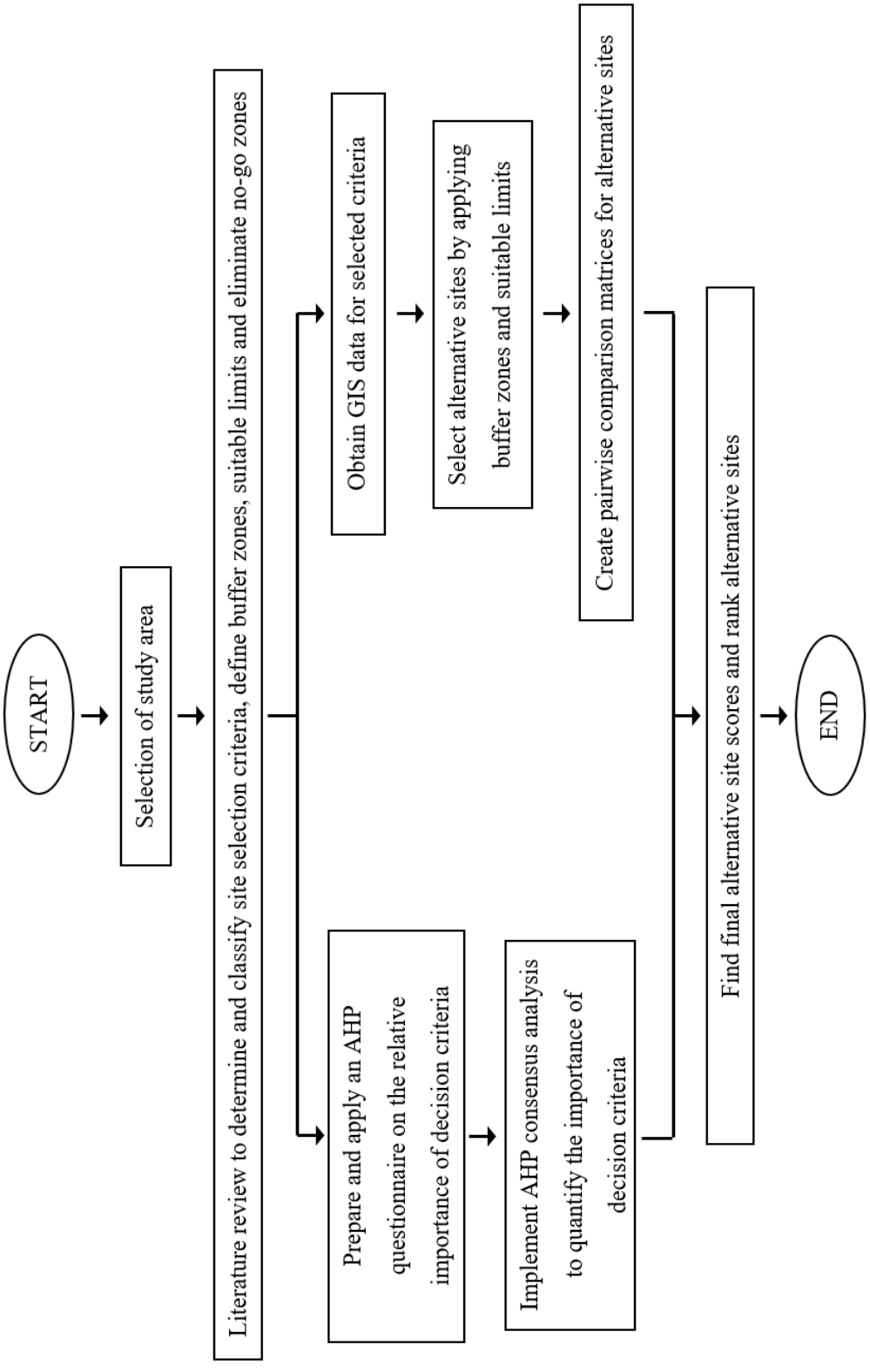



Figure 3.1. Workflow of Site Selection Study

Meanwhile, a questionnaire to consult expert opinions on relative importance of decision criteria has been prepared. It should be noted that pairwise comparisons of decision criteria have been done by experts via this questionnaire, yet the alternative sites are compared pairwise by the author. The questionnaire, which is given in Appendix A, has been answered by 11 experts. Among them, 8 answers have been found to be consistent in accordance with AHP consistency measures (Section 2.1.3 gives details on consistency). The participants are from Türkiye, Denmark, Japan and Portugal. This diversity aims to put together the experience of countries with existing OWPPs with local concerns for Türkiye. Furthermore, experts have different backgrounds, which is believed to reflect the multidisciplinary nature of OWPP site selection. The selected occupations are civil engineer, electrical engineer, biologist, offshore wind project manager and renewable energy project manager.

The next step is to apply consensus analysis to the abovementioned 8 consistent expert opinions. More details are given in Section 2.1.3.1 on the methodology of consensus analysis. After consensus analysis, relative importance values for decision criteria have been quantified. At the end, relative weights of decision criteria and pairwise comparisons of alternative sites have been combined to find the final scores and rank the alternative sites.

## 3.2 Study Area

This study focuses on Marmara Region, one of the seven geographical regions of Türkiye. This preselection eases the site selection process by simplifying GIS data acquisition. The exact frame of the study area is given in Figure 3.2. The study area covers the whole Marmara Sea along with Western Black Sea and Northern Aegean Sea.

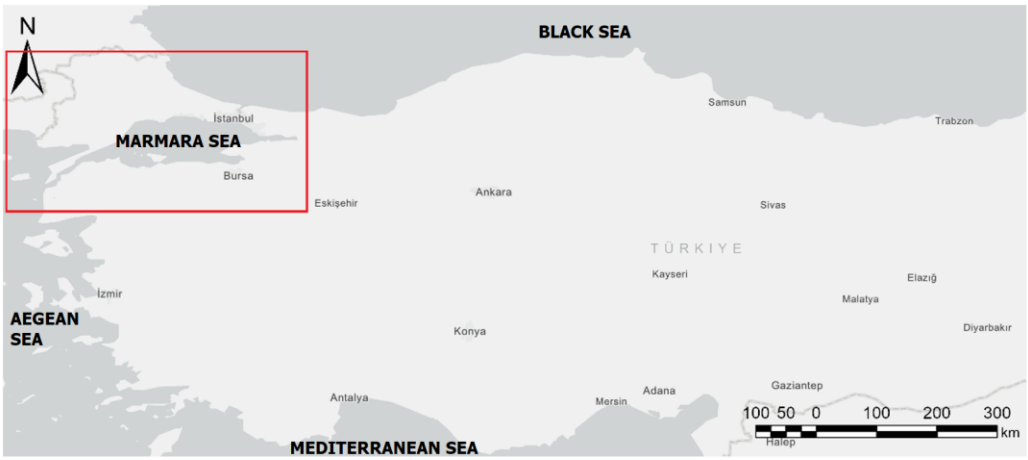



Figure 3.2. Study Area of the Thesis

The preselection of Marmara Region is based on offshore wind speed, population and energy self-sufficiency of the region.

- **Offshore wind speed:** Examining the open-source average annual wind speed data such as Global Wind Atlas, it can be seen that Marmara Region has higher wind speeds compared to the other parts of the country (Figure 3.3).




Figure 3.3. Average Annual Offshore Wind Speed Map of Türkiye at 100 m Height (Modified from Global Wind Atlas (n.d.) by Caceoğlu et al., 2022)

- **Population:** Marmara Region is the most crowded region of Türkiye by far with a population of about 25 million (Ministry of Interior, 2021) corresponding to 30% of the country. Therefore, a potential offshore wind power plant provides the opportunity to serve a significant population.
- **Energy self-sufficiency of the region:** Despite having the highest electricity consumption, energy production in Marmara Region is the lower than its consumption (Enerji Atlası, 2022).This results in the need to transmit electricity for long distances produced in other regions. Although Türkiye has a single electricity grid system, about 12% of electricity is lost during transmission for long distances (TEİAŞ, 2022).

## 3.3 Site Selection Criteria in This Study

In this section, determined site selection criteria are presented separately for decision and exclusion criteria. All criteria are selected based on the literature review presented in Section 2.1. Although a brief discussion is provided each criterion, Caceoğlu et al. (2022) includes a more detailed discussion.

### 3.3.1 Decision Criteria

Decision criteria are the ones that have been evaluated in the questionnaire and obtained relative weights have been used in ranking of alternative sites. Table 3.1 provides information on selected decision criteria, suitable limits (if any) and open-source data obtained to be utilized in ArcGIS Pro.

Table 3.1. Summary of Decision Criteria

| **Criterion** | **Suitable limits** | **Data Source in GIS** |
|---|---|---|
| Average annual offshore wind speed at 100 m | ≥ 6.5 m/s | Global Wind Atlas (n.d.) |
| Commercial fishery | Dense areas excluded | Global Fishing Watch (2021) |
| Distance to shipping routes | ≥ 1 km from densely used corridors | EMODnet Human Activities (2019) |
| Distance to existing large ports | All | Data added manually |
| Social acceptance | ≥ 1.5 km from the coastline | No GIS data |
| Water depth | ≤ 100 m | GEBCO (2021) |
| Earthquake hazard | ≥ 2 km from earthquake fault lines | **Fault line locations:** MTA (2013) SHARE Project (2021) |
| Distance to bird migration routes | ≥ 1 km | Birdmap (2021) |
| Distance to Key Biodiversity Areas | ≥ 1 km | Key Biodiversity Areas (KBA) Partnership (2021) |
| Length of onshore and offshore cables | 380-400 kV cable lines needed | Open Street Map (2021) |

Next, these criteria have been organized in a “hierarchy”. Note that there is a total of 11 criteria listed in Table 3.1. It would require 55 pairwise comparisons, which would make more difficult for experts to produce consistent answers. This is why commercial fishery and distance to shipping routes are considered as subcriteria of a main criterion called “offshore human activities”. Similarly, distance to bid migration routes and distance to Key Biodiversity Areas are

grouped as “environmental concerns”. Finally, lengths of onshore and offshore cables are considered as separate subcriteria of “electricity grid connection” as onshore and offshore cables do not have the same cost. Figure 3.5 visualizes the final hierarchy of decision criteria. In the final proposed hierarchy, there are 8 main decision criteria. It results in a total 28 pairwise comparisons, which is halved down compared to 11 decision criteria. On the other hand, 3 main criteria have 2 subcriteria each, which adds up 3 more pairwise comparisons. As a result, experts have been asked to make 31 pairwise comparisons.

In the next paragraphs, the data that is used in ArcGIS Pro is presented. Each figure includes one decision criteria followed by a discussion and observations related to this criterion.

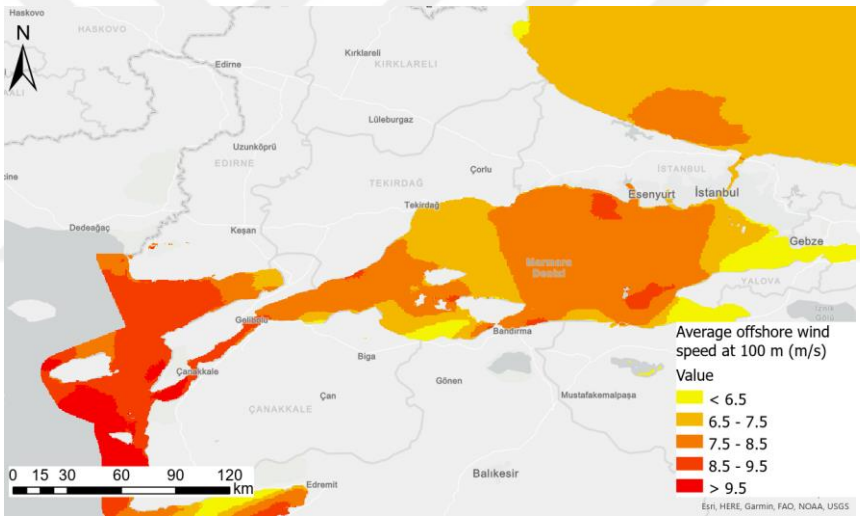



Figure 3.4. Average Annual Wind Speed at 100 m at the Study Area

High wind speed is obviously critical for any wind energy project to maximize enegy production and profit. Section 3.2 already showed that Northwest Türkiye has the highest wind speed in Türkiye. As seen from Figure 3.4, Çanakkale Province, where average wind speeds exceed 9.5 m/s, has the highest wind speeds in the study area. On the other hand, most of the Black Sea coasts in the study area have wind speeds between 6.5 – 7 m/s.

Figure 3.5. Hierarchy of Decision Criteria in This Study

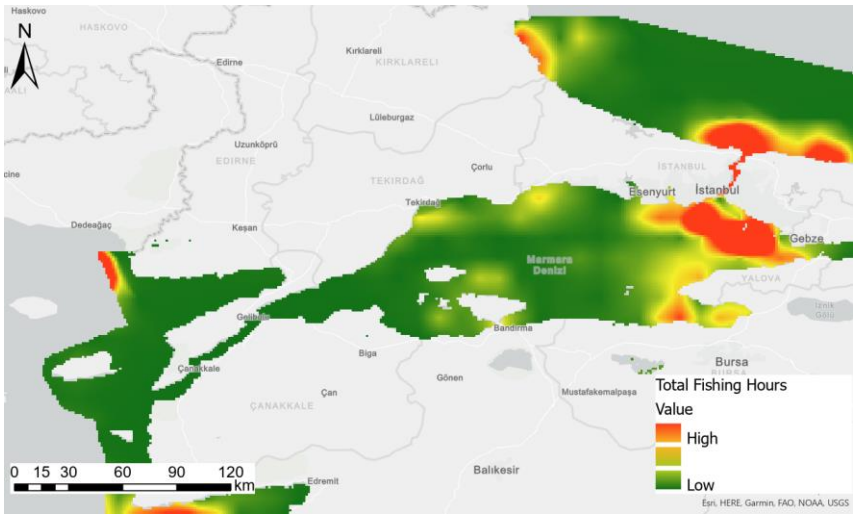



Figure 3.6. Commercial Fishery at The Study Area

Fishery is a traditionally important source of income for most coastal communities. Fishery areas may be reduced by OWPPs, therefore dense fishery areas should be defined during preliminary site selection, and ideally an OWPP should be far enough from these areas to prevent any conflicts. Figure 3.6 includes data for 2012 – 2016. Commercial fishery does not seem to be a major concern for the area except for Kırklareli coasts, Bosphorus Strait and Gemlik bay.

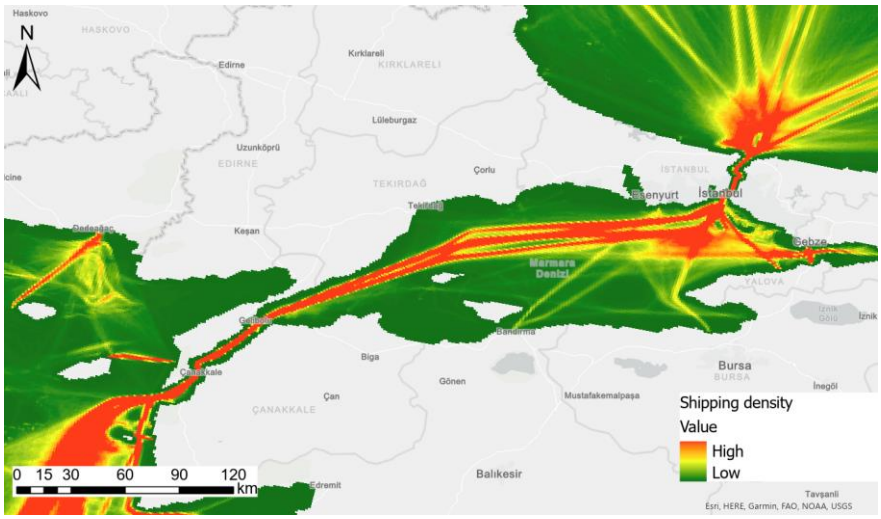



Figure 3.7. Shipping Routes at The Study Area

Dense shipping routes should be defined as ships pose collision risk with offshore wind turbines. Also, radar systems of ships may be affected by wind turbines. As observed from Figure 3.7, Bosphorus and Dardanelles Straits form the busiest international shipping routes. Their approach and connection routes are busy shipping routes as well. This may be a problem for Çanakkale Province where the wind speeds are the highest.

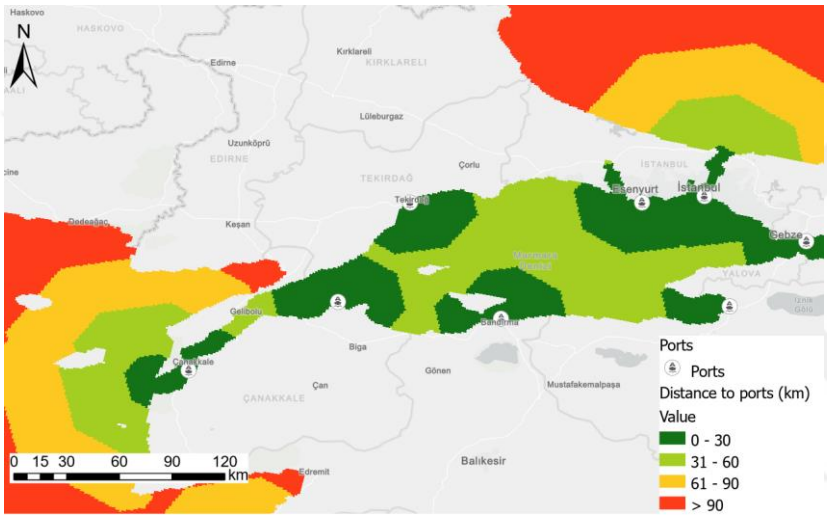
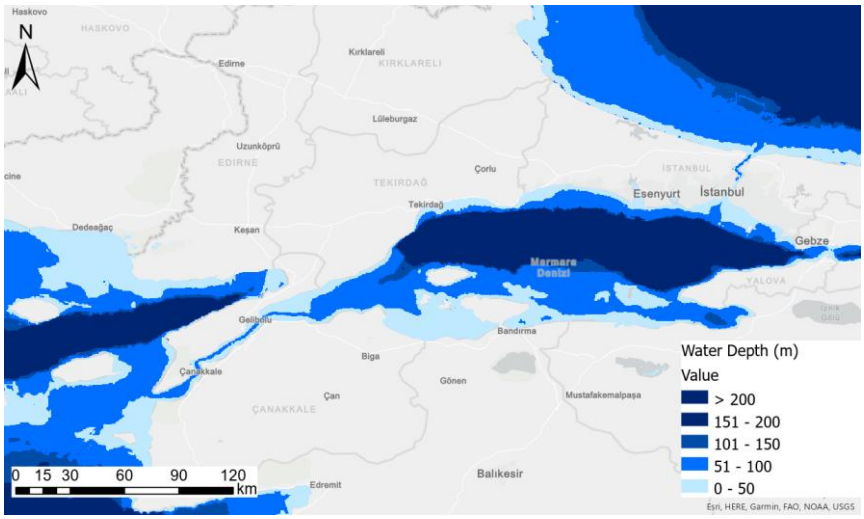
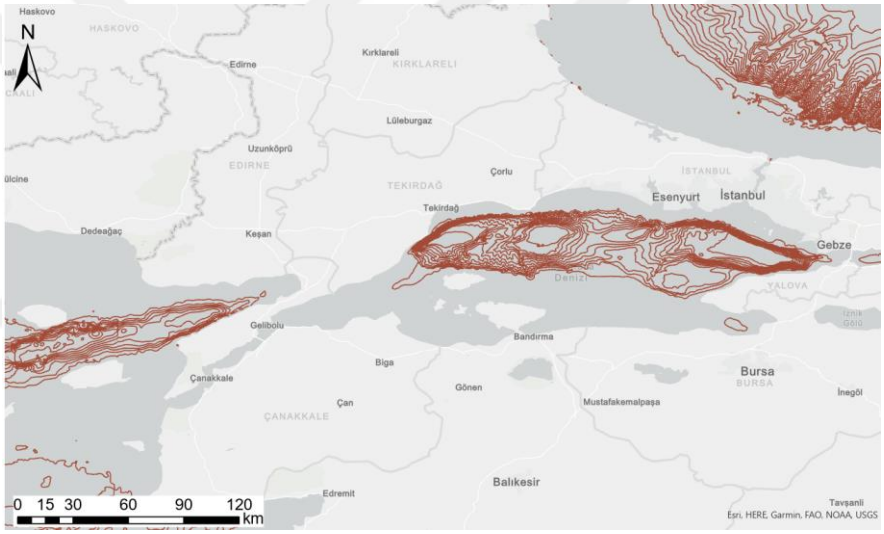



Figure 3.8. Existing Ports and Distance to Ports at the Study Area

Specialized port facilities are required for construction, operation, maintenance and decommissioning of OWPPs. Existing large ports are considered in this study. In most of the study area, there is an existing large port closer than 90 km. However, the most prominent exception is the shores of Kırklareli Province (Figure 3.8). In this thesis, it is assumed that port authorities would apply necessary upgrades to manage the specialized needs of offshore wind industry.




(a)




(b)

Figure 3.9. (a) Water Depth (b) Bathymetry Contours (Shown with Red) with 100 m Intervals at the Study Area

Water depth directly affects the foundation design including the foundation type, therefore the cost is directly affected by water depth. Figure 3.9 (a) clearly shows water depth quickly reaches to 50 m in most of the study area, which may limit the applicability of fixed-bottom foundations. In this thesis, maximum water depth is limited to 100 m as seabed slope is observed to be too high after this depth (Figure 3.9). It is not desirable to construct OWPPs on

high seabed slope regions because this may induce risks to cables and turbines via various geohazards such as earthquake induced submarine landslides.

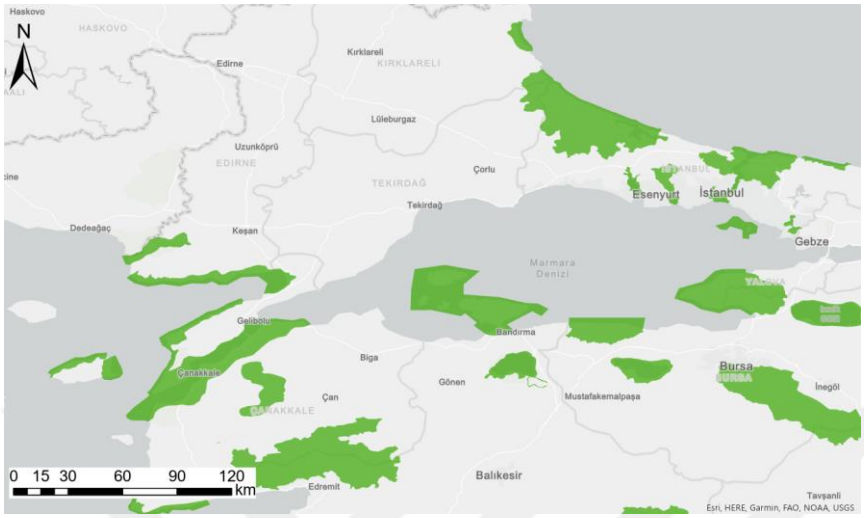



Figure 3.10. Key Biodiversity Areas (KBAs) at the Study Area

As KBAs are valuable areas for global biodiversity, effect of an OWPP should be minimized on a KBA (Figure 3.10). In the absence of detailed observations, distance may be regarded as a sufficient preliminary indicator. However, Environmental Impact Assessment is a crucial step in OWPP deployment.

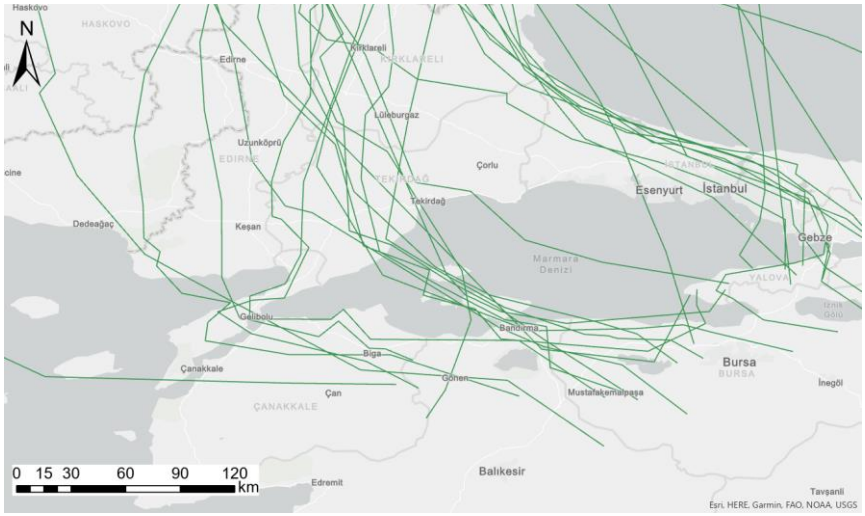



Figure 3.11. Bird Migration Routes at the Study Area

Arguably, birds are one of the most affected species from wind turbines due to collision risk. As a result, it is preferable to maximize the distance between OWPPs and bird migration routes. However, Marmara Region is located on a dense network of bird migration routes (Figure 3.11). Also, it should be noted that detected routes do not represent each individual bird as it is not possible to place a GPS on each bird, but they give a precious idea on the general behavior.

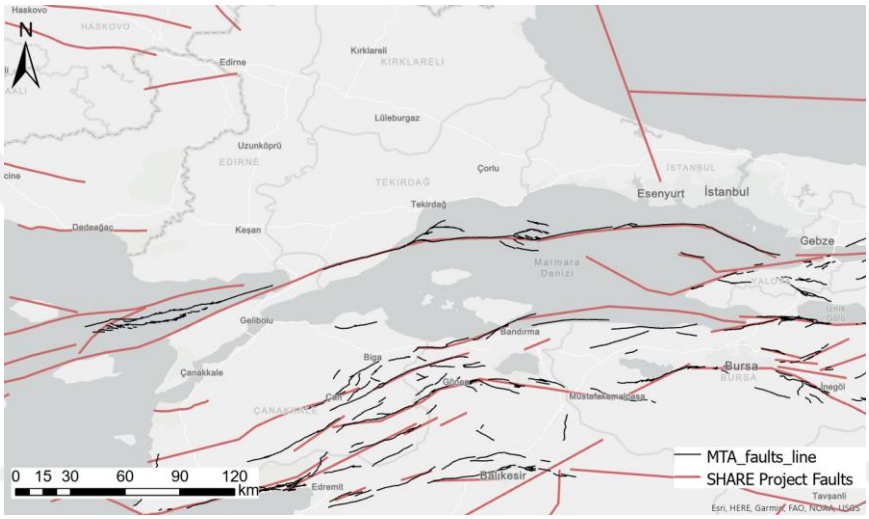



Figure 3.12. Earthquake Fault Lines at the Study Area

Offshore wind turbines may fail or lose their serviceability as a result of large earthquakes. Other seismic hazards include submarine landslides and soil liquefaction. As Marmara Region is a high earthquake hazard area due to numerous fault lines such as North Anatolian Fault, seismic loads must be considered in the final design stage. On the other hand, higher distance from fault lines typically results in lower PGA, which eases the seismic design. This is why alternative sites farther to fault lines are assigned higher desirability for site selection purposes.

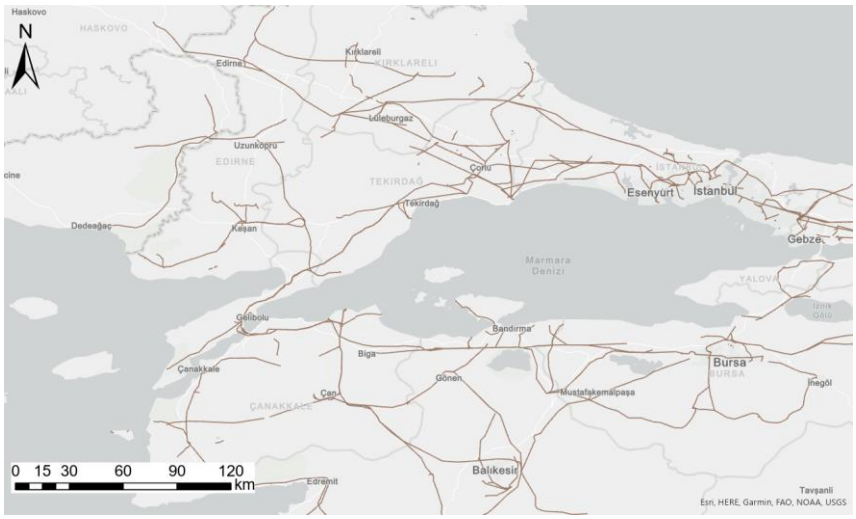



Figure 3.13. High Voltage Electricity Cable Lines at the Study Area

Any produced electricity needs to be connected to a grid system. Since OWPPs typically produce massive amounts of energy (in the order of GW nowadays), high voltage cables must be identified. Please note that grid connection is a completely different study area. Still, being closer to an existing high voltage cable reduces the cable cost and transmission losses. Furthermore, it may eliminate need for an offshore substation, which is expensive to build. As a rule of thumb, installation and maintenance of offshore cables cost more than onshore counterparts. Marmara Region has a widespread network of high voltage cables as it consumes the most electricity in the country (Figure 3.13).

### 3.3.2 Exclusion Criteria

Exclusion criteria immediately result some areas to be defined as unsuitable, also known as no-go zones. Therefore, exclusion criteria do not need to be compared pairwise. In this study, there are 4 exclusion criteria, which are given in Table 3.2.

Table 3.2. Summary of Exclusion Criteria

| **Criterion** | **Buffer zone** | **Data Source in GIS** |
|---|---|---|
| Distance to civil aviation devices/airports | ≥ 2-15 km (depending on type of device) | Republic of Türkiye Energy Market Regulatory Authority (2017) |
| Shipwrecks | ≥ 1 km | EMODnet Human Activities (2021) |
| Subsea communication cables | ≥ 750 m | TeleGeography (2022) |
| Subsea pipelines | ≥ 750 m | TurkStream (2017) |
| Military areas | - | Turkish Naval Forces Office of Navigation Hydrography and Oceanography (2021) |

As in Section 3.3.1, the next paragraphs discuss the selected exclusion criteria.

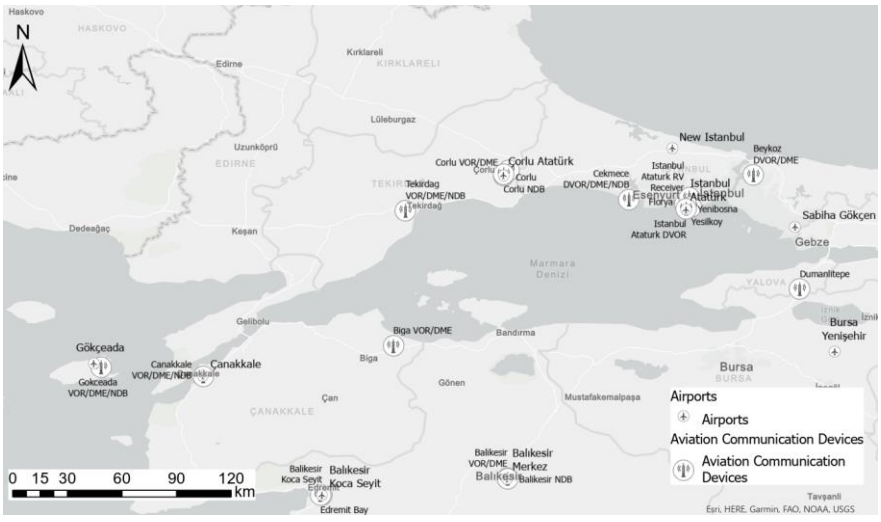



Figure 3.14. Airports and Aviation Communication Devices at the Study Area

Civil aviation industry has concerns over OWPPs due to collision risk and possible effects on communication systems. This is why it needs to be ensured that an OWPP would have the minimum effect on civil aviation industry. This may be achieved by selecting the site far enough from airports and crucial communication devices. Energy Market Regulatory Authority has set this value as 2-15 km depending on the device type. Hosting the most crowded airports in Türkiye such as New Istanbul Airport and Sabiha Gökçen Airport (Figure 3.14), OWPPs should be carefully located in Marmara Region.

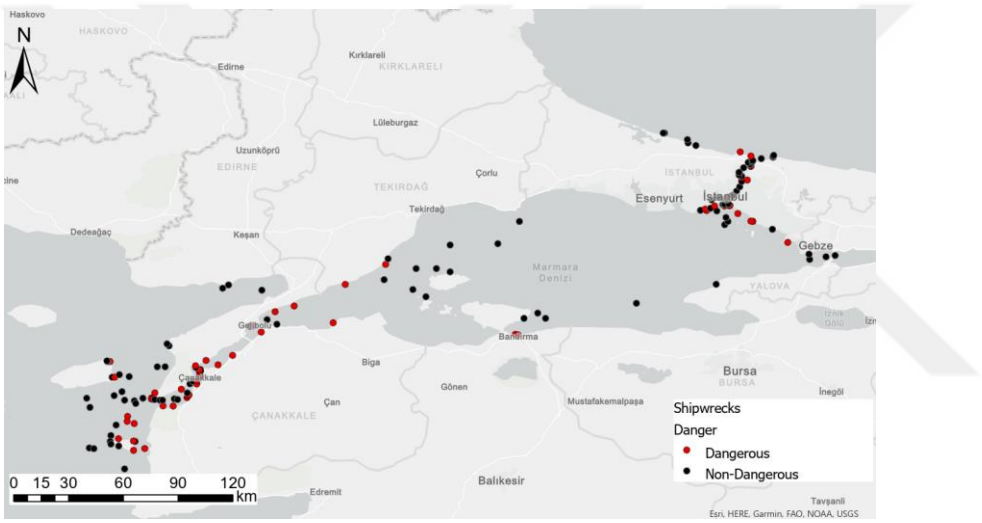



Figure 3.15. Shipwrecks at the Study Area

Shipwrecks may be dangerous as they may carry unexploded objects such as bombs. As a result, a small buffer zone may be necessary to ensure safety. In Türkiye, most of the dangerous shipwrecks concentrate in Dardanelles and Bosphorus straits (Figure 3.15), which are probably remnants from World War I.

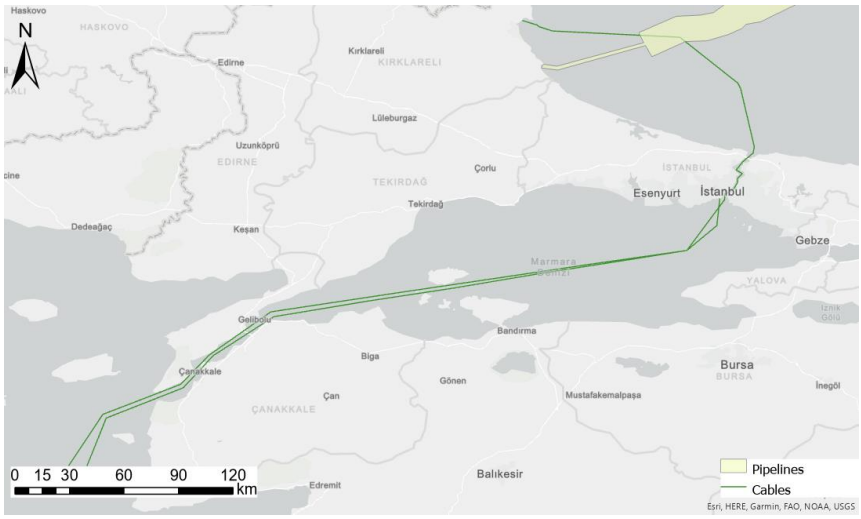



Figure 3.16. Existing Subsea Communication Cables and Natural Gas Pipelines at the Study Area

Existing subsea communication cables are important infrastructure components. Hence, a buffer zone between them and OWPPs are required to prevent possible interaction which may be caused by various reasons such as construction works, foundations and anchors of ships. In the study area, undersea communication cables exist cover a considerable length in Marmara Sea and Western Black Sea (Figure 3.16).

The potential risks between OWPPs and existing subsea pipelines are similar with the ones between communication cables. As a result, a buffer zone is needed for pipelines as well. In Marmara Region, the most important subsea natural gas pipeline by far is TurkStream (visualized in Figure 3.16), which connects Russia and Türkiye beneath the Black Sea.

Finally, military training and forbidden zones are excluded, which are not presented here for confidentiality.

## 3.4 Alternative Sites

In this section, selected alternative sites are given and grouped. After applying suitable limits in Table 3.1 and buffer zones in Table 3.2, total of 12 sites are found to be suitable in the study area (Figure 3.17). Note that this figure also illustrates all unsuitable areas with blue color except for military areas, water depth and wind speed. Bird migration routes, earthquake fault lines and water depth are found to be significant restrictions.

Suitable areas are grouped into 5 regions which is based on their geographical proximity: Bozcaada, Gökçeada, Karabiga, Bandırma and Kıyıköy. All assessments done after this point consider these 5 regions (hereafter referred as "alternative sites") instead of 12 to reduce the number of pairwise comparisons. Please remember that all alternative sites are suitable sites for OWPP installations, the remaining calculations aim to outrank the already suitable sites.

Then, Table 3.3 summarizes the properties of the alternative sites, which are measured via ArcGIS Pro. This table is important in the sense that it forms the basis of comparisons given in Section 3.5.2.

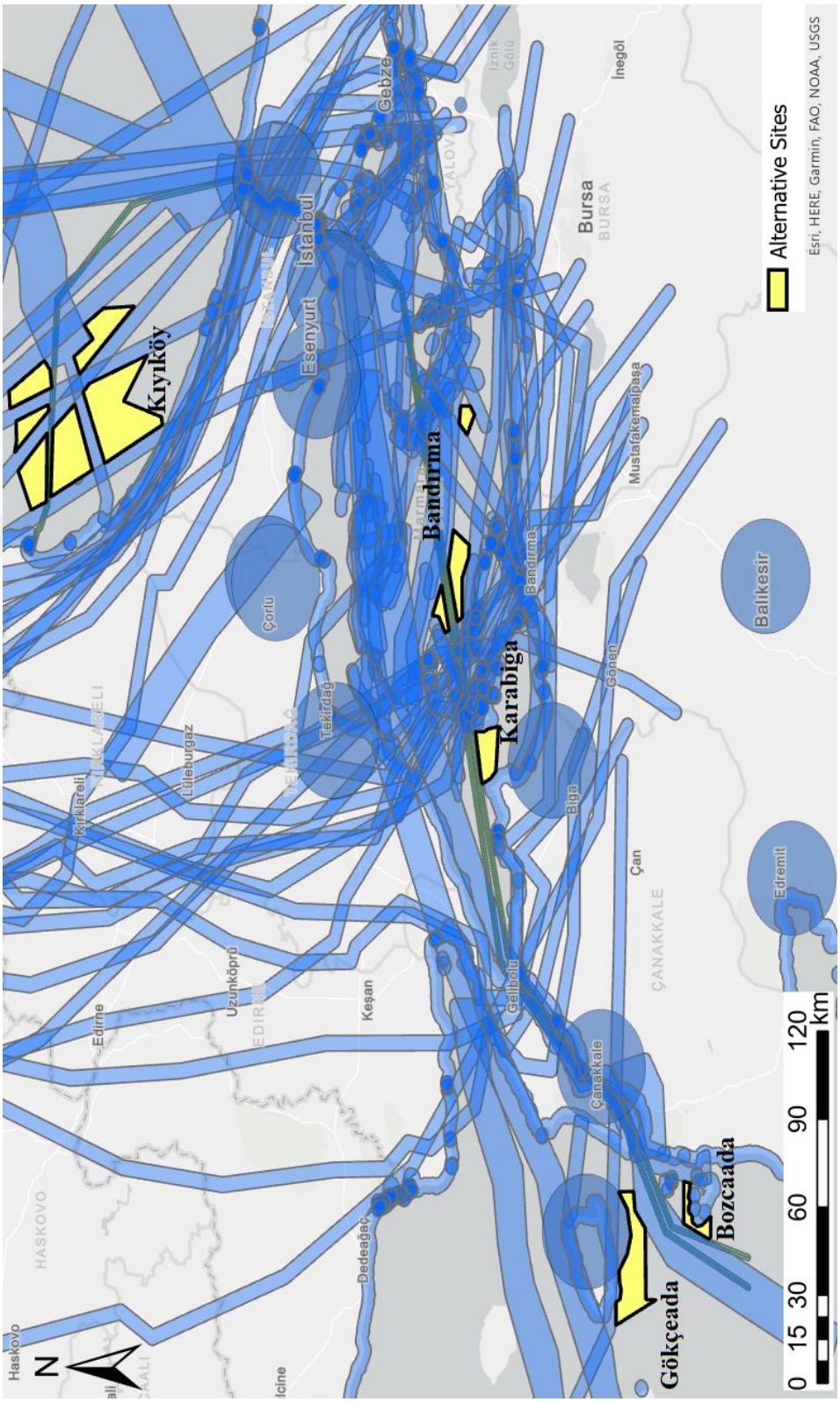



Figure 3.17. Alternative Sites (indicated with yellow)

Table 3.3. Main Properties of 5 Alternative Sites

| Sites | Bozcaada | Gökçeada | Karabiga | Bandırma | Kıyıköy |
|---|---|---|---|---|---|
| Average annual offshore wind speed at 100 m height (m/s) | 8.95 – 9.50 | 8.34 – 9.42 | 6.87 – 7.20 | 7.10 – 7.95 | 6.64 – 6.95 |
| Commercial activity | No | No | Low to medium | Low to medium | Highest |
| Minimum distance to shipping routes (km) | 1.5 (to dense routes) | 2 (to dense routes) | 9 (to dense routes) | 1 (to moderately used routes) | 2 (to lightly used routes) |
| Distance to a large port (km) | 40 | 28 | 3 | 25 | 103 |
| Distance to the nearest large settlement (km) | 3.5 | 10 | 5 | 12 | 16 |
| Distance to bird migration routes (km) | 15 (only one route) | 2 (only one route) | 5 (multiple routes) | 5 (multiple routes) | 1 (multiple routes) |
| Water depth (m) | 8 – 37 | 71 – 81 | 47 – 64 | 46 – 92 | 55 – 90 |
| Distance to active earthquake fault lines (km) | 17 | 9 | 8 | 3 | > 50 |
| Required offshore cable length (km) | ~12 | ~110 | ~32 | ~60-100 | 32 |
| Required onshore cable length (km) | 90 | 6.25 | 25 | 25 | 40 |

Some of the data such as commercial fishery is evaluated as qualitative data. It is considered that qualitative data would provide sufficient basis for such pairwise comparisons. It is to be noted that required offshore and onshore cable length values are calculated considering opinions of experts from TEİAŞ, which are confidential.

## 3.5 Results and Discussion of Site Selection

This section includes the "Relative Weights of Decision Criteria" (Section 3.5.1), "Alternative Site Scores" (Section 3.5.2) and concludes the site selection study in the last subsection (Section 3.5.3), which is "Final Alternative Site Scores and Discussion".

### 3.5.1 Relative Weights of Decision Criteria

Individual answers to the questionnaire cannot be presented here due to ethical considerations. Experts have been said that their answers will be kept confidential by the author. Among the 11 participants, 8 individual answers have been consistent in accordance with Eqs. (2.1) – (2.3).

Table 3.4 gives the first candidate group PCM, which is obtained by applying Eq. (2.1) to 8 consistent individual PCMs. This PCM is the used input in the first iteration.

Table 3.4. First Candidate Group PCM

| | **WND** | **HUM** | **PRT** | **SOC** | **WD** | **EQH** | **ENV** | **EGC** |
|---|---|---|---|---|---|---|---|---|
| **WND** | 1.00 | 3.27 | 3.03 | 2.83 | 1.36 | 1.27 | 0.98 | 0.72 |
| **HUM** | 0.31 | 1.00 | 0.86 | 1.05 | 0.31 | 0.28 | 0.41 | 0.23 |
| **PRT** | 0.33 | 1.16 | 1.00 | 2.36 | 0.36 | 0.29 | 0.46 | 0.24 |
| **SOC** | 0.35 | 0.95 | 0.42 | 1.00 | 0.20 | 0.21 | 0.32 | 0.20 |
| **WD** | 0.74 | 3.26 | 2.81 | 5.12 | 1.00 | 1.16 | 0.90 | 0.54 |
| **EQH** | 0.79 | 3.57 | 3.50 | 4.76 | 0.86 | 1.00 | 0.96 | 0.60 |
| **ENV** | 1.02 | 2.45 | 2.18 | 3.15 | 1.11 | 1.04 | 1.00 | 0.81 |
| **EGC** | 1.38 | 4.26 | 4.23 | 4.98 | 1.86 | 1.67 | 1.23 | 1.00 |

From Table 3.4, it can be observed that diagonal elements are equal to 1, and the condition of $a_{ij} = 1/a_{ji}$ is satisfied. Please remember that these observations were made in Section 2.1.3.1, and they can be deemed significant checkpoints. This first candidate group PCM is then fed into the consensus analysis, which is the Step 3 introduced in Section 2.1.3.1.

In Iteration 12, the consensus has been reached as standard deviation is smaller than the set threshold of 0.01. The final group PCM, which is given in Table 3.5, is obtained in this iteration.

Table 3.5. Final Group PCM

| | **WND** | **HUM** | **PR** | **SOC** | **WD** | **EQH** | **ENV** | **EGC** |
|---|---|---|---|---|---|---|---|---|
| **WND** | 1.00 | 3.44 | 3.09 | 2.93 | 1.46 | 1.45 | 0.93 | 0.69 |
| **HUM** | 0.29 | 1.00 | 0.85 | 1.03 | 0.29 | 0.28 | 0.33 | 0.22 |
| **PRT** | 0.32 | 1.17 | 1.00 | 2.44 | 0.34 | 0.29 | 0.37 | 0.22 |
| **SOC** | 0.34 | 0.97 | 0.41 | 1.00 | 0.19 | 0.22 | 0.28 | 0.19 |
| **WD** | 0.68 | 3.40 | 2.97 | 5.17 | 1.00 | 1.28 | 0.78 | 0.50 |
| **EQH** | 0.69 | 3.53 | 3.48 | 4.65 | 0.78 | 1.00 | 0.80 | 0.51 |
| **ENV** | 1.07 | 3.02 | 2.67 | 3.62 | 1.28 | 1.25 | 1.00 | 0.83 |
| **EGC** | 1.44 | 4.55 | 4.57 | 5.22 | 2.01 | 1.97 | 1.20 | 1.00 |

The consistency check can be performed by Eqs.(2.7) – (2.9). This leads to $CI = 0.015 < 0.1$. Therefore, it is concluded that the final GCM is consistent whose results are trustable. It should be noted that this result is expected as individual PCMs were checked if they are consistent before the consensus analysis. Group PCM would be consistent as it is formed by consensus of consistent individual PCMs. As this is an iterative method, a table is useful in summarizing the iterations as given in Table 3.6 (in the next page).

From Table 3.6, it can be observed that GCI values get closer to 1 with each iteration. Also, standard deviations of GCI get smaller. These are indicators that the algorithm converges to a group PCM reflecting the more common opinion of the group. However, each expert's individual matrix has been updated at least once, which shows that there is no expert with too deviant opinions.

Table 3.6. Summary of Consensus Iterations

| **Iteration no.** | | **1** | **2** | **3** | **4** | **5** | **6** | **7** | **8** | **9** | **10** | **11** | **12** |
|---|---|---|---|---|---|---|---|---|---|---|---|---|---|
| **Group consensus index (GCI)** | **Exp. 1** | 1.800 | 1.773 | 1.794 | 1.206 | 1.191 | 1.186 | 1.191 | 1.183 | 1.182 | 1.181 | 1.179 | 1.178 |
| | **Exp. 2** | 1.551 | 1.566 | 1.538 | 1.553 | 1.513 | 1.494 | 1.187 | 1.185 | 1.186 | 1.185 | 1.185 | 1.183 |
| | **Exp. 3** | 2.275 | 1.288 | 1.314 | 1.315 | 1.305 | 1.284 | 1.285 | 1.265 | 1.172 | 1.169 | 1.171 | 1.168 |
| | **Exp. 4** | 1.784 | 1.824 | 1.220 | 1.235 | 1.222 | 1.218 | 1.207 | 1.191 | 1.195 | 1.194 | 1.193 | 1.192 |
| | **Exp. 5** | 1.574 | 1.535 | 1.493 | 1.476 | 1.454 | 1.437 | 1.430 | 1.168 | 1.163 | 1.162 | 1.166 | 1.165 |
| | **Exp. 6** | 1.270 | 1.261 | 1.251 | 1.227 | 1.217 | 1.203 | 1.192 | 1.215 | 1.213 | 1.211 | 1.174 | 1.173 |
| | **Exp. 7** | 1.713 | 1.653 | 1.633 | 1.606 | 1.675 | 1.244 | 1.234 | 1.225 | 1.219 | 1.179 | 1.216 | 1.177 |
| | **Exp. 8** | 1.845 | 1.808 | 1.775 | 1.735 | 1.190 | 1.215 | 1.201 | 1.192 | 1.189 | 1.193 | 1.188 | 1.191 |
| **St. dev. Of GCI** | | 0.271 | 0.207 | 0.211 | 0.188 | 0.169 | 0.109 | 0.078 | 0.029 | 0.018 | 0.014 | 0.015 | **0.009** |
| **Expert no. whose PCM is to be updated** | | 3 | 4 | 1 | 8 | 7 | 2 | 5 | 3 | 7 | 6 | 7 | None |

Then, relative weights are calculated using Eqs. (2.5) – (2.6). The results are presented in Figure 3.18.

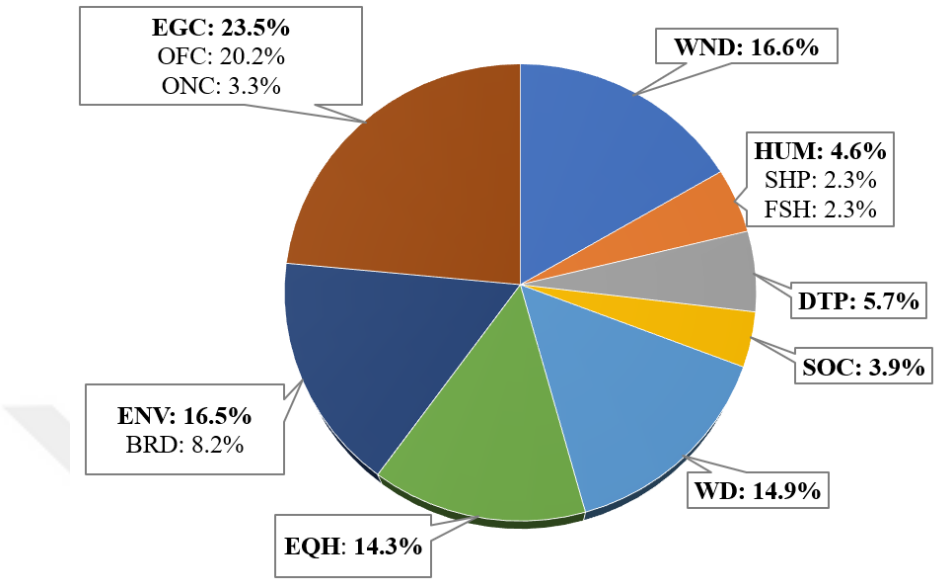



Figure 3.18. Relative Weights of Decision Criteria.

According to the expert group, electricity grid connection (EGC) is the most important decision criterion. Annual average offshore wind speed (WND) takes up the second place closely followed by environmental concerns (ENV). On the other hand, social acceptance (SOC) and existing offshore human activities (HUM) are regarded as the least important decision criteria.

The expert group tended to give more importance to the technical criteria like electricity grid connection and average wind speed. It is reasonable in the sense that maximum energy could be produced without causing serious problems in electricity transmission system. On the other hand, social criteria such as social acceptance obtained lower relative weights. The experts may have considered these criteria as manageable by proper communication with the locals throughout the detailed planning stage.

The previous studies for OWPP site selection in Türkiye did not the same criteria as in this study, therefore the relative weights of criteria obtained in this study may not be directly comparable to previous studies. However, among the common criteria, when compared with the existing literature, the results seem to be more in line with Akalın (2018) (Table 2.7), who concluded earthquake fault lines and distance to substations as important decision criteria whilst distance to shipping routes were deemed as much less important. Isiacik et al. (2020) considered that electricity grid connection is less important than the current thesis does. Similarly, Tercan et al. (2020) assigned a considerably larger importance to distance to ports. Therefore, it can be seen that there is still no definite consensus on relative importance of OWPP site selection criteria.

### 3.5.2 Alternative Site Scores

In this section, methodology presented in Section 2.1.3.2 is applied and the results are discussed for each decision criterion.

In the next paragraphs, a detailed discussion is provided. Please note that consistency ratios for PCMs are given in respective table captions. All PCMs are consistent as $CR < 0.1$ condition is satisfied.

Table 3.7. Alternative Site Scores for WND ($CR = 0.040$)

| | Bozcaada | Gökçeada | Bandırma | Karabiga | Kıyıköy | **Scores** |
|---|---|---|---|---|---|---|
| Bozcaada | 1.00 | 2.00 | 3.00 | 5.00 | 5.00 | **0.413** |
| Gökçeada | 0.50 | 1.00 | 3.00 | 4.00 | 4.00 | **0.288** |
| Bandırma | 0.33 | 0.33 | 1.00 | 3.00 | 3.00 | **0.158** |
| Karabiga | 0.20 | 0.25 | 0.33 | 1.00 | 2.00 | **0.081** |
| Kıyıköy | 0.20 | 0.25 | 0.33 | 0.50 | 1.00 | **0.060** |

As Table 3.7 points out, Bozcaada and Gökçeada obtained the highest scores from WND criterion. It is reasonable as they have some of the highest wind speeds (>9 m/s at 100 m height) in the country. On the other hand, Kıyıköy and Karabiga offers significantly lower wind speeds (6.5 – 7 m/s at 100 m height).

Table 3.8. Alternative Site Scores for FSH ($CR = 0.037$)

| | Bozcaada | Gökçeada | Bandırma | Karabiga | Kıyıköy | **Scores** |
|---|---|---|---|---|---|---|
| Bozcaada | 1.00 | 1.00 | 3.00 | 2.00 | 4.00 | **0.316** |
| Gökçeada | 1.00 | 1.00 | 3.00 | 2.00 | 4.00 | **0.316** |
| Bandırma | 0.33 | 0.33 | 1.00 | 0.50 | 4.00 | **0.135** |
| Karabiga | 0.50 | 0.50 | 2.00 | 1.00 | 3.00 | **0.182** |
| Kıyıköy | 0.25 | 0.25 | 0.25 | 0.33 | 1.00 | **0.063** |

From Table 3.8, it is seen that Bozcaada and Gökçeada obtained the same score. This is because there is no noteworthy commercial fishery activity around these islands. On the other hand, the highest activity among the alternative sites is observed around Kıyıköy, therefore this site obtained the lowest score from this criterion.

Table 3.9. Alternative Site Scores for SHP ($CR = 0.031$)

| | Bozcaada | Gökçeada | Bandırma | Karabiga | Kıyıköy | **Scores** |
|---|---|---|---|---|---|---|
| Bozcaada | 1.00 | 0.25 | 0.33 | 0.20 | 0.14 | **0.047** |
| Gökçeada | 4.00 | 1.00 | 0.50 | 0.33 | 0.20 | **0.107** |
| Bandırma | 3.00 | 2.00 | 1.00 | 0.50 | 0.33 | **0.150** |
| Karabiga | 5.00 | 3.00 | 2.00 | 1.00 | 0.50 | **0.257** |
| Kıyıköy | 7.00 | 5.00 | 3.00 | 2.00 | 1.00 | **0.438** |

Since Bozcaada and Gökçeada are closely located to Dardanelles Strait, their scores are the lowest among 5 alternative sites as given in Table 3.9 Bandırma sites are close to less crowded shipping routes, which are mostly domestic routes, resulting in being slightly more favorable. On the other hand, Kıyıköy is close to the least used corridors in the Black Sea, therefore it is assigned to have the highest desirability.

Table 3.10. Alternative Site Scores for PRT ($CR = 0.038$)

| | Bozcaada | Gökçeada | Bandırma | Karabiga | Kıyıköy | **Scores** |
|---|---|---|---|---|---|---|
| Bozcaada | 1.00 | 1.00 | 0.33 | 0.17 | 5.00 | **0.106** |
| Gökçeada | 1.00 | 1.00 | 0.33 | 0.17 | 5.00 | **0.106** |
| Bandırma | 3.00 | 3.00 | 1.00 | 0.50 | 8.00 | **0.268** |
| Karabiga | 6.00 | 6.00 | 2.00 | 1.00 | 9.00 | **0.487** |
| Kıyıköy | 0.20 | 0.20 | 0.13 | 0.11 | 1.00 | **0.032** |

Karabiga and Bandırma have close port facilities (<30 km), which is desirable. Yet, the closest large port to Kıyıköy site is Haydarpaşa Port, farther than 100 km to the site. Thus, Kıyıköy is assigned the lowest score for this criterion as seen in Table 3.10.

Table 3.11. Alternative Site Scores for SOC ($CR = 0.035$)

| | Bozcaada | Gökçeada | Bandırma | Karabiga | Kıyıköy | **Scores** |
|---|---|---|---|---|---|---|
| Bozcaada | 1.00 | 0.50 | 0.17 | 2.00 | 0.17 | **0.074** |
| Gökçeada | 2.00 | 1.00 | 0.20 | 1.00 | 0.20 | **0.087** |
| Bandırma | 6.00 | 5.00 | 1.00 | 5.00 | 1.00 | **0.381** |
| Karabiga | 0.50 | 1.00 | 0.20 | 1.00 | 0.17 | **0.065** |
| Kıyıköy | 6.00 | 5.00 | 1.00 | 6.00 | 1.00 | **0.394** |

It is important to note that this study considers distance to shore as a preliminary indicator for social acceptance, which may not be necessarily accurate. A comprehensive study for social acceptance is needed. However, as Kıyıköy site is the farthest from the shore, it obtained the highest score in this study (Table 3.11). It should be noted that Bozcaada and Karabiga sites are the nearest ones to the shoreline.

Table 3.12. Alternative Site Scores for WD ($CR = 0.038$)

| | Bozcaada | Gökçeada | Bandırma | Karabiga | Kıyıköy | **Scores** |
|---|---|---|---|---|---|---|
| Bozcaada | 1.00 | 3.00 | 3.00 | 3.00 | 4.00 | **0.436** |
| Gökçeada | 0.33 | 1.00 | 1.00 | 0.50 | 1.00 | **0.124** |
| Bandırma | 0.33 | 1.00 | 1.00 | 2.00 | 1.00 | **0.164** |
| Karabiga | 0.33 | 2.00 | 0.50 | 1.00 | 1.00 | **0.147** |
| Kıyıköy | 0.25 | 1.00 | 1.00 | 1.00 | 1.00 | **0.130** |

Nowadays, fixed-bottom foundations are considerably cheaper than floating ones. Therefore, lower water depth is desired, which Bozcaada complies with (8-37 m). It should be noted that other alternatives have water depths larger than 50 m. As a result, Bozcaada has significantly larger score (Table 3.12). Still, floating foundations are expected to become more economically feasible in the future, which may close the gap between Bozcaada and the remaining sites.

Table 3.13. Alternative Site Scores for EQH ($CR = 0.075$)

| | Bozcaada | Gökçeada | Bandırma | Karabiga | Kıyıköy | **Scores** |
|---|---|---|---|---|---|---|
| Bozcaada | 1.00 | 0.50 | 3.00 | 1.00 | 0.17 | **0.112** |
| Gökçeada | 2.00 | 1.00 | 1.00 | 0.50 | 0.17 | **0.103** |
| Bandırma | 0.33 | 1.00 | 1.00 | 0.50 | 0.14 | **0.067** |
| Karabiga | 1.00 | 2.00 | 2.00 | 1.00 | 0.14 | **0.124** |
| Kıyıköy | 6.00 | 6.00 | 7.00 | 7.00 | 1.00 | **0.594** |

Four sites except for Kıyıköy are characterized by their relatively lower distance to distinct branches of North Anatolian Fault, closest of which is Bandırma sites. This gave Bandırma the lowest desirability in terms of earthquake hazard (Table 3.13). On the other hand, Kıyıköy obtained a significantly higher score thanks to being far from large earthquake fault lines.

Table 3.14. Alternative Site Scores for BRD ($CR = 0.009$)

| | Bozcaada | Gökçeada | Bandırma | Karabiga | Kıyıköy | **Scores** |
|---|---|---|---|---|---|---|
| Bozcaada | 1.00 | 3.00 | 2.00 | 2.00 | 3.00 | **0.373** |
| Gökçeada | 0.33 | 1.00 | 1.00 | 1.00 | 2.00 | **0.168** |
| Bandırma | 0.50 | 1.00 | 1.00 | 1.00 | 2.00 | **0.181** |
| Karabiga | 0.50 | 1.00 | 1.00 | 1.00 | 2.00 | **0.181** |
| Kıyıköy | 0.33 | 0.50 | 0.50 | 0.50 | 1.00 | **0.097** |

Kıyıköy is found to be closest site to important bird migration routes, which increases the environmental concerns for this site. So, its score is considerably lower compared to the other sites (Table 3.14). Yet, Bozcaada is the most desirable alternative site in terms of bird migration routes.

Table 3.15. Alternative Site Scores for DKBA ($CR = 0.054$)

| | Bozcaada | Gökçeada | Bandırma | Karabiga | Kıyıköy | **Scores** |
|---|---|---|---|---|---|---|
| Bozcaada | 1.00 | 3.00 | 1.00 | 3.00 | 0.50 | **0.253** |
| Gökçeada | 0.33 | 1.00 | 1.00 | 1.00 | 0.50 | **0.134** |
| Bandırma | 1.00 | 1.00 | 1.00 | 3.00 | 1.00 | **0.231** |
| Karabiga | 0.33 | 1.00 | 0.33 | 1.00 | 0.50 | **0.103** |
| Kıyıköy | 2.00 | 2.00 | 1.00 | 2.00 | 1.00 | **0.279** |

In Section 3.3.1, it was stated that KBAs are observed in all of study area. It resulted in alternative sites having relatively closer scores from this criterion (Table 3.15). An interesting fact is that KBA network does not cover open seas, which results in higher desirability for sites further than the coastline. Therefore, Kıyıköy obtained a high value despite having considerably lower score for distance to bird migration routes (Table 3.14).

Table 3.16. Alternative Site Scores for OFC ($CR = 0.049$)

| | Bozcaada | Gökçeada | Bandırma | Karabiga | Kıyıköy | **Scores** |
|---|---|---|---|---|---|---|
| Bozcaada | 1.00 | 7.00 | 7.00 | 3.00 | 3.00 | **0.467** |
| Gökçeada | 0.14 | 1.00 | 0.33 | 0.20 | 0.17 | **0.041** |
| Bandırma | 0.14 | 3.00 | 1.00 | 0.33 | 0.20 | **0.073** |
| Karabiga | 0.33 | 5.00 | 3.00 | 1.00 | 0.50 | **0.167** |
| Kıyıköy | 0.33 | 6.00 | 5.00 | 2.00 | 1.00 | **0.252** |

As quantified in Table 3.16, Bozcaada is the most desirable site for OFC criterion by far. On the other hand, from TEİAŞ experts, it was learnt that electricity grid connection for Gökçeada and Bandırma sites would be more difficult due to current working loads of the national grid system. Those sites, thus, may require new offshore cables for long distances, reducing their desirability by increasing the cost.

Table 3.17. Alternative Site Scores for ONC ($CR = 0.057$)

| | Bozcaada | Gökçeada | Bandırma | Karabiga | Kıyıköy | **Scores** |
|---|---|---|---|---|---|---|
| Bozcaada | 1.00 | 0.14 | 0.20 | 0.20 | 0.20 | **0.041** |
| Gökçeada | 7.00 | 1.00 | 3.00 | 3.00 | 5.00 | **0.459** |
| Bandırma | 5.00 | 0.33 | 1.00 | 1.00 | 3.00 | **0.198** |
| Karabiga | 5.00 | 0.33 | 1.00 | 1.00 | 3.00 | **0.198** |
| Kıyıköy | 5.00 | 0.20 | 0.33 | 0.33 | 1.00 | **0.104** |

When required onshore cable length values are compared, it is observed that Gökçeada is the most advantageous as it requires the shortest. So, it obtained the highest score in this criterion. On the other hand, the neighbor island Bozcaada is the least desired one. The reason is locations of possible electricity connections are different for these locations.

### 3.5.3 Final Alternative Site Scores and Discussion

Table 3.18 summarizes the obtained final alternative site scores, which are obtained through Eq. (2.12), which utilizes relative weights and alternative site scores of each decision criterion. Note that final alternative site scores add up to unity at the end.

Table 3.18. Final Alternative Site Scores

| **Decision Criteria** | **RW** | **Alternative Site Scores** | | | | |
|---|---|---|---|---|---|---|
| | | Bozcaada | Gökçeada | Bandırma | Karabiga | Kıyıköy |
| WND | 0.166 | 0.413 | 0.288 | 0.158 | 0.081 | 0.060 |
| FSH | 0.023 | 0.316 | 0.316 | 0.135 | 0.182 | 0.063 |
| SHP | 0.023 | 0.047 | 0.107 | 0.150 | 0.257 | 0.438 |
| PRT | 0.057 | 0.106 | 0.106 | 0.268 | 0.487 | 0.032 |
| SOC | 0.039 | 0.074 | 0.087 | 0.381 | 0.065 | 0.394 |
| WD | 0.149 | 0.436 | 0.124 | 0.164 | 0.147 | 0.130 |
| EQH | 0.143 | 0.112 | 0.103 | 0.067 | 0.124 | 0.594 |
| BRD | 0.082 | 0.373 | 0.168 | 0.181 | 0.181 | 0.097 |
| DKBA | 0.083 | 0.253 | 0.134 | 0.231 | 0.103 | 0.279 |
| OFC | 0.202 | 0.467 | 0.041 | 0.073 | 0.167 | 0.252 |
| ONC | 0.033 | 0.041 | 0.459 | 0.198 | 0.198 | 0.104 |
| **Final Score** | | **0.314** | **0.149** | **0.152** | **0.157** | **0.228** |
| **Ranking** | | **1** | **5** | **4** | **3** | **2** |

An example application of Eq. (2.12) for Bozcaada is given below.

$$s_{Bozcaada,final} = 0.166 \times 0.413 + 0.023 \times 0.316 + (\dots) + 0.033 \times 0.041 = 0.314$$

In the end, Bozcaada is found to be the most suitable alternative site. The most powerful aspects of Bozcaada are its high wind speed, low water depth, low distance of required offshore cable length and high distance from bird migration routes. These are condemned as the more important decision criteria by the experts. Note that this finding supports the previous findings given in Section 2.1.3.

However, this study concludes that Kıyıköy has been overlooked in the previous studies as Kıyıköy has obtained the second highest score here. The strengths of Kıyıköy are found to be the low earthquake hazard, high distance to shipping routes and high distance to shore, which resulted in the assumption of social acceptability. Yet, it is the farthest alternative site from a large port, and it is the closest to the bird migration routes. For this reason, detailed bird migration route observations should be made in this site.

Karabiga and Bandırma, both of which are in Marmara Sea, are found to have similar scores. Both alternative sites have close port facilities. The weakest aspect of Bandırma is to be the closest to earthquake fault lines. On the other hand, Karabiga is the closest to the shoreline whereas the Bandırma is the farthest along with Kıyıköy.

Interestingly, Gökçeada is found to be the least suitable alternative site in this study, which opposes the previous studies. Despite its high wind speed, grid connection seems to be problematic, which is concluded after communicating with experts from TEİAŞ. The site would require considerably longer offshore cable length reducing the desirability significantly. Also, the island is close to the North Anatolian Fault Line, which increases the earthquake hazard.

# CHAPTER 4

# PRELIMINARY MONOPILE DESIGN

This chapter represents the preliminary monopile design process in detail.

The chapter starts by presenting the workflow in Section 4.1. Then, Section 4.2 introduces 3 idealized soil profiles from Marmara Sea which has been studied in this thesis. Meanwhile, turbine selection process and selected turbine is given in Section 4.3. Section 4.4 aims to provide realistic load estimations that would act on an OWT in Marmara Region. This thesis does not utilize any meteorological measurements, therefore, wind and wave parameters are selected based on available literature. Also, since loads depend on pile geometry, justifications related with selected pile diameters is given in this section. Sections 4.5 deals with creation and validation of Jeanjean et al. (2022) curves and check of these curves entered in LPILE. After listing design criteria and assumptions in Section 4.6, Section 4.7 presents details of results along with comparative discussions.

The reader should be aware that concluded pile diameters do not represent final design. Thus, a practicing engineer will still need to perform detailed final design, utilizing met-ocean measurements as well as site-specific soil profile and soil properties. From a practical point of view, this part of the thesis is intended to give an educated guess for a starting point to engineers who will work in OWPP planning in Marmara Region. On the other hand, from theoretical point of view, the focus is on the effect of soil types and selected p-y curves to the estimated pile response.

## 4.1 Workflow of Monopile Design

Workflow of this part of the study is given in Figure 4.1.

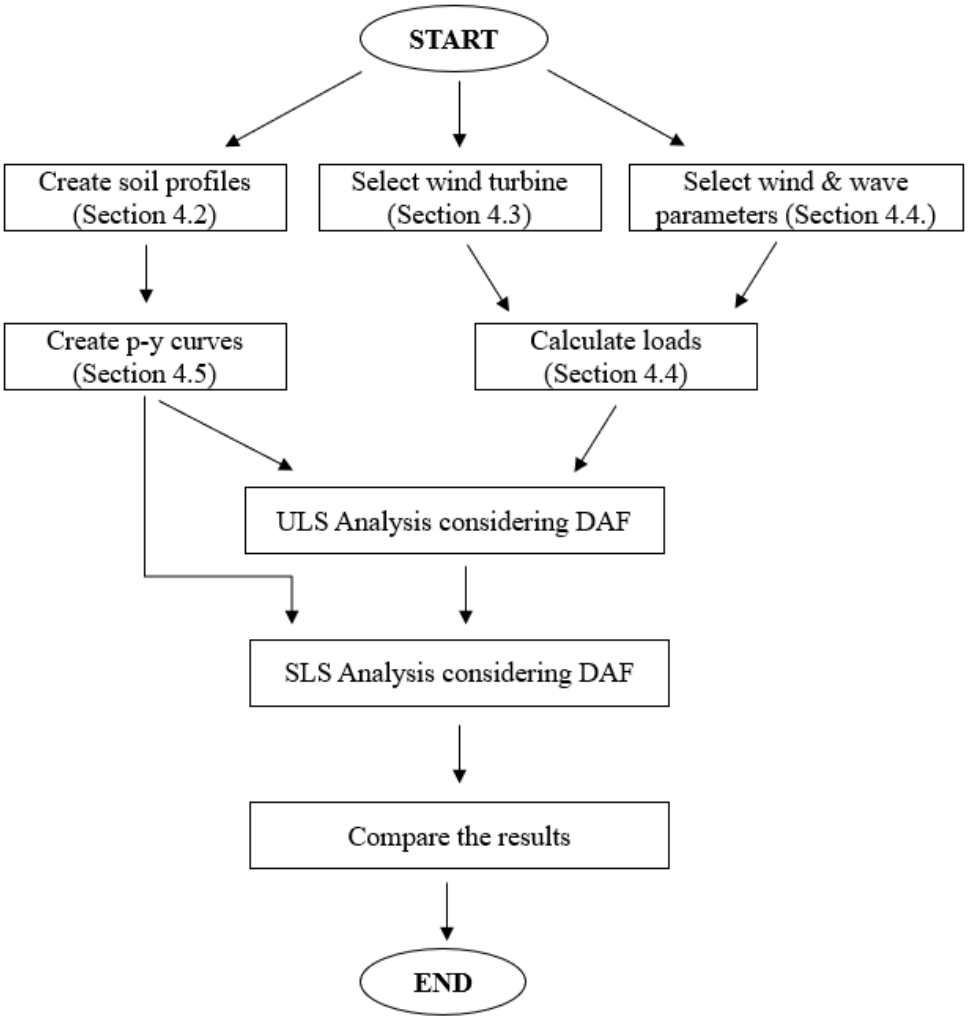



Figure 4.1. Workflow of Monopile Design

The first step is to determine input parameters needed for design: idealized soil profile, wind turbine along with wind and wave parameters.

Idealized soil profiles are needed to create p-y curves representing soil reaction. This will represent the available resistance of the pile. On the other hand, wind

turbine and sea environment parameters (wind and wave) should be decided to be able to estimate loads, constituting the actions.

First, Ultimate Limit State (ULS) checks have been done. Then, the analyses continued with Serviceability Limit State (SLS). If the pile dimensions are found to be insufficient, necessary updates have been done.

Laterally loaded pile analysis has been done on LPILE software via finite difference method. LPILE is a widely recognized special-purpose computer program based on rational processes for assessing a pile under lateral loading using p-y curves. LPILE uses a finite difference technique to solve the differential equation for an elastic beam. Over the length of the pile, the program computes deflection, bending moment, shear force and soil reaction. Nonlinear p-y curves are created internally using published recommendations for various types of soils. Alternatively, p-y curves can be specified by the user. Although the programme is useful, it has two main backdraws:

1. It is not possible to specify misaligned loads from wind and wave. Thus, only collinear loading case is considered in this study.

2. Only one amplitude can be entered, therefore it is not possible to perform time domain analysis. Therefore, random nature of a storm needs to be simplified.

Using LPILE, a total of 12 design cases are studied, which are summarized in Table 4.1.

Table 4.1. Studied Design Cases

| **Case No** | **Soil Profile** | **Method** | **Pile diameter (m)** | **Wall thickness (mm)** |
|---|---|---|---|---|
| 1 | Soil Profile 1 | Current recommendations | 8.5 | 92 |
| 2 | Soil Profile 1 | Current recommendations | 9.5 | 102 |
| 3 | Soil Profile 2 | Current recommendations | 7.5 | 82 |
| 4 | Soil Profile 2 | Current recommendations | 8.5 | 92 |
| 5 | Soil Profile 3 | Current recommendations | 7.5 | 82 |
| 6 | Soil Profile 3 | Current recommendations | 8.5 | 92 |
| 7 | Soil Profile 1 | Jeanjean et al. (2022) | 8.5 | 92 |
| 8 | Soil Profile 1 | Jeanjean et al. (2022) | 9.5 | 102 |
| 9 | Soil Profile 2 | Jeanjean et al. (2022) | 7.5 | 82 |
| 10 | Soil Profile 2 | Jeanjean et al. (2022) | 8.5 | 92 |
| 11 | Soil Profile 3 | Jeanjean et al. (2022) | 7.5 | 82 |
| 12 | Soil Profile 3 | Jeanjean et al. (2022) | 8.5 | 92 |

Pile wall thickness ($t_p$) should be decided at this stage. A commonly used estimation is provided in American Petroleum Institute (2014), which is given by Eq. (4.1).

$$t_p \geq 6.35 + \frac{D_{pile}}{100} \ (in\ mm) \tag{4.1}$$

However, final wall thickness should be decided from pile driving analysis so that the pile would not deform excessively during transportation and installation.

Justification of selected pile diameters are based on tower dimensions of selected wind turbine (Section 4.3) and applicability intervals of wave load calculation (Section 4.4).

## 4.2 Idealized Soil Profiles

When an OWT is to be installed at a specific location, site investigation is carried out according to international guidelines, typically including cone penetration test (CPT) and boreholes/soil sampling/laboratory testing. In this study, site-specific geotechnical investigation data are not available. Instead, to be able to develop idealized soil profiles that may represent Southern Marmara Sea, findings on literature review along with confidential reports have been utilized.

In Section 3, sites in Southern Marmara Sea, i.e., Bandırma and Karabiga were not concluded to be the most suitable sites, however, this section focuses on Southern Marmara due to geotechnical data availability.

Laboratory tests include identification tests such as saturated unit weight, sieve analysis and Atterberg limits along with shear strength tests like monotonic UU triaxial and torvane tests. Note that no cyclic test was performed on samples.

The locations of the tests do not match selected suitable sites in Section 3. As a result, there is a good chance to encounter different soil conditions, considering soil variability in Marmara Sea as already shown in Section 2. Figure 4.2 visualizes the idealized soil profiles, and then each soil profile is briefly introduced. Please note that water depth is 50 m in all profiles.




Figure 4.2. Idealized Soil Profiles Used in This Study

### 4.2.1 Soil Profile 1

Soil Profile 1 is the most challenging profile with a 35 m thick lightly overconsolidated very soft sensitive clay, underlain by a weak mudstone treated as hard clay. This very soft clay layer was studied in detail by both CPTs, and lab tests whose results are summarized in Figure 4.3.

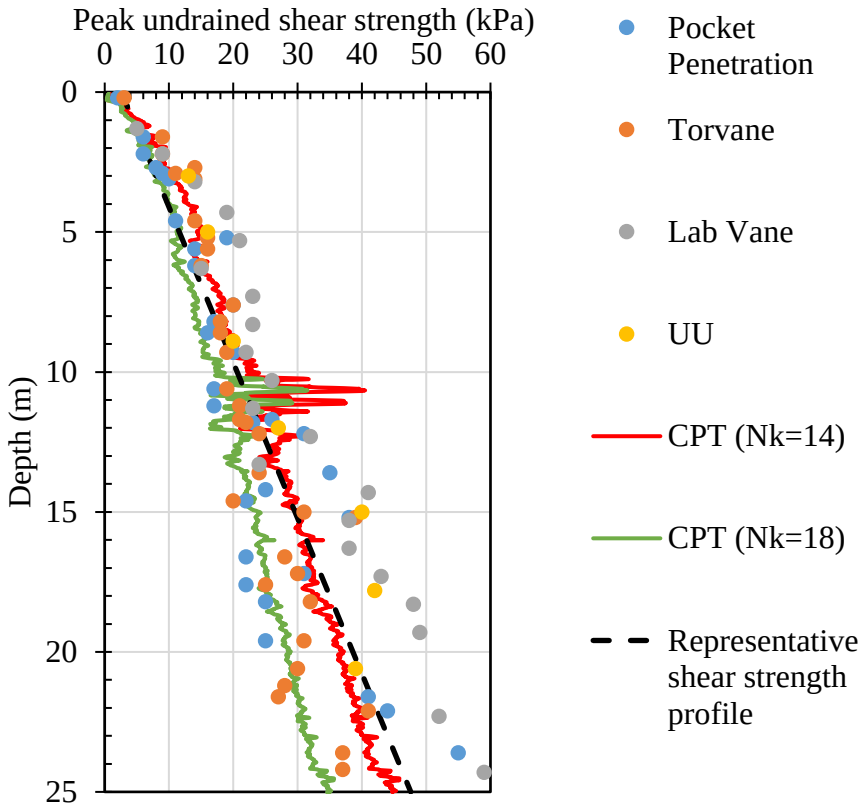



Figure 4.3. Representative Test Results in Very Soft Clay Layer

In Figure 4.3, laboratory test results are directly taken from a confidential report whereas CPT measurements were used to estimate peak undrained shear strength using Eq. (4.2).

$$s_{u,peak} = \frac{q_t - \sigma_v}{N_k} \tag{4.2}$$

The figure shows results from only the first 25 m. After this depth, there are no lab tests although CPT tends to follow the same trend between 25-35 m with the top 25 m.

Despite considerable deviations between different tests, peak undrained shear strength of this profile is approximated by $s_{u,peak} = 2.6 + 1.8z$, with a sensitivity ($s_{u,peak} \,/\, s_{u,residual}$) of about 10. Since monopiles are driven into the seabed, which disturbs the soil at the vicinity considerably, remoulded (or residual) shear strength, $s_{u,residual} = 0.26 + 0.18z$ for very soft clay layer, is used in all analysis. No remoulded tests were performed on the weak mudstone, so it is assumed to be non-sensitive.

### 4.2.2 Soil Profile 2

Soil Profile 2 consists of a 10 m thick overconsolidated medium stiff clay layer with constant peak and residual shear strengths of 80 and 64 kPa, respectively. This layer has been underlain by medium dense sand, which has a constant relative density of 50% and saturated unit weight of 19 kN/m$^3$. In this soil profile, weak mudstone starts at 30 m depth from the seabed.

### 4.2.3 Soil Profile 3

This soil profile consists of the same medium stiff clay and medium dense layers as Soil Profile 2. However, this time, the top layer is medium dense sand.

It should be noted that the distances between Soil Profiles are around 1.5 km in confidential reports, which is a small distance considering the total area of offshore wind farms. The general rule of thumb for spacing of individual turbines in the dominant wind direction is about 7 times the rotor diameter (164 m for LW 8 MW turbine) and 5 times the rotor diameter in the direction perpendicular to the dominant wind direction.

## 4.3 Selected Wind Turbine

In this study, two wind turbines were considered. In the literature review, average OWT rated power was stated as 8 MW as of 2021 in OWPP projects around the world. Thus, the considered wind turbines have similar rated powers between 8 – 10 MW. The basic properties of the considered wind turbines are presented in Table 4.2.

Table 4.2. Considered Wind Turbines

| | **LW 8 MW (Desmond et al., 2016)** | **DTU 10 MW (Bak et al., 2013)** |
|---|---|---|
| Rotor diameter | 164 m | 178.3 m |
| Hub height | 110 m | 119 m |
| Cut-in, rated and cut-out wind speeds | 4 m/s, 12.5 m/s, 25 m/s | 4 m/s, 11.4 m/s, 25 m/s |
| Rotor speed range | 6.3 – 10.5 rpm | 6 – 9.6 rpm |
| 1P frequency band | 0.105 – 0.175 Hz | 0.10 – 0.16 Hz |
| 3P frequency band | 0.315 – 0.525 Hz | 0.30 – 0.48 Hz |
| Mass of rotor nacelle assembly | 480 tons | 694.7 tons |
| Tower mass | 558 tons | 605 tons |
| Tower height | 106.3 m | 115.6 m |
| Tower top and bottom diameter | 5 m, 7.7 m | 5.5 m, 8.3 m |
| Tower average wall thickness | 29 mm | 29 mm |
| Fixed-base natural frequency (calculated using method in Section 2.2.2.4.1) | 0.27 Hz | 0.22 Hz |

In this thesis, the final selection of the turbine is based on natural frequencies instead of cost or detailed power production analysis.

As Section 4.4 reveals, wave periods in Southern Marmara Sea are close to 0.22 Hz, which is the fixed base frequency of DTU 10MW turbine. This situation increases the dynamic amplification of wave forces. Furthermore, it is known that foundation deformability will result in reduction of fixed-base natural frequency, so DTU 10MW turbine may experience significant dynamic amplification. In the light of this discussion, **LW 8MW** wind turbine is chosen.

## 4.4 Load Calculations

Load calculations are based on Table 2.8 with the exception of Combination 5, which includes misalignment of wind and wave loads as it is not possible to model misaligned loads in LPILE. Yet, it may not be the most critical load combination because dominant wind and wave directions are concurrent in Southern Marmara Sea (Global Wind Atlas, n.d.; Özhan & Abdalla, 1999).

Furthermore, as an adjustment, 2-year wave load cases are used in this thesis instead of 1-year. This is because recent literature (Kutupoğlu et al., 2023) provides wave height information on 2-year storms, which has been estimated based on long term wave measurements. It should be noted that this adjustment adds conservatism to concluded monopile dimensions.

Table 4.3 presents the estimated wind loads acting on LW 8MW turbine on Southern Marmara Sea, full details of which are given in Appendix B.

Table 4.3. Calculated Wind Loads

| **Wind Load Case** | **Force (MN)** | **Moment (MN·m)** |
|---|---|---|
| Case 1: Normal turbulence at rated wind speed | 1.35 | 215.8 |
| Case 2: Extreme turbulence at rated wind speed | 1.64 | 288.5 |
| Case 3: Extreme operating gust at rated wind speed | 2.93 | 467.7 |
| Case 4: Extreme operating gust at cut-out speed | 0.83 | 132.1 |

Although wind speed is the largest at Case 4, it results in the lowest wind force because of the lower drag coefficient at high wind speeds. The most critical case turns out to be Case 3. In this case, an extreme gust is acting when non-turbulent wind force is already at the highest level. In all cases, moment arm of wind force is 160 m, the summation of hub height (110 m) and water depth (50 m).

Then, Table 4.4 summarizes the wave forces.

Table 4.4. Calculated Non-Amplified Wave Loads

| | **D=7.5 m** | | **D=8.5 m** | | **D=9.5 m** | |
|---|---|---|---|---|---|---|
| | **Force (MN)** | **Moment (MN·m)** | **Force (MN)** | **Moment (MN·m)** | **Force (MN)** | **Moment (MN·m)** |
| Case 1: 2-year Extreme Sea State (Period: 5.5 s) | 1.56 | 68.7 | 2.00 | 87.8 | 2.48 | 109.3 |
| Case 2: 2-year Extreme Wave Height (Period: 8.3 s) | 2.87 | 121.3 | 3.65 | 154.6 | 4.54 | 191.9 |

Table 4.4 (cont'd)

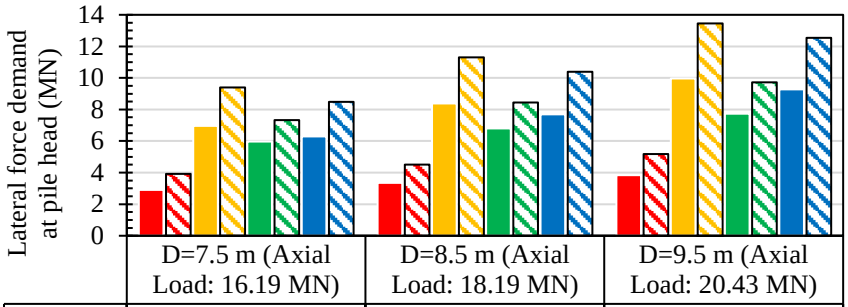
| | **D=7.5 m** | | **D=8.5 m** | | **D=9.5 m** | |
|---|---|---|---|---|---|---|
| | **Force (MN)** | **Moment (MN·m)** | **Force (MN)** | **Moment (MN·m)** | **Force (MN)** | **Moment (MN·m)** |
| Case 3: 50-year Extreme Wave Height (Period: 10.8 s) | 5.32 | 188.5 | 6.74 | 238.2 | 8.32 | 293.7 |

Since wave force changes with monopile diameter, it is calculated at different values. Wave force increases with increasing pile diameter. As LW 8MW has a bottom tower diameter of 7.7 m, minimum reasonable monopile diameter is deemed as 7.5 m. On the other hand, Table 4.4 is obtained using Morison's equation, which is valid when pile diameter ($D_{pile}$) to wavelength ($L$) ratio is smaller than 0.2. Case 1 has an estimated wavelength of 47 m, so largest monopile diameter is 9.5 m which barely remains inside applicability limits of Morison's equation. The reader is referred to Appendix C for more details.

In the next step, wind and wave loads have been combined for Serviceability Limit State (SLS) and Ultimate Limit State (ULS) analysis (see Figure 4.4 where the letter "C" represents "combination"). Note that the former limit state does not require any partial load factors albeit the latter one does.

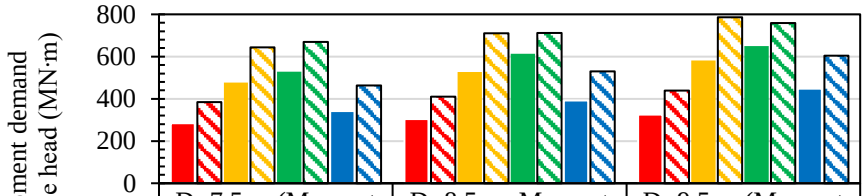
As an important note, no live load is considered on the monopile because load cases are expected to occur at storm events during which no maintenance activity is assumed.

As pile diameter increases, moment arm reduces because wave loads increase whereas wind load is not dependent on monopile diameter.




| | D=7.5 m (Axial Load: 16.19 MN) | D=8.5 m (Axial Load: 18.19 MN) | D=9.5 m (Axial Load: 20.43 MN) |
|---|---|---|---|
| C1 SLS | 2.91 | 3.34 | 3.83 |
| C1 ULS | 3.93 | 4.51 | 5.17 |
| C2 SLS | 6.96 | 8.38 | 9.96 |
| C2 ULS | 9.40 | 11.31 | 13.45 |
| C3 SLS | 5.97 | 6.80 | 7.74 |
| C3 ULS | 7.32 | 8.45 | 9.72 |
| C4 SLS | 6.29 | 7.70 | 9.28 |
| C4 ULS | 8.49 | 10.40 | 12.53 |

(a)




| | D=7.5 m (Moment arm: 55-98 m) | D=8.5 m: Moment arm: 51-91 m) | D=9.5 m (Moment arm: 48-85 m) |
|---|---|---|---|
| C1 SLS | 284.5 | 303.6 | 325.1 |
| C1 ULS | 384.0 | 409.8 | 438.9 |
| C2 SLS | 477.0 | 526.7 | 582.2 |
| C2 ULS | 644.0 | 711.1 | 786.0 |
| C3 SLS | 528.5 | 613.9 | 649.0 |
| C3 ULS | 669.5 | 711.8 | 759.2 |
| C4 SLS | 342.6 | 392.3 | 447.8 |
| C4 ULS | 462.5 | 529.6 | 604.5 |

(b)

Figure 4.4. Calculated (a) Lateral Force and (b) Bending Moments at the Pile Head

Combination 1 consists of the lowest loading on the pile; however, moment arm is the highest (97, 91, 85 m for 7.5 m, 8.5 m, 9.5 m diameter respectively). Also, this case includes the waves with smaller periods, therefore dynamic amplification is expected to be larger. Combination 2 has the largest lateral loads because it represents the extreme wave load case. On the other hand, Combination 3 considers the extreme wind load, which results in the largest moment in SLS. Combinations 2&4 considers the largest waves with largest periods, therefore dynamic amplification should be lower when compared to Combination 1. Combination 4 has the lowest moment arm (55, 51, 48 m for 7.5 m, 8.5 m, 9.5 m diameter respectively) because wind load is the lowest in this combination.

Set 1 in Table 2.9 is not considered in ULS analysis since this combination is expected to be more critical in axially loaded piles instead of laterally loaded monopiles. Also, Set 3, increasing loads by 10%, is only applied to wind load in Combination 3 since it represents abnormal wind load case. Remaining load factors are taken from Set 2, which increases loads by 35%.

Note that moment arms of Combination 3 are slightly different for SLS and ULS. This is because wind load is factored by 1.1 whilst by 1.35 for wave load. Therefore, wave load is more pronounced in ULS, resulting in lower moment arm than in SLS.

Finally, vertical load, which was already presented in Figure 4.4, includes weight of the OWT components and effective self-weight of the monopile portion in the water. Load factor is not needed in neither ULS nor SLS analysis.

This study does not consider earthquake loading as seismis analysis require separate detailed analysis considering liquefaction, lateral spreading etc. together with detailed site-specific cyclic soil strength and stiffness degradation related parameters.

## 4.5 Creation and Validation of Jeanjean et al. (2022) p-y Curves

As Jeanjean et al. (2022) is not yet implemented in LPILE, a spreadsheet is prepared for this method. The next sections discuss the monotonic and cyclic curves separately.

### 4.5.1 Monotonic Curves

Monotonic p-y curves are created by utilizing Eqs. (2.37) - (2.41) and Figure 2.11.

The validation of the prepared spreadsheet is done via lateral bearing capacity factors given in Jeanjean et al. (2022), where the researchers provided lateral bearing capacity factor variation with depth for two different large piles whose properties are given in Table 4.5.

Table 4.5. Pile Properties Used for Validation (Jeanjean et al., 2022)

| **Pile no.** | **Pile diameter (m)** | **Pile length (m)** | $\alpha_{ave}$ |
|---|---|---|---|
| 1 | 10 | 60 | 0.62 |
| 2 | 5 | 30 | 0.53 |

Cases in Table 4.5 gives the opportunity to compare the effect of pile diameter and average adhesion factor, $\alpha_{ave}$ in the same soil profile.

For validation, firstly, provided undrained shear strength profile is approximated by Eq. (4.3).

$$s_u = \begin{cases} 70 + 36z \quad for\ 0 \le z < 2.5\ m \\ 210 - 20z \quad for\ 2.5\ m \le z < 5\ m \\ 95 + 3z \quad for\ z \ge 5\ m \end{cases} \tag{4.3}$$

The comparison of Eq. (4.3) and the provided profile in Jeanjean et al. (2022) is given in Figure 4.5.

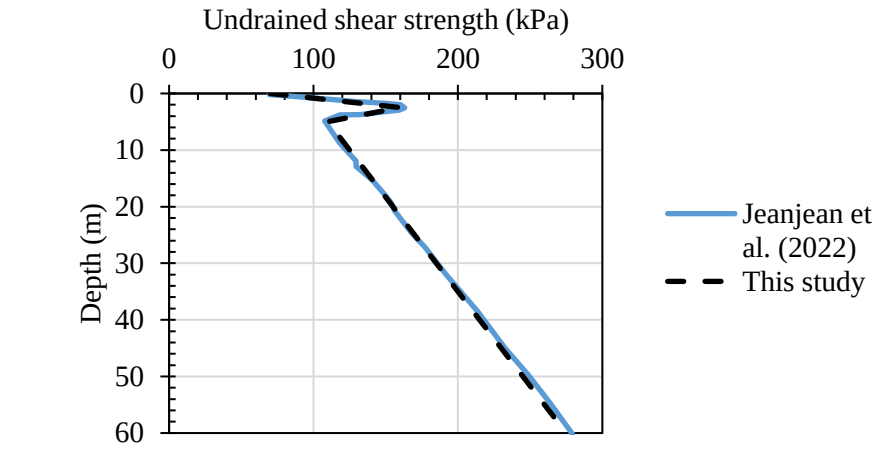



Figure 4.5. Validation of Undrained Shear Strength Profiles

As Figure 4.5 shows, there is satisfactory match. Also, please observe that it is possible to study clay layers whose undrained shear strength decreasing with depth, i.e., $s_{u1} < 0$ although Jeanjean et al. (2022) noted that the method is mostly intended to simulate profiles with $s_{u1} \geq 0$.

In the next stage, lateral bearing capacity factors are calculated assuming soil unit weight constant as 20 kN/m$^3$. As can be seen in Figure 4.6, match is satisfactory, which validates the prepared spreadsheet under monotonic loads.

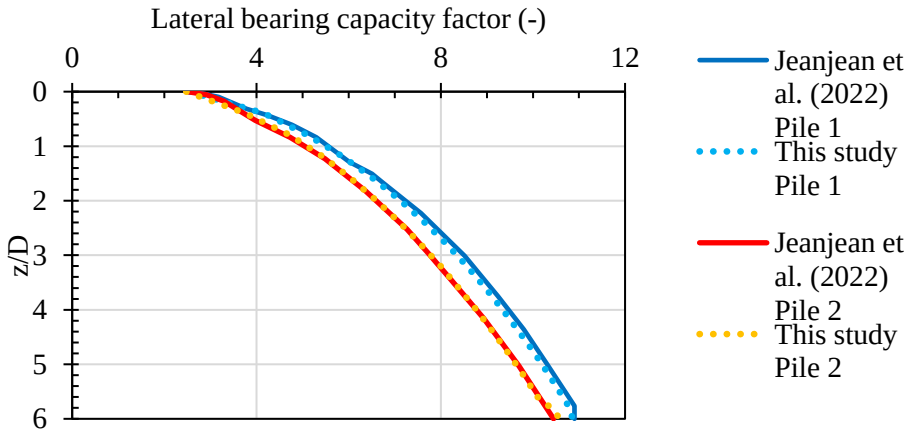



Figure 4.6. Validation of Monotonic Lateral Bearing Capacity Factors

### 4.5.2 Cyclic Curves

Unfortunately, it was not possible to validate cyclic curves due to lack of publicly available data.

In the current study, North Sea conditions have been assumed as it is possible to study both soft and stiff clay conditions. As a reminder from Section 2.2.8, cyclic loading parameters are summarized in Table 4.6. Importantly, this assumption may be overestimating both soil hardening and softening since North Sea wave climate is harsher than Marmara Sea. Jeanjean (2022) noted that if wave conditions differ considerably from Gulf of Mexico and North Sea, site specific studies would be needed. This lacks in the current study, imposing a limitation.

Table 4.6. Cyclic p-y Curve Model Parameters for North Sea (Jeanjean et al., 2022)

| **Condition** | **Modification factor for mobilized soil resistance ($p_{mod}$)** | **Modification factor for lateral deflection ($y_{mod}$)** | **$g$ (needed for equivalent number of cycles, $N_{eq}$)** |
|---|---|---|---|
| Soft clay | $1.63 - 0.15\ln(N_{eq})$ | $1.2 - 0.17\ln(N_{eq})$ | 1.25 |
| Stiff clay | $1.45 - 0.17\ln(N_{eq})$ | $1.2 - 0.17\ln(N_{eq})$ | 2.5 |

As pointed out Section 2.2.8, a monotonic analysis is needed to obtain cyclic curves because cyclic curves are a function of depth of rotation, which changes with pile length.

Regarding the model parameters in cyclic curves, some observations are as follows:

- Hybrid factor, $h_f$, is a negative number below center of rotation. This results in significantly lower number of equivalent cycles.
- Number of equivalent cycles ($N_{eq}$) is a larger number at larger deflections. It is reasonable considering more cycles are needed to cause more deflection.
- Number of equivalent cycles ($N_{eq}$) takes larger values at shallower depths, likely to reflect the fact that upper soil layers are more affected from lateral loads.
- As number of equivalent cycles increases, the model tends to simulate softening model. However, the softening and hardening boundary depends on the other model parameters, such as $g$.

### 4.5.3 Comparison of Monotonic and Cyclic Curves

In this section, example comparisons between monotonic and cyclic curves have been presented for various cases to provide more insight into new method.

Figure 4.7 visualizes the first example.

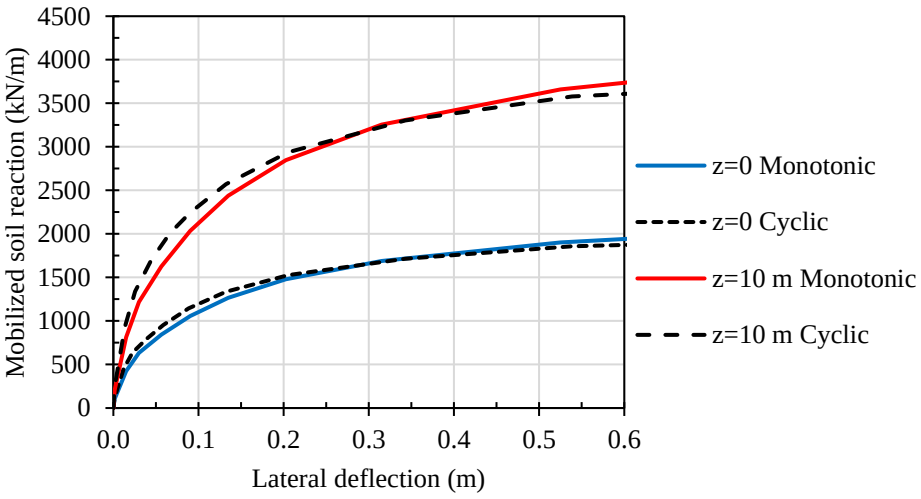



Figure 4.7. Example p-y Curves from Soil Profile 2, ULS, L=31 m, D=7.5 m (Depth of rotation under monotonic loading: 21 m)

Figure 4.7 shows monotonic and cyclic p-y curves at seabed and 10 m depth, which are the boundaries of medium stiff clay layer. Note that these depths are much above the depth of rotation. It can be observed that soil is estimated to harden up to about 30 cm lateral deflection under cyclic loading. This corresponds to lateral strain of 4%. After that point, mobilized soil reaction under monotonic action is observed to be higher, indicating softening behavior.

The next example is about simulated behavior of weak mudstone, which is important as it is expected to contribute considerably to the capacity of the pile.

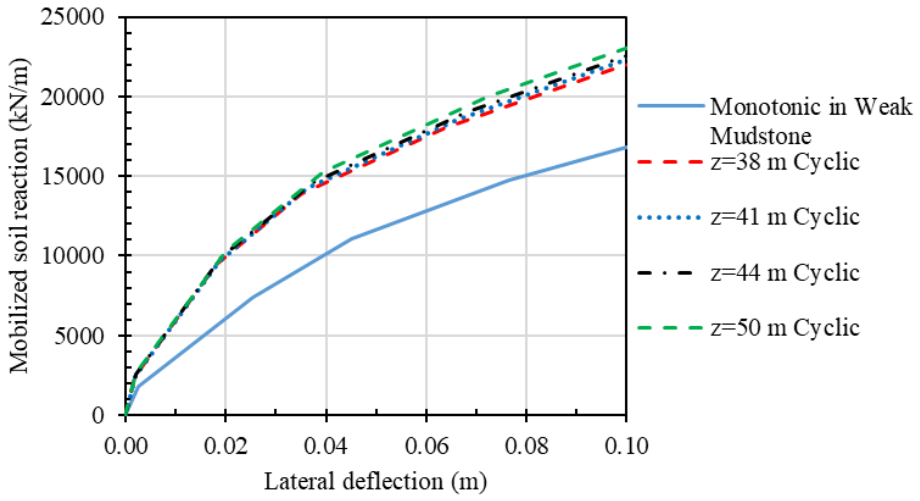



Figure 4.8. Example p-y Curves from Soil Profile 1, SLS, L=58 m, D=8.5 m (Depth of rotation under monotonic load: 47 m)

In this case, the model estimates hardening of already hard clay. It is investigated if hardening is simulated above the zero deflection point as well. As Figure 4.8 visualizes, hardening is observed both above and below the zero-deflection point. There could be two explanations for that:

1. Normally, small deflections are expected at the vicinity of the zero-deflection point, which is very likely to result in hardening.

2. When there is deflection at pile tip, i.e., pile is not flexible, an additional soil resistance should mobilize. This is unlikely to be anticipated by Matlock (1970) method because this method considers flexible piles only.

However, in Jeanjean et al. (2022) model, although not shown in Figure 4.8, estimated hardening behavior continues for large deflections as well. For flexible piles, it should not be a problem as no significant pile tip deflection is expected, however, for rigid piles, this phenomenon should be kept in mind.

The final example (Figure 4.9) investigates Soil Profile 3, where depth of rotation is in medium stiff clay. Please note curves at 25 m & 30 m depths exactly coincide with each other.

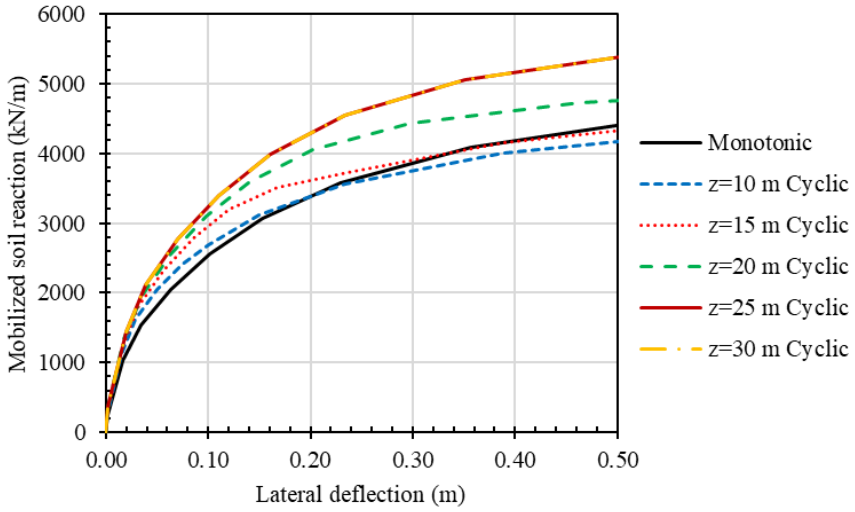



Figure 4.9. Example p-y Curves from Soil Profile 3, ULS, L=36 m, D=8.5 m (Depth of rotation under monotonic load: 25 m)

This example combines both behaviors discussed above. Hardening of soil is modelled below the centre of rotation. However, please observe that there is hardening behavior as well at 20 m depth, which is about 0.5D above depth of rotation. However, at shallower depths, behavior is the same as Figure 4.8, where soil softens at large lateral strains.

### 4.5.4 Check of p-y Curves in LPILE

As a checkpoint, it is investigated if p-y curves have been generated correctly in LPILE. Calculated Jeanjean et al. (2022) curves have been entered with 5 m intervals to LPILE. But it may result in slight inaccuracies in p-y curves at intermediate depths because LPILE utilizes interpolation at these depths. So, at selected depths, calculated curves in the spreadsheet and extracted curves from LPILE have been compared to ensure that there are no excessive deviations.

The example checks on Soil Profile 1 are given in Figure 4.10.

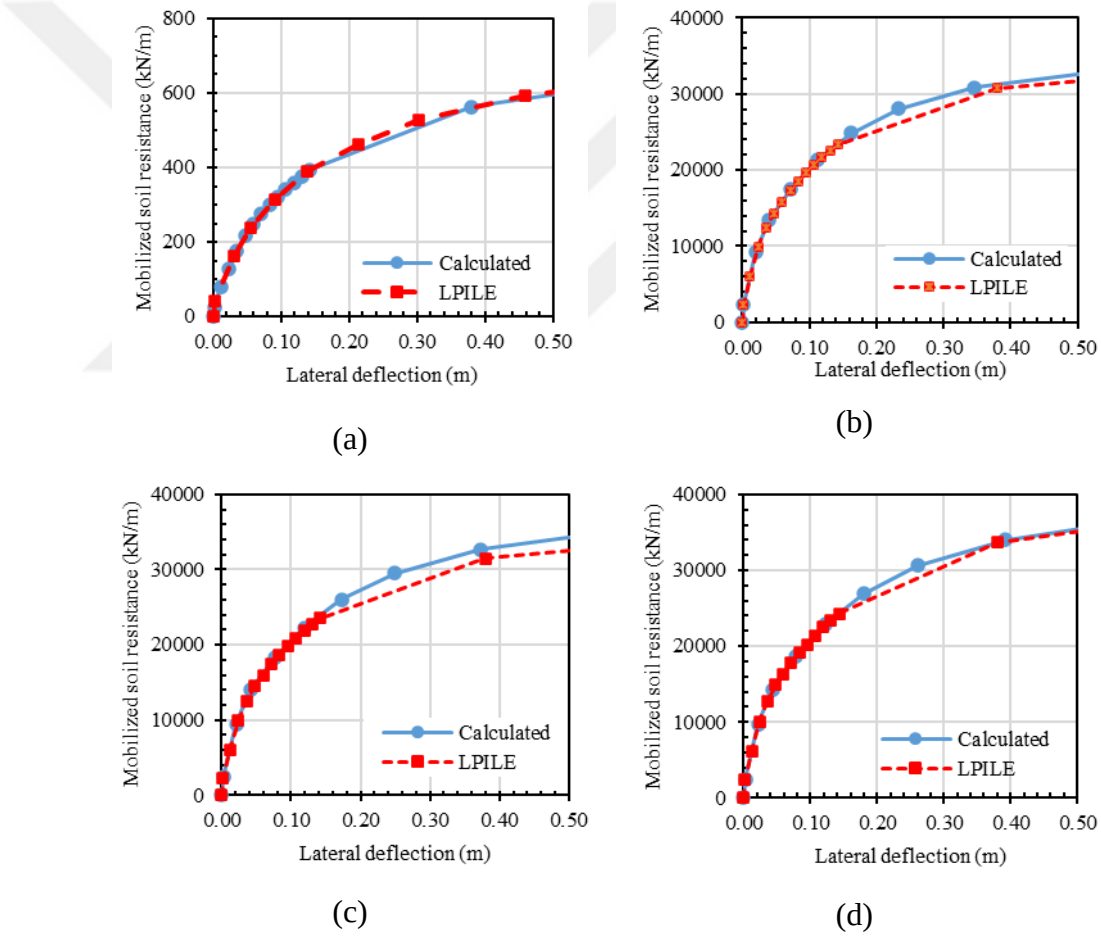



Figure 4.10. Comparison of Calculated and Extracted Cyclic p-y Curves at (a) 32 m, (b) 38 m, (c) 42 m and (d) 46 m depth (ULS, Soil Profile 1, D=9.5 m)

Three selected depths are in the hard clay layer ($z \geq 35\ m$) as this layer is expected to dominate the behavior. Also, to ensure the soft clay was modelled accurately as well, curves from 32 m depth has also been compared. Please notice the satisfactory match for all cases.

## 4.6 Design Criteria and Assumptions

**Ultimate Limit State:** The pile must have sufficient capacity under extreme loads. This is calculated by methods presented in Section 2.2.2.2.1.

**Serviceability Limit State:** In this study, short term serviceability is being investigated. Pile head rotation must be smaller than 0.5° and lateral deflection must be smaller than 0.2 m, when unfactored loads are applied. Long term serviceability is not studied due to lack of data.

**Natural Frequency:** 1P and 3P frequency bands must be avoided with 10% factor of safety. So, target natural frequency band is 0.193-0.27 Hz.

**Fatigue Limit State:** Although it may be an important control from structural engineering point of view, this limit state is not studied because it is concerns with loads created by average waves, which falls outside the Morison's equation applicability limits.

During all analysis in this thesis, following assumptions have been made.

- No gapping is assumed for all soil profiles. Therefore, for hard clay/weak mudstone, p-y curves without free water are used. In the field, it can be achieved by proper scour protection.
- Jeanjean et al. (2022) gives normalized p-y curves for three overconsolidation ratios, which are OCR<2, OCR=4 and OCR=10. Only the first two are used as idealized soil profiles fit to these categories.

- In Jeanjean et al. (2022) method, average adhesion factor, $\alpha_{ave}$ changes with pile length. Nonetheless, it has a negligible effect on the maximum lateral bearing capacity factor since studied pile lengths do not differ dramatically in the same soil profile. So, a constant $\alpha_{ave}$ is used for each soil profile, which is calculated by Eq. (4.4) (American Petroleum Institute, 2014).

$$\alpha = \begin{cases} 0.5\left(\frac{s_u}{\sigma_v'}\right)^{-0.5} \leq 1.0 \; for \; \frac{s_u}{\sigma_v'} \leq 1.0 \\ 0.5\left(\frac{s_u}{\sigma_v'}\right)^{-0.25} \leq 1.0 \; for \; \frac{s_u}{\sigma_v'} > 1.0 \end{cases} \quad (4.4)$$

  Calculated $\alpha_{ave}$ values are as follows:

  - Soil Profile 1 (deep very soft clay at seabed): $\alpha_{ave} = 0.8$
  - Soil Profile 2 (medium stiff clay at the seabed): $\alpha_{ave} = 0.53$
  - Soil Profile 3 (medium dense sand at the seabed): $\alpha_{ave} = 0.92$

  Soil Profile 3 resulted in the largest $\alpha_{ave}$ as this profile includes medium stiff clay between 10-30 m depths. In this layer, effective stress values are much larger than undrained shear strength (64 kPa for SLS), increasing adhesion factor significantly.

- Depth of rotation ($z_{rot}$) changes with pile length, however, in this study, a single conservative depth of rotation, which is slightly deeper, is assumed while studying slightly different pile lengths. These depths have been obtained from monotonic analysis.
  - Soil Profile 1: $z_{rot} = 47\ m$ (in weak mudstone/hard clay)
  - Soil Profile 2: $z_{rot} = 21\ m$ (in medium dense sand)
  - Soil Profile 3: $z_{rot} = 25\ m$ (in medium stiff clay)
- North Sea conditions have been assumed for cyclic loads as already stated in Section 4.5.2.

- Damping ratio of monopile is assumed as 3% (Det Norske Veritas, 2014) in all dynamic amplification factor calculations.
- In the “current recommendations” analysis, weak mudstone/hard clay layer is modeled by stiff clay without free water p-y curves whereas medium stiff and very soft clays are modelled by Matlock (1970) recommendation.
- In both “current practice” and Jeanjean et al. (2022) analyses, sand is modelled by American Petroleum Institute method.
- In Soil Profiles 2 and 3 with sandy layers, angle of internal friction (Φ’) is taken as 30°. As mentioned in Chapter 2, for sands the current recommendations do not specify whether the partial resistance factor should be applied to the angle of internal friction (Φ’) or the tangent of it (tanΦ’). If partial resistance factor is directly applied to the angle of friction, a reduced value of 29.5° is obtained. If it isapplied to tangent of angle of friction, the result is 30.4°. The average of these two calculations gives 30°.

## 4.7 Results and Discussion of Monopile Design

This section starts with an example process for 1 design problem in Section 4.7.1. Then, Section 4.7.2 gives a complete summary of 12 design cases, which is followed by comparative discussions about the effect of selected p-y curves and soil properties (Section 4.7.3).

### 4.7.1 Example Design Problem (Soil Profile 1 – L=70 m & D=9.5 m Using Current Practice)

The example monopile has a penetration length of 70 m. In idealized soil profiles, maximum soil depth is given as 60 m. It is assumed that hard clay

continues into greater depths with the same engineering properties. The pile diameter, on the other hand, is 9.5 m with a wall thickness of 102 mm.

In the next sections, limit state checks are explained step by step. Please note that natural frequency estimations are needed in both limit states to estimate amplified loads.

#### 4.7.1.1 Ultimate Limit State (ULS) Checks

This step includes trial and error to reach satisfactory pile length. Here, only the satisfactory pile is presented for brevity.

**Step 1: Ultimate pile capacity**

First step is the estimation of ultimate pile capacity, which differs for each load combination due to varying moment arms. As a result, each load combination needs to be analyzed separately.

In LPILE, for each load combination, lateral load and corresponding moment have been applied with increments of 1 MN until analysis diverge. Maximum deflection limit is specified as 10 m.

The results are presented in Figure 4.11.

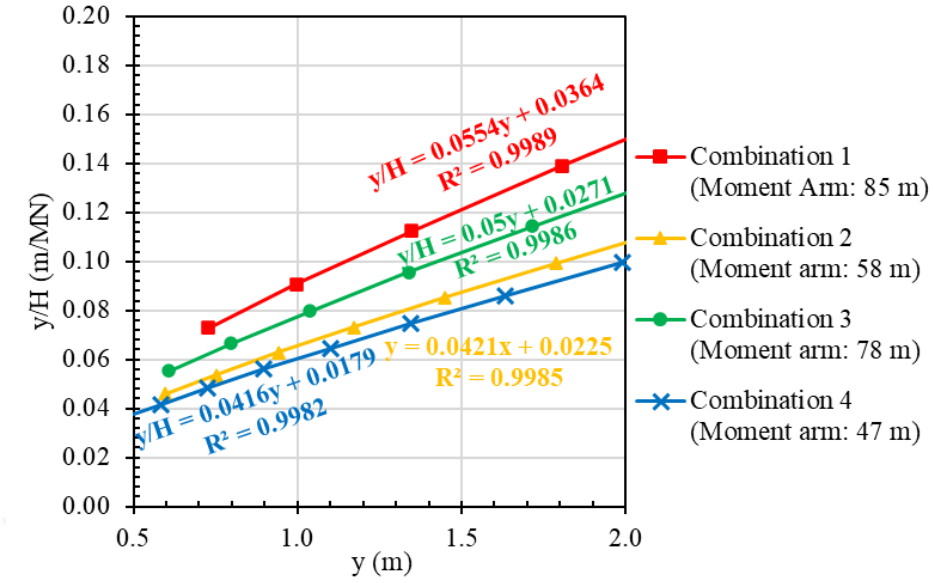



Figure 4.11. ULS Analysis Plot for the Example Monopile

In Figure 4.11, only the linear portions are plotted, and equations of best fit lines is given with the same color as in the legend. For example, best fit line equation for Combination 3 is given by $y/H = 0.0421y + 0.0225$.

Ultimate capacity of this pile under each load combination are calculated in Table 4.7.

Table 4.7. Ultimate Pile Capacity Values for the Example Monopile

| **Load combination** | **Ultimate lateral capacity of monopile** |
|---|---|
| C1 | $H_{ult} = 1/0.0544 = 18.1\ MN$ |
| C2 | $H_{ult} = 1/0.0421 = 23.8\ MN$ |
| C3 | $H_{ult} = 1/0.05 = 20\ MN$ |
| C4 | $H_{ult} = 1/0.0416 = 24\ MN$ |

Note that Combination 4 has the lowest slope in Figure 4.11. However, since ultimate pile capacity is the inverse of the slope, this combination provides the

largest capacity. This is expected because the moment arm is the lowest. Also, the minimum and the maximum pile capacities have a difference of 5.9 MN. This exemplifies importance of moment arm on pile capacity under lateral loads.

**Step 2: ULS Natural frequency**

Natural frequency is needed to be able to estimate how much wave load and moment will be amplified. Using the method of Arany et al. (2016), Table 4.8 is formed.

Table 4.8. Estimated ULS Natural Frequencies for the Example Monopile

| | **C1** | **C2** | **C3** | **C4** |
|---|---|---|---|---|
| Load ($MN$) | 5.17 | 13.45 | 9.72 | 12.53 |
| Moment ($MN \cdot m$) | 438.9 | 786.0 | 759.2 | 604.5 |
| $K_L$ $(MN/m)$ | 305.4 | 98.4 | 147 | 143.1 |
| $K_{LR}$ $(MN)$ | -10244 | -3209 | -4777 | -4732 |
| $K_R$ $(MN \cdot m/rad)$ | 432812 | 130815 | 185297 | 189860 |
| Natural frequency (Hz) | 0.243 | 0.194 | 0.202 | 0.207 |

Combination 2 is the most critical one in terms of natural frequency. Target natural frequency interval is barely achieved. This load combination imposes the largest lateral load, resulting in higher lateral deflection and rotation. Therefore, it is expected to observe lower natural frequency, i.e., higher period in this case. Note that foundation deformability results in 30% reduction of fixed base natural frequency, which is 0.27 Hz.

**Step 3: ULS amplified loads and moments**

In this step, dynamic amplification factor is calculated for each load combination, which enables to estimate how much wave loads will be amplified on the monopile.

Table 4.9 summarizes the amplified load calculations.

Table 4.9. Amplified ULS Loads and Moments Acting on the Example Monopile

| | **C1** | **C2** | **C3** | **C4** |
|---|---|---|---|---|
| Natural freq. (Hz) | 0.243 | 0.194 | 0.202 | 0.207 |
| Wave frequency (Hz) | 0.182 | 0.093 | 0.121 | 0.093 |
| Non-amplified total force (MN) | 5.17 | 13.45 | 9.72 | 12.53 |
| Non-amplified total moment (MN·m) | 438.9 | 786.0 | 759.2 | 604.5 |
| DAF | 3.94 | 1.91 | 2.47 | 1.81 |
| Amplified total load (MN) | 15.1 | 23.8 | 19.3 | 21.7 |
| Amplified total moment (MN·m) | 877 | 1145 | 1117 | 928 |

The largest dynamic amplification is observed in Combination 1 because this combination considers smallest waves compared to other combinations. On the contrary, Combinations 2 and 4 have the smallest dynamic amplification. Yet, these remain the combinations with largest lateral load demands because they already consider 50-year extreme wave height scenario.

Amplified loads have lower moment arms compared to non-amplified loads because only the wave loads are amplified.

**Step 4: Comparison of pile capacity and amplified loads/moments**

The last step is the comparison of ultimate pile capacity (Step 1) with amplified loads and moments (Step 3) to ensure pile has sufficient capacity under extreme lateral loads.

As noted in the previous step, dynamic amplification reduces the moment arm despite increasing loads and moments. As a result, pile capacity increases. However, if the pile length is shortened, natural frequency changes as well, which changes the forces once more. This means there is an iterative process requiring detailed modeling of wave-pile interaction. Yet, since this thesis focuses on preliminary dimensioning, this iteration is ignored, and pile capacities are taken as ones calculated in Step 1.

Table 4.10. Safety Check for the Example Monopile

| | **C1** | **C2** | **C3** | **C4** |
|---|---|---|---|---|
| Pile capacity (Table 4.7) | 18.1 MN | 23.8 MN | 20.0 MN | 24.0 MN |
| Amplified load (Table 4.9) | 15.1 MN | 23.8 MN | 19.3 MN | 21.7 MN |
| Is pile safe? | Yes | Yes | Yes | Yes |

From Table 4.10, the example monopile can be concluded as safe against extreme loads. Therefore, calculations will proceed with SLS checks.

#### 4.7.1.2 Serviceability Limit State (SLS) Checks

In this limit state, no pile capacity is needed. Thus, calculations start from natural frequency estimations. At the end, deflection and rotation at pile head will be checked under amplified loads.

**Step 1: SLS Natural frequency**

Similar with ULS, natural frequencies are estimated (Table 4.11).

Table 4.11. Estimated SLS Natural Frequencies for the Example Monopile

| | **C1** | **C2** | **C3** | **C4** |
|---|---|---|---|---|
| Load ($MN$) | 3832 | 9959 | 7739 | 9144 |
| Moment ($MN \cdot m$) | 325083 | 582217 | 649007 | 425747 |
| $K_L$ $(MN/m)$ | 432.7 | 281.4 | 287.0 | 327.5 |
| $K_{LR}$ $(MN)$ | -12792 | -9812 | -9893 | -10882 |
| $K_R$ $(MN \cdot m/rad)$ | 491614 | 423876 | 426306 | 456066 |
| Natural frequency (Hz) | 0.247 | 0.239 | 0.240 | 0.243 |

From allowable natural frequency point of view, ULS is the more critical limit state. This is because both partial load and resistance factors tend to increase foundation deformations, which causes lower natural frequency.

**Step 2: SLS amplified loads and moments**

Amplified loads are amplified as the same way as Ultimate Limit State.

Table 4.12. Amplified SLS Loads and Moments Acting on the Example Monopile

| | **C1** | **C2** | **C3** | **C4** |
|---|---|---|---|---|
| Natural freq. (Hz) | 0.247 | 0.239 | 0.240 | 0.243 |
| Wave frequency (Hz) | 0.182 | 0.093 | 0.121 | 0.093 |
| Non-amplified total load (MN) | 3.83 | 9.96 | 7.74 | 9.28 |
| Non-amplified total moment (MN·m) | 325.1 | 582.2 | 649.0 | 447.8 |

Table 4.12 (cont'd)

| | **C1** | **C2** | **C3** | **C4** |
|---|---|---|---|---|
| DAF | 2.17 | 1.18 | 1.34 | 1.17 |
| **Amplified total load (MN)** | **6.75** | **11.44** | **9.35** | **10.55** |
| **Amplified total moment (MN·m)** | **454.5** | **633.8** | **710.0** | **473.7** |

**Step 3: Pile head deflection and rotation**

In the last step, LPILE analysis is performed to estimate pile head deflection and rotation under amplified loads. The results are presented in Table 4.13.

Table 4.13. Pile Head Deflection and Rotation of the Example Monopile

| | **C1** | **C2** | **C3** | **C4** |
|---|---|---|---|---|
| Deflection (m) | 0.139 | 0.286 | 0.276 | 0.194 |
| Rotation (°) | 0.27 | 0.48 | 0.48 | 0.35 |

The pile satisfies requirements under Combinations 1 and 4. However, Combinations 2 and 3 have lateral deflections larger than 20 cm, therefore SLS requirements are not satisfied. Notice that pile head rotation is within allowable limits in each combination, so lateral deflection turns out to be more critical.

**Step 4: Change the pile length and repeat Steps 1 – 3**

Since the design is not satisfactory against SLS requirements, pile length will be increased to reduce the lateral deflection and rotation. The pile length is increased with 3 m increments, and repeating Steps 1 – 3, lateral deflection and rotation values are plotted in Figure 4.12.

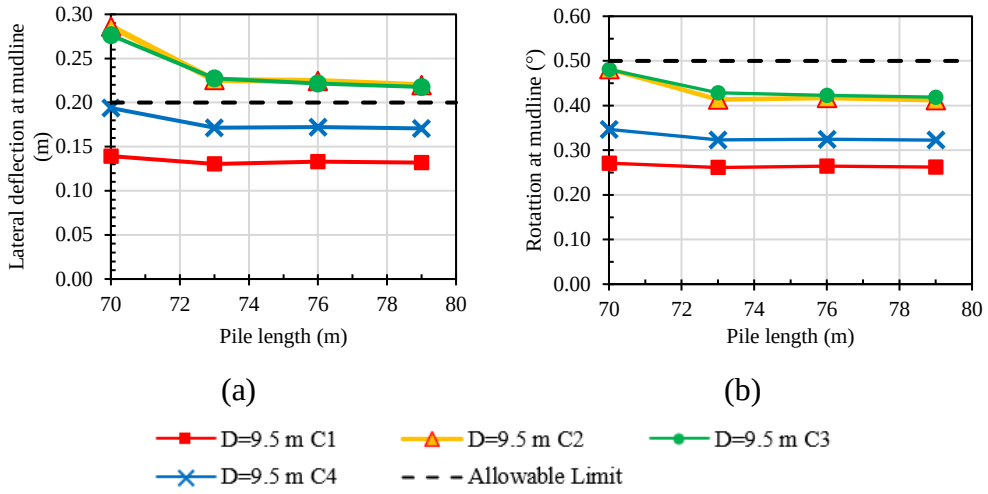



Figure 4.12. (a) Pile Head Deflection and (b) Rotation Values for Increased Pile Lengths for the Example Monopile

As observed from Figure 4.12, increasing the length to 73 m makes an improvement, however further increase does not because pile starts to behave in a flexible manner where the lateral load is not transferred to the pile tip. As a result, it can be understood that further increasing pile length will not help. The remedy is to increase the pile diameter, which falls outside the studied cases in this thesis.

Therefore, using currently recommended methods, no monopile with 9.5 m diameter is possible on Soil Profile 1.

### 4.7.2 Summary of Results

In this section, resulting pile diameters are summarized separately for Ultimate Limit State (ULS) and Serviceability Limit State (SLS). At the end, suggested monopiles are presented which has satisfactory performance for both limit states.

#### 4.7.2.1 Ultimate Limit State (ULS)

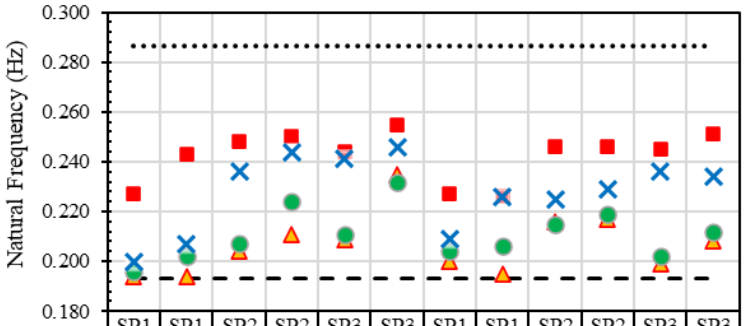
Complete details have been provided in Appendix D, which includes analysis results used to find ultimate pile capacity.

Before comparing load demands and pile capacities, natural frequencies will be discussed as stated in the previous section, natural frequency is more critical in Ultimate Limit State.

However, following figures include some abbreviations, which are explained as follows:

- SP : Soil Profile
- CUR/JJ : Current recommendations / Jeanjean et al. (2022)
- There are two numbers given under either CUR or JJ abbreviation. Thsese numbers give pile length and diameter in meters, respectively.

For example, first column in Figure 4.13 reads: Soil Profile 1 using Current recommendations for a pile length: 73 m and pile diameter: 8.5 m.



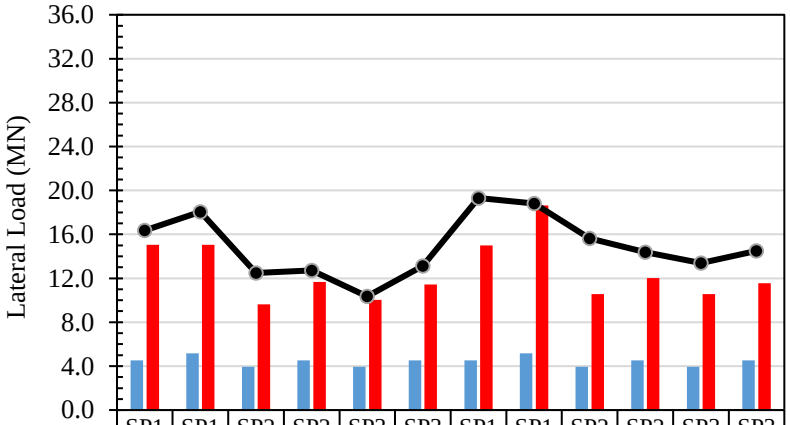

| | SP1 CUR 73 8.5 | SP1 CUR 70 9.5 | SP2 CUR 44 7.5 | SP2 CUR 43 8.5 | SP3 CUR 47 7.5 | SP3 CUR 46 8.5 | SP1 JJ 52 8.5 | SP1 JJ 50 9.5 | SP2 JJ 31 7.5 | SP2 JJ 30 8.5 | SP3 JJ 37 7.5 | SP3 JJ 36 8.5 |
|---|---|---|---|---|---|---|---|---|---|---|---|---|
| C1 | 0.227 | 0.243 | 0.248 | 0.250 | 0.244 | 0.255 | 0.227 | 0.226 | 0.246 | 0.246 | 0.245 | 0.251 |
| C2 | 0.194 | 0.194 | 0.204 | 0.211 | 0.209 | 0.235 | 0.200 | 0.195 | 0.216 | 0.217 | 0.199 | 0.208 |
| C3 | 0.196 | 0.202 | 0.207 | 0.224 | 0.211 | 0.232 | 0.204 | 0.206 | 0.215 | 0.219 | 0.202 | 0.212 |
| C4 | 0.200 | 0.207 | 0.236 | 0.244 | 0.241 | 0.246 | 0.209 | 0.226 | 0.225 | 0.229 | 0.236 | 0.234 |
| Allowable Minimum Limit | 0.193 | 0.193 | 0.193 | 0.193 | 0.193 | 0.193 | 0.193 | 0.193 | 0.193 | 0.193 | 0.193 | 0.193 |
| Allowable Maximum Limit | 0.286 | 0.286 | 0.286 | 0.286 | 0.286 | 0.286 | 0.286 | 0.286 | 0.286 | 0.286 | 0.286 | 0.286 |

Figure 4.13. Estimated Natural Frequencies of the Design Cases

It is reminded that fixed base natural frequency is 0.27 Hz for LW 8MW turbine. Therefore, it is seen that foundation deformability reduction of natural frequency at least by 0.015 Hz (5.6%). In general, the following trends are observed.

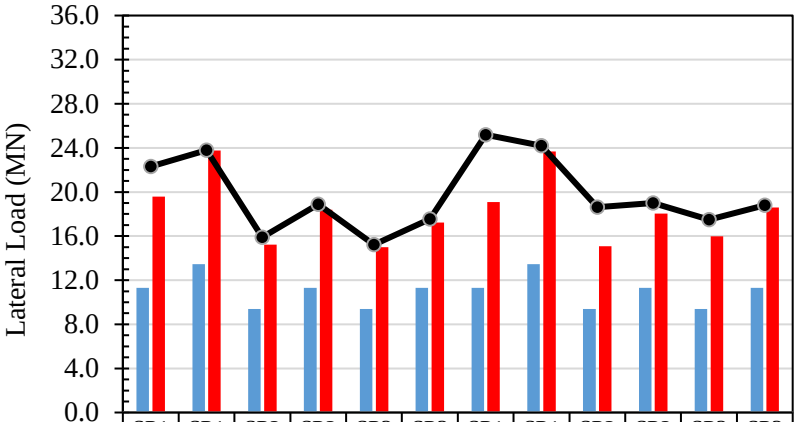
- Lowest natural frequency values are obtained in monopiles over Soil Profile 1. Yet, there is no pile violating the natural frequency requirement.
- Combination 1 results in highest natural frequencies whereas Combinations 2 & 3 yields the lowest. This is due to the non-linear behavior of soil. Combination 4 takes an intermediate value between the othe load combinations.
- Irregularities in behavior are estimated due to from iteration convergence limits in LPILE.

Detailed ultimate limit comparisons are presented in Figure 4.14 - Figure 4.17.



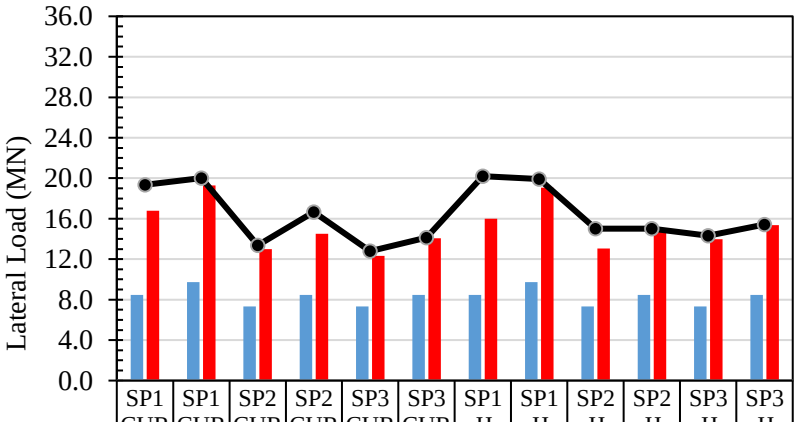

| | SP1 CUR 73 8.5 | SP1 CUR 70 9.5 | SP2 CUR 44 7.5 | SP2 CUR 43 8.5 | SP3 CUR 47 7.5 | SP3 CUR 46 8.5 | SP1 JJ 52 8.5 | SP1 JJ 50 9.5 | SP2 JJ 31 7.5 | SP2 JJ 30 8.5 | SP3 JJ 37 7.5 | SP3 JJ 36 8.5 |
|---|---|---|---|---|---|---|---|---|---|---|---|---|
| Non-amplified demand | 4.5 | 5.2 | 3.9 | 4.5 | 3.9 | 4.5 | 4.5 | 5.2 | 3.9 | 4.5 | 3.9 | 4.5 |
| Amplified demand | 15.0 | 15.1 | 9.6 | 11.7 | 10.0 | 11.4 | 15.0 | 18.6 | 10.6 | 12.0 | 10.6 | 11.6 |
| Capacity | 16.4 | 18.1 | 12.5 | 12.7 | 10.4 | 13.1 | 19.3 | 18.8 | 15.6 | 14.4 | 13.4 | 14.5 |

Figure 4.14. Ultimate Limit State Load Demands and Pile Capacities for Load Combination 1



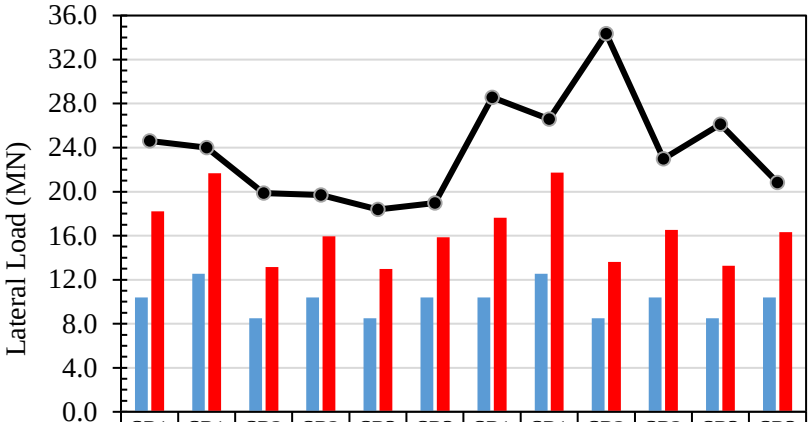

| | SP1 CUR 73 8.5 | SP1 CUR 70 9.5 | SP2 CUR 44 7.5 | SP2 CUR 43 8.5 | SP3 CUR 47 7.5 | SP3 CUR 46 8.5 | SP1 JJ 52 8.5 | SP1 JJ 50 9.5 | SP2 JJ 31 7.5 | SP2 JJ 30 8.5 | SP3 JJ 37 7.5 | SP3 JJ 36 8.5 |
|---|---|---|---|---|---|---|---|---|---|---|---|---|
| Non-amplified demand | 11.3 | 13.5 | 9.4 | 11.3 | 9.4 | 11.3 | 11.3 | 13.5 | 9.4 | 11.3 | 9.4 | 11.3 |
| Amplified demand | 19.6 | 23.8 | 15.2 | 18.4 | 15.0 | 17.2 | 19.1 | 23.7 | 15.1 | 18.0 | 16.0 | 18.6 |
| Capacity | 22.3 | 23.8 | 15.9 | 18.9 | 15.2 | 17.5 | 25.2 | 24.2 | 18.6 | 19.0 | 17.5 | 18.8 |

Figure 4.15. Ultimate Limit State Load Demands and Pile Capacities for Load Combination 2




| | SP1 CUR 73 8.5 | SP1 CUR 70 9.5 | SP2 CUR 44 7.5 | SP2 CUR 43 8.5 | SP3 CUR 47 7.5 | SP3 CUR 46 8.5 | SP1 JJ 52 8.5 | SP1 JJ 50 9.5 | SP2 JJ 31 7.5 | SP2 JJ 30 8.5 | SP3 JJ 37 7.5 | SP3 JJ 36 8.5 |
|---|---|---|---|---|---|---|---|---|---|---|---|---|
| Non-amplified demand | 8.5 | 9.7 | 7.3 | 8.5 | 7.3 | 8.5 | 8.5 | 9.7 | 7.3 | 8.5 | 7.3 | 8.5 |
| Amplified demand | 16.8 | 19.3 | 13.0 | 14.5 | 12.3 | 14.1 | 16.0 | 19.1 | 13.1 | 14.8 | 14.0 | 15.4 |
| Capacity | 19.3 | 20.0 | 13.4 | 16.7 | 12.8 | 14.1 | 20.2 | 19.9 | 15.0 | 15.0 | 14.3 | 15.4 |

Figure 4.16. Ultimate Limit State Load Demands and Pile Capacities for Load Combination 3




| | SP1 CUR 73 8.5 | SP1 CUR 70 9.5 | SP2 CUR 44 7.5 | SP2 CUR 43 8.5 | SP3 CUR 47 7.5 | SP3 CUR 46 8.5 | SP1 JJ 52 8.5 | SP1 JJ 50 9.5 | SP2 JJ 31 7.5 | SP2 JJ 30 8.5 | SP3 JJ 37 7.5 | SP3 JJ 36 8.5 |
|---|---|---|---|---|---|---|---|---|---|---|---|---|
| Non-amplified loads | 10.4 | 12.5 | 8.5 | 10.4 | 8.5 | 10.4 | 10.4 | 12.5 | 8.5 | 10.4 | 8.5 | 10.4 |
| Amplified loads | 18.2 | 21.7 | 13.1 | 15.9 | 13.0 | 15.9 | 17.6 | 21.7 | 13.6 | 16.5 | 13.3 | 16.3 |
| Capacity | 24.6 | 24.0 | 19.9 | 19.7 | 18.4 | 19.0 | 28.6 | 26.6 | 34.4 | 23.0 | 26.1 | 20.8 |

Figure 4.17. Ultimate Limit State Load Demands and Pile Capacities for Load Combination 4

Load Combination 1, called “normal operation conditions” is characterized by having both the lowest loads and pile capacity. However, it does not make this combination a negligible one. Significant dynamic amplification of forces can be observed. In most cases, lateral load is amplified by about 3-4 times (only the waves are amplified, so dynamic amplification factor turns out to be more). Load Combinations 2 & 3 are the most critical ones in almost all design cases. Load Combination 4 turns out to be the least critical load combination, which might be considered as ironic because wind speed of 90 km/h is considered in this combination. However, as stated before, wind force is at lowest due to significantly lower drag coefficient.

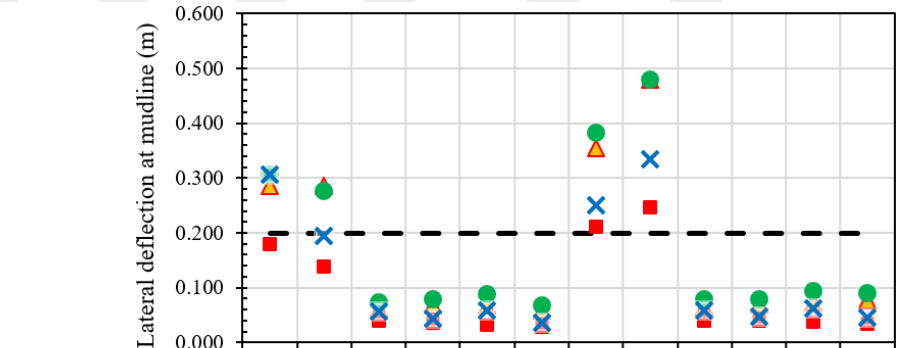
In general, all of the presented piles have sufficient capacity. Therefore, these piles are satisfactory for ULS requirements, and dimensions of these piles are summarized in Table 4.14.

Table 4.14. Monopile Penetration Depths Satisfying ULS Requirements

| | **Soil Profile 1** | | **Soil Profile 2** | | **Soil Profile 3** | |
|---|---|---|---|---|---|---|
| **Pile diameter (m)** | **8.5** | **9.5** | **7.5** | **8.5** | **7.5** | **8.5** |
| Current practice | 73 m | 70 m | 44 m | 43 m | 47 m | 46 m |
| Jeanjean et al. (2022) | 52 m | 50 m | 31 m | 30 m | 37 m | 36 m |

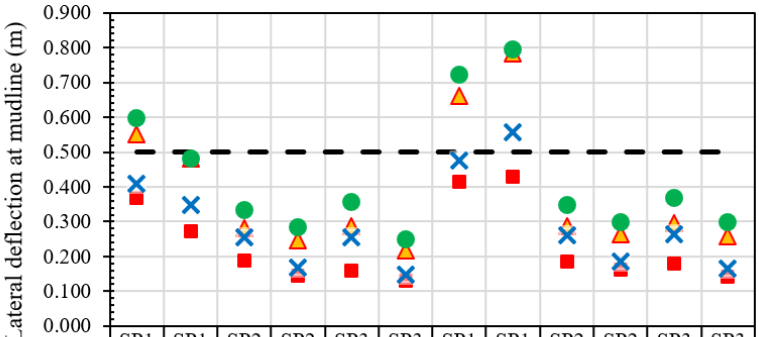
#### 4.7.2.2 Serviceability Limit State (SLS)

Although detailed analysis results have been provided in Appendix E, a summary has been provided in Figure 4.18 - Figure 4.19. As a reminder, studied piles are the shortest ones that satisfy ULS requirements.




| | SP1 CUR 73 8.5 | SP1 CUR 70 9.5 | SP2 CUR 44 7.5 | SP2 CUR 43 8.5 | SP3 CUR 47 7.5 | SP3 CUR 46 8.5 | SP1 JJ 52 8.5 | SP1 JJ 50 9.5 | SP2 JJ 31 7.5 | SP2 JJ 30 8.5 | SP3 JJ 37 7.5 | SP3 JJ 36 8.5 |
|---|---|---|---|---|---|---|---|---|---|---|---|---|
| C1 | 0.180 | 0.139 | 0.040 | 0.036 | 0.033 | 0.030 | 0.211 | 0.246 | 0.040 | 0.040 | 0.038 | 0.035 |
| C2 | 0.286 | 0.286 | 0.062 | 0.068 | 0.068 | 0.058 | 0.355 | 0.479 | 0.065 | 0.069 | 0.074 | 0.077 |
| C3 | 0.305 | 0.276 | 0.073 | 0.079 | 0.088 | 0.067 | 0.384 | 0.480 | 0.079 | 0.078 | 0.094 | 0.090 |
| C4 | 0.305 | 0.194 | 0.056 | 0.044 | 0.059 | 0.036 | 0.251 | 0.334 | 0.058 | 0.047 | 0.063 | 0.045 |
| Allowable Limit | 0.2 | 0.2 | 0.2 | 0.2 | 0.2 | 0.2 | 0.2 | 0.2 | 0.2 | 0.2 | 0.2 | 0.2 |

Figure 4.18. Summary of SLS Analysis Showing Lateral Deflection of Pile Head




| | SP1 CUR 73 8.5 | SP1 CUR 70 9.5 | SP2 CUR 44 7.5 | SP2 CUR 43 8.5 | SP3 CUR 47 7.5 | SP3 CUR 46 8.5 | SP1 JJ 52 8.5 | SP1 JJ 50 9.5 | SP2 JJ 31 7.5 | SP2 JJ 30 8.5 | SP3 JJ 37 7.5 | SP3 JJ 36 8.5 |
|---|---|---|---|---|---|---|---|---|---|---|---|---|
| C1 | 0.367 | 0.271 | 0.187 | 0.145 | 0.158 | 0.129 | 0.416 | 0.428 | 0.185 | 0.161 | 0.179 | 0.140 |
| C2 | 0.552 | 0.482 | 0.280 | 0.246 | 0.287 | 0.217 | 0.660 | 0.784 | 0.288 | 0.263 | 0.297 | 0.258 |
| C3 | 0.598 | 0.481 | 0.333 | 0.284 | 0.356 | 0.249 | 0.721 | 0.795 | 0.347 | 0.299 | 0.368 | 0.299 |
| C4 | 0.410 | 0.347 | 0.256 | 0.167 | 0.256 | 0.148 | 0.474 | 0.557 | 0.260 | 0.184 | 0.263 | 0.166 |
| Allowable Limit | 0.5 | 0.5 | 0.5 | 0.5 | 0.5 | 0.5 | 0.5 | 0.5 | 0.5 | 0.5 | 0.5 | 0.5 |

Figure 4.19. Summary of SLS Analysis Showing Rotation of Pile Head

The most interesting observation is that all piles in Soil Profiles in 2 & 3 satisfy SLS requirements although this is not the case for Soil Profile 1. The same conclusion can be drawn from both methods. Furthermore, in Soil Profile 1, Jeanjean et al. (2022) estimates larger deflections at pile head compared to current recommendations. However, it should be remembered that Jeanjean et al. (2022) analysis is done for much shorter piles.

As consistent with ULS analysis, Load Combinations 2 & 3 are the most critical ones as they produce the largest deflections.

In Section 4.7.1, it was shown that current methods do not provide an acceptable design in Soil Profile 1. Therefore, these will not be repeated here. Instead, Figure 4.20 visualizes the pile head deflections for 9.5 m diameter as no pile was found to be satisfactory with 8.5 m diameter.

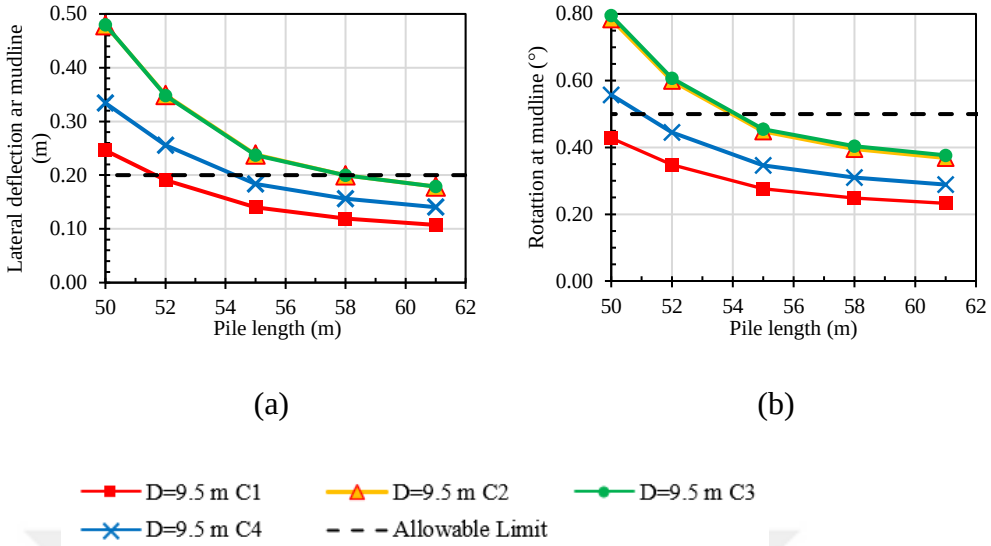



Figure 4.20. (a) Pile Head Deflection and (b) Rotation Values for Increased Pile Lengths (Jeanjean et al. (2022) Soil Profile 1 – D=9.5 m)

At the end, it is seen that when pile length is 58 m, both lateral deflection and rotation requirements are met. It can be noticed that lateral deflection criterion is found to be governing. It can be explained by the depth of the soft clay layer.

#### 4.7.2.3 Suggested Monopile Dimensions

In Table 4.15, monopile dimensions which satisfy both ULS and SLS requirements are summarized. Note that this thesis does not aim to find the most economical solution. Therefore, none of the piles will be recommended as "the solution".

Table 4.15. Concluded Preliminary Monopile Penetration Depths

| | **Soil Profile 1** | | **Soil Profile 2** | | **Soil Profile 3** | |
|---|---|---|---|---|---|---|
| **Pile diameter (m)** | **8.5** | **9.5** | **7.5** | **8.5** | **7.5** | **8.5** |
| Current practice | - | - | 44 m | 43 m | 47 m | 46 m |
| Jeanjean et al. (2022) | - | 58 m | 31 m | 30 m | 37 m | 36 m |

### 4.7.3 Comparison of Results

When two methods are compared, striking differences can be observed. Jeanjean et al. (2022) was already expected to result in lower pile lengths, but general highlights can be listed as follows:

- Savings in pile length is between 10-13 m or 20-30% on Soil Profiles 2 and 3 compared to current practice.
- Using current practice, a satisfactory design could not be reached for a 9.5 m diameter pile. However, Jeanjean et al. (2022) helped to reach a sufficient penetration depth of 58 m in Soil Profile 1, when pile diameter is 9.5 m. Still, this monopile is challenging in terms of logistics because it will need to have a total length of at least 108 m (58 m penetration depth + 50 m water depth).

In both methods, increasing the diameter do not result in significant reduction of pile length because wave loads increase with diameter. In ULS, partial load factors govern how much a pile can be shortened. On the other hand, SLS performance improves greatly by increasing diameter. This is exemplified in Figure 4.21, where two unsatisfactory cases have been compared.

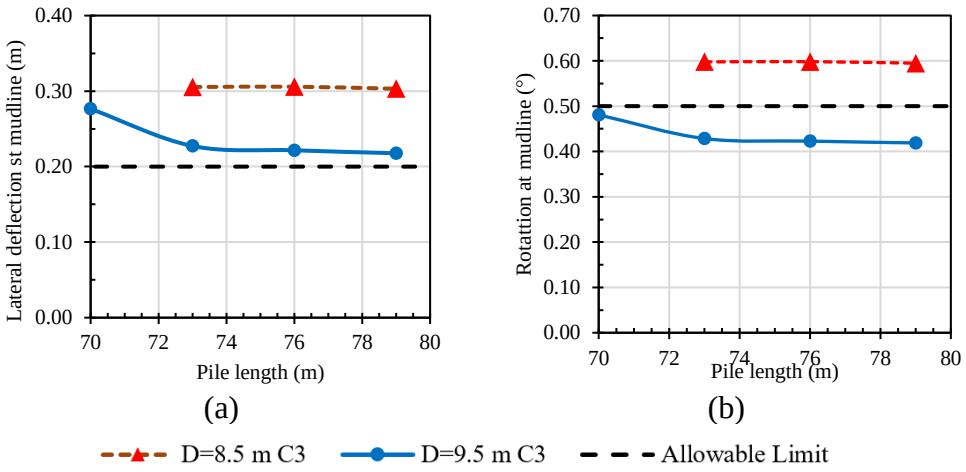



Figure 4.21. Effect of Diameter in Pile Head Deflection and Rotation (Soil Profile 1 – Current Recommendation – SLS – Load Combination 3)

It can be noted lateral deflections reduces from 30 cm to almost 20 cm increasing the pile diameter from 8.5 m to 9.5 m. Similarly, in terms of pile head rotation, 8.5 m diameter pile could not satisfy the allowable limit of 0.5°. However, increasing the dimeter helps to reduce the rotation almost by 50%.

Another similarity is related with simulated pile behaviors in Soil Profile 1 as illustrated in Figure 4.20. As a reminder, current practice curve does not represent a satisfactory design whilst Jeanjean et al. (2022) curve does.

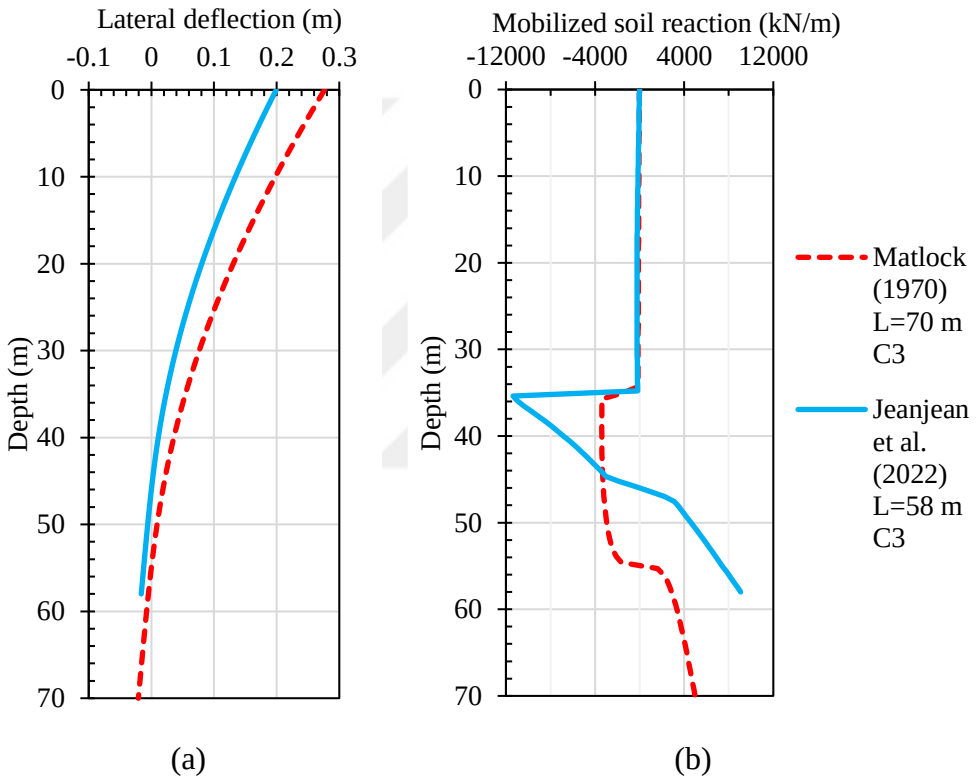



Figure 4.22. (a) Lateral Deflection and (b) Mobilized Soil Reactions for Example Comparison (SLS, Soil Profile 1, D=9.5 m)

For both cases, it can be observed that there is noticeable pile tip deflection, which is about 2 cm, however, slope of deflected shape is not constant. So, it is understood that both piles show translational behavior, i.e., not perfectly neither

rigid nor flexible. However, mobilized soil reactions in hard clay differ considerably. This was the typical pile behavior observed in most analysis.

Required pile lengths vary not only for chosen method but also the soil profiles. A special focus may be given into Soil Profiles 2 and 3, where the only difference is the order of medium dense and medium stiff clay layers.

The final noteworthy effect is related with governing limit states. In Soil Profile 1, the design is governed by Serviceability Limit State. Yet, Ultimate Limit State is more pronounced in Soil Profiles 2 & 3. The reason can be stated as the existence of very soft deep clay layer in Soil Profile 1. This layer did not have noteworthy contribution to the pile response, but it increases pile deformation.

As a final note, although Jeanjean et al. (2022) increases lateral bearing capacity factors, striking differences should not be attributed only to this. As different from current methods, Jeanjean et al. (2022) also models hardening soil at the vicinity of center of rotation under cyclic loads. This model is very likely to rely on assumption of small strains, which is more reasonable at flexible piles. Yet, it is understandable considering that Jeanjean et al. (2022) also concerns flexible piles, which are commonly utilized in offshore oil and gas platforms.

Furthermore, increase bearing capacity factors has a second effect on pile response. Since Jeanjean et al. (2022) estimates lower pile deflection and rotation, dynamic amplification factors will be lower. This further increases the differences between method.

# CHAPTER 5

# CONCLUSION AND FUTURE WORK

## 5.1 Conclusion

Within the scope of this thesis, site selection and conservative preliminary geotechnical designs of monopile have been performed for future offshore wind power plants (OWPPs) in Marmara Region, Türkiye. Marmara Region is studied due to its high wind speeds and hosting a large population whereas local electricity production is limited.

Site selection is done via implementation of Analytical Hierarchy Process (AHP) and Geographic Information Systems (GIS). GIS is utilized to detect potentially suitable sites by using open-source data for 15 site selection criteria. Based on literature review, threshold values for separating suitable and unsuitable sites have been decided. As a result, it is found that 5 regions in Marmara Region are potential candidates for OWPP implementations.

On the other hand, AHP helped in outranking of desirability of these alternative sites. As different from previous studies, where researchers had total control over relative weights of decision criteria, this thesis collected and analyzed opinions of 11 international experts via consensus analysis. Although experts had various backgrounds, analysis reached to a consensus. Expert opinions indicated that "electricity grid connection" is the most important site selection criterion. The second and third most important criteria are found as "average wind speed" and "environmental concerns". Then, 5 suitable regions have been compared pairwise in terms of each decision criterion. Combination of relative weights and alternative site comparison completed the outranking of 5 suitable regions. Site selection study confirmed previous studies to some extent as Bozcaada is concluded as the most

desirable site for an OWPP. However, previously overlooked regions such as Kıyıköy emerged as a strong candidate.

Then, the second part focused on a preliminary monopile design in Southern Marmara Sea, which is chosen due to offshore geotechnical data availability from a confidential report. Three idealized soil profiles have been obtained, each of which are about 1.5 km away from each other. It should be noted that only a limited amount of data was available without any cyclic laboratory tests.

Geotechnical properties of these profiles are found to vary significantly with challenging conditions such as 35 m deep very soft sensitive clays.

To support an 8 MW offshore wind turbine, preliminary monopile dimensioning for 12 cases (2 pile diameters in 3 idealized soil profiles utilizing 2 design recommendations) has been performed using currently recommended p-y curves and recently proposed p-y curves by Jeanjean et al. (2022). As Jeanjean et al. (2022) method is not yet implemented in common software like LPILE, which is used in this thesis, the method is applied on a spreadsheet first. Written spreadsheet has been validated, and then fed as input to LPILE. This study is one of the first applications of Jeanjean et al. (2022) methodology to the best knowledge of the author.

Results showed that monopile dimensions are likely to vary significantly in a future OWPP in Marmara Sea. For the studied soil profiles, suggested monopiles have penetration lengths between 30-58 m and diameters ranging between 7.5-9.5 m.

This may be the case even in a single OWPP because it was shown that soil conditions differ significantly in distances like 1.5 km. This is a short distance considering the general rule of thumb for spacing of individual turbines in the dominant wind direction is about 7 times the rotor diameter (164 m for LW 8 MW turbine) and 5 times the rotor diameter in the direction perpendicular to the dominant wind direction. Furthermore, challenging soil conditions like very thick very soft clay may be encountered, which would challenge current limits of the industry practice like Arcadis Ost 1 OWPP.

It is found that recently proposed offshore pile design methods would result in about 20-30% reduction in required pile penetration depth compared to the currently recommended practice. More interestingly, unlike current recommendations, using Jeanjean et al. (2022) method, a satisfactory preliminary design was obtained in challenging soil conditions. Still, this pile, whose total length is 108 m and diameter is 9.5 m, would be among the largest monopiles in the world if implemented. In general, reduction in monopile penetration depth is expected to help offshore wind energy be more competitive economically.

Also, this study shows that dynamic amplification may be an important design concern in Turkish waters because waves as noticeably smaller when compared to the North Sea. It results in coincidence of wave periods and allowable natural frequencies. This issue may be overcome though by careful dimensioning or implementing mass dampers on turbines.

## 5.2 Future Work

Although it is hoped that this thesis will be a valuable resource for helping future OWPP planning and design process in Marmara Sea, there are noteworthy limitations. These limitations can be overcome by the suggested future works below:

- Sensitivity analysis (e.g. considering different weights for criteria) for obtained relative weights can be performed to investigate the effects of relative weights on the outranking of suitable areas. This is because each MCDM method inevitably includes subjectivity although it is believed that asking multiple expert opinions may reduce this subjectivity.
- Observation and recording offshore met-ocean data such as wind and wave data for the alternative sites. This will give reliable data to estimate energy production and loads that must be resisted by foundations, including the effect of dynamic amplification.
- More detailed social acceptability studies and bird migration route observations are needed at the local level.

- Detailed geophysical and geotechnical site investigation programs should be conducted at the suggested alternative sites. These studies should include detailed identification of geohazards such as liquefaction, lateral spreading, submarine landslides and shallow gas.
- Suitability of foundation solutions other than monopiles should be studied if deep clays are encountered in the field. For example, jacket foundations may be more suitable for Soil Profile 1 as jacket foundations transfer lateral load on the turbine as axial loads to the foundation.
- Site specific earthquake hazard assessment is needed to be able to perform seismic design, which is a major concern in Marmara Sea. Monopile dimensions found in this study are likely to change based on seismic pile response analysis.
- Fatigue Limit State (FLS) analysis are needed. It may be a critical issue in Marmara Sea due to dynamic amplification.
- Cyclic laboratory tests such as cyclic triaxial and cyclic simple shear tests must be performed on soil samples taken from the recommended alternative sites. If these tests are performed under realistic load histories for Marmara Sea, which is to be obtained from meteorological measurements, accurate model parameters for Jeanjean et al. (2022) can be determined. This would enable fast, reliable and more economical designs compared to the current practice.

## REFERENCES


Abdel-Basset, M., Gamal, A., Chakrabortty, R. K., & Ryan, M. (2021). A new hybrid multi-criteria decision-making approach for location selection of sustainable offshore wind energy stations: A case study. *Journal of Cleaner Production*, *280*, 124462. https://doi.org/10.1016/j.jclepro.2020.124462

Akalın, S. (2018). *Açık Deniz Rüzgâr Enerjisi Türbinlerinin Kurulum Yeri Seçimi İçin Bir Model Önerisi*. Gazi University.

Allamehzadeh, H. (2017). Wind energy history, technology and control. *2016 IEEE Conference on Technologies for Sustainability, SusTech 2016*, 119–126. https://doi.org/10.1109/SusTech.2016.7897153

Altuzarra, A., Moreno-Jimenez, J. M., & Salvador, M. (2009). Searching for consensus in AHP-Group decision making. A Bayesian perspective. *Estadística Matemàtica*, 1–17.

American Petroleum Institute. (2014). *ANSI/API RECOMMENDED PRACTICE 2GEO-Specific requirements for offshore structures, Part 4-Geotechnical and foundation design considerations*.

Andersen, L. V., Vahdatirad, M. J., Sichani, M. T., & Sørensen, J. D. (2012). Natural frequencies of wind turbines on monopile foundations in clayey soils-A probabilistic approach. *Computers and Geotechnics*, *43*, 1–11. https://doi.org/10.1016/j.compgeo.2012.01.010

Anh Quang, M. (2012). *Design Monopile Foundation of Offshore Wind Turbines*. University of Liege & Vietnam Water Resources University.

Arany, L., Bhattacharya, S., MacDonald, J. H. G., & Hogan, S. J. (2015). A Critical Review of Serviceability Limit State Requirements for Monopile Foundations of Offshore Wind Turbines. *Proceedings of the Annual Offshore Technology Conference*, *4*, 2570–2587. https://doi.org/10.4043/25874-MS

Arany, L., Bhattacharya, S., Macdonald, J. H. G., & Hogan, S. J. (2016). Closed form solution of Eigen frequency of monopile supported offshore wind turbines in deeper waters incorporating stiffness of substructure and SSI. *Soil Dynamics and Earthquake Engineering*, *83*, 18–32. https://doi.org/10.1016/j.soildyn.2015.12.011

Arany, L., Bhattacharya, S., Macdonald, J., & Hogan, S. J. (2017). Design of monopiles for offshore wind turbines in 10 steps. *Soil Dynamics and Earthquake Engineering*, *92*, 126–152. https://doi.org/10.1016/j.soildyn.2016.09.024

Argin, M., Yerci, V., Erdogan, N., Kucuksari, S., & Cali, U. (2019). Exploring the offshore wind energy potential of Turkey based on multi-criteria site selection. *Energy Strategy Reviews*, *23*(March 2018), 33–46. https://doi.org/10.1016/j.esr.2018.12.005

Aydıner, İ. (2020). *CBS Tabanlı Analitik Hiyerarşi Yöntemi ile Ege Denizi'nde Rüzgâr ve Dalga Enerji Sistemleri İçin Yer Seçimi*. Ondokuz Mayis University, Turkey.

Bak, C., Zahle, F., Bitsche, R., Kim, T., Yde, A., Henriksen, L. C., Hansen, M. H., Blasques, J. P. A. A., Gaunaa, M., Natarajan, A. (2013). *The DTU 10-MW Reference Wind Turbine). The DTU 10-MW Reference Wind Turbine. Sound/Visual production (digital)*.

Bhattacharya, S. (2014). Challenges in Design of Foundations for Offshore Wind Turbines. *Engineering & Technology Reference*. https://doi.org/10.1049/etr.2014.0041

Bhattacharya, S. (2019). *Design of foundations for offshore wind turbines*. JohnWiley & Sons Ltd.

Bilgili, M., Yasar, A., & Simsek, E. (2011). Offshore wind power development in Europe and its comparison with onshore counterpart. *Renewable and Sustainable Energy Reviews*, *15*, 905–915. https://doi.org/doi:10.1016/j.rser.2010.11.006

Birdmap. (2021). *Major bird migration routes*. http://birdmap.5dvision.ee/en

Broms, B. B. (1964a). Lateral Resistance of Piles in Cohesionless Soils. *The Journal of the Soil Mechanics and Foundations*.

Broms, B. B. (1964b). Lateral Resistance of Piles in Cohesive Soils. *The Journal of the Soil Mechanics and Foundations*.

Buljan, A. (2021a, April 19). *Offshore Wind Costs in 2050 Could Be Lower than Previously Expected*. Offshore Wind. https://www.offshorewind.biz/2021/04/19/offshore-wind-costs-in-2050-could-be-lower-than-previously-expected/

Buljan, A. (2021b, October 8). *Seabed Issue Could Relocate Danish Offshore Wind Farm*. https://www.offshorewind.biz/2021/10/08/seabed-issue-could-relocate-danish-offshore-wind-farm/

Byrne, B. W., Houlsby, G. T., Burd, H. J., Gavin, K. G., Igoe, D. J. P., Jardine, R. J., Martin, C. M., McAdam, R. A., Potts, D. M., Taborda, D. M. G., & Zdravkovic, L. (2020). PISA design model for monopiles for offshore wind turbines: Application to a stiff glacial clay till. *Geotechnique*, *70*(11), 1030–1047. https://doi.org/10.1680/jgeot.18.P.255

Caceoğlu, E., Yildiz, H. K., Oğuz, E., Huvaj, N., & Guerrero, J. M. (2022). Offshore wind power plant site selection using Analytical Hierarchy Process for Northwest Turkey. *Ocean Engineering*, *252*, 111178. https://doi.org/10.1016/j.oceaneng.2022.111178

Cradden, L., Kalogeri, C., Barrios, I. M., Galanis, G., Ingram, D., & Kallos, G. (2016). Multi-criteria site selection for offshore renewable energy platforms. *Renewable Energy*, *87*, 791–806. https://doi.org/10.1016/j.renene.2015.10.035

Cuéllar, P. (2011). *Pile Foundations for Offshore Wind Turbines: Numerical and Experimental Investigations on the Behaviour under Short-Term and Long-Term Cyclic Loading*.

DEME Group. (2022, July 22). *Monopile Installation Completed at Arcadis Ost 1 Offshore Wind Farm*. Retrieved June 16, 2023, from https://www.deme-group.com/news/monopile-installation-completed-arcadis-ost-1-offshore-wind-farm

Desmond, C., Murphy, J., Blonk, L., & Haans, W. (2016). Description of an 8 MW reference wind turbine. *Journal of Physics: Conference Series*, *753*(9). https://doi.org/10.1088/1742-6596/753/9/092013

Det Norske Veritas. (2014). *DNV-OS-J101: Design of Offshore Wind Turbine Structures*. www.dnvgl.com.

Díaz, H., & Soares, C. G. (2021). A multi-criteria approach to evaluate floating offshore wind farms siting in the canary islands (Spain). *Energies*, *14*(4). https://doi.org/10.3390/en14040865

Dong, Q., & Saaty, T. L. (2014). An analytic hierarchy process model of group consensus. *Journal of Systems Science and Systems Engineering*, *23*(3), 362–374. https://doi.org/10.1007/s11518-014-5247-8

Duzcan, A., & Kara, Y. A. (2023). Offshore wind energy potential analysis of Turkish Marmara and Aegean seas. *International Journal of Environmental Science and Technology*, *20*(3), 5571–5584. https://doi.org/10.1007/s13762-022-04577-y

Emeksiz, C., & Demirci, B. (2019). The determination of offshore wind energy potential of Turkey by using novelty hybrid site selection method. *Sustainable Energy Technologies and Assessments*, *36*(October), 100562. https://doi.org/10.1016/j.seta.2019.100562

EMODnet Human Activities. (2019, March). *Vessel Density*. https://www.emodnet-humanactivities.eu/search-results.php?dataname=Vessel+Density+

EMODnet Human Activities. (2021). *Shipwrecks*. https://www.emodnet-humanactivities.eu/search-results.php?dataname=Ship+Wrecks

EMODnet Geology (2021). *EMODnet Map Viewer*. https://emodnet.ec.europa.eu/geoviewer/

Enerji Atlası. (2022). *Şehirlerin Elektrik Santrali Kurulu Güçleri ile Üretim ve Tüketim Bilgileri*. https://www.enerjiatlasi.com/sehir/

Ergin, M., Kapur, S., Karakaş, Z., Akca, E., Kangal, Ö., & Keskin, Ş. (1999). Grain size and clay mineralogy of Late Quaternary sediments on a tectonically active shelf, the southern Sea of Marmara: clues to hydrographic, tectonic and climatic evolution. *Geological Journal*, *34*, 199–210.

Esteban, M. D., Diez, J. J., López, J. S., & Negro, V. (2011). Why offshore wind energy?. *Renewable Energy*, *36*(2), 444–450. https://doi.org/10.1016/j.renene.2010.07.009

European MSP Platform. (2018). *Conflict fiche 1: Maritime tourism (incl. local communities) and offshore wind*. https://maritime-spatial-planning.ec.europa.eu/sites/default/files/sector/pdf/1_tourism_offshore_wind.pdf

Fetanat, A., & Khorasaninejad, E. (2015). A novel hybrid MCDM approach for offshore wind farm site selection: A case study of Iran. *Ocean and Coastal Management*, *109*, 17–28. https://doi.org/10.1016/j.ocecoaman.2015.02.005

Fleming, K., Weltman, A., Randolph, M., & Elson, K. (1985). *Piling Engineering*. Kluwer Academic Publishers.

GEBCO. (2021). *GEBCO - The General Bathymetric Chart of the Oceans*. https://www.gebco.net/

Genç, M. S., Karipoğlu, F., Koca, K., & Azgın, Ş. T. (2021). Suitable site selection for offshore wind farms in Turkey's seas: GIS-MCDM based approach. *Earth Science Informatics*, *14*(3), 1213–1225. https://doi.org/10.1007/s12145-021-00632-3

Gilbert, R. B., Wang, S.-T., Senanayake, A., & Rendon, E. (2015). *Design of Wind Turbine Monopiles for Lateral Loads*. https://www.boem.gov/sites/default/files/renewable-energy-program/Studies/TAP/757AA.pdf.

Global Fishing Watch. (2021). *Datasets and Code: Fishing effort*. https://globalfishingwatch.org/dataset-and-code-fishing-effort/

*Global Wind Atlas*. (n.d.). Retrieved June 8, 2022, from https://globalwindatlas.info/download/maps-country-and-region

Global Wind Energy Council. (2021). *Global Offshore Wind Report 2021*. www.gwec.net

Guinan, J., McKeon, C., O'Keeffe, E., Monteys, X., Sacchetti, F., Coughlan, M., & Nic Aonghusa, C. (2021). INFOMAR data supports offshore energy development and marine spatial planning in the Irish offshore via the EMODnet Geology portal. *Quarterly Journal of Engineering Geology and Hydrogeology*, *54*(1), 2020-033.

Güzel, B. (2012). *Açık Deniz Rüzgar Enerjisi, Fizibilite Adımları ile Bozcaada ve Gökçeada Örnek Çalışması*. https://polen.itu.edu.tr/bitstream/11527/12875/1/301091038.pdf

Haiderali, A. E., & Madabhushi, G. S. P. (2013). Evaluation of the p-y method in the design of monopiles for offshore wind turbines. *Offshore Technology Conference, Proceedings*, *3*, 1824–1844. https://doi.org/10.4043/24088-ms

Hermans, K. W., & Peeringa, J. M. (2016). *Future XL monopile foundation design for a 10 MW wind turbine in deep water*.

Hong, L., & Möller, B. (2011). *Offshore wind energy potential in China: Under technical, spatial and economic constraints*. https://doi.org/10.1016/j.energy.2011.03.071

Irawan, C. A., Ouelhadj, D., Jones, D., Stålhane, M., & Sperstad, I. B. (2017). Optimisation of maintenance routing and scheduling for offshore wind farms. *European Journal of Operational Research*, *256*(1), 76–89. https://doi.org/10.1016/j.ejor.2016.05.059

Isenhower, W. M., Shin-Tower, P. E., Wang, P. E. L., & Gonzalo Vasquez, P. E. (2019). *Technical Manual for LPile 2019 (Using Data Format Version 11) A Program for the Analysis of Deep Foundations Under Lateral Loading*.

Isiacik Colak, T. A., Senel, G., & Goksel, C. (2021). GIS-based maritime spatial planning for site selection of offshore wind farms with exergy efficiency analysis: A case study. *International Journal of Exergy*, *34*(2), 255–268. https://doi.org/10.1504/IJEX.2021.113008

Jay, S. (2009). Planners to the rescue: Spatial planning facilitating the development of offshore wind energy. *Marine Pollution Bulletin*.

Jeanjean, P. (2009). Re-Assessment of P-Y Curves for Soft Clays from Centrifuge Testing and Finite Element Modeling. *Offshore Technology Conference*. http://onepetro.org/OTCONF/proceedings-pdf/09OTC/All-09OTC/OTC-20158-MS/1760108/otc-20158-ms.pdf/1

Jeanjean, P., Zakeri, A., Zhang, Y., & Andersen, K. H. (2022). The New ISO/API P-Y Curves in Clays and their Reconciliation with the PISA Framework. *Proceedings of the Annual Offshore Technology Conference*. https://doi.org/10.4043/31860-MS

Kaldellis, J. K., & Zafirakis, D. (2011). The wind energy (r)evolution: A short review of a long history. In *Renewable Energy* (Vol. 36, Issue 7, pp. 1887–1901). Elsevier Ltd. https://doi.org/10.1016/j.renene.2011.01.002

Karthikeyan, R., Venkatesan, K. G. S., & Chandrasekar, A. (2016). A Comparison of Strengths and Weaknesses for Analytical Hierarchy Process. *Journal of Chemical and Pharmaceutical Sciences*, *9*(3). www.jchps.com

KBA Partnership. (2021). *Key Biodiversity Areas GIS Data Request*. http://www.keybiodiversityareas.org/kba-data/request

Kim, C. K., Jang, S., & Kim, T. Y. (2018). Site selection for offshore wind farms in the southwest coast of South Korea. *Renewable Energy*, *120*, 151–162. https://doi.org/10.1016/J.RENENE.2017.12.081

Krolis, V. D., van der Tempel, J., & de Vries, W. E. (2007). *Evaluation of foundation design for monopile support structures for offshore wind turbines*.

Kutupoğlu, V., Çalışır, E., & Akpınar, A. (2023). Characterization and classification of wave storm events and wave climate on the Sea of Marmara. *Ocean Engineering*, *279*. https://doi.org/10.1016/j.oceaneng.2023.114448

Langemeyer, J., Gómez-Baggethun, E., Haase, D., Scheuer, S., & Elmqvist, T. (2016). Bridging the gap between ecosystem service assessments and land-use planning through Multi-Criteria Decision Analysis (MCDA). *Environmental Science and Policy*, *62*, 45–56. https://doi.org/10.1016/J.ENVSCI.2016.02.013

LeBlanc, C., Houlsby, G. T., & Byrne, B. W. (2010). Response of stiff piles in sand to long-term cyclic lateral loading. *Geotechnique*, *60*(2), 79–90. https://doi.org/10.1680/GEOT.7.00196

Lesny, K., & Richwien, W. (2011). Design, construction and installation of support structures. In J. D. Sørensen & J. N. Sørensen (Eds.), *Wind Energy Systems* (pp. 479–518). Woodhead Publishing.

Lesny, K., & Wiemann, J. (2005). Design Aspects of Monopiles in German Offshore Wind Farms. In M. Cassidy & S. Gourvenec (Eds.), *Proceedings of the International Symposium on Frontiers in Offshore Geotechnics* (pp. 383–389).

Lewis, M. (2023). *This record-breaking monopile is headed to the US's first commercial offshore wind farm*. https://electrek.co/2023/02/17/us-first-commercial-offshore-wind-farm-monopile/

Matlock, H. (1970), *Correlations for Design of Laterally Loaded Piles in Soft Clay*. In: Proc. 2nd Annual Offshore Technology Conf., OTC 1204, Houston, Texas, April, 1970.

Mayaki, E. A., Adedipe, O., & Lawal, S. A. (2018). Multi-Criteria Evaluation of the Appropriate Offshore Wind Farm Location in Nigeria. *IOP Conference Series: Materials Science and Engineering*, *413*(1). https://doi.org/10.1088/1757-899X/413/1/012041

Ministry of Energy and Natural Resources. (2022). *Türkiye Ulusal Enerji Planı*. https://enerji.gov.tr/Media/Dizin/EIGM/tr/Raporlar/TUEP/T%C3%BCrkiye_Ulusal_Enerji_Plan%C4%B1.pdf

MTA. (2013). *Yenilenmiş Diri Fay Haritaları*.

Murphy, G., Igoe, D., Doherty, P., & Gavin, K. (2018). 3D FEM approach for laterally loaded monopile design. *Computers and Geotechnics*, *100*, 76–83. https://doi.org/10.1016/j.compgeo.2018.03.013

Nasab, N. M., Kilby, J., & Bakhtiaryfard, L. (2022). Analysis and Design of Monopile Foundations for Offshore Wind and Tidal Turbine Structures. *Water 2022, Vol. 14, Page 3555*, *14*(21), 3555. https://doi.org/10.3390/W14213555

Negro, V., López-Gutiérrez J., Esteba, M. D., Alberdi, P., Imaz, M., Serraclara, J. (2017). Monopiles in offshore wind: Preliminary estimate of main dimensions. *Ocean Engineering, 133,* 253-261. https://doi.org/10.1016/j.oceaneng.2017.02.011.

New European Wind Atlas. (2022). *New European Wind Atlas 1.1*. https://map.neweuropeanwindatlas.eu/

Oguz, E. A., & Huvaj, N. (2020). Spatial probabilistic evaluation of offshore/nearshore sea bottom soils based on cone penetration tests. *Bulletin of Engineering Geology and the Environment*, *79*(2), 971–983. https://doi.org/10.1007/s10064-019-01608-w

Oguztimur, S. (2011). Why fuzzy analytic hierarchy process approach for transport problems? *European Regional Science Association*, *September*, 438. https://www.econstor.eu/bitstream/10419/120007/1/ERSA2011_0438.pdf

Oh, K. Y., Nam, W., Ryu, M. S., Kim, J. Y., & Epureanu, B. I. (2018). A review of foundations of offshore wind energy convertors: Current status and future perspectives. In *Renewable and Sustainable Energy Reviews* (Vol. 88, pp. 16–36). Elsevier Ltd. https://doi.org/10.1016/j.rser.2018.02.005

Open Street Map. (2021). *OpenStreetMap*. https://www.openstreetmap.org/#map=10/40.9721/29.4090

Orakcı, O. (2022). *How to Account For Uncertainty In Soil Properties In Offshore Monopile Design By Means Of Probabilistic Analysis*.

Ørsted. (2019). *Making green energy affordable: How the offshore wind energy industry matured-and what we can learn from it*. https://orsted.com/en/about-us/whitepapers/making-green-energy-affordable/1991-to-2001-the-first-offshore-wind-farms

Özdilim, A. M. (2017). *Türkiye'de Kurulabilecek Deniz Üstü Rüzgar Santrallerinin Teknik ve Ekonomik Analizi*. Yıldız Technical University.

Özhan, E., & Abdalla, S. (1999). *Türkiye Kıyıları için Rüzgar ve Derin Deniz Dalga Atlası*.

Page, A. M., Klinkvort, R. T., Bayton, S., Zhang, Y., & Jostad, H. P. (2021). A procedure for predicting the permanent rotation of monopiles in sand supporting offshore wind turbines. *Marine Structures, 75*. https://doi.org/10.1016/J.MARSTRUC.2020.102813

Parker, J., Castelli, R., Zelenko, B., O'Connor, R., Montesi, M., & Godfrey, E. (2018). *Geotechnical Engineering Circular: Design, Analysis, and Testing of Laterally Loaded Deep Foundations that Support Transportation Facilities*. U.S. Department of Transportation Federal Highway Administration. https://rosap.ntl.bts.gov/view/dot/62720

Peters, J. L., Remmers, T., Wheeler, A. J., Murphy, J., & Cummins, V. (2020). A systematic review and meta-analysis of GIS use to reveal trends in offshore wind energy research and offer insights on best practices. In *Renewable and Sustainable Energy Reviews* (Vol. 128). Elsevier Ltd. https://doi.org/10.1016/j.rser.2020.109916

Prendergast, L. J., & Gavin, K. (2016). A comparison of initial stiffness formulations for small-strain soil-pile dynamic Winkler modelling. *Soil Dynamics and Earthquake Engineering, 81*, 27–41. https://doi.org/10.1016/J.SOILDYN.2015.11.006

Providakis, S., Rogers, C. D. F., & Chapman, D. N. (2021). 3D spatiotemporal risk assessment analysis of the tunnelling-induced settlement in an urban area using analytical hierarchy process and BIM 3D spatiotemporal risk assessment analysis of the tunnelling-induced settlement in an urban area using analytical hierarchy process and BIM. *Georisk: Assessment and Management of Risk for Engineered Systems and Geohazards*. https://doi.org/10.1080/17499518.2021.1952607

Republic of Turkey Energy Market Regulatory Authority. (2017). *Devlet Hava Meydanları İşletmesi Genel Müdürlüğü Sorumluluğunda Hizmet Vermekte Olan Seyrüsefer Yardımcı Sistemlerine ve Hava/Yer Haberleşme İstasyonlarına İlişkin Bilgiler*. https://www.epdk.gov.tr/Detay/Icerik/4-348/dhmi-sorumlulugunda-hizmet-vermekte-olan-seyrusefer-yardimci-sistemlerine-ve-havayer-haberlesme-istasyonlarina-iliskin-bilgiler

Republic of Turkey Ministry of Interior. (2021, July 11). *Türkiye'nin Nüfus Haritası (in Turkish)*. https://www.icisleri.gov.tr/turkiyenin-nufus-haritasi-10072021

Robertson, P. K., & Cabal, K. L. (2012). *Guide to Cone Penetration Testing*. www.greggdrilling.com

Rocscience Inc. (2022). *RSPile- Laterally Loaded Piles Theory Manual*.

Saadatkhah, N., Kassim, A., Lee, •, & Lee, M. (2015). Susceptibility Assessment of Shallow Landslides in Hulu Kelang Area, Kuala Lumpur, Malaysia Using Analytical Hierarchy Process and Frequency Ratio. *Geological and Geotechnical Engineering*, *33*, 43–57. https://doi.org/10.1007/s10706-014-9818-8

Saaty, R. W. (1987). The analytic hierarchy process-what it is and how it is used. *Mathematical Modelling*, *9*(3–5), 161–176. https://doi.org/10.1016/0270-0255(87)90473-8

Saaty, T. L. (1980). *The Analytic Hierarchy Process*. McGraw-Hill, New York. - References- Scientific Research Publishing. https://doi.org/10.1016/b978-0-08-032599-6.50008-8

Senanayake, A. I. M. J. (2016). *Design of Large Diameter Monopiles for Offshore Wind Turbines in Clay*. The University of Texas at Austin.

SHARE Project. (2021). *Documents | SHARE*. http://www.share-eu.org/node/61.html

Spyridonidou, S., & Vagiona, D. G. (2020). Systematic review of site-selection processes in onshore and offshore wind energy research. *Energies*, *13*(22). https://doi.org/10.3390/en13225906

TEİAŞ. (2022). *Türkiye Elektrik Üretim-İletim İstatistikleri*. https://www.teias.gov.tr/turkiye-elektrik-uretim-iletim-istatistikleri

TeleGeography. (2022). *Submarine Cable Map*. https://www.submarinecablemap.com/

Tercan, E., Tapkın, S., Latinopoulos, D., Dereli, M. A., Tsiropoulos, A., & Ak, M. F. (2020). A GIS-based multi-criteria model for offshore wind energy power plants site selection in both sides of the Aegean Sea. *Environmental Monitoring and Assessment*, *192*(10). https://doi.org/10.1007/s10661-020-08603-9

The UK Maritime and Coastguard Agency. (2021). *MARINE GUIDANCE NOTE MGN 654 (M+F) Safety of Navigation: Offshore Renewable Energy Installations (OREIs)-Guidance on UK Navigational Practice, Safety and Emergency Response*. www.gov.uk/guidance/offshore

The United Kingdom Government. (2020, October 6). *New plans to make UK world leader in green energy*. https://www.gov.uk/government/news/new-plans-to-make-uk-world-leader-in-green-energy

Tricoli, C., Barsanti, M., & Delbono, I. (2006). Offshore wind farms along the Italian coasts: a first selection of suitable areas based on wind and bathymetric data. *Offshore Wind and Other Marine Renewable Energies in Mediterranean and European Seas. OWEMES, Civitavecchia (Rome) Italy, April 20-22, 2006.*, *April*, 93–102.

Turkish Naval Forces Office of Navigation Hydrography and Oceanography. (2021). *Annual Notices to Mariners*. https://www.shodb.gov.tr/shodb_esas/orj/2021_YILIK_e5be1.pdf

TurkStream. (2017). *TurkStream Natural Gas Pipeline-Offshore Section: Final EIA Report Turkey*. https://www.turkstream.info/r/9F7E28DC-996C-4C52-80A2-3C4024ABC98B/Final-Turkey-EIA-2017-ENG.pdf

Vagiona, D. G., & Karanikolas, N. M. (2012). A multicriteria approach to evaluate offshore wind farms siting in Greece. *Global Nest Journal*, *14*(2), 235–243. https://doi.org/10.30955/gnj.000868

Vardar, D., & Alpar, B. (2016). High-resolution seismic characterization of shallow gas accumulations in the southern shelf of Marmara Sea, Turkey. In *Acta Geophysica* (Vol. 64, Issue 3, pp. 589–609). De Gruyter Open Ltd. https://doi.org/10.1515/acgeo-2015-0059

Vasileiou, M., Loukogeorgaki, E., & Vagiona, D. G. (2017). GIS-based multi-criteria decision analysis for site selection of hybrid offshore wind and wave energy systems in Greece. *Renewable and Sustainable Energy Reviews*, *73*, 745–757. https://doi.org/10.1016/J.RSER.2017.01.161

Velarde, J. (2016). *Design of Monopile Foundations to Support the DTU 10 MW Offshore Wind Turbine*.

Wan, J.-H., Bai, R., Li, X.-Y., & Liu, S.-W. (2023). Natural Frequency Analysis of Monopile Supported Offshore Wind Turbines Using Unified Beam-Column Element Model. *Journal of Marine Science and Engineering*, *11*(3), 628. https://doi.org/10.3390/jmse11030628

Wang, M.; Wang, M.; Cheng, X.; Lu, Q.; Lu, J. (2022). A New p–y Curve for Laterally Loaded Large-Diameter Monopiles in Soft Clays. *Sustainability, 14*, 15102. https://doi.org/10.3390/su142215102

WindEurope. (2021). *Offshore Wind in Europe (2020)*. https://windeurope.org/intelligence-platform/product/offshore-wind-in-europe-key-trends-and-statistics-2020/

World Bank. (2019). *Going Global: Expanding Offshore Wind to Emerging Markets* (Issue October). https://documents1.worldbank.org/curated/en/716891572457609829/pdf/Going-Global-Expanding-Offshore-Wind-To-Emerging-Markets.pdf

Wu, Z., & Xu, J. (2012). A consistency and consensus based decision support model for group decision making with multiplicative preference relations. *Decision Support Systems*, *52*(3), 757–767. https://doi.org/10.1016/j.dss.2011.11.022

Yıldız, H. K. (2021). *Offshore wind farm site selection for Aegean and Mediterranean Sea, Turkey*. Middle East Technical University.

Yilmaz, I., & Üstünkaya, M. (2004). Unconsolidated clays from the inner shore of the Gemlik Gulf in the Marmara Sea (Bursa-Turkey). *Bulletin of Engineering Geology and the Environment*, *63*(2), 133–139. https://doi.org/10.1007/s10064-004-0229-6

Zabel, P. (2012). *Diplomarbeit ILR-RSN DA 12-03 System Analysis & Evaluation of Greenhouse Modules within Moon/Mars Habitats*.

Zlaugotne, B., Zihare, L., Balode, L., Kalnbalkite, A., Khabdullin, A., & Blumberga, D. (2020). Multi-Criteria Decision Analysis Methods Comparison. *Environmental and Climate Technologies*, *24*(1), 454–471. https://doi.org/10.2478/rtuect-2020-0028

# APPENDICES

## A. Site Selection AHP Questionnaire

**OFFSHORE WIND FARM SITE SELECTION IN TURKEY**

Please read this introduction before answering the questions.

This questionnaire consists of 31 questions. It would take about 15 minutes. It is approved by Middle East Technical University Human Subject Ethics Committee on15 April 2021.

This research is part of the "Offshore Wind Farms Large-Scale Integration in Turkey – WindFlag" project (www.windflag.et.aau.dk) funded by Danida Fellowship Centre and the Ministry of Foreign Affairs of Denmark to conduct research in growth and transition countries under the grant no. 19-M03-AAU.

This research aims to select the most suitable site for a potential offshore wind farm in Turkey carried out by Middle East Technical University (METU). It is planned to be published in an academic peer-reviewed journal.

Your answers, including the ones in this page, and identity will be kept confidential. However, the analysis results based on your answers will be non-confidential. Your participation in this questionnaire is completely voluntary. *We kindly ask not to share this questionnaire with other people.*

While answering, please keep in mind that areas having at least one of the following properties have already been excluded from the suitable areas for a potential offshore wind farm:

- Less than 6.5 m/s of average wind speed at 100 m height
- More than 100 m water depth (due to seabed slope being too high after 100 m depth in Turkey and note that suitability of floating foundations is also under consideration.)
- Nearer than 15 km to a civil/military airport
- Nearer than 1 km to internationally used shipping routes
- Nearer than 1 km to offshore natural gas/petroleum wells
- Nearer than 1 km to shipwrecks and unexploded objects
- Nearer than 750 m to undersea communication cables and pipelines
- Military areas
- MetOcean data will be considered in the design process

Analytical Hierarchy Process (AHP), requiring expert opinions on pairwise comparison of decision criteria, will be used in site selection. It is one of the Multi-Criteria Decision-Making methods.

In this method, based on their personal experiences, attendees of questionnaire compare the importance of all decision criteria (and sub-criteria if needed) pairwise in decision making. Using these answers, researchers quantitatively calculate relative weights of each decision criteria. These weights can be used to compare the suitability of different alternatives (possible offshore wind farm sites in this study) for the problem.

The decision criteria for this study are given in the next page.

You can ask your questions by e-mail to either eray.caceoglu@metu.edu.tr or kubra.yildiz@metu.edu.tr.

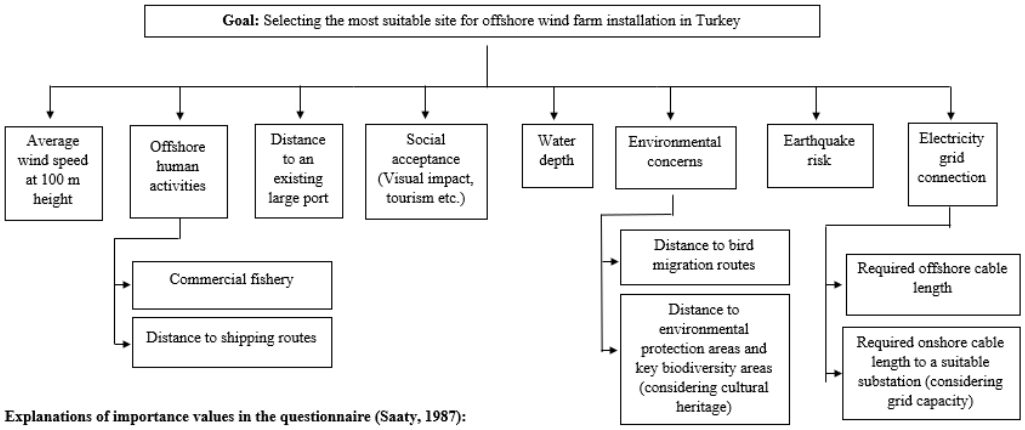
Thank you for your participation in the study.

**YOUR INFORMATION**

| | |
|---|---|
| Occupation | Click here to enter text. |
| Country where you live | Click here to enter text. |
| Field | Chose an item. |
| Professional experience | Choose an item. |
| Have you participated in an offshore wind farm site selection process? | Choose an item. |

Figure A1. Questionnaire Page 1

**Hierarchy formed in the study:**




**Explanations of importance values in the questionnaire (Saaty, 1987):**

| Importance value | Definition | Explanation |
|---|---|---|
| 1 | Equal importance | Two criteria have *equal* contribution on the decision. |
| 3 | Moderate importance | Experience and judgement *slightly* favour one criterion. |
| 5 | Strong importance | Experience and judgement *strongly* favour one criterion. |
| 7 | Very strong importance | *Evidence* favouring one criterion *exists* in the industry |
| 9 | Extreme importance | *Evidence* favours one criterion *at the highest level* possible |
| 2, 4, 6, 8 | Intermediate values in the case of compromise needed between two adjacent judgement | |

Figure A2. Questionnaire Page 2

**Questionnaire:** Based on your experience, please compare the relative importance of the main criteria given pairwise by *choosing one box in each row*.

| 1st criterion | 1st criterion is more important. | | | | | | | | Equal importance | 2nd criterion is more important. | | | | | | | | 2nd criterion |
|---|---|---|---|---|---|---|---|---|---|---|---|---|---|---|---|---|---|---|
| | 9 | 8 | 7 | 6 | 5 | 4 | 3 | 2 | 1 | 2 | 3 | 4 | 5 | 6 | 7 | 8 | 9 | |
| Average wind speed at 100 m | ☐ | ☐ | ☐ | ☐ | ☐ | ☐ | ☐ | ☐ | ☐ | ☐ | ☐ | ☐ | ☐ | ☐ | ☐ | ☐ | ☐ | Offshore human activity |
| Average wind speed at 100 m | ☐ | ☐ | ☐ | ☐ | ☐ | ☐ | ☐ | ☐ | ☐ | ☐ | ☐ | ☐ | ☐ | ☐ | ☐ | ☐ | ☐ | Distance to a large port |
| Average wind speed at 100 m | ☐ | ☐ | ☐ | ☐ | ☐ | ☐ | ☐ | ☐ | ☐ | ☐ | ☐ | ☐ | ☐ | ☐ | ☐ | ☐ | ☐ | Social acceptance |
| Average wind speed at 100 m | ☐ | ☐ | ☐ | ☐ | ☐ | ☐ | ☐ | ☐ | ☐ | ☐ | ☐ | ☐ | ☐ | ☐ | ☐ | ☐ | ☐ | Water depth |
| Average wind speed at 100 m | ☐ | ☐ | ☐ | ☐ | ☐ | ☐ | ☐ | ☐ | ☐ | ☐ | ☐ | ☐ | ☐ | ☐ | ☐ | ☐ | ☐ | Environmental concerns |
| Average wind speed at 100 m | ☐ | ☐ | ☐ | ☐ | ☐ | ☐ | ☐ | ☐ | ☐ | ☐ | ☐ | ☐ | ☐ | ☐ | ☐ | ☐ | ☐ | Earthquake risk |
| Average wind speed at 100 m | ☐ | ☐ | ☐ | ☐ | ☐ | ☐ | ☐ | ☐ | ☐ | ☐ | ☐ | ☐ | ☐ | ☐ | ☐ | ☐ | ☐ | Electricity grid connection |
| Offshore human activity | ☐ | ☐ | ☐ | ☐ | ☐ | ☐ | ☐ | ☐ | ☐ | ☐ | ☐ | ☐ | ☐ | ☐ | ☐ | ☐ | ☐ | Distance to a large port |
| Offshore human activity | ☐ | ☐ | ☐ | ☐ | ☐ | ☐ | ☐ | ☐ | ☐ | ☐ | ☐ | ☐ | ☐ | ☐ | ☐ | ☐ | ☐ | Social acceptance |
| Offshore human activity | ☐ | ☐ | ☐ | ☐ | ☐ | ☐ | ☐ | ☐ | ☐ | ☐ | ☐ | ☐ | ☐ | ☐ | ☐ | ☐ | ☐ | Water depth |
| Offshore human activity | ☐ | ☐ | ☐ | ☐ | ☐ | ☐ | ☐ | ☐ | ☐ | ☐ | ☐ | ☐ | ☐ | ☐ | ☐ | ☐ | ☐ | Environmental concerns |
| Offshore human activity | ☐ | ☐ | ☐ | ☐ | ☐ | ☐ | ☐ | ☐ | ☐ | ☐ | ☐ | ☐ | ☐ | ☐ | ☐ | ☐ | ☐ | Earthquake risk |
| Offshore human activity | ☐ | ☐ | ☐ | ☐ | ☐ | ☐ | ☐ | ☐ | ☐ | ☐ | ☐ | ☐ | ☐ | ☐ | ☐ | ☐ | ☐ | Electricity grid connection |
| Distance to a large port | ☐ | ☐ | ☐ | ☐ | ☐ | ☐ | ☐ | ☐ | ☐ | ☐ | ☐ | ☐ | ☐ | ☐ | ☐ | ☐ | ☐ | Social acceptance |
| Distance to a large port | ☐ | ☐ | ☐ | ☐ | ☐ | ☐ | ☐ | ☐ | ☐ | ☐ | ☐ | ☐ | ☐ | ☐ | ☐ | ☐ | ☐ | Water depth |
| Distance to a large port | ☐ | ☐ | ☐ | ☐ | ☐ | ☐ | ☐ | ☐ | ☐ | ☐ | ☐ | ☐ | ☐ | ☐ | ☐ | ☐ | ☐ | Environmental concerns |
| Distance to a large port | ☐ | ☐ | ☐ | ☐ | ☐ | ☐ | ☐ | ☐ | ☐ | ☐ | ☐ | ☐ | ☐ | ☐ | ☐ | ☐ | ☐ | Earthquake risk |
| Distance to a large port | ☐ | ☐ | ☐ | ☐ | ☐ | ☐ | ☐ | ☐ | ☐ | ☐ | ☐ | ☐ | ☐ | ☐ | ☐ | ☐ | ☐ | Electricity grid connection |
| Social acceptance | ☐ | ☐ | ☐ | ☐ | ☐ | ☐ | ☐ | ☐ | ☐ | ☐ | ☐ | ☐ | ☐ | ☐ | ☐ | ☐ | ☐ | Water depth |
| Social acceptance | ☐ | ☐ | ☐ | ☐ | ☐ | ☐ | ☐ | ☐ | ☐ | ☐ | ☐ | ☐ | ☐ | ☐ | ☐ | ☐ | ☐ | Environmental concerns |
| Social acceptance | ☐ | ☐ | ☐ | ☐ | ☐ | ☐ | ☐ | ☐ | ☐ | ☐ | ☐ | ☐ | ☐ | ☐ | ☐ | ☐ | ☐ | Earthquake risk |
| Social acceptance | ☐ | ☐ | ☐ | ☐ | ☐ | ☐ | ☐ | ☐ | ☐ | ☐ | ☐ | ☐ | ☐ | ☐ | ☐ | ☐ | ☐ | Electricity grid connection |
| Water depth | ☐ | ☐ | ☐ | ☐ | ☐ | ☐ | ☐ | ☐ | ☐ | ☐ | ☐ | ☐ | ☐ | ☐ | ☐ | ☐ | ☐ | Environmental concerns |
| Water depth | ☐ | ☐ | ☐ | ☐ | ☐ | ☐ | ☐ | ☐ | ☐ | ☐ | ☐ | ☐ | ☐ | ☐ | ☐ | ☐ | ☐ | Earthquake risk |
| Water depth | ☐ | ☐ | ☐ | ☐ | ☐ | ☐ | ☐ | ☐ | ☐ | ☐ | ☐ | ☐ | ☐ | ☐ | ☐ | ☐ | ☐ | Electricity grid connection |
| Environmental concerns | ☐ | ☐ | ☐ | ☐ | ☐ | ☐ | ☐ | ☐ | ☐ | ☐ | ☐ | ☐ | ☐ | ☐ | ☐ | ☐ | ☐ | Earthquake risk |
| Environmental concerns | ☐ | ☐ | ☐ | ☐ | ☐ | ☐ | ☐ | ☐ | ☐ | ☐ | ☐ | ☐ | ☐ | ☐ | ☐ | ☐ | ☐ | Electricity grid connection |
| Earthquake risk | ☐ | ☐ | ☐ | ☐ | ☐ | ☐ | ☐ | ☐ | ☐ | ☐ | ☐ | ☐ | ☐ | ☐ | ☐ | ☐ | ☐ | Electricity grid connection |

Figure A3. Questionnaire Page 3

Based on your experience, please compare the relative importance of the sub-criteria given pairwise by *choosing one box in each row*.

| 1st criterion | 1st criterion is more important. | | | | | | | | Equal importance | 2nd criterion is more important. | | | | | | | | 2nd criterion |
|---|---|---|---|---|---|---|---|---|---|---|---|---|---|---|---|---|---|---|
| | 9 | 8 | 7 | 6 | 5 | 4 | 3 | 2 | 1 | 2 | 3 | 4 | 5 | 6 | 7 | 8 | 9 | |
| Commercial fishery | ☐ | ☐ | ☐ | ☐ | ☐ | ☐ | ☐ | ☐ | ☐ | ☐ | ☐ | ☐ | ☐ | ☐ | ☐ | ☐ | ☐ | Distance to shipping routes |
| Distance to bird migration routes | ☐ | ☐ | ☐ | ☐ | ☐ | ☐ | ☐ | ☐ | ☐ | ☐ | ☐ | ☐ | ☐ | ☐ | ☐ | ☐ | ☐ | Distance to environmental protection areas and key biodiversity areas |
| Length of offshore cables | ☐ | ☐ | ☐ | ☐ | ☐ | ☐ | ☐ | ☐ | ☐ | ☐ | ☐ | ☐ | ☐ | ☐ | ☐ | ☐ | ☐ | Length of onshore cables to a suitable substation |

If you have any comments regarding this survey, please write them down here (optional).

Click here to enter text.

Thank you for your participation!

Figure A4. Questionnaire Page 4

## B. Wind Load Calculations

Table B1. Input parameters for wind load calculations

| Parameter | Value | Reference |
|---|---|---|
| Integral length scale, $L_k$ (m) | 340.2 | Det Norske Veritas (2014) |
| Reference turbulence, $I_{ref}$ | 0.18 | |
| Rated wind speed, $U_R$ (m/s) | 12.5 | Desmond et al. (2016) |
| Cut-out speed, $U_{cut}$ (m/s) | 25 | |
| Hub height, $z_{hub}$ (m) | 110 | |
| Rotor diameter, $D_{rot}$ (m) | 164 | |
| $f_{1,max}$ (Hz) | 0.175 | |
| Average wind speed, $U_{avg}$ (m/s) | 7.05 | New European Wind Atlas (2022) |
| Shape parameter, $S$ | 1.78 | Duzcan & Kara (2023) |
| Scale parameter, $K$ (m/s) | 7.93 | Modified from Duzcan & Kara (2023) |
| Water depth, $s$ (m) | 50 | GEBCO (2021) |

In their recent study, Duzcan & Kara (2023) calculated scale parameter as 10.32 m/s for an estimated average wind speed of 9.17 m/s. However, since the current study uses 7.05 m/s for long term average wind speed, scale parameter is linearly interpolated to find 7.93 m/s.

This appendix explains load calculations following Det Norske Veritas (2014) and International Electrochemical Commission (2005).

**Wind Case 1: Normal Turbulence (NTM) at Rated Wind Speed:**

$$\sigma_{u,NTM} = I_{ref}(0.75U_R + 5.6) = 2.70\ m/s$$

$$u_{NTM} = 1.28\sigma_{u,NTM}\sqrt{\frac{1}{\left(\frac{6L_k}{U_R}f_{1P,max} + 1\right)^{\frac{2}{3}}}} = 1.12\ m/s$$

Force: $F_{NTM} = 0.5 \times \rho_{air} A C_T (U_R + u_{NTM})^2, where\ C_T = 7/U_R$

$$F_{NTM} = 0.5 \times 1.23 \times \frac{\pi \times 164^2}{4} \times \frac{7}{12.5} \times (12.5 + 1.12)^2 \times 10^{-3} = 1349\ kN$$

Moment: $M_{NTM} = F_{NTM}(z_{hub} + s) = 1349 \times (110 + 50) = 215793\ kN \cdot m$

**Wind Case 2: Extreme Turbulence (ETM) at Rated Wind Speed:**

$$\sigma_{u,ETM} = 2I_{ref}\left[0.072\left(\frac{U_{avg}}{2} + 3\right)\left(\frac{U_R}{2} - 4\right) + 10\right] = 2.51\ m/s$$

$$u_{ETM} = 1.28\sigma_{u,ETM}\sqrt{\frac{1}{\left(\frac{6L_k}{U_R}f_{1P,max} + 1\right)^{\frac{2}{3}}}} = 2.51\ m/s$$

Force: $F_{ETM} = 0.5 \times \rho_{air}A(7/U_R)(U_R + u_{ETM})^2 = 1640\ kN$

Moment: $M_{NTM} = 1640 \times (110 + 50) = 288532\ kN \cdot m$

**Wind Case 3: Extreme Operating Gust (EOG) at Rated Wind Speed**

$$U_{10,50-year} = K\left[-\ln\left(1 - 0.98^{1/52596}\right)\right]^{\frac{1}{s}} = 36\ m/s$$

$$U_{10,1-year} = 0.8U_{10,1-year} = 28.8\ m/s$$

$$u_{EOG} = \min\left[1.35(U_{10,1-year} - U_R, \frac{3.3 \times 0.11U_{10,1-year}}{1 + \frac{0.1D_{rot}}{0.125L_k}}\right] = \min[22\ , 7.54] = 7.54\ m/s$$

Force: $F_{EOG,U_R} = 0.5 \times 1.23 \times \frac{\pi \times 164^2}{4} \times \frac{7}{12.5} \times (12.5 + 7.54)^2 \times 10^{-3} = 2923\ kN$

Moment: $M_{EOG_U_R} = 2923 \times (110 + 50) = 467665\ kN \cdot m$

**Wind Case 4: Extreme operating gust (EOG) at cut-out speed**

Using same equation with Case 3 but replacing $U_R$ with $U_{cut}$, $u_{EOG} = 5.13\ m/s$

Force: $F_{ETM} = 0.5 \times \rho_{air}A(7U_R^2/U_{cut}^3)(U_{cut} + u_{NTM})^2 = 963\ kN$

Moment: $M_{NTM} = 963 \times (110 + 50) = 154105\ kN \cdot m$

## C. Wave Load Calculations

Linear wave theory is applicable when pile diameter / wavelength ratio is less than 0.2. This condition is satisfied, so, Morison's equation can be used.

**Calculation Process:**

1. Wave frequency, $\omega$: $\omega = 2\pi/T$
2. Wave number, $k$, using wave frequency: $\omega = \sqrt{gk\ tanh(ks)}$, $s$: water depth
3. Wavelength, $L$, using wave number: $L = 2\pi/k > 5D_{pile}$
4. Unitless parameters ($P_D, Q_D, P_I, Q_I$) where $H$ denotes wave height:

$$P_D = \frac{e^{2k(s+0.5H)} - e^{-2k(s+0.5H)}}{8k} + \frac{s+0.5H}{2}$$

$$Q_D = \left(\frac{s+0.5H}{8k} - \frac{1}{16k^2}\right)e^{2k(s+0.5H)} - \left(\frac{s+0.5H}{8k} + \frac{1}{16k^2}\right)e^{-2k(s+0.5H)} + \left(\frac{s+0.5H}{2}\right)^2 + \frac{1}{8k^2}$$

$$P_I = \frac{sinh(k(s+0.5H))}{k}$$

$$Q_I = \left(\frac{s+0.5H}{2k} - \frac{1}{2k^2}\right)e^{k(s+0.5H)} - \left(\frac{s+0.5H}{2k} + \frac{1}{2k^2}\right)e^{-k(s+0.5H)} + \frac{1}{k^2}$$

5. Force and moment components (density of sea water is taken as $\rho_w$=1030 kg/m$^3$):
   - Maximum drag force:

$$F_{D,max} = \frac{1}{2}\rho_w D_{pile} C_D \frac{\pi^2 H^2}{T^2 \sinh^2(kS)} P_D$$

   - Maximum drag moment at seabed level:

$$M_{D,max} = \frac{1}{2}\rho_w D_{pile} C_D \frac{\pi^2 H^2}{T^2 \sinh^2(kS)} Q_D$$

   - Maximum inertia force:

$$F_{I,max} = \frac{1}{2}\rho_w D_{pile}^2 C_m \frac{\pi^3 H}{T^2 \sinh(kS)} P_I$$

- Maximum inertia moment at seabed level:

$$M_{I,max} = \frac{1}{2}\rho_w D_{pile}^2 C_m \frac{\pi^3 H}{T^2 \sinh(kS)} Q_I$$

6. Total force and moment:
   - $F_{max} = F_{D,max} + F_{I,max}$
   - $M_{max} = M_{D,max} + M_{I,max}$

Step 6 shows a conservative approach (including a summation of maximum wave load and moment) since maximum drag and inertia forces do not act at the same time. However, in this thesis, wave force is dominated by inertia forces, therefore, this approach is not expected to result in too much conservativeness.

Due to the same reason (since inertia forces dominate the problem), it was confirmed that inertia coefficient can be taken as 2, and effect of drag coefficient is negligible, which is taken as 1 conservatively. These values are based on common literature due to lack of publicly available site-specific measurements.

Meanwhile, a literature review has been carried out to select representative wave parameters (see Table C1).

Table C1. Literature review on wave parameters at northern shores of Kapıdağ Peninsula

| | **Kutupoğlu et al. (2023)** | **Özhan & Abdalla (1999)** |
|---|---|---|
| $H_s$ for 50-year storm (m) | 4.4 – 4.8 m | 4.6 – 4.9 (extrapolated) |
| $T_p$ for 50-year storm (s) | 6 s (for a "severe" storm) | 6.4 – 6.6 (extrapolated) |
| $H_s$ for 2-year storm (m) | 2.6 – 2.8 | ~3 m |
| $T_p$ for 2-year storm (m) | Not given | ~5.5 s when $H_s \approx 3$ m |

In this study, representative wave parameters are selected following Table C1. Table C2 summarizes the selected sea parameters. Using significant wave height ($H_s$) and peak period ($T_p$), maximum wave parameters are estimated from Det Norske Veritas (2014).

Table C2. Selected sea parameters

| | **Extreme Sea State** | | **Extreme Sea Height** | |
|---|---|---|---|---|
| | **2-year** | **50-year** | **2-year** | **50-year** |
| **Wave height (m)** | **2.8** | **4.8** | **5.45** | **9.24** |
| **Wave period (s)** | **5.5** | **6.5** | **8.3** | **10.8** |
| $\omega$ | 1.142397 | 0.966644 | 0.759188 | 0.583078 |
| $k$ | 0.133076 | 0.095293 | 0.059091 | 0.036515 |
| Wave length (m) | 48 | 66 | 106 | 172 |
| $P_D$ | 820474 | 28538 | 1102 | 212 |
| $Q_D$ | 39089078 | 1345105 | 48335 | 8401 |
| $P_I$ | 3511 | 774 | 190 | 99 |
| $Q_I$ | 154160 | 32526 | 7104 | 3440 |

Load calculations are presented in the following tables (Tables C3 – C5).

Table C3. Wave loads for $D_{pile} = 7.5\ m$

| | **Extreme Sea State** | | **Extreme Sea Height** | |
|---|---|---|---|---|
| **Return period** | **2-year** | **50-year** | **2-year** | **50-year** |
| $F_{D,max}$ (kN) | 54 | 173 | 199 | 651 |
| $F_{I,max}$ (kN) | 1505 | 2692 | 2845 | 4671 |
| $F_{max}$ (kN) | **1559** | **2865** | **3044** | **5322** |
| $M_{D,max}$ (kN·m) | 2567 | 8132 | 8730 | 25780 |
| $M_{I,max}$ (kN·m) | 66090 | 113201 | 106133 | 162692 |
| $M_{max}$ (kN·m) | **68657** | **121332** | **114863** | **188472** |

Table C4. Wave loads for $D_{pile} = 8.5\ m$

| | **Extreme Sea State** | | **Extreme Sea Height** | |
|---|---|---|---|---|
| **Return period** | **2-year** | **50-year** | **2-year** | **50-year** |
| $F_{D,max}$ (kN) | 61 | 196 | 226 | 738 |
| $F_{I,max}$ (kN) | 1934 | 3458 | 3654 | 6000 |
| $F_{max}$ (kN) | **1995** | **3653** | **3880** | **6737** |
| $M_{D,max}$ (kN·m) | 2909 | 9216 | 9894 | 29217 |
| $M_{I,max}$ (kN·m) | 84889 | 145400 | 136322 | 208969 |
| $M_{max}$ (kN·m) | **87798** | **154616** | **146215** | **238186** |

Table C5. Wave loads for $D_{pile} = 9.5\ m$

| | **Extreme Sea State** | | **Extreme Sea Height** | |
|---|---|---|---|---|
| **Return period** | **2-year** | **50-year** | **2-year** | **50-year** |
| $F_{D,max}$ (kN) | 68 | 219 | 252 | 824 |
| $F_{I,max}$ (kN) | 2415 | 4319 | 4564 | 7495 |
| $F_{max}$ (kN) | **2484** | **4538** | **4816** | **8319** |
| $M_{D,max}$ (kN·m) | 3252 | 10300 | 11058 | 32654 |
| $M_{I,max}$ (kN·m) | 106037 | 181624 | 170284 | 261031 |
| $M_{max}$ (kN·m) | **109289** | **191924** | **181342** | **293685** |

**Calculation of Number of Cycles**

**2-year Extreme Sea State:** $N = 3\ hr/5.5\ s = \mathbf{1964}$

**2-year Extreme Wave Height:** Extreme wave height represents a single wave with maximum wave height. So, it is unreasonable to expose the pile to this wave period for 3 hours. On the other hand, applying a monotonic load is not a realistic case either. Therefore, equivalent number of cycles may be estimated using wave energy equation (Jeanjean et al., 2022). Still, it is reminded that time domain analysis would give more reliable results.

$$E_{single\ wave} = \frac{\rho g H^2 L}{8} \rightarrow E_{total\ storm} = N\frac{\rho g H^2 L}{8}$$

For a 2-year storm,

$$N_1\frac{\rho g H_s^2 L_1}{8} = N_2\frac{\rho g H_m^2 L_2}{8} \rightarrow N_2 = N_1\frac{H_s^2 L_1}{H_m^2 L_2} = 1964\frac{2.8^2 \times 48}{5.45^2 \times 106} = \mathbf{234}$$

**50-year Extreme Wave Height:** Following the same procedure with previous case,

$$N = N_1\frac{H_s^2 L_1}{H_m^2 L_2} = \frac{10800}{6.5} \times \frac{4.8^2 \times 66}{9.24^2 \times 172} = \mathbf{172}$$

## D. LPILE Ultimate Limit State Analysis Results

### Design Case 1: Soil Profile 1 - Current Recommendations - L=73 m & D=8.5 m

Table D1. LPILE Analysis for Ultimate Pile Capacity in Design Case 1

| H (MN) | COMBINATION 1 | | | COMBINATION 2 | | | COMBINATION 3 | | | COMBINATION 4 | | |
|---|---|---|---|---|---|---|---|---|---|---|---|---|
| | M (MN*m) | y (m) | y/H (m/MN) | M (MN*m) | y (m) | y/H (m/MN) | M (MN*m) | y (m) | y/H (m/MN) | M (MN*m) | y (m) | y/H (m/MN) |
| 1 | 91 | 0.019 | 0.019 | 63 | 0.019 | 0.019 | 168 | 0.024 | 0.024 | 49 | 0.015 | 0.015 |
| 2 | 182 | 0.043 | 0.022 | 126 | 0.043 | 0.022 | 252 | 0.055 | 0.028 | 98 | 0.036 | 0.018 |
| 3 | 273 | 0.072 | 0.024 | 189 | 0.072 | 0.024 | 336 | 0.091 | 0.030 | 147 | 0.059 | 0.020 |
| 4 | 364 | 0.102 | 0.026 | 252 | 0.102 | 0.026 | 420 | 0.130 | 0.033 | 196 | 0.085 | 0.021 |
| 5 | 455 | 0.136 | 0.027 | 315 | 0.136 | 0.027 | 504 | 0.172 | 0.034 | 245 | 0.113 | 0.023 |
| 6 | 546 | 0.171 | 0.028 | 378 | 0.171 | 0.028 | 588 | 0.219 | 0.036 | 294 | 0.142 | 0.024 |
| 7 | 637 | 0.209 | 0.030 | 441 | 0.209 | 0.030 | 672 | 0.272 | 0.039 | 343 | 0.174 | 0.025 |
| 8 | 728 | 0.252 | 0.032 | 504 | 0.252 | 0.032 | 756 | 0.337 | 0.042 | 392 | 0.208 | 0.026 |
| 9 | 819 | 0.303 | 0.034 | 567 | 0.303 | 0.034 | 840 | 0.416 | 0.046 | 441 | 0.247 | 0.027 |
| 10 | 910 | 0.362 | 0.036 | 630 | 0.362 | 0.036 | 924 | 0.514 | 0.051 | 490 | 0.292 | 0.029 |
| 11 | 1001 | 0.434 | 0.039 | 693 | 0.434 | 0.039 | 1008 | 0.639 | 0.058 | 539 | 0.345 | 0.031 |
| 12 | 1092 | 0.519 | 0.043 | 756 | 0.519 | 0.043 | 1092 | 0.988 | 0.082 | 588 | 0.408 | 0.034 |
| 13 | 1183 | 0.624 | 0.048 | 819 | 0.624 | 0.048 | | | | 637 | 0.482 | 0.037 |
| 14 | 1274 | 0.762 | 0.054 | 882 | 0.762 | 0.054 | | | | 686 | 0.570 | 0.041 |
| 15 | 1365 | 0.964 | 0.064 | 945 | 0.964 | 0.064 | | | | 735 | 0.676 | 0.045 |
| 16 | | | | | | | | | | 784 | 0.806 | 0.050 |
| 17 | | | | | | | | | | 833 | 0.979 | 0.058 |

Table D2. Amplification of Ultimate Forces in Design Case 1

| | C1 | C2 | C3 | C4 |
|---|---|---|---|---|
| Load (MN) | 4.51 | 11.31 | 8.45 | 10.4 |
| Moment (MN) | 409.8 | 711.1 | 711.8 | 529.6 |
| $K_L$ (MN/m) | 241.0 | 118.8 | 141.8 | 158.8 |
| $K_{LR}$ (MN) | -6974 | -3184 | -3798 | -4396 |
| $K_R$ (MN*m/rad) | 254873 | 110690 | 127672 | 149919 |
| Nat. freq. (Hz) | 0.227 | 0.194 | 0.196 | 0.200 |
| DAF | 4.885 | 1.912 | 2.591 | 1.864 |
| Amplified load (MN) | 16.79 | 19.57 | 16.79 | 18.21 |
| Amplified moment (MN*m) | 1028.9 | 1003.0 | 1028.9 | 808.8 |

**Design Case 2: Soil Profile 1 - Current Recommendations - L=70 m & D=9.5 m**

Table D3. LPILE Analysis for Ultimate Pile Capacity in Design Case 2

| H (MN) | COMBINATION 1 | | | COMBINATION 2 | | | COMBINATION 3 | | | COMBINATION 4 | | |
|---|---|---|---|---|---|---|---|---|---|---|---|---|
| | M (MN*m) | y (m) | y/H (m/MN) | M (MN*m) | y (m) | y/H (m/MN) | M (MN*m) | y (m) | y/H (m/MN) | M (MN*m) | y (m) | y/H (m/MN) |
| 1 | 85 | 0.017 | 0.017 | 58 | 0.012 | 0.012 | 78 | 0.015 | 0.015 | 47 | 0.010 | 0.010 |
| 2 | 170 | 0.040 | 0.020 | 116 | 0.027 | 0.014 | 156 | 0.034 | 0.017 | 94 | 0.023 | 0.012 |
| 3 | 255 | 0.066 | 0.022 | 174 | 0.045 | 0.015 | 234 | 0.057 | 0.019 | 141 | 0.038 | 0.013 |
| 4 | 340 | 0.096 | 0.024 | 232 | 0.064 | 0.016 | 312 | 0.081 | 0.020 | 188 | 0.055 | 0.014 |
| 5 | 425 | 0.135 | 0.027 | 290 | 0.085 | 0.017 | 390 | 0.110 | 0.022 | 235 | 0.073 | 0.015 |
| 6 | 510 | 0.191 | 0.032 | 348 | 0.110 | 0.018 | 468 | 0.147 | 0.025 | 282 | 0.094 | 0.016 |
| 7 | 595 | 0.270 | 0.039 | 406 | 0.140 | 0.020 | 546 | 0.196 | 0.028 | 329 | 0.118 | 0.017 |
| 8 | 680 | 0.378 | 0.047 | 464 | 0.179 | 0.022 | 624 | 0.261 | 0.033 | 376 | 0.149 | 0.019 |
| 9 | 765 | 0.528 | 0.059 | 522 | 0.228 | 0.025 | 702 | 0.348 | 0.039 | 423 | 0.188 | 0.021 |
| 10 | 850 | 0.729 | 0.073 | 580 | 0.291 | 0.029 | 780 | 0.461 | 0.046 | 470 | 0.236 | 0.024 |
| 11 | 935 | 0.997 | 0.091 | 638 | 0.371 | 0.034 | 858 | 0.609 | 0.055 | 517 | 0.297 | 0.027 |
| 12 | 1020 | 1.348 | 0.112 | 696 | 0.472 | 0.039 | 936 | 0.798 | 0.066 | 564 | 0.374 | 0.031 |
| 13 | 1105 | 1.807 | 0.139 | 754 | 0.597 | 0.046 | 1014 | 1.038 | 0.080 | 611 | 0.468 | 0.036 |
| 14 | 1190 | 2.438 | 0.174 | 812 | 0.752 | 0.054 | 1092 | 1.338 | 0.096 | 658 | 0.584 | 0.042 |
| 15 | 1275 | 3.350 | 0.223 | 870 | 0.942 | 0.063 | 1170 | 1.716 | 0.114 | 705 | 0.725 | 0.048 |
| 16 | 1360 | 4.740 | 0.296 | 928 | 1.172 | 0.073 | 1248 | 2.206 | 0.138 | 752 | 0.895 | 0.056 |
| 17 | | | | 986 | 1.4498 | 0.085 | 1326 | 2.872 | 0.169 | 799 | 1.100 | 0.065 |
| 18 | | | | 1044 | 1.788 | 0.099 | | | | 846 | 1.344 | 0.075 |
| 19 | | | | 1102 | 2.211 | 0.116 | | | | 893 | 1.634 | 0.086 |
| 20 | | | | 1160 | 2.755 | 0.138 | | | | 940 | 1.989 | 0.099 |

Table D4. Amplification of Ultimate Forces in Design Case 2

| | C1 | C2 | C3 | C4 |
|---|---|---|---|---|
| Load (MN) | 4.51 | 11.31 | 8.45 | 10.4 |
| Moment (MN) | 409.8 | 711.1 | 711.8 | 529.6 |
| $K_L$ (MN/m) | 305.4 | 98.4 | 146.9 | 143.1 |
| $K_{LR}$ (MN) | -10244 | -3209 | -4777 | -4732 |
| $K_R$ (MN*m/rad) | 423812 | 130815 | 185297 | 189860 |
| Nat. freq. (Hz) | 0.243 | 0.194 | 0.202 | 0.207 |
| DAF | 3.938 | 1.914 | 2.471 | 1.81 |
| Amplified load (MN) | 15.06 | 23.76 | 19.29 | 21.67 |
| Amplified moment (MN*m) | 877.3 | 1114.5 | 1116.6 | 927.8 |

**Design Case 3: Soil Profile 2 - Current Recommendations - L=44 m & D=7.5 m**

Table D5. LPILE Analysis for Ultimate Pile Capacity in Design Case 3

| H (MN) | COMBINATION 1 | | | COMBINATION 2 | | | COMBINATION 3 | | | COMBINATION 4 | | |
|---|---|---|---|---|---|---|---|---|---|---|---|---|
| | M (MN*m) | y (m) | y/H (m/MN) | M (MN*m) | y (m) | y/H (m/MN) | M (MN*m) | y (m) | y/H (m/MN) | M (MN*m) | y (m) | y/H (m/MN) |
| 1 | 98 | 0.010 | 0.010 | 69 | 0.007 | 0.007 | 91 | 0.009 | 0.009 | 52 | 0.005 | 0.005 |
| 2 | 196 | 0.023 | 0.012 | 138 | 0.016 | 0.008 | 182 | 0.021 | 0.011 | 104 | 0.012 | 0.006 |
| 3 | 294 | 0.039 | 0.013 | 207 | 0.027 | 0.009 | 273 | 0.036 | 0.012 | 156 | 0.021 | 0.007 |
| 4 | 392 | 0.057 | 0.014 | 276 | 0.039 | 0.010 | 364 | 0.052 | 0.013 | 208 | 0.030 | 0.007 |
| 5 | 490 | 0.080 | 0.016 | 345 | 0.053 | 0.011 | 455 | 0.072 | 0.014 | 260 | 0.040 | 0.008 |
| 6 | 588 | 0.111 | 0.018 | 414 | 0.069 | 0.011 | 546 | 0.098 | 0.016 | 312 | 0.051 | 0.009 |
| 7 | 686 | 0.154 | 0.022 | 483 | 0.088 | 0.013 | 637 | 0.131 | 0.019 | 364 | 0.064 | 0.009 |
| 8 | 784 | 0.217 | 0.027 | 552 | 0.112 | 0.014 | 728 | 0.178 | 0.022 | 416 | 0.078 | 0.010 |
| 9 | 882 | 0.316 | 0.035 | 621 | 0.142 | 0.016 | 819 | 0.247 | 0.027 | 468 | 0.096 | 0.011 |
| 10 | 980 | 0.489 | 0.049 | 690 | 0.183 | 0.018 | 910 | 0.353 | 0.035 | 520 | 0.117 | 0.012 |
| 11 | | | | 759 | 0.240 | 0.022 | 1001 | 0.554 | 0.050 | 572 | 0.143 | 0.013 |
| 12 | | | | 828 | 0.320 | 0.027 | 1092 | | | 624 | 0.176 | 0.015 |
| 13 | | | | 897 | 0.439 | 0.034 | 1183 | | | 676 | 0.220 | 0.017 |
| 14 | | | | 966 | 0.836 | 0.060 | 1274 | | | 728 | 0.278 | 0.020 |
| 15 | | | | | | | | | | 780 | 0.358 | 0.024 |
| 16 | | | | | | | | | | 832 | 0.477 | 0.030 |

Table D6. Amplification of Ultimate Forces in Design Case 3

| | C1 | C2 | C3 | C4 |
|---|---|---|---|---|
| Load (MN) | 3.93 | 9.40 | 7.32 | 8.49 |
| Moment (MN) | 384.0 | 644.0 | 669.5 | 462.5 |
| $K_L$ (MN/m) | 1549.3 | 553.0 | 578.3 | 742.5 |
| $K_{LR}$ (MN) | -18808 | -9073 | -9403 | -12370 |
| $K_R$ (MN*m/rad) | 347188 | 177283 | 183124 | 271428 |
| Nat. freq. (Hz) | 0.248 | 0.204 | 0.207 | 0.236 |
| DAF | 3.688 | 1.831 | 2.381 | 1.645 |
| Amplified load (MN) | 9.62 | 15.24 | 12.99 | 13.14 |
| Amplified moment (MN*m) | 631.7 | 857.9 | 882.1 | 626.5 |

**Design Case 4: Soil Profile 2 - Current Recommendations - L=43 m & D=8.5 m**

Table D7. LPILE Analysis for Ultimate Pile Capacity in Design Case 4

| H (MN) | COMBINATION 1 | | | COMBINATION 2 | | | COMBINATION 3 | | | COMBINATION 4 | | |
|---|---|---|---|---|---|---|---|---|---|---|---|---|
| | M (MN*m) | y (m) | y/H (m/MN) | M (MN*m) | y (m) | y/H (m/MN) | M (MN*m) | y (m) | y/H (m/MN) | M (MN*m) | y (m) | y/H (m/MN) |
| 1 | 91 | 0.006 | 0.006 | 63 | 0.004 | 0.004 | 84 | 0.006 | 0.006 | 49 | 0.003 | 0.003 |
| 2 | 182 | 0.015 | 0.007 | 126 | 0.010 | 0.005 | 168 | 0.014 | 0.007 | 98 | 0.008 | 0.004 |
| 3 | 273 | 0.025 | 0.008 | 189 | 0.017 | 0.006 | 252 | 0.023 | 0.008 | 147 | 0.014 | 0.005 |
| 4 | 364 | 0.038 | 0.010 | 252 | 0.025 | 0.006 | 336 | 0.034 | 0.009 | 196 | 0.020 | 0.005 |
| 5 | 455 | 0.054 | 0.011 | 315 | 0.035 | 0.007 | 420 | 0.048 | 0.010 | 245 | 0.027 | 0.005 |
| 6 | 546 | 0.077 | 0.013 | 378 | 0.046 | 0.008 | 504 | 0.066 | 0.011 | 294 | 0.035 | 0.006 |
| 7 | 637 | 0.108 | 0.015 | 441 | 0.059 | 0.008 | 588 | 0.090 | 0.013 | 343 | 0.044 | 0.006 |
| 8 | 728 | 0.155 | 0.019 | 504 | 0.076 | 0.009 | 672 | 0.124 | 0.016 | 392 | 0.055 | 0.007 |
| 9 | 819 | 0.228 | 0.025 | 567 | 0.098 | 0.011 | 756 | 0.174 | 0.019 | 441 | 0.068 | 0.008 |
| 10 | 910 | 0.345 | 0.035 | 630 | 0.127 | 0.013 | 840 | 0.250 | 0.025 | 490 | 0.084 | 0.008 |
| 11 | 1001 | 0.554 | 0.050 | 693 | 0.168 | 0.015 | 924 | 0.369 | 0.034 | 539 | 0.105 | 0.010 |
| 12 | 1092 | | | 756 | 0.225 | 0.019 | 1008 | 0.585 | 0.049 | 588 | 0.132 | 0.011 |
| 13 | 1183 | | | 819 | 0.306 | 0.024 | | | | 637 | 0.167 | 0.013 |
| 14 | 1274 | | | 882 | 0.424 | 0.030 | | | | 686 | 0.213 | 0.015 |
| 15 | 1365 | | | 945 | 0.679 | 0.045 | | | | 735 | 0.277 | 0.018 |
| 16 | | | | | | | | | | 784 | 0.365 | 0.023 |
| 17 | | | | | | | | | | 833 | 0.488 | 0.029 |

Table D8. Amplification of Ultimate Forces in Design Case 4

| | C1 | C2 | C3 | C4 |
|---|---|---|---|---|
| Load (MN) | 4.51 | 11.31 | 8.45 | 10.4 |
| Moment (MN) | 409.8 | 711.1 | 711.8 | 529.6 |
| $K_L$ (MN/m) | 1193.5 | 601.5 | 708.5 | 870.9 |
| $K_{LR}$ (MN) | -20239 | -11624 | -13558 | -16997 |
| $K_R$ (MN*m/rad) | 473450 | 257760 | 305180 | 421266 |
| Nat. freq. (Hz) | 0.250 | 0.211 | 0.224 | 0.244 |
| DAF | 3.642 | 1.784 | 2.155 | 1.612 |
| Amplified load (MN) | 11.67 | 18.40 | 14.51 | 15.93 |
| Amplified moment (MN*m) | 723.9 | 961.9 | 942.0 | 727.3 |

**Design Case 5: Soil Profile 3 - Current Recommendations - L=47 m & D=7.5 m**

Table D9. LPILE Analysis for Ultimate Pile Capacity in Design Case 5

| H (MN) | COMBINATION 1 | | | COMBINATION 2 | | | COMBINATION 3 | | | COMBINATION 4 | | |
|---|---|---|---|---|---|---|---|---|---|---|---|---|
| | M (MN*m) | y (m) | y/H (m/MN) | M (MN*m) | y (m) | y/H (m/MN) | M (MN*m) | y (m) | y/H (m/MN) | M (MN*m) | y (m) | y/H (m/MN) |
| 1 | 98 | 0.009 | 0.009 | 69 | 0.007 | 0.007 | 91 | 0.009 | 0.009 | 52 | 0.005 | 0.005 |
| 2 | 196 | 0.021 | 0.010 | 138 | 0.015 | 0.007 | 182 | 0.019 | 0.010 | 104 | 0.011 | 0.006 |
| 3 | 294 | 0.034 | 0.011 | 207 | 0.024 | 0.008 | 273 | 0.031 | 0.010 | 156 | 0.018 | 0.006 |
| 4 | 392 | 0.052 | 0.013 | 276 | 0.034 | 0.009 | 364 | 0.065 | 0.013 | 208 | 0.026 | 0.007 |
| 5 | 490 | 0.083 | 0.017 | 345 | 0.047 | 0.009 | 455 | 0.092 | 0.015 | 260 | 0.035 | 0.007 |
| 6 | 588 | 0.150 | 0.025 | 414 | 0.062 | 0.010 | 546 | 0.139 | 0.020 | 312 | 0.045 | 0.008 |
| 7 | 686 | 0.280 | 0.040 | 483 | 0.082 | 0.012 | 637 | 0.218 | 0.027 | 364 | 0.057 | 0.008 |
| 8 | 784 | 0.495 | 0.062 | 552 | 0.114 | 0.014 | 728 | 0.338 | 0.038 | 416 | 0.073 | 0.009 |
| 9 | 882 | 0.907 | 0.101 | 621 | 0.163 | 0.018 | 819 | 0.513 | 0.051 | 468 | 0.094 | 0.010 |
| 10 | | | | 690 | 0.238 | 0.024 | 910 | 0.782 | 0.071 | 520 | 0.126 | 0.013 |
| 11 | | | | 759 | 0.342 | 0.031 | 1001 | 1.953 | 0.163 | 572 | 0.172 | 0.016 |
| 12 | | | | 828 | 0.484 | 0.040 | | | | 624 | 0.237 | 0.020 |
| 13 | | | | 897 | 0.673 | 0.052 | | | | 676 | 0.323 | 0.025 |
| 14 | | | | 966 | 1.092 | 0.078 | | | | 728 | 0.434 | 0.031 |
| 15 | | | | | | | | | | 780 | 0.574 | 0.038 |
| 16 | | | | | | | | | | 832 | 0.779 | 0.049 |
| 17 | | | | | | | | | | 884 | 1.310 | 0.077 |

Table D10. Amplification of Ultimate Forces in Design Case 5

| | C1 | C2 | C3 | C4 |
|---|---|---|---|---|
| Load (MN) | 3.93 | 9.40 | 7.32 | 8.49 |
| Moment (MN) | 384.0 | 644.0 | 669.5 | 462.5 |
| $K_L$ (MN/m) | 705.8 | 348.8 | 375.5 | 535.1 |
| $K_{LR}$ (MN) | -10868 | -6786 | -7258 | -9548 |
| $K_R$ (MN*m/rad) | 262928 | 167846 | 180523 | 248759 |
| Nat. freq. (Hz) | 0.244 | 0.209 | 0.219 | 0.241 |
| DAF | 3.875 | 1.794 | 2.217 | 1.625 |
| Amplified load (MN) | 10.02 | 14.98 | 12.31 | 12.99 |
| Amplified moment (MN*m) | 649.0 | 848.4 | 856.8 | 621.5 |

**Design Case 6: Soil Profile 3 - Current Recommendations - L=46 m & D=8.5 m**

Table D11. LPILE Analysis for Ultimate Pile Capacity in Design Case 6

| H (MN) | COMBINATION 1 | | | COMBINATION 2 | | | COMBINATION 3 | | | COMBINATION 4 | | |
|---|---|---|---|---|---|---|---|---|---|---|---|---|
| | M (MN*m) | y (m) | y/H (m/MN) | M (MN*m) | y (m) | y/H (m/MN) | M (MN*m) | y (m) | y/H (m/MN) | M (MN*m) | y (m) | y/H (m/MN) |
| 1 | 91 | 0.006 | 0.006 | 63 | 0.004 | 0.004 | 84 | 0.006 | 0.006 | 49 | 0.003 | 0.003 |
| 2 | 182 | 0.014 | 0.007 | 126 | 0.010 | 0.005 | 168 | 0.013 | 0.006 | 98 | 0.008 | 0.004 |
| 3 | 273 | 0.023 | 0.008 | 189 | 0.016 | 0.005 | 252 | 0.021 | 0.007 | 147 | 0.013 | 0.004 |
| 4 | 364 | 0.033 | 0.008 | 252 | 0.023 | 0.006 | 336 | 0.030 | 0.008 | 196 | 0.018 | 0.005 |
| 5 | 455 | 0.047 | 0.009 | 315 | 0.030 | 0.006 | 420 | 0.042 | 0.008 | 245 | 0.024 | 0.005 |
| 6 | 546 | 0.068 | 0.011 | 378 | 0.040 | 0.007 | 504 | 0.058 | 0.010 | 294 | 0.031 | 0.005 |
| 7 | 637 | 0.106 | 0.015 | 441 | 0.052 | 0.007 | 588 | 0.085 | 0.012 | 343 | 0.039 | 0.006 |
| 8 | 728 | 0.178 | 0.022 | 504 | 0.070 | 0.009 | 672 | 0.135 | 0.017 | 392 | 0.049 | 0.006 |
| 9 | 819 | 0.293 | 0.033 | 567 | 0.099 | 0.011 | 756 | 0.217 | 0.024 | 441 | 0.063 | 0.007 |
| 10 | 910 | 0.461 | 0.046 | 630 | 0.147 | 0.015 | 840 | 0.340 | 0.034 | 490 | 0.083 | 0.008 |
| 11 | 1001 | 0.699 | 0.064 | 693 | 0.218 | 0.020 | 924 | 0.512 | 0.047 | 539 | 0.114 | 0.010 |
| 12 | 1092 | 1.335 | 0.111 | 756 | 0.315 | 0.026 | 1008 | 0.755 | 0.063 | 588 | 0.162 | 0.013 |
| 13 | 1183 | | | 819 | 0.446 | 0.034 | 1092 | 1.521 | 0.117 | 637 | 0.227 | 0.017 |
| 14 | 1274 | | | 882 | 0.614 | 0.044 | | | | 686 | 0.312 | 0.022 |
| 15 | 1365 | | | 945 | 0.873 | 0.058 | | | | 735 | 0.421 | 0.028 |
| 16 | | | | | | | | | | 784 | 0.557 | 0.035 |
| 17 | | | | | | | | | | 833 | 0.731 | 0.043 |

Table D12. Amplification of Ultimate Forces in Design Case 6

| | C1 | C2 | C3 | C4 |
|---|---|---|---|---|
| Load (MN) | 4.51 | 11.31 | 8.45 | 10.4 |
| Moment (MN) | 409.8 | 711.1 | 711.8 | 529.6 |
| $K_L$ (MN/m) | 976.3 | 371.3 | 451.7 | 586.9 |
| $K_{LR}$ (MN) | -15840 | -7880 | -10411 | -12673 |
| $K_R$ (MN*m/rad) | 408813 | 230665 | 298919 | 373627 |
| Nat. freq. (Hz) | 0.252 | 0.235 | 0.232 | 0.246 |
| DAF | 3.557 | 1.653 | 2.074 | 1.604 |
| Amplified load (MN) | 11.44 | 17.22 | 14.08 | 15.86 |
| Amplified moment (MN*m) | 713.8 | 920.0 | 925.9 | 724.7 |

**Design Case 7: Soil Profile 1 – Jeanjean et al. (2022) - L=52 m & D=8.5 m**

Table D13. LPILE Analysis for Ultimate Pile Capacity in Design Case 7

| H (MN) | COMBINATION 1 | | | COMBINATION 2 | | | COMBINATION 3 | | | COMBINATION 4 | | |
|---|---|---|---|---|---|---|---|---|---|---|---|---|
| | M (MN*m) | y (m) | y/H (m/MN) | M (MN*m) | y (m) | y/H (m/MN) | M (MN*m) | y (m) | y/H (m/MN) | M (MN*m) | y (m) | y/H (m/MN) |
| **1** | **91** | 0.031 | 0.001 | **63** | 0.023 | 0.023 | **84** | 0.029 | 0.029 | **49** | 0.020 | 0.020 |
| **2** | **182** | 0.074 | 0.003 | **126** | 0.053 | 0.026 | **168** | 0.068 | 0.034 | **98** | 0.043 | 0.022 |
| **3** | **273** | 0.126 | 0.004 | **189** | 0.091 | 0.030 | **252** | 0.117 | 0.039 | **147** | 0.074 | 0.025 |
| **4** | **364** | 0.182 | 0.006 | **252** | 0.133 | 0.033 | **336** | 0.169 | 0.042 | **196** | 0.109 | 0.027 |
| **5** | **455** | 0.245 | 0.008 | **315** | 0.176 | 0.035 | **420** | 0.226 | 0.045 | **245** | 0.146 | 0.029 |
| **6** | **546** | 0.318 | 0.010 | **378** | 0.224 | 0.037 | **504** | 0.293 | 0.049 | **294** | 0.184 | 0.031 |
| **7** | **637** | 0.407 | 0.013 | **441** | 0.279 | 0.040 | **588** | 0.371 | 0.053 | **343** | 0.226 | 0.032 |
| **8** | **728** | 0.516 | 0.016 | **504** | 0.341 | 0.043 | **672** | 0.467 | 0.058 | **392** | 0.273 | 0.034 |
| **9** | **819** | 0.645 | 0.019 | **567** | 0.415 | 0.046 | **756** | 0.581 | 0.065 | **441** | 0.326 | 0.036 |
| **10** | **910** | 0.797 | 0.023 | **630** | 0.501 | 0.050 | **840** | 0.714 | 0.071 | **490** | 0.386 | 0.039 |
| **11** | **1001** | 0.974 | 0.028 | **693** | 0.600 | 0.055 | **924** | 0.867 | 0.079 | **539** | 0.457 | 0.042 |
| **12** | **1092** | 1.188 | 0.033 | **756** | 0.712 | 0.059 | **1008** | 1.048 | 0.087 | **588** | 0.537 | 0.045 |
| **13** | **1183** | 1.459 | 0.040 | **819** | 0.839 | 0.065 | **1092** | 1.266 | 0.097 | **637** | 0.626 | 0.048 |
| **14** | **1274** | 1.817 | 0.049 | **882** | 0.984 | 0.070 | **1176** | 1.544 | 0.110 | **686** | 0.726 | 0.052 |
| **15** | **1365** | 2.345 | 0.061 | **945** | 1.152 | 0.077 | **1260** | 1.915 | 0.128 | **735** | 0.838 | 0.056 |
| **16** | **1456** | 3.2406 | 0.08205 | **1008** | 1.3537 | 0.085 | **1344** | 2.458 | 0.154 | **784** | 0.963 | 0.060 |
| **17** | **1547** | 5.6127 | 0.1366 | **1071** | 1.6031 | 0.094 | **1428** | 3.389 | 0.199 | **833** | 1.105 | 0.065 |
| **18** | | | | **1134** | 1.928 | 0.107 | **1512** | 6.101 | 0.339 | **882** | 1.269 | 0.071 |
| **19** | | | | **1197** | 2.3723 | 0.125 | | | | **931** | 1.468 | 0.077 |
| **20** | | | | **1260** | 3.0566 | 0.153 | | | | **980** | 1.708 | 0.085 |

Table D14. Amplification of Ultimate Forces in Design Case 7

| | **C1** | **C2** | **C3** | **C4** |
|---|---|---|---|---|
| Load (MN) | 4.51 | 11.31 | 8.45 | 10.4 |
| Moment (MN) | 409.8 | 711.1 | 711.8 | 529.6 |
| $K_L$ (MN/m) | 291.5 | 132.0 | 156.6 | 184.4 |
| $K_{LR}$ (MN) | -8662 | -3535 | -4231 | -5119 |
| $K_R$ (MN*m/rad) | 310771 | 123092 | 144670 | 175638 |
| Nat. freq. (Hz) | 0.227 | 0.200 | 0.204 | 0.209 |
| DAF | 4.868 | 1.861 | 2.438 | 1.800 |
| Amplified load (MN) | 14.99 | 19.10 | 15.99 | 17.63 |
| Amplified moment (MN*m) | 869.6 | 986.4 | 988.5 | 787.9 |

**Design Case 8: Soil Profile 1 – Jeanjean et al. (2022) - L=50 m & D=9.5 m**

Table D15. LPILE Analysis for Ultimate Pile Capacity in Design Case 8

| H (MN) | COMBINATION 1 | | | COMBINATION 2 | | | COMBINATION 3 | | | COMBINATION 4 | | |
|---|---|---|---|---|---|---|---|---|---|---|---|---|
| | M (MN*m) | y (m) | y/H (m/MN) | M (MN*m) | y (m) | y/H (m/MN) | M (MN*m) | y (m) | y/H (m/MN) | M (MN*m) | y (m) | y/H (m/MN) |
| **1** | **85** | 0.116 | 0.039 | **58** | 0.018 | 0.018 | **78** | 0.022 | 0.022 | **47** | 0.016 | 0.016 |
| **2** | **170** | 0.171 | 0.043 | **116** | 0.045 | 0.022 | **156** | 0.060 | 0.030 | **94** | 0.037 | 0.018 |
| **3** | **255** | 0.237 | 0.047 | **174** | 0.082 | 0.027 | **234** | 0.107 | 0.036 | **141** | 0.069 | 0.023 |
| **4** | **340** | 0.315 | 0.052 | **232** | 0.123 | 0.031 | **312** | 0.158 | 0.040 | **188** | 0.104 | 0.026 |
| **5** | **425** | 0.414 | 0.059 | **290** | 0.166 | 0.033 | **390** | 0.217 | 0.043 | **235** | 0.141 | 0.028 |
| **6** | **510** | 0.537 | 0.067 | **348** | 0.215 | 0.036 | **468** | 0.287 | 0.048 | **282** | 0.181 | 0.030 |
| **7** | **595** | 0.688 | 0.076 | **406** | 0.273 | 0.039 | **546** | 0.372 | 0.053 | **329** | 0.227 | 0.032 |
| **8** | **680** | 0.865 | 0.087 | **464** | 0.339 | 0.042 | **624** | 0.479 | 0.060 | **376** | 0.279 | 0.035 |
| **9** | **765** | 1.077 | 0.098 | **522** | 0.421 | 0.047 | **702** | 0.609 | 0.068 | **423** | 0.339 | 0.038 |
| **10** | **850** | 1.340 | 0.112 | **580** | 0.518 | 0.052 | **780** | 0.763 | 0.076 | **470** | 0.411 | 0.041 |
| **11** | **935** | 1.681 | 0.129 | **638** | 0.631 | 0.057 | **858** | 0.944 | 0.086 | **517** | 0.495 | 0.045 |
| **12** | **1020** | 2.156 | 0.154 | **696** | 0.761 | 0.063 | **936** | 1.159 | 0.097 | **564** | 0.592 | 0.049 |
| **13** | **1105** | 2.895 | 0.193 | **754** | 0.910 | 0.070 | **1014** | 1.428 | 0.110 | **611** | 0.702 | 0.054 |
| **14** | **1190** | 4.318 | 0.270 | **812** | 1.081 | 0.077 | **1092** | 1.775 | 0.127 | **658** | 0.826 | 0.059 |
| **15** | | | | **870** | 1.285 | 0.086 | **1170** | 2.260 | 0.151 | **705** | 0.966 | 0.064 |
| **16** | | | | **928** | 1.532 | 0.096 | **1248** | 3.018 | 0.189 | **752** | 1.125 | 0.070 |
| **17** | | | | **986** | 1.847 | 0.109 | **1326** | 4.472 | 0.263 | **799** | 1.314 | 0.077 |
| **18** | | | | **1044** | 2.266 | 0.126 | | | | **846** | 1.539 | 0.085 |
| **19** | | | | **1102** | 2.874 | 0.151 | | | | **893** | 1.818 | 0.096 |
| **20** | | | | **1160** | 3.876 | 0.194 | | | | **940** | 2.175 | 0.109 |

Table D16. Amplification of Ultimate Forces in Design Case 8

| | **C1** | **C2** | **C3** | **C4** |
|---|---|---|---|---|
| Load (MN) | 4.51 | 11.31 | 8.45 | 10.4 |
| Moment (MN) | 409.8 | 711.1 | 711.8 | 529.6 |
| $K_L$ (MN/m) | 355.6 | 107.9 | 144.1 | 153.8 |
| $K_{LR}$ (MN) | -11556 | -3195 | -4347 | -4698 |
| $K_R$ (MN*m/rad) | 426183 | 126030 | 161788 | 175789 |
| Nat. freq. (Hz) | 0.226 | 0.195 | 0.204 | 0.206 |
| DAF | 5.004 | 1.905 | 2.438 | 1.816 |
| Amplified load (MN) | 1864 | 23.66 | 19.08 | 21.73 |
| Amplified moment (MN*m) | 1036.4 | 1141.5 | 1108.5 | 930.0 |

**Design Case 9: Soil Profile 2 – Jeanjean et al. (2022) - L=31 m & D=7.5 m**

Table D17. LPILE Analysis for Ultimate Pile Capacity in Design Case 9

| H (MN) | COMBINATION 1 | | | COMBINATION 2 | | | COMBINATION 3 | | | COMBINATION 4 | | |
|---|---|---|---|---|---|---|---|---|---|---|---|---|
| | M (MN*m) | y (m) | y/H (m/MN) | M (MN*m) | y (m) | y/H (m/MN) | M (MN*m) | y (m) | y/H (m/MN) | M (MN*m) | y (m) | y/H (m/MN) |
| 1 | 98 | 0.010 | 0.010 | 69 | 0.007 | 0.007 | 91 | 0.009 | 0.009 | 52 | 0.005 | 0.005 |
| 2 | 196 | 0.023 | 0.011 | 138 | 0.016 | 0.008 | 182 | 0.021 | 0.011 | 104 | 0.012 | 0.006 |
| 3 | 294 | 0.038 | 0.013 | 207 | 0.027 | 0.009 | 273 | 0.036 | 0.012 | 156 | 0.020 | 0.007 |
| 4 | 392 | 0.057 | 0.014 | 276 | 0.040 | 0.010 | 364 | 0.054 | 0.013 | 208 | 0.029 | 0.007 |
| 5 | 490 | 0.078 | 0.016 | 345 | 0.054 | 0.011 | 455 | 0.074 | 0.015 | 260 | 0.039 | 0.008 |
| 6 | 588 | 0.102 | 0.017 | 414 | 0.070 | 0.012 | 546 | 0.097 | 0.016 | 312 | 0.050 | 0.008 |
| 7 | 686 | 0.130 | 0.019 | 483 | 0.088 | 0.013 | 637 | 0.124 | 0.018 | 364 | 0.062 | 0.009 |
| 8 | 784 | 0.164 | 0.020 | 552 | 0.108 | 0.014 | 728 | 0.158 | 0.020 | 416 | 0.075 | 0.009 |
| 9 | 882 | 0.209 | 0.023 | 621 | 0.132 | 0.015 | 819 | 0.202 | 0.022 | 468 | 0.090 | 0.010 |
| 10 | 980 | 0.268 | 0.027 | 690 | 0.160 | 0.016 | 910 | 0.262 | 0.026 | 520 | 0.105 | 0.009 |
| 11 | 1078 | 0.357 | 0.032 | 759 | 0.196 | 0.018 | 1001 | 0.351 | 0.032 | 572 | 0.123 | 0.010 |
| 12 | 1176 | 0.501 | 0.042 | 828 | 0.241 | 0.020 | 1092 | 0.504 | 0.042 | 624 | 0.142 | 0.010 |
| 13 | 1274 | 0.816 | 0.063 | 897 | 0.303 | 0.023 | 1183 | 0.910 | 0.070 | 676 | 0.165 | 0.011 |
| 14 | | | | 966 | 0.391 | 0.028 | | | | 728 | 0.192 | 0.012 |
| 15 | | | | 1035 | 0.536 | 0.036 | | | | 780 | 0.225 | 0.013 |
| 16 | | | | 1104 | 0.8771 | 0.055 | | | | 832 | 0.264 | 0.014 |
| 17 | | | | | | | | | | 884 | 0.314 | 0.016 |
| 18 | | | | | | | | | | 936 | 0.381 | 0.017 |
| 19 | | | | | | | | | | 988 | 0.474 | 0.020 |
| 20 | | | | | | | | | | 1040 | 0.615 | 0.024 |

Table D18. Amplification of Ultimate Forces in Design Case 9

| | C1 | C2 | C3 | C4 |
|---|---|---|---|---|
| Load (MN) | 3.93 | 9.40 | 7.32 | 8.49 |
| Moment (MN) | 384.0 | 644.0 | 669.5 | 462.5 |
| $K_L$ (MN/m) | 1175.4 | 744.6 | 772.8 | 772.8 |
| $K_{LR}$ (MN) | -16626 | -10285 | -10617 | -10617 |
| $K_R$ (MN*m/rad) | 327726 | 177987 | 181665 | 181665 |
| Nat. freq. (Hz) | 0.245 | 0.216 | 0.215 | 0.226 |
| DAF | 3.816 | 1.754 | 2.263 | 1.695 |
| Amplified load (MN) | 10.56 | 15.07 | 13.06 | 13.62 |
| Amplified moment (MN*m) | 697.6 | 862.4 | 906.2 | 658.5 |

**Design Case 10: Soil Profile 2 – Jeanjean et al. (2022) - L=30 m & D=8.5 m**

Table D19. LPILE Analysis for Ultimate Pile Capacity in Design Case 10

| H (MN) | COMBINATION 1 | | | COMBINATION 2 | | | COMBINATION 3 | | | COMBINATION 4 | | |
|---|---|---|---|---|---|---|---|---|---|---|---|---|
| | M (MN*m) | y (m) | y/H (m/MN) | M (MN*m) | y (m) | y/H (m/MN) | M (MN*m) | y (m) | y/H (m/MN) | M (MN*m) | y (m) | y/H (m/MN) |
| 1 | 91 | 0.009 | 0.009 | 63 | 0.006 | 0.006 | 84 | 0.009 | 0.009 | 49 | 0.005 | 0.005 |
| 2 | 182 | 0.021 | 0.010 | 126 | 0.015 | 0.007 | 168 | 0.019 | 0.010 | 98 | 0.012 | 0.006 |
| 3 | 273 | 0.035 | 0.012 | 189 | 0.024 | 0.008 | 252 | 0.032 | 0.011 | 147 | 0.019 | 0.006 |
| 4 | 364 | 0.051 | 0.013 | 252 | 0.035 | 0.009 | 336 | 0.047 | 0.012 | 196 | 0.027 | 0.007 |
| 5 | 455 | 0.071 | 0.014 | 315 | 0.047 | 0.009 | 420 | 0.065 | 0.013 | 245 | 0.036 | 0.007 |
| 6 | 546 | 0.094 | 0.016 | 378 | 0.061 | 0.010 | 504 | 0.085 | 0.014 | 294 | 0.047 | 0.008 |
| 7 | 637 | 0.121 | 0.017 | 441 | 0.077 | 0.011 | 588 | 0.108 | 0.015 | 343 | 0.059 | 0.008 |
| 8 | 728 | 0.155 | 0.019 | 504 | 0.094 | 0.012 | 672 | 0.137 | 0.017 | 392 | 0.071 | 0.009 |
| 9 | 819 | 0.200 | 0.022 | 567 | 0.114 | 0.013 | 756 | 0.173 | 0.019 | 441 | 0.085 | 0.009 |
| 10 | 910 | 0.265 | 0.027 | 630 | 0.138 | 0.014 | 840 | 0.222 | 0.022 | 490 | 0.101 | 0.010 |
| 11 | 1001 | 0.376 | 0.034 | 693 | 0.166 | 0.015 | 924 | 0.294 | 0.027 | 539 | 0.118 | 0.011 |
| 12 | 1092 | 0.634 | 0.053 | 756 | 0.203 | 0.017 | 1008 | 0.420 | 0.035 | 588 | 0.138 | 0.012 |
| 13 | | | | 819 | 0.251 | 0.019 | 1092 | 0.755 | 0.058 | 637 | 0.162 | 0.012 |
| 14 | | | | 882 | 0.320 | 0.023 | | | | 686 | 0.191 | 0.014 |
| 15 | | | | 945 | 0.431 | 0.029 | | | | 735 | 0.228 | 0.015 |
| 16 | | | | 1008 | 0.669 | 0.042 | | | | 784 | 0.275 | 0.017 |
| 17 | | | | | | | | | | 833 | 0.342 | 0.020 |
| 18 | | | | | | | | | | 882 | 0.444 | 0.025 |
| 19 | | | | | | | | | | 931 | 0.637 | 0.034 |

Table D20. Amplification of Ultimate Forces in Design Case 10

| | C1 | C2 | C3 | C4 |
|---|---|---|---|---|
| Load (MN) | 4.51 | 11.31 | 8.45 | 10.4 |
| Moment (MN) | 409.8 | 711.1 | 711.8 | 529.6 |
| $K_L$ (MN/m) | 1383.2 | 768.8 | 877.7 | 1119.9 |
| $K_{LR}$ (MN) | -22760 | -12304 | -13988 | -18337 |
| $K_R$ (MN*m/rad) | 472511 | 234600 | 262419 | 325241 |
| Nat. freq. (Hz) | 0.246 | 0.217 | 0.219 | 0.229 |
| DAF | 3.771 | 1.744 | 2.215 | 1.678 |
| Amplified load (MN) | 12.02 | 18.04 | 14.82 | 16.53 |
| Amplified moment (MN*m) | 739.2 | 949.1 | 954.0 | 748.6 |

**Design Case 11: Soil Profile 3 – Jeanjean et al. (2022) - L=37 m & D=7.5 m**

Table D21. LPILE Analysis for Ultimate Pile Capacity in Design Case 11

| H (MN) | COMBINATION 1 | | | COMBINATION 2 | | | COMBINATION 3 | | | COMBINATION 4 | | |
|---|---|---|---|---|---|---|---|---|---|---|---|---|
| | M (MN*m) | y (m) | y/H (m/MN) | M (MN*m) | y (m) | y/H (m/MN) | M (MN*m) | y (m) | y/H (m/MN) | M (MN*m) | y (m) | y/H (m/MN) |
| 1 | 98 | 0.010 | 0.010 | 69 | 0.007 | 0.007 | 91 | 0.009 | 0.009 | 52 | 0.006 | 0.006 |
| 2 | 196 | 0.022 | 0.011 | 138 | 0.016 | 0.008 | 182 | 0.020 | 0.010 | 104 | 0.013 | 0.006 |
| 3 | 294 | 0.036 | 0.012 | 207 | 0.026 | 0.009 | 273 | 0.034 | 0.011 | 156 | 0.020 | 0.007 |
| 4 | 392 | 0.056 | 0.014 | 276 | 0.037 | 0.009 | 364 | 0.051 | 0.013 | 208 | 0.028 | 0.007 |
| 5 | 490 | 0.082 | 0.016 | 345 | 0.051 | 0.010 | 455 | 0.074 | 0.015 | 260 | 0.038 | 0.008 |
| 6 | 588 | 0.121 | 0.020 | 414 | 0.070 | 0.012 | 546 | 0.107 | 0.018 | 312 | 0.050 | 0.008 |
| 7 | 686 | 0.176 | 0.025 | 483 | 0.095 | 0.014 | 637 | 0.152 | 0.022 | 364 | 0.064 | 0.009 |
| 8 | 784 | 0.252 | 0.032 | 552 | 0.129 | 0.016 | 728 | 0.215 | 0.027 | 416 | 0.083 | 0.010 |
| 9 | 882 | 0.368 | 0.041 | 621 | 0.172 | 0.019 | 819 | 0.304 | 0.034 | 468 | 0.108 | 0.012 |
| 10 | 980 | 0.548 | 0.055 | 690 | 0.228 | 0.023 | 910 | 0.442 | 0.044 | 520 | 0.138 | 0.011 |
| 11 | 1078 | 0.813 | 0.074 | 759 | 0.304 | 0.028 | 1001 | 0.639 | 0.058 | 572 | 0.176 | 0.013 |
| 12 | 1176 | 1.315 | 0.110 | 828 | 0.414 | 0.035 | 1092 | 0.943 | 0.079 | 624 | 0.223 | 0.015 |
| 13 | | | | 897 | 0.563 | 0.043 | 1183 | 1.636 | 0.126 | 676 | 0.284 | 0.017 |
| 14 | | | | 966 | 0.767 | 0.055 | | | | 728 | 0.366 | 0.020 |
| 15 | | | | 1035 | 1.082 | 0.072 | | | | 780 | 0.476 | 0.024 |
| 16 | | | | 1104 | 1.8464 | 0.115 | | | | 832 | 0.613 | 0.030 |
| 17 | | | | | | | | | | 884 | 0.798 | 0.036 |
| 18 | | | | | | | | | | 936 | 1.067 | 0.044 |
| 19 | | | | | | | | | | 988 | 1.606 | 0.056 |

Table D22. Amplification of Ultimate Forces in Design Case 11

| | C1 | C2 | C3 | C4 |
|---|---|---|---|---|
| Load (MN) | 3.93 | 9.40 | 7.32 | 8.49 |
| Moment (MN) | 384.0 | 644.0 | 669.5 | 462.5 |
| $K_L$ (MN/m) | 804.5 | 436.8 | 470.0 | 606.8 |
| $K_{LR}$ (MN) | -12463 | -7720 | -8219 | -10883 |
| $K_R$ (MN*m/rad) | 286787 | 162136 | 171182 | 259148 |
| Nat. freq. (Hz) | 0.245 | 0.199 | 0.202 | 0.236 |
| DAF | 3.812 | 1.873 | 2.466 | 1.649 |
| Amplified load (MN) | 10.55 | 15.97 | 13.98 | 13.27 |
| Amplified moment (MN*m) | 697.2 | 897.0 | 944.2 | 645.5 |

**Design Case 12: Soil Profile 3 – Jeanjean et al. (2022) - L=36 m & D=8.5 m**

Table D23. LPILE Analysis for Ultimate Pile Capacity in Design Case 12

| H (MN) | COMBINATION 1 | | | COMBINATION 2 | | | COMBINATION 3 | | | COMBINATION 4 | | |
|---|---|---|---|---|---|---|---|---|---|---|---|---|
| | M (MN*m) | y (m) | y/H (m/MN) | M (MN*m) | y (m) | y/H (m/MN) | M (MN*m) | y (m) | y/H (m/MN) | M (MN*m) | y (m) | y/H (m/MN) |
| 1 | 91 | 0.008 | 0.008 | 63 | 0.006 | 0.006 | 84 | 0.007 | 0.007 | 49 | 0.005 | 0.005 |
| 2 | 182 | 0.017 | 0.009 | 126 | 0.012 | 0.006 | 168 | 0.016 | 0.008 | 98 | 0.010 | 0.005 |
| 3 | 273 | 0.028 | 0.009 | 189 | 0.020 | 0.007 | 252 | 0.026 | 0.009 | 147 | 0.016 | 0.005 |
| 4 | 364 | 0.042 | 0.011 | 252 | 0.028 | 0.007 | 336 | 0.038 | 0.010 | 196 | 0.023 | 0.006 |
| 5 | 455 | 0.062 | 0.012 | 315 | 0.039 | 0.008 | 420 | 0.055 | 0.011 | 245 | 0.030 | 0.006 |
| 6 | 546 | 0.090 | 0.015 | 378 | 0.052 | 0.009 | 504 | 0.079 | 0.013 | 294 | 0.039 | 0.007 |
| 7 | 637 | 0.131 | 0.019 | 441 | 0.070 | 0.010 | 588 | 0.113 | 0.016 | 343 | 0.051 | 0.007 |
| 8 | 728 | 0.190 | 0.024 | 504 | 0.094 | 0.012 | 672 | 0.160 | 0.020 | 392 | 0.065 | 0.008 |
| 9 | 819 | 0.267 | 0.030 | 567 | 0.126 | 0.014 | 756 | 0.224 | 0.025 | 441 | 0.084 | 0.009 |
| 10 | 910 | 0.381 | 0.038 | 630 | 0.169 | 0.017 | 840 | 0.310 | 0.031 | 490 | 0.108 | 0.011 |
| 11 | 1001 | 0.557 | 0.051 | 693 | 0.222 | 0.020 | 924 | 0.437 | 0.040 | 539 | 0.139 | 0.013 |
| 12 | 1092 | 0.814 | 0.068 | 756 | 0.289 | 0.024 | 1008 | 0.625 | 0.052 | 588 | 0.178 | 0.015 |
| 13 | 1183 | 1.264 | 0.097 | 819 | 0.381 | 0.029 | 1092 | 0.902 | 0.069 | 637 | 0.225 | 0.017 |
| 14 | | | | 882 | 0.513 | 0.037 | 1176 | 1.414 | 0.101 | 686 | 0.281 | 0.020 |
| 15 | | | | 945 | 0.685 | 0.046 | | | | 735 | 0.356 | 0.024 |
| 16 | | | | 1008 | 0.932 | 0.058 | | | | 784 | 0.456 | 0.028 |
| 17 | | | | 1071 | 1.3407 | 0.079 | | | | 833 | 0.587 | 0.035 |
| 18 | | | | | | | | | | 882 | 0.754 | 0.042 |

Table D24. Amplification of Ultimate Forces in Design Case 12

| | C1 | C2 | C3 | C4 |
|---|---|---|---|---|
| Load (MN) | 4.51 | 11.31 | 8.45 | 10.4 |
| Moment (MN) | 409.8 | 711.1 | 711.8 | 529.6 |
| $K_L$ (MN/m) | 987.9 | 541.8 | 562.8 | 695.8 |
| $K_{LR}$ (MN) | -17642 | -9237 | -11386 | -14636 |
| $K_R$ (MN*m/rad) | 434205 | 220071 | 264099 | 369621 |
| Nat. freq. (Hz) | 0.251 | 0.208 | 0.212 | 0.234 |
| DAF | 3.597 | 1.805 | 2.316 | 1.655 |
| Amplified load (MN) | 11.55 | 18.60 | 15.35 | 16.32 |
| Amplified moment (MN*m) | 718.5 | 968.8 | 974.2 | 741.2 |

## E. LPILE Serviceability Limit State Analysis Results

Table E1. SLS Results – Current Recommendation – Soil Profile 1

| Pile length (m) | Pile diameter (m) | Wall thickness (mm) | Load Combination | V (kN) | H (kN) | M (kN*m) | $K_L$ (kN/m) | $K_{LR}$ (kN) | $K_R$ (kN*m/rad) | Natural Frequency (Hz) | DAF | Amplified H (kN) | Amplified M (kN*m) | Amplified y (m) | Amplified rot. (rad) | Amplified rot. (deg) |
|---|---|---|---|---|---|---|---|---|---|---|---|---|---|---|---|---|
| 73 | 8.5 | 92 | C1 | 19546 | 3343 | 303592 | 3.23E+05 | -9.02E+06 | 3.31E+08 | **0.239** | **2.356** | 6062 | 422942 | 0.180 | 6.41E-03 | 0.367 |
| 73 | 8.5 | 92 | C2 | 19546 | 8377 | 526718 | 2.34E+05 | -7.03E+06 | 2.67E+08 | **0.229** | **1.197** | 9695 | 573323 | 0.286 | 9.63E-03 | 0.552 |
| 73 | 8.5 | 92 | C3 | 19546 | 6802 | 613880 | 2.29E+05 | -6.78E+06 | 2.53E+08 | **0.226** | **1.395** | 8332 | 672013 | 0.305 | 1.04E-02 | 0.598 |
| 73 | 8.5 | 92 | C4 | 19546 | 7563 | 370248 | 2.68E+05 | -8.05E+06 | 3.13E+08 | **0.236** | **1.182** | 8762 | 411413 | 0.209 | 7.15E-03 | 0.410 |
| 76 | 8.5 | 92 | C1 | 19546 | 3343 | 303592 | 3.22E+05 | -8.96E+06 | 3.29E+08 | **0.240** | **2.352** | 6055 | 422625 | 0.184 | 6.48E-03 | 0.371 |
| 76 | 8.5 | 92 | C2 | 19546 | 8377 | 526718 | 2.39E+05 | -7.05E+06 | 2.65E+08 | **0.229** | **1.195** | 9686 | 573023 | 0.288 | 9.67E-03 | 0.554 |
| 76 | 8.5 | 92 | C3 | 19546 | 6802 | 613880 | 2.33E+05 | -6.80E+06 | 2.51E+08 | **0.227** | **1.391** | 8320 | 671547 | 0.306 | 1.04E-02 | 0.598 |
| 76 | 8.5 | 92 | C4 | 19546 | 7563 | 370248 | 2.71E+05 | -8.07E+06 | 3.13E+08 | **0.237** | **1.181** | 8756 | 411196 | 0.214 | 7.24E-03 | 0.415 |
| 79 | 8.5 | 92 | C1 | 19546 | 3343 | 303592 | 3.26E+05 | -9.02E+06 | 3.30E+08 | **0.240** | **2.346** | 6042 | 422078 | 0.182 | 6.45E-03 | 0.370 |
| 79 | 8.5 | 92 | C2 | 19546 | 8377 | 526718 | 2.51E+05 | -7.21E+06 | 2.66E+08 | **0.230** | **1.193** | 9670 | 572456 | 0.286 | 9.62E-03 | 0.551 |
| 79 | 8.5 | 92 | C3 | 19546 | 6802 | 613880 | 2.46E+05 | -6.96E+06 | 2.52E+08 | **0.228** | **1.385** | 8296 | 670670 | 0.303 | 1.04E-02 | 0.595 |
| 79 | 8.5 | 92 | C4 | 19546 | 7563 | 370248 | 2.82E+05 | -8.16E+06 | 3.15E+08 | **0.239** | **1.177** | 8728 | 410243 | 0.212 | 7.20E-03 | 0.413 |
| 70 | 9.5 | 102 | C1 | 21787 | 3832 | 325083 | 4.33E+05 | -1.28E+07 | 4.92E+08 | **0.247** | **2.171** | 6749 | 454502 | 0.139 | 4.73E-03 | 0.271 |
| 70 | 9.5 | 102 | C2 | 21787 | 9959 | 582217 | 2.81E+05 | -9.81E+06 | 4.24E+08 | **0.239** | **1.177** | 11442 | 633812 | 0.286 | 8.41E-03 | 0.482 |
| 70 | 9.5 | 102 | C3 | 21787 | 7739 | 649007 | 2.87E+05 | -9.89E+06 | 4.26E+08 | **0.240** | **1.336** | 9350 | 710004 | 0.276 | 8.39E-03 | 0.481 |
| 70 | 9.5 | 102 | C4 | 21787 | 9144 | 425747 | 3.28E+05 | -1.09E+07 | 4.56E+08 | **0.243** | **1.171** | 10548 | 473682 | 0.194 | 6.05E-03 | 0.347 |
| 73 | 9.5 | 102 | C1 | 21787 | 3832 | 325083 | 4.64E+05 | -1.33E+07 | 5.01E+08 | **0.248** | **2.151** | 6698 | 452270 | 0.130 | 4.56E-03 | 0.261 |
| 73 | 9.5 | 102 | C2 | 21787 | 9959 | 582217 | 3.20E+05 | -1.05E+07 | 4.42E+08 | **0.243** | **1.170** | 11382 | 631729 | 0.226 | 7.22E-03 | 0.414 |
| 73 | 9.5 | 102 | C3 | 21787 | 7739 | 649007 | 3.24E+05 | -1.06E+07 | 4.42E+08 | **0.244** | **1.323** | 9287 | 707636 | 0.227 | 7.48E-03 | 0.429 |
| 73 | 9.5 | 102 | C4 | 21787 | 9144 | 425747 | 3.63E+05 | -1.15E+07 | 4.67E+08 | **0.245** | **1.167** | 10517 | 472614 | 0.171 | 5.64E-03 | 0.323 |
| 76 | 9.5 | 102 | C1 | 21787 | 3832 | 325083 | 4.66E+05 | -1.33E+07 | 5.00E+08 | **0.249** | **2.147** | 6688 | 451808 | 0.133 | 4.61E-03 | 0.264 |
| 76 | 9.5 | 102 | C2 | 21787 | 9959 | 582217 | 3.30E+05 | -1.07E+07 | 4.44E+08 | **0.244** | **1.168** | 11368 | 631264 | 0.225 | 7.28E-03 | 0.417 |
| 76 | 9.5 | 102 | C3 | 21787 | 7739 | 649007 | 3.33E+05 | -1.07E+07 | 4.43E+08 | **0.245** | **1.320** | 9273 | 707105 | 0.222 | 7.38E-03 | 0.423 |
| 76 | 9.5 | 102 | C4 | 21787 | 9144 | 425747 | 3.70E+05 | -1.16E+07 | 4.68E+08 | **0.246** | **1.166** | 10508 | 472326 | 0.172 | 5.66E-03 | 0.324 |
| 79 | 9.5 | 102 | C1 | 21787 | 3832 | 325083 | 4.78E+05 | -1.35E+07 | 5.02E+08 | **0.249** | **2.140** | 6672 | 451103 | 0.132 | 4.58E-03 | 0.262 |
| 79 | 9.5 | 102 | C2 | 21787 | 9959 | 582217 | 3.49E+05 | -1.10E+07 | 4.49E+08 | **0.245** | **1.167** | 11355 | 630805 | 0.220 | 7.19E-03 | 0.412 |
| 79 | 9.5 | 102 | C3 | 21787 | 7739 | 649007 | 3.52E+05 | -1.10E+07 | 4.48E+08 | **0.245** | **1.317** | 9258 | 706547 | 0.218 | 7.31E-03 | 0.419 |
| 79 | 9.5 | 102 | C4 | 21787 | 9144 | 425747 | 3.89E+05 | -1.19E+07 | 4.74E+08 | **0.247** | **1.164** | 10498 | 471962 | 0.171 | 5.63E-03 | 0.323 |

Table E2. SLS Results – Current Recommendation – Soil Profile 2

| Pile length (m) | Pile diameter (m) | Wall thickness (mm) | Load Combination | V (kN) | H (kN) | M (kN*m) | $K_L$ (kN/m) | $K_{LR}$ (kN) | $K_R$ (kN*m/rad) | Natural Frequency (Hz) | DAF | Amplified H (kN) | Amplified M (kN*m) | Amplified y (m) | Amplified rot. (rad) | Amplified rot. (deg) |
|---|---|---|---|---|---|---|---|---|---|---|---|---|---|---|---|---|
| 44 | 7.5 | 82 | C1 | 17545 | 2908 | 284450 | 2.88E-02 | 2.42E-03 | 1.81E+06 | **0.249** | **2.147** | 4709 | 362766 | 0.040 | 3.26E-03 | 0.187 |
| 44 | 7.5 | 82 | C2 | 17545 | 6962 | 477004 | 5.62E-02 | 4.48E-03 | 1.51E+06 | **0.236** | **1.183** | 7930 | 511909 | 0.062 | 4.89E-03 | 0.280 |
| 44 | 7.5 | 82 | C3 | 17545 | 5967 | 582527 | 6.58E-02 | 5.30E-03 | 1.36E+06 | **0.232** | **1.368** | 7086 | 625368 | 0.073 | 5.81E-03 | 0.333 |
| 44 | 7.5 | 82 | C4 | 17545 | 6147 | 432721 | 4.99E-02 | 4.01E-03 | 1.60E+06 | **0.239** | **1.177** | 7074 | 474963 | 0.056 | 4.47E-03 | 0.256 |
| 43 | 8.5 | 92 | C1 | 19546 | 3343 | 303592 | 2.35E-02 | 1.76E-03 | 1.89E+06 | **0.253** | **2.061** | 5471 | 396987 | 0.036 | 2.53E-03 | 0.145 |
| 43 | 8.5 | 92 | C2 | 19546 | 8377 | 526718 | 5.80E-02 | 3.78E-03 | 1.34E+06 | **0.243** | **1.170** | 9515 | 566960 | 0.068 | 4.29E-03 | 0.246 |
| 43 | 8.5 | 92 | C3 | 19546 | 6802 | 613880 | 6.54E-02 | 4.28E-03 | 1.27E+06 | **0.238** | **1.343** | 8132 | 664437 | 0.079 | 4.96E-03 | 0.284 |
| 43 | 8.5 | 92 | C4 | 19546 | 7563 | 370248 | 3.75E-02 | 2.56E-03 | 1.61E+06 | **0.251** | **1.157** | 8598 | 405789 | 0.044 | 2.91E-03 | 0.167 |

Table E3. SLS Results – Current Recommendation – Soil Profile 3

| Pile length (m) | Pile diameter (m) | Wall thickness (mm) | Load Combination | V (kN) | H (kN) | M (kN*m) | $K_L$ (kN/m) | $K_{LR}$ (kN) | $K_R$ (kN*m/rad) | Natural Frequency (Hz) | DAF | Amplified H (kN) | Amplified M (kN*m) | Amplified y (m) | Amplified rot. (rad) | Amplified rot. (deg) |
|---|---|---|---|---|---|---|---|---|---|---|---|---|---|---|---|---|
| 47 | 7.5 | 82 | C1 | 17545 | 2908 | 284450 | 1.37E+06 | -1.60E+07 | 3.10E+08 | **0.249** | **2.138** | 4694 | 362116 | 0.033 | 2.76E-03 | 0.158 |
| 47 | 7.5 | 82 | C2 | 17545 | 6962 | 477004 | 8.26E+05 | -1.13E+07 | 2.27E+08 | **0.238** | **1.179** | 7911 | 511222 | 0.068 | 5.01E-03 | 0.287 |
| 47 | 7.5 | 82 | C3 | 17545 | 5967 | 582527 | 7.21E+05 | -9.92E+06 | 1.89E+08 | **0.229** | **1.384** | 7135 | 627241 | 0.088 | 6.21E-03 | 0.356 |
| 47 | 7.5 | 82 | C4 | 17545 | 6147 | 432721 | 9.23E+05 | -1.24E+07 | 2.53E+08 | **0.242** | **1.172** | 7043 | 473553 | 0.059 | 4.46E-03 | 0.256 |
| 46 | 8.5 | 92 | C1 | 19546 | 3343 | 303592 | 1.73E+06 | -2.20E+07 | 4.69E+08 | **0.255** | **2.030** | 5408 | 394250 | 0.030 | 2.25E-03 | 0.129 |
| 46 | 8.5 | 92 | C2 | 19546 | 8377 | 526718 | 1.06E+06 | -1.68E+07 | 4.04E+08 | **0.251** | **1.158** | 9437 | 564212 | 0.058 | 3.78E-03 | 0.217 |
| 46 | 8.5 | 92 | C3 | 19546 | 6802 | 613880 | 9.88E+05 | -1.57E+07 | 3.75E+08 | **0.249** | **1.305** | 7985 | 658831 | 0.067 | 4.35E-03 | 0.249 |
| 46 | 8.5 | 92 | C4 | 19546 | 7563 | 370248 | 1.38E+06 | -1.95E+07 | 4.47E+08 | **0.254** | **1.154** | 8577 | 405050 | 0.036 | 2.58E-03 | 0.148 |

Table E4. SLS Results – Jeanjean et al. (2022) – Soil Profile 1

| Pile length (m) | Pile diameter (m) | Wall thickness (mm) | Load Combination | V (kN) | H (kN) | M (kN*m) | $K_L$ (kN/m) | $K_{LR}$ (kN) | $K_R$ (kN*m/rad) | Natural Frequency (Hz) | DAF | Amplified H (kN) | Amplified M (kN*m) | Amplified y (m) | Amplified rot. (rad) | Amplified rot. (deg) |
|---|---|---|---|---|---|---|---|---|---|---|---|---|---|---|---|---|
| 52 | 8.5 | 92 | C1 | 19546 | 3353 | 305052 | 3.56E+05 | -9.87E+06 | 3.48E+08 | **0.239** | **2.364** | 6097 | 425733 | 0.211 | 7.26E-03 | 0.416 |
| 52 | 8.5 | 92 | C2 | 19546 | 8377 | 526718 | 2.67E+05 | -7.15E+06 | 2.32E+08 | **0.219** | **1.218** | 9839 | 578442 | 0.355 | 1.15E-02 | 0.660 |
| 52 | 8.5 | 92 | C3 | 19546 | 6802 | 613880 | 2.58E+05 | -6.80E+06 | 2.18E+08 | **0.217** | **1.445** | 8526 | 679380 | 0.384 | 1.26E-02 | 0.721 |
| 52 | 8.5 | 92 | C4 | 19546 | 7563 | 370248 | 3.18E+05 | -9.03E+06 | 3.14E+08 | **0.232** | **1.191** | 8819 | 413375 | 0.251 | 8.28E-03 | 0.474 |
| 55 | 8.5 | 92 | C1 | 19546 | 3353 | 305052 | 4.12E+05 | -1.06E+07 | 3.57E+08 | **0.243** | **2.260** | 5888 | 416532 | 0.165 | 6.11E-03 | 0.350 |
| 55 | 8.5 | 92 | C2 | 19546 | 8377 | 526718 | 3.42E+05 | -8.68E+06 | 2.76E+08 | **0.231** | **1.192** | 9660 | 572112 | 0.262 | 9.31E-03 | 0.533 |
| 55 | 8.5 | 92 | C3 | 19546 | 6802 | 613880 | 3.35E+05 | -8.33E+06 | 2.59E+08 | **0.229** | **1.383** | 8289 | 670367 | 0.280 | 1.01E-02 | 0.578 |
| 55 | 8.5 | 92 | C4 | 19546 | 7563 | 370248 | 3.74E+05 | -9.99E+06 | 3.43E+08 | **0.240** | **1.175** | 8715 | 409795 | 0.195 | 6.94E-03 | 0.398 |
| 58 | 8.5 | 92 | C1 | 19546 | 3353 | 305052 | 4.45E+05 | -1.10E+07 | 3.62E+08 | **0.245** | **2.222** | 5811 | 413160 | 0.147 | 5.68E-03 | 0.325 |
| 58 | 8.5 | 92 | C2 | 19546 | 8377 | 526718 | 3.81E+05 | -9.34E+06 | 2.95E+08 | **0.237** | **1.181** | 9592 | 569697 | 0.232 | 8.59E-03 | 0.492 |
| 58 | 8.5 | 92 | C3 | 19546 | 6802 | 613880 | 3.75E+05 | -9.00E+06 | 2.77E+08 | **0.234** | **1.358** | 8191 | 666658 | 0.247 | 9.29E-03 | 0.532 |
| 58 | 8.5 | 92 | C4 | 19546 | 7563 | 370248 | 4.09E+05 | -1.05E+07 | 3.53E+08 | **0.243** | **1.170** | 8684 | 408716 | 0.175 | 6.46E-03 | 0.370 |
| 61 | 8.5 | 92 | C1 | 19546 | 3353 | 305052 | 4.71E+05 | -1.13E+07 | 3.67E+08 | **0.246** | **2.202** | 5772 | 411419 | 0.139 | 5.49E-03 | 0.315 |
| 61 | 8.5 | 92 | C2 | 19546 | 8377 | 526718 | 4.13E+05 | -9.82E+06 | 3.06E+08 | **0.239** | **1.177** | 9560 | 568572 | 0.215 | 8.21E-03 | 0.470 |
| 61 | 8.5 | 92 | C3 | 19546 | 6802 | 613880 | 4.08E+05 | -9.48E+06 | 2.88E+08 | **0.237** | **1.346** | 8145 | 664922 | 0.223 | 8.67E-03 | 0.497 |
| 61 | 8.5 | 92 | C4 | 19546 | 7563 | 370248 | 4.39E+05 | -1.09E+07 | 3.59E+08 | **0.244** | **1.168** | 8668 | 408188 | 0.163 | 6.20E-03 | 0.355 |
| 50 | 9.5 | 102 | C1 | 21787 | 3832 | 325083 | 4.39E+05 | -1.38E+07 | 5.16E+08 | **0.242** | **2.290** | 7044 | 467614 | 0.246 | 7.47E-03 | 0.428 |
| 50 | 9.5 | 102 | C2 | 21787 | 9959 | 582217 | 2.69E+05 | -8.07E+06 | 2.87E+08 | **0.222** | **1.211** | 11726 | 643722 | 0.479 | 1.37E-02 | 0.784 |
| 50 | 9.5 | 102 | C3 | 21787 | 7739 | 649007 | 2.79E+05 | -8.32E+06 | 2.93E+08 | **0.222** | **1.417** | 9741 | 724834 | 0.480 | 1.39E-02 | 0.795 |
| 50 | 9.5 | 102 | C4 | 21787 | 9144 | 425747 | 3.62E+05 | -1.12E+07 | 4.01E+08 | **0.228** | **1.198** | 10770 | 481259 | 0.334 | 9.73E-03 | 0.557 |
| 52 | 9.5 | 102 | C1 | 21787 | 3832 | 325083 | 4.68E+05 | -1.40E+07 | 5.17E+08 | **0.246** | **2.200** | 6821 | 457705 | 0.191 | 6.07E-03 | 0.348 |
| 52 | 9.5 | 102 | C2 | 21787 | 9959 | 582217 | 3.49E+05 | -1.03E+07 | 3.57E+08 | **0.230** | **1.194** | 11585 | 638808 | 0.349 | 1.05E-02 | 0.599 |
| 52 | 9.5 | 102 | C3 | 21787 | 7739 | 649007 | 3.57E+05 | -1.05E+07 | 3.61E+08 | **0.230** | **1.379** | 9556 | 717836 | 0.348 | 1.06E-02 | 0.607 |
| 52 | 9.5 | 102 | C4 | 21787 | 9144 | 425747 | 4.12E+05 | -1.27E+07 | 4.68E+08 | **0.239** | **1.178** | 10606 | 475670 | 0.256 | 7.77E-03 | 0.445 |
| 55 | 9.5 | 102 | C1 | 21787 | 3832 | 325083 | 5.44E+05 | -1.49E+07 | 5.30E+08 | **0.250** | **2.115** | 6609 | 448291 | 0.140 | 4.82E-03 | 0.276 |
| 55 | 9.5 | 102 | C2 | 21787 | 9959 | 582217 | 4.53E+05 | -1.29E+07 | 4.52E+08 | **0.243** | **1.171** | 11387 | 631893 | 0.238 | 7.81E-03 | 0.447 |
| 55 | 9.5 | 102 | C3 | 21787 | 7739 | 649007 | 4.56E+05 | -1.29E+07 | 4.51E+08 | **0.243** | **1.325** | 9299 | 708085 | 0.237 | 7.94E-03 | 0.455 |
| 55 | 9.5 | 102 | C4 | 21787 | 9144 | 425747 | 4.85E+05 | -1.41E+07 | 5.16E+08 | **0.248** | **1.163** | 10486 | 471567 | 0.183 | 6.04E-03 | 0.346 |
| 58 | 9.5 | 102 | C1 | 21787 | 3832 | 325083 | 5.95E+05 | -1.56E+07 | 5.38E+08 | **0.252** | **2.083** | 6529 | 444757 | 0.119 | 4.33E-03 | 0.248 |
| 58 | 9.5 | 102 | C2 | 21787 | 9959 | 582217 | 5.07E+05 | -1.39E+07 | 4.89E+08 | **0.248** | **1.162** | 11316 | 629450 | 0.200 | 6.90E-03 | 0.395 |
| 58 | 9.5 | 102 | C3 | 21787 | 7739 | 649007 | 5.09E+05 | -1.39E+07 | 4.87E+08 | **0.248** | **1.308** | 9215 | 704889 | 0.199 | 7.04E-03 | 0.403 |
| 58 | 9.5 | 102 | C4 | 21787 | 9144 | 425747 | 5.36E+05 | -1.47E+07 | 5.25E+08 | **0.250** | **1.159** | 10452 | 470403 | 0.156 | 5.40E-03 | 0.309 |
| 61 | 9.5 | 102 | C1 | 21787 | 3832 | 325083 | 6.40E+05 | -1.62E+07 | 5.47E+08 | **0.253** | **2.065** | 6485 | 442825 | 0.107 | 4.06E-03 | 0.233 |
| 61 | 9.5 | 102 | C2 | 21787 | 9959 | 582217 | 5.56E+05 | -1.47E+07 | 5.09E+08 | **0.251** | **1.159** | 11286 | 628389 | 0.179 | 6.43E-03 | 0.368 |
| 61 | 9.5 | 102 | C3 | 21787 | 7739 | 649007 | 5.58E+05 | -1.47E+07 | 5.07E+08 | **0.251** | **1.300** | 9178 | 703511 | 0.179 | 6.57E-03 | 0.376 |
| 61 | 9.5 | 102 | C4 | 21787 | 9144 | 425747 | 5.84E+05 | -1.54E+07 | 5.34E+08 | **0.252** | **1.157** | 10434 | 469783 | 0.140 | 5.04E-03 | 0.289 |

Table E5. SLS Results – Jeanjean et al. (2022) – Soil Profile 2

| Pile length (m) | Pile diameter (m) | Wall thickness (mm) | Load Combination | V (kN) | H (kN) | M (kN*m) | $K_L$ (kN/m) | $K_{LR}$ (kN) | $K_R$ (kN*m/rad) | Natural Frequency (Hz) | DAF | Amplified H (kN) | Amplified M (kN*m) | Amplified y (m) | Amplified rot. (rad) | Amplified rot. (deg) |
|---|---|---|---|---|---|---|---|---|---|---|---|---|---|---|---|---|
| 31 | 7.5 | 82 | C1 | 17545 | 2908 | 284450 | 1.77E+06 | -2.09E+07 | 3.68E+08 | **0.249** | **2.139** | 4696 | 362187 | 0.040 | 3.23E-03 | 0.185 |
| 31 | 7.5 | 82 | C2 | 17545 | 6962 | 477004 | 1.44E+06 | -1.86E+07 | 3.35E+08 | **0.244** | **1.169** | 7856 | 509242 | 0.065 | 5.02E-03 | 0.288 |
| 31 | 7.5 | 82 | C3 | 17545 | 5967 | 582527 | 1.34E+06 | -1.70E+07 | 2.89E+08 | **0.238** | **1.342** | 7008 | 622371 | 0.079 | 6.06E-03 | 0.347 |
| 31 | 7.5 | 82 | C4 | 17545 | 6147 | 432721 | 1.50E+06 | -1.94E+07 | 3.55E+08 | **0.246** | **1.166** | 7013 | 472158 | 0.058 | 4.54E-03 | 0.260 |
| 30 | 8.5 | 92 | C1 | 19546 | 3343 | 303592 | 2.14E+06 | -2.88E+07 | 5.47E+08 | **0.253** | **2.065** | 5480 | 397391 | 0.040 | 2.81E-03 | 0.161 |
| 30 | 8.5 | 92 | C2 | 19546 | 8377 | 526718 | 1.72E+06 | -2.63E+07 | 5.18E+08 | **0.248** | **1.162** | 9463 | 565127 | 0.069 | 4.59E-03 | 0.263 |
| 30 | 8.5 | 92 | C3 | 19546 | 6802 | 613880 | 1.66E+06 | -2.51E+07 | 4.84E+08 | **0.246** | **1.314** | 8021 | 660206 | 0.078 | 5.22E-03 | 0.299 |
| 30 | 8.5 | 92 | C4 | 19546 | 7563 | 370248 | 1.94E+06 | -2.79E+07 | 5.43E+08 | **0.251** | **1.158** | 8601 | 405872 | 0.047 | 3.21E-03 | 0.184 |

Table E6. SLS Results – Jeanjean et al. (2022) – Soil Profile 3

| Pile length (m) | Pile diameter (m) | Wall thickness (mm) | Load Combination | V (kN) | H (kN) | M (kN*m) | $K_L$ (kN/m) | $K_{LR}$ (kN) | $K_R$ (kN*m/rad) | Natural Frequency (Hz) | DAF | Amplified H (kN) | Amplified M (kN*m) | Amplified y (m) | Amplified rot. (rad) | Amplified rot. (deg) |
|---|---|---|---|---|---|---|---|---|---|---|---|---|---|---|---|---|
| 37 | 7.5 | 82 | C1 | 17545 | 2908 | 284450 | 1.33E+06 | -1.59E+07 | 3.13E+08 | **0.249** | **2.136** | 4692 | 362000 | 0.038 | 3.13E-03 | 0.179 |
| 37 | 7.5 | 82 | C2 | 17545 | 6962 | 477004 | 8.86E+05 | -1.35E+07 | 2.96E+08 | **0.243** | **1.170** | 7863 | 509500 | 0.074 | 5.18E-03 | 0.297 |
| 37 | 7.5 | 82 | C3 | 17545 | 5967 | 582527 | 8.51E+05 | -1.31E+07 | 2.89E+08 | **0.242** | **1.329** | 6968 | 620840 | 0.094 | 6.42E-03 | 0.368 |
| 37 | 7.5 | 82 | C4 | 17545 | 6147 | 432721 | 9.71E+05 | -1.40E+07 | 3.01E+08 | **0.245** | **1.167** | 7022 | 472567 | 0.063 | 4.59E-03 | 0.263 |
| 36 | 8.5 | 92 | C1 | 19546 | 3343 | 303592 | 1.61E+06 | -2.16E+07 | 4.74E+08 | **0.255** | **2.036** | 5421 | 394817 | 0.035 | 2.45E-03 | 0.140 |
| 36 | 8.5 | 92 | C2 | 19546 | 8377 | 526718 | 1.06E+06 | -1.86E+07 | 4.49E+08 | **0.248** | **1.162** | 9461 | 565050 | 0.077 | 4.51E-03 | 0.258 |
| 36 | 8.5 | 92 | C3 | 19546 | 6802 | 613880 | 1.00E+06 | -1.82E+07 | 4.42E+08 | **0.247** | **1.311** | 8008 | 659691 | 0.090 | 5.22E-03 | 0.299 |
| 36 | 8.5 | 92 | C4 | 19546 | 7563 | 370248 | 1.33E+06 | -2.03E+07 | 4.64E+08 | **0.252** | **1.156** | 8589 | 405462 | 0.045 | 2.90E-03 | 0.166 |